Investigating the metabolic effects of conjugated linoleic acid isomers as monotherapy or combined with rosiglitazone: *In vitro* and *in vivo* studies

A Dissertation for the fulfilment of Master of Philosophy (MPhil) in Biomedical Sciences

CHAI BOON KHENG

Supervisors: ASSOCIATE PROF. DR. MUSTAFA AHMED AL-SHAGGA

PROF. DR. SURESH KUMAR MOHANKUMAR

Division of Biomedical Sciences

UNMC

August 2019

Table of Contents

Acknowledgements 8
Declaration of Work 9
Abstract 12
CHAPTER 1
Introduction 14
1.1 Insulin 16
1.2 Insulin action in classically insulin sensitive organs 17
1.3 Lipoprotein metabolism 19
1.4 Insulin resistance 22
1.5 Current therapeutic options for diabetes 23
1.6 Peroxisome proliferator activated receptors 25
1.7 Rosiglitazone 28
1.8 Conjugated linoleic acid 30
1.9 Rationale and hypothesis 32
Aims and Objectives 34

CHAPTER 2
Method 35
2.1 *In vitro* studies 35
2.2 *In vivo* studies 40

CHAPTER 3
Results 46
3.1 Cell viability assay 46
3.2 Effect of isomers of CLA on hepatic glucose production 47
3.3 Effect of CLA isomers on PEPCK and G6P expression in HepG2 50
3.4 Effect of PPAR agonist or antagonist on HGP 52
3.5 Effect of PPAR agonist or antagonist on PEPCK and G6P expression in HepG2 57
3.6 Body weight and energy intake 62
3.7 Liver weight 66
3.8 Adipose weight 66

3.9 Fasting and random blood glucose 67
3.10 Oral glucose tolerance test 69
3.11 Hormone levels 70
3.12 Lipid levels 76
3.13 Derived data (*insulin resistance)* 86

CHAPTER 4
Discussion 90
4.1 *In vitro* results discussion 90
4.2 *In vivo* results discussion 94
4.3 Limitations of study 96
4.4 Conclusions 97

References 98
Supplementary Data 110
Appendices 112
Appendix 1 – Scientific Principles Behind the Assays 113
Appendix 2 – HepG2 Cell Line Data Sheet 116
Appendix 3 – H4IIE Cell Line Data Sheet 119
Appendix 4 - Amplex Red Glucose/Glucose Oxidase Assay Kit Data Sheet 121
Appendix 5 – Bioline TRIsure RNA Lysis Kit Data Sheet 127
Appendix 6 – Bioline Tetro cDNA Synthesis Kit Data Sheet 129
Appendix 7 – KAPA Biosystems SYBR Fast qPCR Master Mix (2x)
Data Sheet 131
Appendix 8 – Altromin 1320 M Maintenance Diet Data Sheet
(Normal Diet) 135
Appendix 9 - Appendix 8 – Research Diets #D12079B Data Sheet
(Western Diet) 139
Appendix 10 – Mouse Leptin ELISA Kit Data Sheet 141
Appendix 11 – Mouse Adiponectin ELISA Kit Data Sheet 155
Appendix 12 – Mouse Insulin ELISA Data Sheet 171
Appendix 13 – Biovision HDL and LDL Quantitation Kit Data Sheet 185
Appendix 14 - Biovision Free Fatty Acid Quantitation Kit Data Sheet 186
Appendix 15– Biovision Triglyceride Quantitation Kit Data Sheet 187

Study outcomes 189
Co-Administration of Conjugated Linoleic Acid and Rosiglitazone Increases Atherogenic Co-Efficient and Alters Isoprenaline-Induced Vasodilatation in Rats Fed High Fat Diet 190
Cis-9, *Trans*-11 Conjugated Linoleic Acid Reduces Phosphoenolpyruvate Carboxykinase Expression and Hepatic Glucose Production in HepG2 Cells 202

List of Figures

Figure 1.1: The action of insulin in insulin sensitive tissues 17
Figure 1.2: Cholesterol transport pathway from the liver and peripheral tissues 20
Figure 1.3: Metabolic functions of PPAR isotypes in insulin sensitive tissues.....25
Figure 1.4: Superposition of ligand binding domain of human PPAR isotypes.....26
Figure 1.5: Mechanism of activation of PPAR.....27
Figure 1.6: Chemical structure of conjugated linoleic acid 30
Figure 2.1: Schematic overview of *in vivo* study.....43
Figure 3.1: Cell viability of HepG2 treated with CLA 46
Figure 3.2: Cell viability of H4IIE treated with CLA.....47
Figure 3.3: Glucose production of HepG2 treated with insulin and fatty acids 48
Figure 3.4: Glucose production of H4IIE treated with insulin and fatty acids.....49
Figure 3.5: PEPCK expression of HepG2 treated with fatty acids.....50
Figure 3.6: G6P expression of HepG2 treated with fatty acids 51
Figure 3.7: PPARγ expression in HepG2 52
Figure 3.8: Glucose production of HepG2 treated with rosiglitazone and fatty acids.....53
Figure 3.9: Glucose production of H4IIE treated with rosiglitazone and CLA.....54
Figure 3.10: Glucose production of HepG2 treated with fenofibrate and CLA 55
Figure 3.11: Glucose production of HepG2 treated with GW 9662 and CLA 56
Figure 3.12: PEPCK expression of HepG2 treated with rosiglitazone and CLA 57
Figure 3.13: G6P expression of HepG2 treated with rosiglitazone and CLA 58
Figure 3.14: PEPCK expression of HepG2 treated with fenofibrate and CLA 59
Figure 3.15: G6P expression of HepG2 treated with fenofibrate and CLA.....59
Figure 3.16: PEPCK expression of HepG2 treated with GW 9662 and CLA 60
Figure 3.17: G6P expression of HepG2 treated with GW 9662 and CLA 61
Figure 3.18a: Body weight of WT and ApoE mice across all treatment groups throughout *in vivo* study 62
Figure 3.18b: Body weight gain of WT and ApoE mice across all treatment groups throughout *in vivo* study.....63
Figure 3.19a: Energy intake of mice before Week 12 64
Figure 3.19b: Energy intake of mice after Week 12.....64
Figure 3.20: Fasting blood glucose of WT and ApoE mice 67
Figure 3.21: Random blood glucose of WT and ApoE mice.....68

Figure 3.22: Oral glucose tolerance test 69
Figure 3.23: Serum insulin level at Week 12.....70
Figure 3.24: Serum insulin level at Week 20.....71
Figure 3.25: Adiponectin level at Week 12 72
Figure 3.26: Adiponectin level at Week 20 73
Figure 3.27: Leptin level at Week 12 74
Figure 3.28: Leptin level at Week 20.....75
Figure 3.29: Total cholesterol at Week 12.....76
Figure 3.30: Total cholesterol at Week 20.....77
Figure 3.31: LDL level at Week 12 78
Figure 3.32: LDL level at Week 20 79
Figure 3.33: HDL level at Week 12.....80
Figure 3.34: HDL level at Week 20.....81
Figure 3.35: Total triglyceride at Week 12.....82
Figure 3.36: Total triglyceride at Week 20.....83
Figure 3.37: Free fatty acid level at Week 12.....84
Figure 3.38: Free fatty acid level at Week 20.....85
Figure 3.39: HOMA-IR 86
Figure 3.40: QUICKI.....87
Figure 3.41: QUICKI-FFA 88
Figure S1: RT-qPCR melting curve of HepG2 RNA 111

List of tables

Table 2.1: Sequences of RT-qPCR primers for in vitro study.....39
Table 3.1: Organ weights at Week 12.....65
Table 3.2: Organ Weights at Week 20 65
Table S1: Extracted RNA concentration from HepG2 cells.....110
Table S2: Synthesised cDNA concentration from HepG2 cells 110

Acknowledgements

I would like to acknowledge my supervisors, Dr. Suresh Kumar Mohankumar for his intellectual guidance and unwavering interest throughout the project and to Dr. Mustafa Al-Shagga for attending to my candidature after Dr. Suresh's return to India. I would like to thank fellow mobility students under my supervision, Raza Yarkhan, Vanessa Pang Kerryn Hudson, Seyed Adel Moulana, Kaushal Kyada, Emily Rose and Andrew Shui-Jezierski for generating data that will be a good lead for further investigation. My gratitude goes to Ibrahim Babangida, Afif and Dr. Aini Hamid for providing cell lines for my project.

Declaration of Work

I declare herewith, that this thesis is my own original work.

Furthermore, I confirm that:

- This work has been composed by me without assistance;
- I have clearly referenced in accordance with departmental requirements in both the text and the bibliography or references, all sources (either from a printed source, internet or any other source) used in the work;
- All data and findings in the work have not been falsified or embellished;
- This work has not been previously, or concurrently, used either for other courses or within other exam processes as an exam work;

I appreciate that any false claim in respect of this work will result in disciplinary action in accordance with university or departmental regulations.

I confirm that I understand that my work may be electronically checked for plagiarism by the use of plagiarism detection software and stored on a third party's server for eventual future comparison.



List of Abbreviations

AF1, AF2 – activation function 1, 2

Akt – protein kinase B

AMP – adenosine monophosphate

AMPK – AMP activated protein kinase

ApoE – apolipoprotein E

ATP – adenosine triphosphate

CETP – cholesteryl ester transfer protein

CLA – conjugated linoleic acid

CO_2 – carbon dioxide

ERK – extracellular signal regulated kinase

FDA – Food and Drug Administration

FFA – free fatty acids

G6P – glucose-6-phosphatase

GLUT4 – glucose transporter 4

GSK3 – glycogen synthase kinase 3

HDL – high density lipoprotein

HL – hepatic lipase

HOMA-IR – homeostatic assessment of insulin resistance

IDF – International Diabetes Federation

IL-6 – interleukin 6

IRS – insulin receptor substrate

JNK – c-Jun N-terminal kinase

LBD – ligand binding domain

LCT=AT – lecithin:cholesterol acyltransferase

LDL – low density lipoprotein

LDLr – low density lipoprotein receptor

MCP-1 – monocyte chemoattractant protein-1

MetS – metabolic syndrome

NCEP ATP – National Cholesterol Education Program-Adult Treatment Panel

NF-κB – nuclear factor kappa B

PEPCK – phosphoenolpyruvate carboxykinase

PI3K – phosphatidylinositol-3-kinase

PP1 – protein phosphatase 1

PPAR – peroxisome proliferator activated receptor

PPARE – PPAR response element

QUICKI – quantitative insulin sensitivity check index

QUICKI-FFA – revised quantitative insulin sensitivity check index

SREBP-1c – sterol regulatory element binding protein 1c

T2DM – type 2 diabetes mellitus

TNFα – tumour necrosis factor α

UK – United Kingdom of Great Britain and Northern Ireland

US, USA – United States of America

vLDL – very low density lipoprotein

WHO – World Health Organisation

Abstract

Conjugated linoleic acids (CLA) are dietary fatty acids commonly found in dairy and ruminant meats. CLA is found to be beneficial in treating the metabolic syndrome (MetS) and its major complication, type 2 diabetes mellitus. CLA is thought to exert its beneficial effect through activation of peroxisome proliferator activated receptors (PPAR) activity. Thus, CLA may be beneficial alone or in combination with current medications where it reduces side effect of conventional insulin sensitisers, such as rosiglitazone. The study was carried out via *in vitro* and *in vivo* approaches. For the *in vitro* study, the effects of CLA isomers and its combination with rosiglitazone on glucose production of HepG2 and H4IIE and gluconeogenic gene expression of HepG2 cells were examined. It was found that c9,t11-CLA isomer reduced glucose production in HepG2 and H4IIE cells compared to untreated control ($p < 0.005$), while, t10,c12-CLA had the opposite effect of increasing glucose production. c9,t11-CLA did not affect the ability of rosiglitazone in directly reducing glucose production. Reduction of glucose production by fenofibrate was not affected by either CLA isomer. c9, t11-CLA was found to decrease PEPCK expression in HepG2 cells ($p < 0.05$). The *in vivo* segment of the study was performed with ApoE null mice (n=29) fed Western diet for 20 weeks, divided into 5 groups, to examine the effect of 3 mg/day 1:1 mixture of c9,t11 and t10,c12 isomers of CLA on lipoprotein metabolism and insulin, leptin and adiponectin. The administration of 1:1 CLA isomeric mixture did not alleviate dyslipidemia caused by Western diet; instead simultaneous administration of CLA and rosiglitazone exacerbated dyslipidemia in ApoE null mice, particularly total plasma cholesterol ($p < 0.001$) and plasma LDL ($p < 0.0001$) compared with normal mice fed normal diet. While glucose, insulin and adiponectin level remain unchanged across groups, early administration of CLA irrespective of rosiglitazone led to reduction of leptin compared with mice fed only Western diet. It can be concluded that while c9,t11-CLA may exert benefits in MetS on the liver *in vitro*, the

administration of CLA isomeric mixture with rosiglitazone exacerbates dyslipidemia *in vivo* that may be caused by t10,c12 isomer and thus, unable to ameliorate side effects of rosiglitazone.

CHAPTER 1

1.0 Introduction

Metabolic syndrome (MetS) is a cluster of disorders of energy consumption, storage and utilization that either individually or together raises the risk for chronic diseases including type 2 diabetes mellitus (T2DM) and cardiovascular disease (CVD). The precise definition of MetS varies according to the criteria set by governing bodies such as World Health Organization (WHO), International Diabetes Federation (IDF) and National Cholesterol Education Program-Adult Treatment Panel III (NCEP ATP III). Despite variations, common diagnostic criteria of MetS include obesity, insulin resistance, hyperglycemia, dyslipidemia and hypertension[1].

The prevalence of MetS is at approximately 25% of the world's population, estimated by IDF[1]. MetS prevalence in US hovers around one fifth of the population[2,3]. Moreover, metabolic syndrome was found to have a higher prevalence among US populations with Asian ancestry[4]. The proportion of body fat distribution in Asians differs from that of Caucasians and corresponds to higher adiposity despite having identical body mass indices with Caucasians[5]. Hence, MetS definition set by NCEP ATP III, IDF and WHO may be more applicable for Caucasians and less for Asians. Accounting for differences in body composition, separate criteria had been applied for the Asian definition of MetS. The Asian definition of obesity is modified to be BMI > 25 kg/m^2 as opposed to BMI > 30 kg/m^2 defined by WHO[6]. The ECEP ATP III definition was modified to apply for Asian populations, which the waist circumference >90 cm apply for men and >80 cm for women[7]. In countries such as South Korea, China, Hong Kong, Singapore and the Philippines, the prevalence of MetS range from 10% to 20% according to the Caucasian definition, and 20% to 30% according to the Asian definition[5].

In the Malaysian context, MetS has a surprisingly high prevalence in the population compared to worldwide and Asian prevalence, also being the highest in South East Asia above Indonesia[8]. Prevalence of MetS among Malaysians is close to 30% according to definitions set by NCEP-ATP III and IDF. Alarmingly, overall prevalence comes to a whopping rate of 43.4% using the new definition set by Joint Interim Statement for a harmonized definition of MetS[9].

Individuals with MetS are at high risk of developing T2DM (odds ratio: 5 to 8 in a 4 year follow up period)[10]. Diabetes is projected to affect approximately 400 – 600 million people worldwide by year 2030 with the most disease burden coming from poor and developing countries[11,12]. Although MetS is characterized by the presence of risk factors such as obesity, dyslipidemia, hyperglycemia, hyperinsulinemia and insulin resistance, many of these risk factors are asymptomatic and it can take years to actually develop frank diabetes.

Based on the projection that the world population is going to be approximately 8.2 billion by year 2030[13], MetS is predicted to affect 2 – 3 billion people worldwide, while diabetes will be affecting approximately 5 to 7% of the world's population by that year. Besides that, morbidity of MetS increases healthcare cost proportional to the number of components present in MetS, such as hyperglycemia, hypertension, low HDL, high triglycerides and increased waist circumference[14,15]. In average, cost increases by 24% for each risk factor present; furthermore healthcare cost doubles for patients with diabetes compared to prediabetics[14]. The syndrome is expected to present a major economic burden especially in lower income countries.

Given that MetS has reached epidemic proportion and its complications has led to increase in T2DM, CVD and all-cause mortality, a good understanding of the disease process is essential to combat MetS and its complications. In order to get a closer picture about the current

understanding of MetS pathogenesis and the hypothesis of this study, it is better to discuss some essential information about insulin and its resistance as well as metabolism of lipoproteins.

1.1 Insulin

The human body utilizes glucose and lipids as main sources of energy. Glucose and lipids undergo processes such as glycolysis, citric acid cycle and oxidative phosphorylation to ultimately yield adenosine triphosphate (ATP).

In humans, excess energy obtained after a meal is stored to meet energetic needs during periods of fasting. Excess glucose is stored in two forms namely; glycogen in the liver[16] and fatty acids stored as triglycerides in adipose tissues[17]. A homeostatic mechanism must exist to ensure perpetual availability and efficient utilization of fuels during periods of satiety and fasting[18]. Energy homeostasis is regulated by hormones, which are chemical messengers that circulate in the blood. There are a number of hormones that governs energy homeostasis, but only insulin will be further discussed for the purpose of this study.

Insulin is a peptide hormone secreted by β cells in islets of Langerhans found in pancreas. It is secreted in response to increased glucose availability in the bloodstream detected by β cells[19]. Briefly, increased β cells utilisation of glucose via glycolysis and oxidative phosphorylation leads to increase in ATP/ADP ratio. Increased ATP concentration leads to closure of ATP sensitive potassium channel and increase in intracellular potassium. The depolarization of β cell triggers opening of voltage gated calcium channel and the presence of calcium leads to release of insulin by exocytosis[19].

On target tissues, insulin binds to insulin receptors, the binding triggers trans-autophosporylation of tyrosine kinase domain of the receptors, leading to activation of

downstream signal transduction pathways that involves insulin receptor substrates (IRS), phosphatitylinositol-3-kinase (PI3K), Protein kinase B (Akt) and extracellular signal regulated kinases (ERK)[19,20].

1.2 Insulin action in "classically" insulin sensitive organs

Insulin is an important hormone for regulating glucose and lipid metabolism, primarily in liver, adipose tissues and skeletal muscle (**Figure 1.1**).

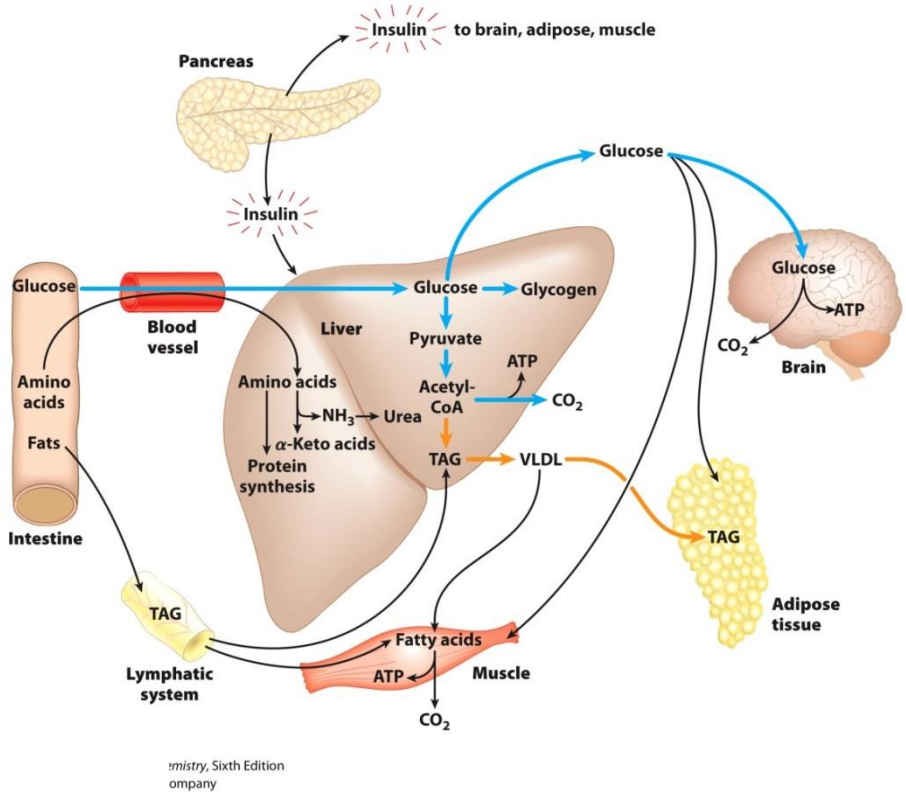


Figure 1.1: The action of insulin in insulin sensitive tissues: liver, adipose tissues and skeletal muscles. Insulin is secreted from the pancreas and act in adipose tissue to promote triacylglycerol uptake and storage; in the skeletal muscle to promote glucose uptake and fatty acid oxidation. In the liver, insulin promotes storage of glucose in the form of glycogen. (taken from Lehninger Principles of Biochemistry, 6th edition, page 952.)

1.2.1 Insulin sensitive organ: Liver

Insulin increases glucose uptake in the liver by upregulating liver glucokinase[21,22], an enzyme responsible for initiating glucose into the metabolic pathway. Insulin expands glycogen stores through stimulation of glycogen synthesis by activation of a rate-limiting enzyme; glycogen synthase and inhibition of glycogen breakdown by deactivation of glycogen phosphorylase in hepatocytes. Moreover, insulin inhibit hepatic gluconeogenesis[20]. Akt activated as a result of insulin binding phosphorylates glycogen synthase kinase 3 (GSK3), leading to GSK3 inactivation. Furthermore, recruitment of Protein Phosphatase 1 (PP1) downstream of PI3K leads to dephosphorylation of the inhibitory phosphate on glycogen synthase and activating phosphate on glycogen phosphorylase, leading to the net outcome of glycogen synthesis[20,23]. The inhibition of gluconeogenesis is mediated through Akt phosphorylation of transcription factor FoxO1. Phosphorylation of FoxO1 sequesters itself in the cytoplasm and decreases expression of two enzymes required for bypass reaction in glucose production: phosphoenolpyruvate carboxykinase (PEPCK) and glucose-6-phosphatase (G6P)[24].

1.2.2 Insulin sensitive organ: Adipose tissues

Adipose tissue is an important organ in mediating insulin sensitivity. Excess energy is converted from glucose and fatty acids into triglycerides. Apart from storing excess energy in the form of fats, adipose tissues garnered attention as an endocrine organ that secretes hormones important in mediating insulin sensitivity and inflammation[25,26]. In adipose tissues, insulin leads to increased glucose and fatty acid uptake and storage (shown in **Figure 1.1**), and decreased breakdown of triglycerides. The net effect is decreased level of circulating plasma free fatty acids (FFA). The increased glucose uptake in adipose tissue is dependent on the insulin responsive glucose transporter, GLUT4, where translocation of GLUT4 to the plasma membrane leads to increased glucose flux into adipocytes[19]. Insulin is known to

stimulate lipogenesis and suppress lipolysis by inhibiting transcriptional activity of SREBP-1c and FoxO1 via protein kinase S6K and Akt, respectively[19,20].

1.2.3 Skeletal muscle

The skeletal muscle accounts for 60 – 70% of insulin stimulated glucose uptake, and thus represents a major glucose sink and regulator of energy balance. In skeletal muscles, the effects of insulin include increase in glucose and free fatty acid uptake (shown in **Figure 1.1**), glycogen synthesis and fatty acid oxidation[19]. The increase in glucose and free fatty acid uptake is achieved by increase in glucose flux via GLUT4 translocation and activation of key enzymes involved in glucose and fatty acid oxidation[19]. Under normal circumstances, insulin does not stimulate lipid storage in skeletal muscles. Under conditions of insulin resistance in T2DM, the skeletal muscle is a primarily affected organ.

1.3 Lipoprotein metabolism

As dyslipidemia is a hallmark of MetS[27], it is imperative to have an understanding of cholesterol and lipoprotein metabolism (**Figure 1.2**). Dietary cholesterol and triglycerides are insoluble in the aqueous environment of the blood plasma; thus they are carried in lipoprotein particles. The liver and adipose tissue are two principal organs involved in the metabolism of lipoproteins. It is well known that excessive low density lipoproteins (LDL) predisposes to high risk of atherosclerosis whereas high density lipoproteins (HDL) lowers it.

Dietary lipids including cholesterol, triglycerides and fatty acids are distributed throughout the body via cholesterol transport pathways as depicted in **Figure 1.2**. From the intestines, dietary lipids enter the circulation in lipoprotein particles of the lowest density called chylomicrons. After much triglyceride (in chylomicrons) are taken up by peripheral tissues,

the liver takes up the remaining contents, known as chylomicron remnants, where free and esterified cholesterol are stored. This is the exogenous pathway of cholesterol transport.

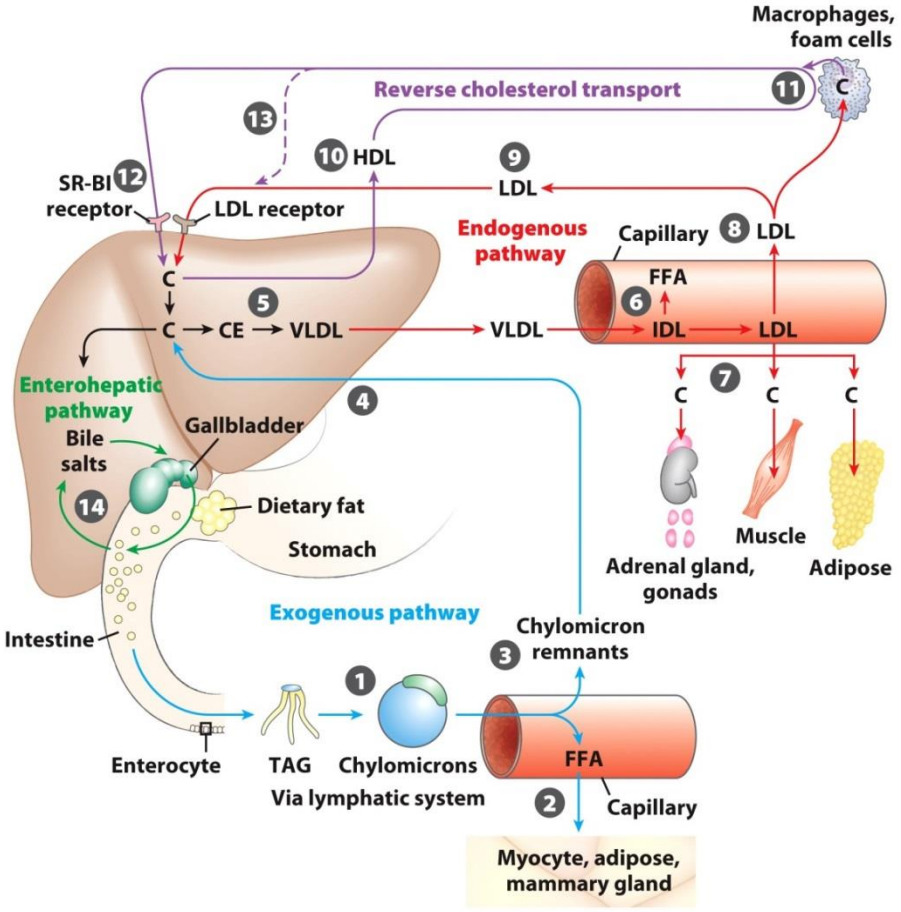


Figure 1.2: Cholesterol transport pathway from the liver and peripheral tissues. Cholesterol and other dietary lipids circulate through the body via enterohepatic pathway involving bile salts and the gallbladder; dietary intake of lipids via exogenous pathway; circulation of vLDL and LDL in the endogenous pathway; and the reverse transport pathway mediated by HDL. (taken from Lehninger Principles of Biochemistry, 6th edition, page 867). *The reader is advised to refer to the main text in the source for details on the pathways and organs denoted by the numbers.* Abbreviations: C: cholesterol; CE: cholesteryl ester; FFA: free fatty acids; HDL: high density lipoproteins; IDL: intermediate density lipoproteins; LDL: low density lipoproteins; vLDL: very low density lipoproteins.

Cholesterol can be distributed in very low density lipoproteins (vLDL) to the peripheral tissues, from the liver. Uptake of triglycerides from vLDL converts them into low density lipoproteins (LDL) that principally contain cholesterol and cholesteryl esters. Cholesterol and

its esters can be taken up by macrophages (which are transformed into foam cells) or taken up by the liver in an endocytic process that involves LDL receptors (LDLr). This is called the endogenous pathway of cholesterol transport.

The reverse cholesterol transport has been reviewed[28]. It is carried out by high density lipoproteins (HDL) originated from the liver. The primary protein component in HDL is ApoA1. HDL is secreted from the liver or intestine as discoidal HDL, also known as pre-β HDL. Discoidal HDL picks up free cholesterol from peripheral cells, including foam cells, and converted into mature HDL particles after esterification of cholesterol. ApoA1 is able to activate lecithin:cholesterol acyltransferase (LCAT) to esterify free cholesterol to cholesteryl esters. The function of LCAT is critical in HDL metabolism[29]. Cholesterol contained in HDL can be transferred to LDL particles via cholesteryl ester transfer protein (CETP) or the liver mediated by hepatic lipase (HL). Cholesterol can be excreted in feces as free cholesterol or bile salts. Increasing evidences pointed that the rate of reverse cholesterol transport does not depend on the overall concentration of HDL but rather on the presence of specific HDL subpopulations, and this is involved in the disease process of diabetes.

Besides the role in reducing cardiovascular risk, HDL is suggested to be beneficial in glycemic control although results are preliminary[30]. ApoE containing LDL and vLDL are able to pick up cholesterol from foam cells to bring cholesterol back into the circulation.

1.4 Insulin resistance

Metabolic syndrome (MetS) has a variety of causes, the major being dietary and minor causes range from genetic, drugs and hormone factors[1]. A hallmark of MetS is insulin resistance, defined as the "*inability of a known quantity of exogenous and endogenous insulin to increase glucose uptake*"[31]. Insulin resistance is characterised by elevated blood glucose despite normal or augmented insulin secretion.

As mentioned earlier, excess energy obtained in the diet is stored as glycogen and triglycerides, in the liver and adipose tissue respectively. In the context of saturated glycogen stores, excess energy is stored as lipids via de novo lipogenesis in the liver, and adipose tissue to a lesser extent[32]. Hepatic and muscular insulin resistance ensues as an adaptive mechanism to protect against lipotoxicity in the organs[33]. Further to that, excess energy is redirected to the adipose tissues.

The increase in lipid store leads to either increase in adipocyte number (hyperplasia) or adipocyte size (hypertrophy). Hypertrophy of adipose tissue leads to necrotic death of adipocytes and secretion of pro-inflammatory cytokines, such as monocyte chemoattractant protein-1 (MCP-1)[34]. Macrophage comprises less than 10% of total cells in healthy adipose tissues, but can rise up to 50% in the inflammatory state[35]. Secretion of proinflammatory cytokines including tumour necrosis factor α (TNFα) and interleukin 6 (IL-6) interferes with insulin signal transduction pathway in adipocytes, leading to adipose insulin resistance. Adipose tissue inflammation is known to be dependent on nuclear factor kappa B (NF-κB) and c-Jun N-terminal kinase (JNK), as suppression of these pathways restores insulin sensitivity[36–38].

The insulin resistant state leads to breakdown of triglycerides (lipolysis) stored in adipose tissues, and release of fatty acids in the circulation. Increased concentration of plasma free

fatty acids leads to ectopic deposition of fats in liver and skeletal muscle, further exacerbating insulin resistance in these organs and their failure to increase glucose uptake in response to insulin. Ectopic fat deposition in the liver occurs through de novo lipogenesis[39], and known as fatty liver or hepatic steatosis. The insulin resistant liver is glycogenolytic and gluconeogenic.

Inflammation and insulin resistance culminates in a vicious positive feedback loop. Over time, insulin resistance in classically insulin sensitive tissues causes elevated blood glucose, a condition known as hyperglycemia[40]. The pancreatic β cells attempt to compensate for insulin resistance by secreting more insulin into the bloodstream (hyperinsulinemia), culminating in the insulin independent stage of T2DM and also inflammation of the islets[40]. Over time, the chronic inflammation leads to decreased functioning β cell mass and subsequently, the insulin dependent stage of diabetes[40].

1.5 Current therapeutic options for diabetes according to drug classes

Diet and lifestyle changes for patients affected with MetS and T2DM are essential steps in patient management. Although diet and lifestyle changes may be as efficacious as medications to maintain normal physiological parameters, many patients struggle with compliance[41]. Furthermore, there is a need for social support for lifetime commitment to altered lifestyle[42,43].

In addition to diet and lifestyle changes, patients are often prescribed medications to manage T2DM. Based on the knowledge of perturbed processes in T2DM, namely reduced insulin secretion, enhanced gluconeogenesis and insulin resistance, several classes of drugs have been developed.

1.5.1 Biguanides

Metformin, a member of biguanides, exerts its antidiabetic effect mainly through interfering with hepatic gluconeogenesis. It acts by transiently inhibiting mitochondrial complex 1 and leads to the accumulation of adenosine monophosphate (AMP). The increased intracellular concentration of AMP leads to activation of AMP activated protein kinase (AMPK) and inhibition of adenylate cyclase. Active AMPK augments insulin signaling by phosphorylation of insulin receptor and IRS-2. On the other hand, inhibition of adenylate cyclase leads to lowered production of cyclic AMP and reduced Protein Kinase A activity. The reduced phosphorylation of phosphofructokinase/fructose-2,6-bisphophatase "bisfunctional enzyme" leads to activation of phosphofructokinase activity and subsequently increased glycolytic flux. Overall, metformin brings about increased hepatic insulin sensitivity and reduced gluconeogenesis[44].

1.5.2 Sulfonylureas and meglitinides

Drugs belonging to the classes of sulfonylureas and meglitinides act by increasing insulin secretion from pancreatic β cells through modulation of ATP sensitive potassium channels on those cells. These drugs lead to closure of ATP sensitive potassium channels on the β cells and insulin release[45], similar to the process described under "Energy Homeostasis". A notable side effect of sulfonylureas is hypoglycemia[46].

1.5.3 Thiazolidinediones

A novel class of anti-diabetic drugs, known as thiazolidinediones (or glitazones) act as insulin sensitisers to make target tissues more responsive to insulin[47]. They will be discussed in detail in the section below, and form the focal point of this study. Generally, they bind to

targets known as peroxisome proliferator activated receptors gamma (PPARγ) to elicit transcriptional cascades in target tissues[48].

1.6 Peroxisome proliferator activated receptors (PPARs)

The peroxisome proliferator activated receptors (PPARs) are a family of evolutionarily related nuclear receptors involved in the regulation of lipid and glucose metabolism in major metabolic organs (**Figure 1.3**).

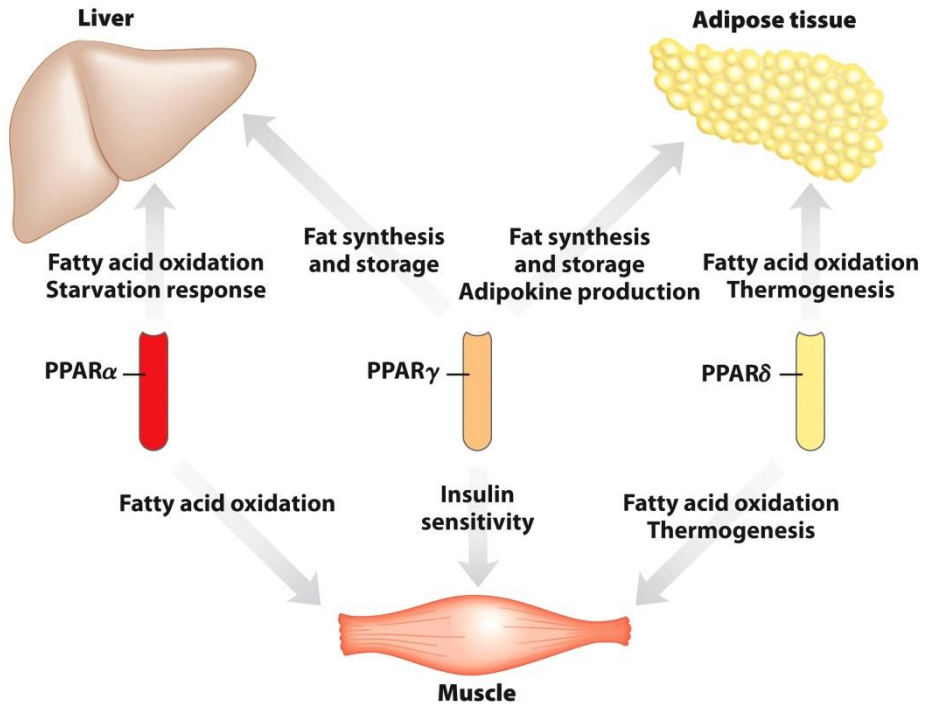


Figure 1.3: Metabolic functions of PPAR isotypes in insulin sensitive tissues, liver, skeletal muscle and adipose tissue. Figure taken from Lehninger Principles of Biochemistry, 6th edition, page 967.

Three isotypes of PPARs have been identified, namely PPARα, PPARβ/δ and PPARγ. All PPAR isotypes are structurally related as revealed in a structural study by Cronet and colleagues in 2001[49] (**Figure 1.4**).

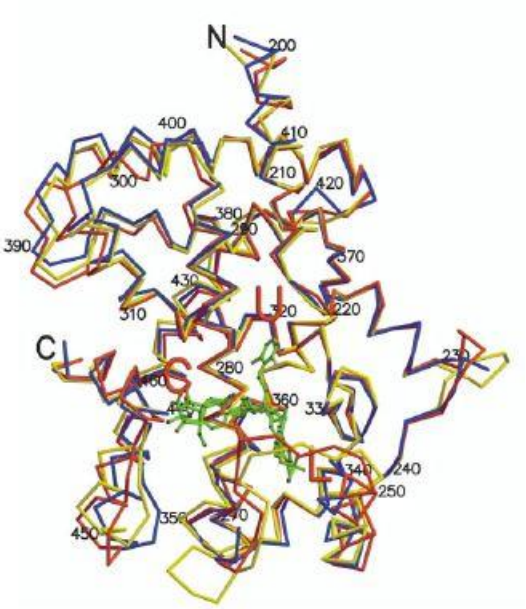


Figure 1.4: Superposition of ligand binding domain (LBD) of human PPAR isotypes, PPARα (red), PPARβ/δ (yellow) and PPARγ (blue). Only the Cα trace is shown. The ligand, AZ 242, is shown in green. Note the structural similarity between PPAR isotypes. Adopted from Cronet et al., 2001[49].

As nuclear receptors, PPARs contain domains common to members of the superfamily[50,51]. The domains of PPARs, from N to C-terminal, are the autonomous activation function (AF1) domain; the DNA binding domain; the hinge domain; and the ligand binding domain (LBD) that encompasses the ligand dependent activation function domain (AF2). The AF1 and LBD domains are particularly important, where the former interacts with transcriptional co-activator proteins and LBD contains the ligand binding pocket[51].

For the purpose of this study, only PPARα and PPARγ will be considered. Ligand bound PPARs form obligate heterodimers with the retinoid X receptor (RXR) and binds to PPAR response element (PPARE) to promote transcription or repression of target genes (illustrated in **Figure 1.5**). Activation of either receptor is sufficient to promote transcription of PPAR responsive genes. Presence of ligands for both receptors showed synergistic response[52].

The ligand binding pocket of PPARα and PPARγ is a large T shaped cavity[49,53]. The large binding pocket in comparison to other nuclear receptors may explain their ability to bind to a wide variety of ligands[54–57], ranging from physiological, pharmacological, nutritional, natural product and xenobiotic ligands. Although ligands belonging to the same drug family may

activate a common PPAR isotype, distinct ligand-receptor complexes have unique conformations that give rise to unique transcriptional profiles and biological response, as evidenced by comparative studies between rosiglitazone, pioglitazone and troglitazone binding[58,59]. A detailed structural study of PPARγ confirmed that distinct ligands vary in their occupancy of the binding pocket, giving minor structural variation of the activated receptor[60].

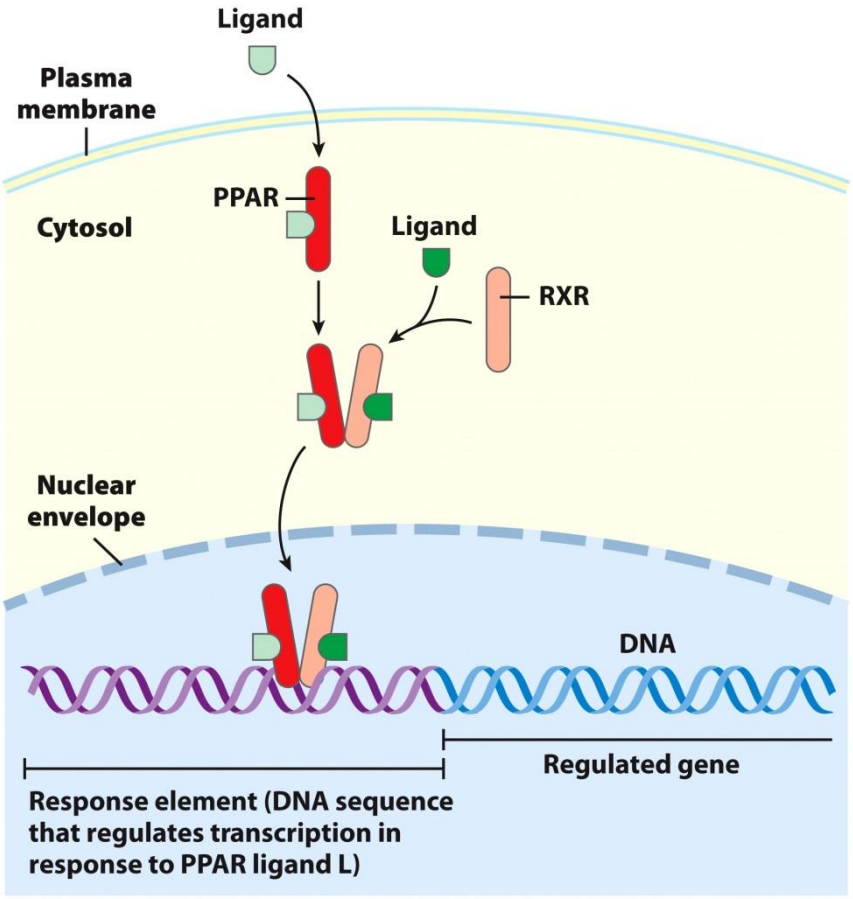


Figure 1.5: Mechanism of activation of PPAR. Figure taken from Lehninger Principles of Biochemistry 6th edition, page 966.

PPARγ is primarily expressed in adipogenic tissues. Alternative splicing of the PPARγ mRNA give rise to two isoforms, PPARγ1 and PPARγ2. Expression of PPARγ1 is ubiquitous, while PPARγ2 is highly expressed in adipocytes[61]. PPARγ is required for the differentiation of preadipocytes into mature adipocytes[62,63] and the maintenance of mature adipocytes[64,65]. It is the receptor for thiazolidinediones, commonly referred as glitazones, which are administered as anti-diabetics. Expression of PPARγ in the adipose tissue[64,66], liver[67] and

skeletal muscle[68,69] has been shown to be important in mediating insulin sensitivity and the efficacy of glitazones.

PPARα is primarily distributed in metabolically active tissues, namely liver and skeletal muscle. It is the receptor for a class of hypolipidemic drugs named fibrates. Physiologically, PPARα is activated in response to fasting and is required for ketogenesis[54,70]. Activation of PPARα promotes fatty acid uptake and utilization, hence explaining the hypolipidemic effect of its ligands[54]. Additional benefits of PPARα activation include the upregulation of circulating HDL in humans[70,71] and improvement of insulin sensitivity[72–74]. It must be noted that several species specific differences in PPARα biology have been documented, especially between humans and rodents. Most notably, human express 90% less PPARα compared to rodents and PPARα induction leads to liver enlargement and hepatocyte proliferation in rodents, but not in humans[75]. Hence, these differences must be taken into account when interpreting the PPARα literature.

1.7 Rosiglitazone

Rosiglitazone is a member of the thiazolidinedione (glitazone) family of drugs used as anti-diabetics. As a specific agonist of PPARγ[76], rosiglitazone improves insulin sensitivity by promoting adipogenesis and hyperplastic expansion of adipose tissue.

Despite strong potency and efficacy, long term administration of rosiglitazone led to increase in heart attacks, according to meta-analyses conducted by Nissen and Wolski[77,78]. Transcriptional profiling of the heart treated with rosiglitazone suggested dysregulation of electrophysiology and atherosclerotic plague rupture as causes for cardiovascular complications[79].

Marketing of rosiglitazone changed frequently due to conflicting reports on its side effects. Major concerns of cardiovascular safety have led to withdrawal of rosiglitazone in UK, India, New Zealand and South Africa. The US Food and Drug Administration imposed sale restriction from November 2011 to November 2013. Currently, rosiglitazone remains freely available in the US after marketing restrictions were lifted[80].

Besides cardiovascular concerns, numerous side effects were documented among members of glitazones, including congestive heart failure, weight gain, fluid retention, bone fractures and oedema[81]. Rosiglitazone was also found to increase plasma triglycerides and LDL[58,82]. The improvement of insulin sensitivity by rosiglitazone is mainly exerted through adipose tissues, due to high level of PPARγ expression, coupled with full agonism of PPARγ. It came to no surprise that rosiglitazone has been classified as an obesogen since it promotes weight gain by expanding the fat store[83].

Despite the availability of several classes of drugs to manage T2DM, many problems remain with pharmacotherapy. Severity of problems is proportional to the number of concomitant medications[84,85]. It was found that concomitant drugs actually led to poor glycemic control and as many as one fourth of patients with diabetes presented contraindications for their medication[84]. The prime reason for change of medication was insufficient glycemic control or adverse effects[85].

The limitations of lifestyle change and medication warrants the consideration of nutritional intervention to prevent the onset of T2DM. Otherwise, nutritional intervention can supplement regimens of lifestyle change and medication. Conjugated linoleic acid (CLA) can potentially serve as a safe substitute. Interestingly, CLA was found to share molecular targets with hypolipidemic and insulin sensitising drugs.

1.8 Conjugated linoleic acid

Conjugated linoleic acids (CLA) refer to positional and geometric isomers of linoleic acids (C18:2) containing conjugated double bonds (**Figure 1.6**). There are 28 possible isomers of conjugated linoleic acids[86], of which the *cis*-9, *trans*-11 isomer is the most abundant in nature and accounts for 90% of dietary CLA[87–90]. The *trans*-7, *cis*-9 (t7,c9) is the second most abundant naturally occurring isomer[89,91] typically constitutes 8-13% of total CLA. There has not been much interest in the t7,c9 isomer due to difficulty obtaining it in sufficient quantity.

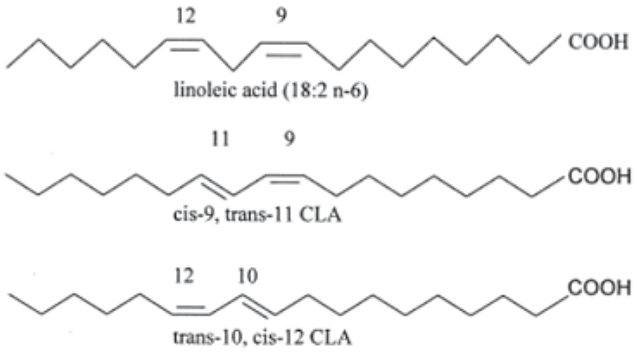


Figure 1.6: Chemical structure of conjugated linoleic acid. Linoleic acid (C18:2) is included for comparison. Figure taken from Evans et al., 2002.

Dietary intake of total conjugated linoleic acid is estimated to be 150 – 200 mg daily and c9,t11-CLA, 140 – 190 mg per day[92]. The health benefits of CLA were discovered accidently and quite unexpectedly when Michael Pariza and colleagues were investigating cancer causing properties of grilled beef[90]. To their surprise, fatty acids in grilled beef actually inhibited carcinogenesis. An explosion of interest in CLA soon followed to characterise the health benefits of CLA. To date, several reviews have been dedicated to highlighting the health benefits of conjugated linoleic acids in obesity, diabetes, cancer, atherosclerosis and immunity[89,90,93].

Natural sources of CLA can be found in meat and butter derived from grass fed ruminants which the c9,t11 isomer is the most abundant[94]. In ruminants, the highest concentration of total CLA has been found in lamb, followed by beef, noting that most studies considered the c9,t11 isomer only[95]. CLA is also present at low levels in meat of monogastric animals[95]. The level of CLA is strongly influenced by diet which such a case has been shown for cow milk[96]. CLA can be biosynthesised by microorganisms in rumen, but the bulk of CLA found in meat actually derived from endogeneous Δ9-desaturation of *trans*-vaccenic acid to c9,t11-CLA. The availability of *trans*-vaccenic acid, the precursor of CLA, comes from biohydrogenation by rumen microorganisms[95].

CLA can be prepared commercially by heating linoleic acid or sunflower and safflower oils under alkaline conditions. This preparation often results in roughly 1:1 ratio of c9,t11 and t10,c12 isomers, with the minor presence of other CLA isomers and other fatty acids[87,89,94]. Many studies of CLA actually consider a mixture of c9,t11 and t10,c12 isomers due to its widespread commercial availability whereas pure isomers are rarely considered due to high cost and scarcity[86,89]. It is known that both c9,t11 and t10,c12 isomers possess biological activity.

The biological effect of CLA is isomer dependent[88,97]. In most studies involving animals, c9,t11 isomer is associated with beneficial effects in ameliorating diabetic complications such as decreasing white adipose inflammation[98], reducing hepatic steatosis[99] and raising plasma HDL[100]. On the other hand, t10,c12-CLA is associated with detrimental effects namely insulin resistance[101,102], white adipose inflammation[103], hepatic steatosis[101,104–106] and lipoatrophy[101,106,107]. A study to profile blood lipids in healthy volunteers showed that t10, c12-CLA increases plasma LDL[108].

Both c9,t11 and t10,c12-CLA were reported to be ligand for all PPAR isotypes and binds at lower affinity compared to the respective pharmacological activators[109–111]. Both isomers of CLA have been found to modulate adipocyte differentiation and fat accumulation through the adipogenic nuclear receptor-transcription factor PPARγ. The c9,t11 isomer is pro-adipogenic[112,113] and t10,c12 isomer, anti-adipogenic[112,114]. The number of functional studies detailing CLA activation of PPARα activation is rather scarce[115,116].

1.9 Rationale and hypothesis

Based on current knowledge of insulin sensitisers, activation of PPARα and PPARγ remained a viable strategy to manage MetS and associated complications. The therapeutic effort using current pharmacological intervention was hampered by non-negligible side effects. Therefore, partial agonists of PPARs might be more appropriate. As CLA has been known to be partial agonists of PPARα and PPARγ, therapeutic goal could be achieved by activating the predominant isotype in respective insulin sensitive tissues, PPARα in the liver and PPARγ in the adipose by using the same substance, while ameliorating many of the side effects. There has been conflicting results regarding CLA benefits and adverse reactions in the literature; hence any isomer specific effect must be taken into account so as to clarify contradictions.

It has been proposed that CLA may be able to increase plasma HDL level through hepatic PPARα activation. Both improvement of blood lipid profile, coupled with the known fact that CLA modulates adipogenesis through PPARγ, would be beneficial for diabetic patients.

The specific hypotheses of this study were:

- Specific CLA isomers might act as dual agonists for PPARα/γ and regulate downstream signaling/metabolic pathways that are identical or distinct from known pharmacological ligands of PPAR receptors

- CLA supplementation could be safely combined with thiazolidinedione, which are full agonists of PPARγ. The former was able to reduce or reverse adverse effects posed by the latter (such as elevated LDL) by binding competitively with the full agonists. It was hypothesised that this combination would lead to an improved lipid profile compared to singular administration of thiazolidinediones

Aims and Objectives

The aim of this study was to examine whether or not CLA is a safe substitute or supplement for conventional insulin sensitisers that act on PPARγ. Two approaches would be utilised to achieve the aim of the study, namely by observing gluconeogenesis *in vitro* and physiological parameters of the blood using genetically modified mice *in vivo*.

The specific objectives of my research project were:

- To examine the effect of CLA isomers on hepatic (HepG2 & H4IIE) gluconeogenesis *in vitro,* and its dynamics with rosiglitazone. Both glucose production and expression of gluconeogenic genes would be examined
- To determine the effect of CLA isomers on the basal expression of PPAR isotypes in hepatic cells, particularly HepG2
- To investigate the effect of CLA in a 1:1 isomer mixture, either alone or with rosiglitazone, on glucose and lipid metabolism in ApoE null mice on C57BL/6 background compared with wild type mice fed normal diet

CHAPTER 2

Materials and Methods

2.1 *In vitro* studies

2.1.1 List of materials

No.	Material/Chemical/Reagent	Source	Catalogue no.	Remark
1	1.5 mL microcentrifuge tube	Goodware	MCT1500	
2	Cryovial	SPL Life Sciences	SPL#43022	
3	HepG2 cell line	American Type Culture Collection	ATCC® HB 8065™	
4	H4IIE	American Type Culture Collection	ATCC®CRL1548 ™	
5	α-MEM with L-glycine, without nucleosides	Nacalai Tesque	21445-95	
6	DMEM high glucose with sodium pyruvate and glycine	Nacalai Tesque	08458-45	
7	DMEM no glucose	Nacalai Tesque	09891-25	
8	DMEM no glucose no glutamine no phenol red	Invitrogen	A14430-01	
9	Fetal bovine serum	Sigma-Aldrich	SIG#F7524	
10	Penicillin-Streptomycin	Nacalai Tesque	#26253-84	
11	Conical tubes 15 mL	SPL Life Sciences Accumax	SPL#50015 ACT-15-B	
12	Conical tubes 50 mL	SPL Life Sciences	SPL#50050	
13	Cell culture flask T-25	SPL Life Sciences	SPL#70025	Surface treatment and sterile packaging
14	Cell culture flask T-75	SPL Life Sciences	SPL#70075	Surface treatment and sterile packaging
15	96-well plate, tissue culture treated	SPL Life Sciences	SPL#30096	
16	Serological pipette	SPL Life Sciences	SPL#91010	

17	Phosphate buffered saline	Self-prepared		Prepared as a 10x concentrate and diluted to the working concentration with distilled water.
18	Trypsin-EDTA	Nacalai Tesque	#35554-64	2.5g/l-Trypsin and 1mmol/l-EDTA
19	Ethanol	RCI Labscan	AR1069	
20	Dimetyl sulfoxide normal grade	Nacalai Tesque	13407-45	
21	Dimetyl sulfoxide biotechnology grade	Nacalai Tesque	09659-14	
22	MTT	Nacalai Tesque	23547-21	
23	Dexamethasone from plant	Nacalai Tesque	11107-51	
24	*cis*-9, *trans*-11-CLA	Cayman Chemicals	90145-50	Purity ≥98%
25	*trans*-10, *cis*-12-CLA	Cayman Chemicals	90140-50	Purity ≥98%
26	Rosiglitazone	Cayman Chemicals	71740-10	Purity ≥98%
27	Forkskolin	Tocris Bioscience	GZ-1099	
28	GW 6471	Tocris Bioscience	GZ-4618	
29	GW 9662	Tocris Bioscience	GZ-1508	
30	Fenofibrate	Tocris Bioscience	GZ-4113	
31	Amplex Red Glucose Assay	Molecular Probes	A22189	
32	Qiagen RNeasy Mini Kit	Qiagen Biotechnologies	74104	
33	Bioline Tetro cDNA synthesis kit	Bioline	BLN#BIO-65042	
34	0.2 ml PCR strip tubes	Axygen	PCR-0208-C	
35	0.2 ml PCR strip caps	Axygen	PCR-2CP-RT-C	
36	KAPA SYBR Fast qPCR Master Mix, 2x	KAPA Biosystems	KAPA-KK4600	
37	Eco 48 Real Time PCR plate	Illumina	ECOPLATE	
38	Eco 48 Real Time PCR Seal	Illumina	ECOSEAL	
39	DEPC-treated water	1st BASE	BUF-1170-200ml	
40	Isopropyl alchohol, biotechnology grade	Inspiro Technologies	0918-500ml	

2.1.2 Cell culture and treatments

Hepatic carcinoma cell lines from human, HepG2 (HB 8065™, American Type Culture Collection; ATCC®, USA) and rat, H4IIE (CRL1548™, ATCC®, USA) were cultured in α-MEM (21445-95, Nacalai Tesque, Japan) supplemented with 10% fetal bovine serum (SIG#F7524, Sigma-Aldrich, USA) and 100 U/ml Penicillin-Streptomycin (#26253-84, Nacalai Tesque, Japan). The cells were grown in a 75ml flask (SPL#70075, SPL Life Sciences, South Korea), maintained in the incubator at 37°C, 5% CO_2. The growth media were refreshed every 2 - 3 days. Upon reaching 80-90% confluence, the cells were passaged. Used culture medium was discarded. Cultured cells were washed with 2 ml of phosphate buffer saline (PBS) to remove dead cells and serum. The cells were then incubated for 5-10 minutes with 2 ml of 0.5% Trypsin-EDTA (#35554-64, Nacalai Tesque, Japan). Following this, 8ml media was added and centrifuged at 3000rpm for 5 min at room temperature. The harvested cells were then rinsed with PBS and homogenized with growth media. The cells were counted in haemocytometer before sub-culturing or seeding experimental plates. Cells were re-seeded in culture flasks at ratios between 1:6 and 1:4. All experiments were carried out within 5-15 passages unless otherwise mentioned.

2.1.3 Cell viability assay

Using tissue culture treated 96-well plates (SPL#30096, SPL Life Sciences, South Korea), HepG2 and H4IIE were seeded at 1×10^4 cells per well and left to incubate for 24 hours at 37°C and 5% CO_2. After that, the incubated cells were washed twice and serum starved for 4 hours in the incubator. Cells were exposed to concentrations of c9, t11- and t10, c12-CLA at 0, 5, 15, 20, 30, 50, 70, 100 µM concentrations in serum free media for 24 hours. Cell viability was determined using the MTT assay[117]. 5 mg/mL of MTT (23547-21, Nacalai Tesque, Japan) dissolved in PBS was used, in which cells were incubated for 4 hours. At the

end of the assay, MTT solution was removed and the insoluble formazan was dissolved in normal grade DMSO (13407-45, Nacalai Tesque, Japan). Absorbance reading was taken at a wavelength of 560 nm on a spectrophotometer.

2.1.4 *In vitro* glucose production assay

The glucose production assay was based on a published protocol[118]. Briefly, the cells were seeded at 2.8×10^5 per well for HepG2 and 2.0×10^5 per well for H4IIE, in a 12-well plate and incubated for 48 hours. Cells were washed twice with PBS and serum starved with serum free α-MEM for 8 hours, then glucose starved with glucose free Dulbecco's modified Eagle's medium (DMEM; 09891-25, Nacalai Tesque, Japan) for 1 hour. The cells were then incubated in 500 µL glucose production medium, consisting of glucose and phenol red free Dulbecco's modified Eagle's medium (A14430-02, Invitrogen, USA) with 20 mM sodium lactate , 2 mM sodium pyruvate (#06977-34, Nacalai Tesque, Japan), 2 mM L-glutamine (#16948-04, Nacalai Tesque, Japan) and 15 mM HEPES (#17557-94, Nacalai Tesque, Japan) for 24 hours. Treatments were added to their final concentrations in the glucose production media and incubated for 24 hours. The final concentration for fatty acids (c9,t11-CLA, t10,c12-CLA and linoleic acid) were 20 µM and other chemicals (rosiglitazone, fenofibrate, GW9662) were 10 µM.

A 50 µL of the glucose production media were assayed with the Amplex Red Glucose/Glucose Oxidase Assay Kit (A22189, Molecular Probes, USA). Glucose concentration in the glucose production media was tabulated in µM. Cells remaining in each plate well were lysed with NP-40[119]. 5 µL of lysates were used to obtain respective protein concentration using the Bradford assay in 96-well plate format[120]. The glucose concentration obtained from each well was normalized with respective protein concentration and presented as µM glucose per µg protein.

2.1.5 RT-qPCR

Primers were synthesised by Integrated DNA Technologies, Singapore. Their sequences are presented in Table 2.1:

Table 2.1: Sequences of primers used for RT-qPCR of HepG2 cells.

Gene of interest	Forward sequence	Reverse sequence	Source
Human PPARg	5'-CGTGGCCGCAGATTTGAA-3'	5'-CTTCCATTACGGAGAGATCCAC-3'	Tachibana, K et. al. (2005)[121]
Human PEPCK	5'-AAGAGACACAGTGCCCATCC-3'	5'-ACGTAGGGTGAATCCGTCAG-3'	Kim, H et. al. (2011)[122]
Human G6P	5'-GAGACTGGCTCAACCTCGTC-3'	5'-CCTGGTCCAGTCTCACAGGT-3'	Kim, H et. al. (2011)[122]
36B4	5'-CCGTGATGCCCAG-3'GGAAGACAG	5'-TTAGTCGAAGAGAC-3'CGAATCCC	Akamine, R et. al. (2007)[123]

The treatment steps for RT-qPCR were identical to those of *in vitro* glucose production assay, except that assay was done in 1 mL of glucose production media in a 6 well plate as adopted[124]. At the end of the treatment, RNA was extracted with Qiagen RNeasy Mini Kit (74104, Qiagen GmbH, Germany), in which 350 µL of Buffer RLT was used for each well. Quality of extracted RNA was measured using a Nanodrop instrument. Subsequent steps were performed according to manufacturer's recommendations. cDNA was synthesised with the Bioline Tetro cDNA Synthesis Kit (BLN#BIO-65042, Bioline, UK) according to

manufacturer's instructions. Quality of cDNA was checked with a Nanodrop instrument. Quantitative PCR was performed with KAPA SYBR Fast qPCR Master Mix (KAPA-KK4600, KAPA Biosystems, USA) using Illumina Eco Real Time PCR System (EC101-1001, Illumina, USA) according to manufacturer's protocol. Gluconeogenesis genes, phosphoenolpyruvate carboxykinase (PEPCK) and glucose-6-phosphatase (G6P) were tested. Target gene expression was normalized against the acidic ribosomal phosphoprotein P0, also known as 36B4[125]. Result were analyzed by the comparative threshold cycle method[126].

2.1.6 Statistical analysis

All data were processed with Prism 7 (GraphPad Software, USA) and presented as mean ± SEM. Statistical significance between groups was determined using one-way ANOVA followed by Tukey's post-hoc tests. Cell viability data was tabulated as percentage viability to look for IC_{50}. For RT-qPCR data, a fold change of more than 2 accompanied by $p < 0.05$ is considered significant.

2.2 *In vivo* studies

2.2.1 List of materials

No.	Material/Chemical/Reagent	Source	Catalogue no.	Remarks
1	Wild type mice	Taconic		C57BL/6J background
2	ApoE null mice	Taconic		C57BL/6J background. Strain generated by Nobuyo Maeda.
3	Normal diet	Altromin	#1324	
4	Western diet	Research Diets	D12079B	Cholesterol content 0.15% w/w
5	Fat free milk	Self-prepared		Prepared as 5% w/v with sterile autoclaved water
6	Steel gavage			
7	1:1 conjugated linoleic acid	Nu-Chek-Prep	UC-59-AX	95% purity. Prepared as 0.015g/mL in 5%

				fat free milk
8	Rosiglitazone	Tokyo Chemicals	R0106-1g	Purity ≥98%. Dissolved in dimethyl sulfoxide at 0.6 mg/mL. Prior to injection into mice, diluted 1:10 in phosphate buffered saline.
9	Accu Chek Performa test strips	Roche		
10	Tissue Tek O.C.T. Compound	Sakura Finetek	4583	
11	Insulin ELISA kit	Merck	EZRMI-13K	
12	Leptin ELISA kit	Merck	EZMADP-60K	
13	Adiponectin ELISA kit	Merck	EZML-82K	
14	HDL and LDL Quantitation kit	BioVision	K613-100	
15	Free Fatty Acid Quantitation Kit	BioVision	K612-100	
16	Triglyceride Quantitation Kit	BioVision	K622-100	

2.2.2 Background of Apolipoprotein E null mice

Apolipoprotein E (ApoE) null mice are also known as ApoE knockout mice. Three strains of ApoE null mice are currently available, one generated by Jan Breslow[127] and another by Nobuyo Maeda[128] and another by Loius Havakes[129]. The ApoE null strain utilised in this study originated from the Maeda Laboratory.

ApoE null mice are leaner than wild type mice due to their less efficient incorporation of lipids into their subcutaneous tissue and retention in the bloodstream when fed normal diet[130].

ApoE null mice become severely hypercholesterolemic irrespective of being fed normal chow or high fat diets[127,131,132]. Their total plasma cholesterol can be five to six times of wild type mice. Compared with wild type mice, ApoE null mice have higher level of vLDL, IDL and triglycerides and decreased HDL[127,131].

ApoE null mice develop atherosclerotic lesions as early as 8 weeks of age when fed Western diet and 10 weeks of age when fed chow diet, and develop lesions of all stages throughout the arterial tree[132]. A study conducted by Maeda group also reached similar conclusions[133]. When

fed Western type diet for seven weeks, ApoE null mice develop severe non-alchoholic hepatosteatitis, whereas wild type mice do not develop the condition on a Western diet[134].

2.2.3 Animal care and treatment

Animal work was conducted at Satellite Animal Facility, Department of Pharmacology at University of Malaya under Institutional Animal Care and Use Committee approval number #2015-180908/PHAR/R/DDM. A total of 10 wild type and 45 ApoE null mice on a C57BL6/J background (Taconic Biosciences, USA) were purchased. All mice were eight-week old and acclimatized for one week.

At Week 1, mice were allocated into groups of five per cage. Wild type mice were designated WT. ApoE null mice were allocated into groups of ApoE, WD and ApoE, WD+CLA(e). After Week 12, mice were placed in groups of three to four per cage. The ApoE, WD group was further divided into ApoE, WD; ApoE, WD+CLA(l) and ApoE, WD+Rosi. ApoE, WD+CLA(e) was further divided into ApoE, WD+CLA(e) and ApoE, WD+CLA(e)+Rosi. The study design is illustrated in a schematic in Figure 2.1.

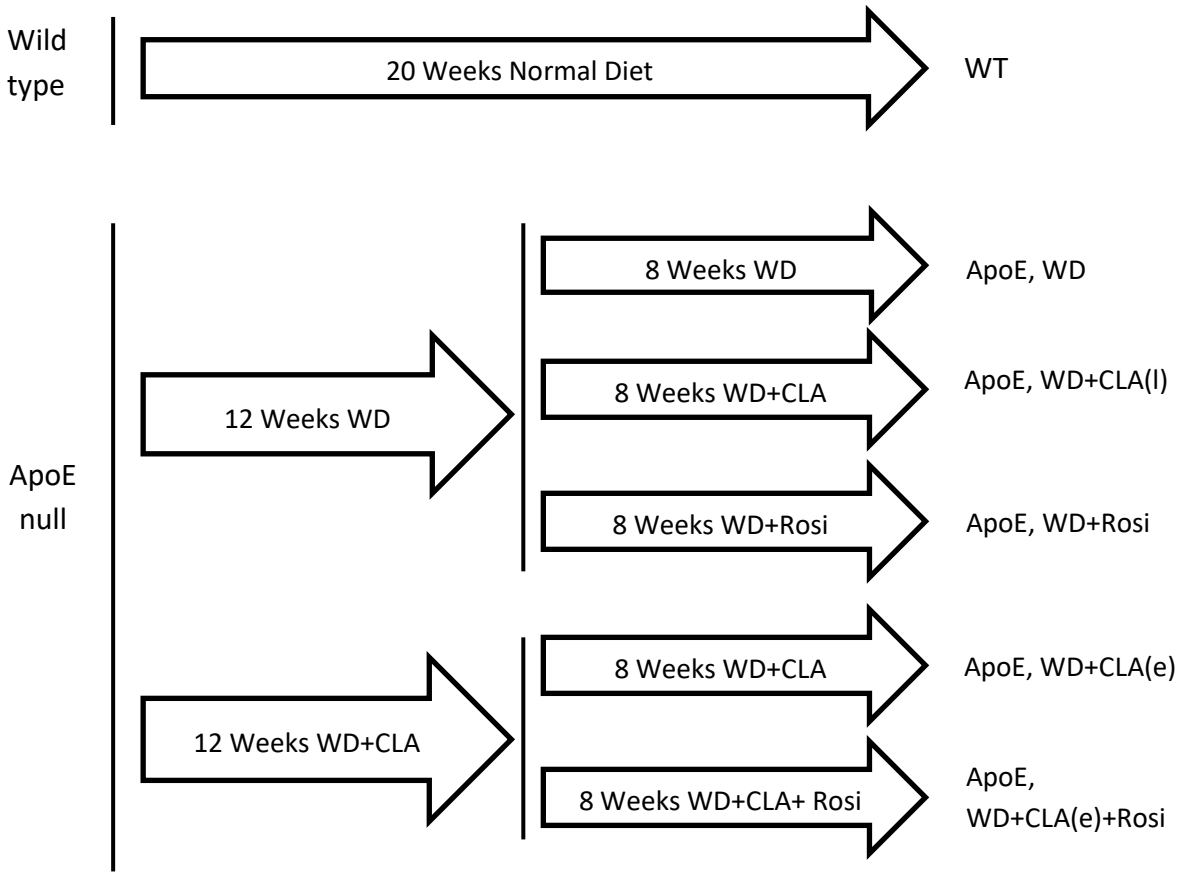


Figure 2.1: Schematic overview of the study design for *in vivo* study. Wild type and ApoE null mice were divided into treatment groups at Week 1 for 12 Weeks, and further divided to receive additional treatments for another 8 8 Weeeks.

Throughout the study, body weight and food intake were monitored on a weekly basis. Blood glucose was measured with Accu-Chek Performa strips and glucose meter (Roche, Switzerland).

2.2.4 Induction of obesity with Western Diet

Wild type mice were fed normal diet containing 3386 kcal/kg consisting of 15% fat and 61% by carbohydrate in terms of calorie content (#1324, Altromin, Germany). ApoE null mice were fed Western diet containing 4679 kcal/kg consisting of 41% calorie by fat and 43% by carbohydrate (D12079B, Research Diets, USA) from Week 1. CLA stock (UC-59-AX, Nu-

Chek-Prep, USA) was a 1:1 mixture of isomers, prepared as a 0.1% w/v mixture in 5% fat free milk, and administered to CLA early treatment group (ApoE, WD+CLA(e)) and CLA early treatment with rosiglitazone (ApoE, WD+CLA(e)+Rosi) from the Week 1 by oral gavage. Each mouse receives 200 µL in oral gavage, which turns out to be 3 mg CLA per mouse per day.

2.2.5 Treatment of obesity from Week 12 with CLA and rosiglitazone

Starting from Week 12, 0.6 mg/kg rosiglitazone (R0106-1g, Tokyo Chemicals, Japan) was administered by intraperitoneal injection for ApoE, WD+Rosi and ApoE, WD+CLA(e)+Rosi groups. CLA-milk mixture was administered to the CLA late treatment group [ApoE, WD+CLA(l)].

2.2.6 Oral glucose tolerance test

Oral glucose tolerance test was performed at Week 19. A 100 mg/mL glucose solution was administered to each mouse at dosage of 2 g/kg body weight. Glucose reading was taken at intervals of 30 minutes, up to 120 minutes.

2.2.6 Termination of animal study

Two mice were sacrificed from WT, ApoE, WD and ApoE, WD+CLA(e) at Week 12. At the conclusion of the study at Week 20, all mice were sacrificed by CO_2 asphyxiation. Blood samples were collected by intercardiac puncture and processed into serum. Livers were extracted, weighed and divided into three lobes, 1 lobe frozen in O.C.T. compound (4583, Sakura Finetek), 1 lobe frozen in liquid nitrogen and another kept in formalin. Epididymal fat, perirenal fat, mesenteric fat, kidney, spleen and pancreas were weighed and frozen in liquid nitrogen.

2.2.7 Serum insulin, leptin and adiponectin

Respective hormone levels were assayed with ELISA kits for insulin (EZRMI-13K, Merck, Germany), leptin (EZMADP-60K, Merck, Germany) and adiponectin (EZML-82K, Merck, Germany). Assays were performed using manufacturer's recommendations.

2.2.8 Serum lipid levels

Assays for total cholesterol, LDL and HDL were performed with HDL and LDL quantitation kit (K613-100, BioVision, USA). Free fatty acid (FFA) was assayed with Free Fatty Acid Quantitation Kit (K612-100, BioVision, USA) and total triglyceride with Triglyceride Quantitation Kit (K622-100, BioVision, USA). Assays were performed according to manufacturer's recommendations.

2.2.9 Statistical analysis

All data were processed with Prism 7 (GraphPad Software, USA) and presented as mean ± SEM. Statistical significance between groups was determined using one-way ANOVA followed by Tukey's post-hoc tests. For body weight data, statistical significance was determined using two-way ANOVA followed by Tukey's post-hoc tests.

To assess insulin resistance, homeostatic model assessment of insulin resistance (HOMA-IR) was calculated using blood glucose in mg/dL and insulin concentration in mU/L divided by 405 as described previously[135]. Quantitative insulin sensitivity check index (QUICKI) was calculated by adding the logarithms of blood glucose in mg/dL and insulin in mU/L, and taking the reciprocal of the sum of logarithms[136]. Revised QUICKI (QUICKI-FFA) was calculated by adding the respective logarithms of blood glucose in mg/dL, insulin in mU/L and FFA in nmol/μL and taking the reciprocal of the sum of logarithms, as described previously[137].

CHAPTER 3

Results

3.1 Cell viability assay

A cell viability assay on HepG2 and H4IIE was conducted to assess cytotoxic effects of CLA on cells as well as to determine a suitable concentration for subsequent experiments. HepG2 and H4IIE cells were treated with increasing concentrations of c9,t11-CLA and t10,c12-CLA in serum free media. Generally, cell viability decreased with increasing concentrations of CLA. In HepG2, the IC_{50} was 37±3.2 μM for c9,t11-CLA and 50±5.1 μM for t10,c12-CLA (Figure 3.1). For H4IIE, the IC_{50} was 76.6±3.0 μM for c9,t11-CLA and 71±3.3 μM for t10,c12-CLA (Figure 3.2). Based on the cell viability assay, 20 μM was chosen for both CLA isomers in subsequent assays, as this concentration showed efficacy without compromising cell viability.

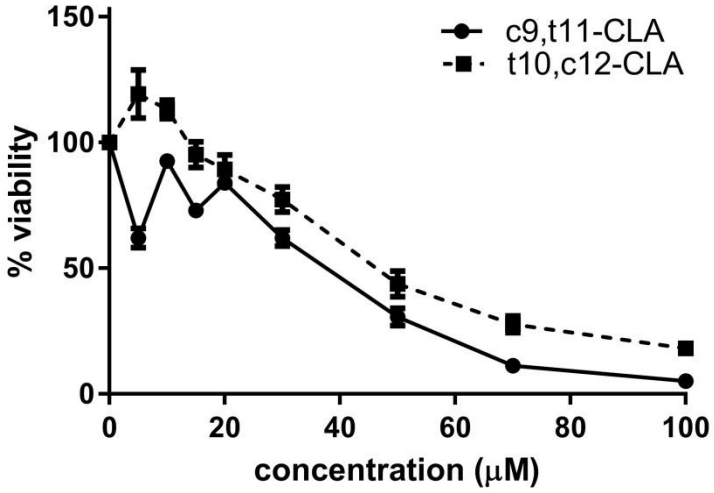


Figure 3.1: Cell viability of HepG2 treated with various concentrations of c9,t11- and t10,c12-CLA.

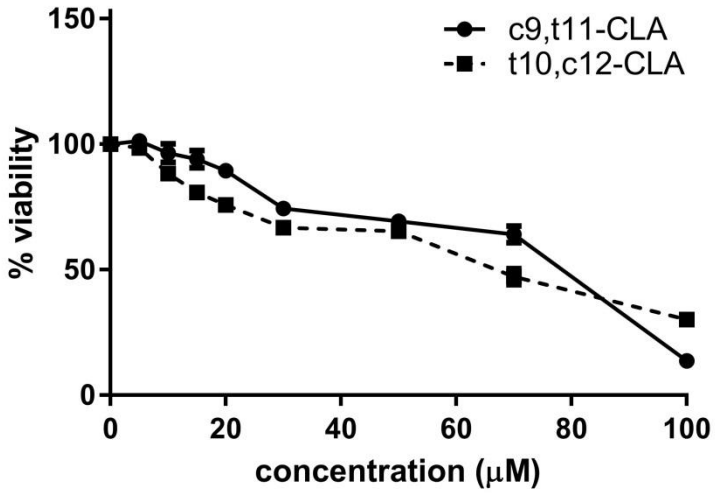


Figure 3.2: Cell viability of H4IIE treated with various concentrations of c9,t11- and t10,c12-CLA.

3.2 Effect of isomers of CLA on hepatic glucose production

The study proceeded to test the effect of c9,t11 and t10,c12-CLA in directly inhibiting glucose production in vitro using hepatoma cells, HepG2 and H4IIE. As insulin has been well demonstrated to suppress gluconeogenesis[138], 100nM of insulin was used as a positive control in all experiments. Also, 20 μM linoleic acid (C18:2n-6) was tested in parallel with CLA isomers to elucidate any molecular structure or isomer-specific effects.

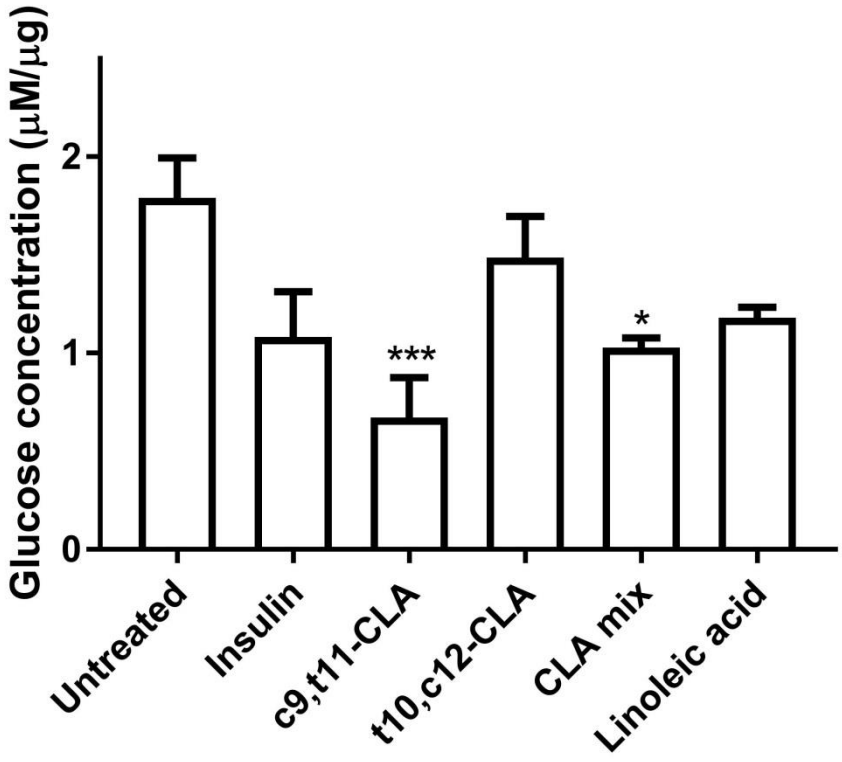


Figure 3.3: Glucose production of HepG2 when treated with fatty acids. Concentrations of the treatments were insulin 100 nM; c9,t11-CLA 20 µM; t10,c12-CLA 20 µM; CLA mix consisted of c9,t11 10 µM and t10,c12 10 µM; linoleic acid 20 µM. * $p < 0.05$ vs. Untreated, *** $p < 0.005$ vs. Untreated.

As shown in Figure 3.3, the HepG2 cells exposed to 100 nM insulin for 24 hours had 40% reduced glucose production compared to untreated control ($p > 0.05$%). Administration of 20 µM of c9,t11-CLA decreased glucose production by 62.5% compared to untreated cells ($p < 0.001$). Conversely, the exposure of HepG2 cells with 20 µM of t10,c12-CLA rendered no change in glucose production ($p > 0.05$%). Of note, administering both CLA isomers (10 µM of c9t11-CLA and 10 µM of t10c12-CLA) or 20 µM linoleic acid reduced the glucose production by 42.6% ($p < 0.05$) and 34.2% ($p > 0.05$%) compared to untreated control.

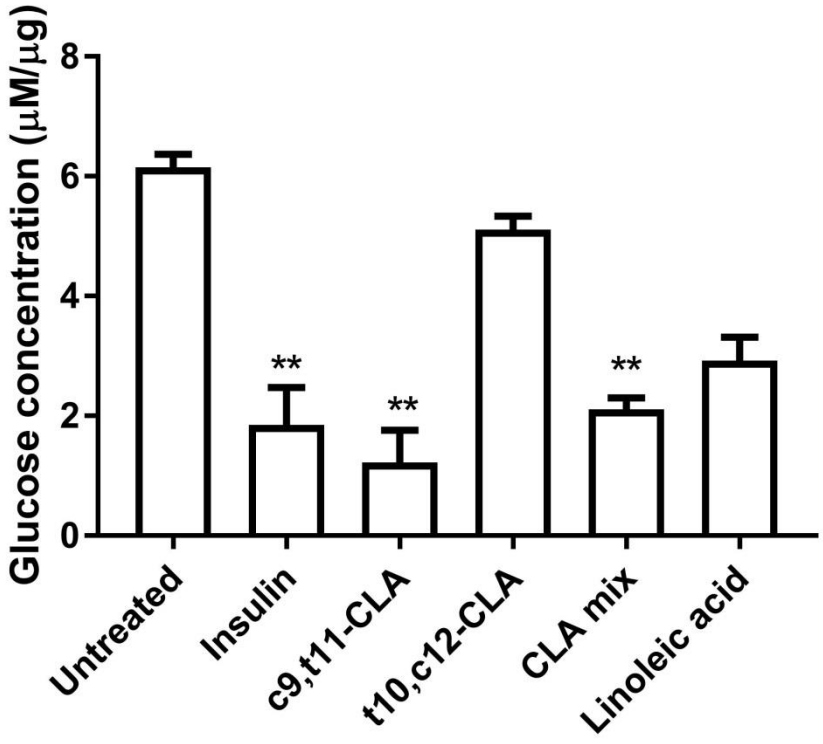


Figure 3.4: Glucose production of H4IIE cells administered with fatty acids. Concentrations of the treatments were insulin 100 nM; c9,t11-CLA 20 μM; t10,c12-CLA 20 μM; CLA mix consisted of c9,t11 10 μM and t10,c12 10 μM; linoleic acid 20 μM. ** $p < 0.01$ vs. Untreated.

To further validate the results obtained from HepG2, the effect of CLA isomers on glucose production were tested in rat hepatoma cells, H411E. In H4IIE cells (Figure 3.4), it was found that administration of 100 nM insulin, 20 μM of c9,t11-CLA and 1:1 mixture of CLA isomers significantly reduced the glucose production by 69.9%, 80.1% and 65.7%, respectively, compared to control ($p < 0.01$). Similar to the observations in HepG2 cells, administration of 20 μM of t10,c12-CLA led to no change in glucose production in H4IIE cells ($p > 0.05$). The glucose production was reduced by 52.5% in 20 μM of linoleic acid treated cells, compared to control. Together, these results were comparable to the results obtained from HepG2 cells.

3.3 Effect of CLA isomers on PEPCK and G6P expression in HepG2.

The rate limiting steps of hepatic glucose production are catalyzed by phosphoenolpyruvate carboxykinase (PEPCK) and glucose-6-phosphatase (G6P). To elucidate the effects of CLA isomers on hepatic glucose production is linked with the downregulation of hepatic gluconeogenic enzymes, the HepG2 cells exposed to CLA isomers were analysed for mRNA level of PEPCK and G6P and compared with untreated control (Figure 3.5).

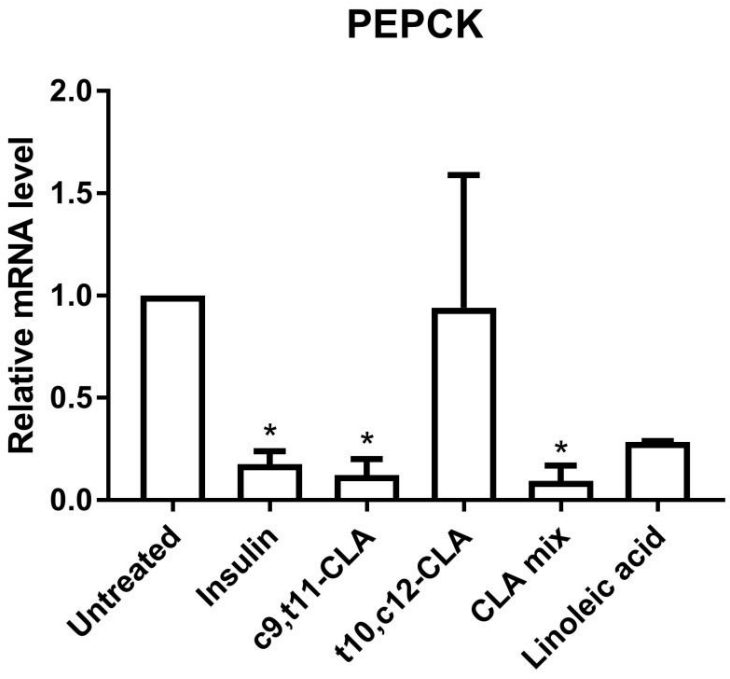


Figure 3.5: PEPCK expression of HepG2 treated with fatty acids. Concentrations of the treatments were insulin 100 nM; c9,t11-CLA 20 µM; t10,c12-CLA 20 µM; CLA mix consisted of c9,t11 10 µM and t10,c12 10 µM; linoleic acid 20 µM. * $p < 0.05$ vs. Untreated.

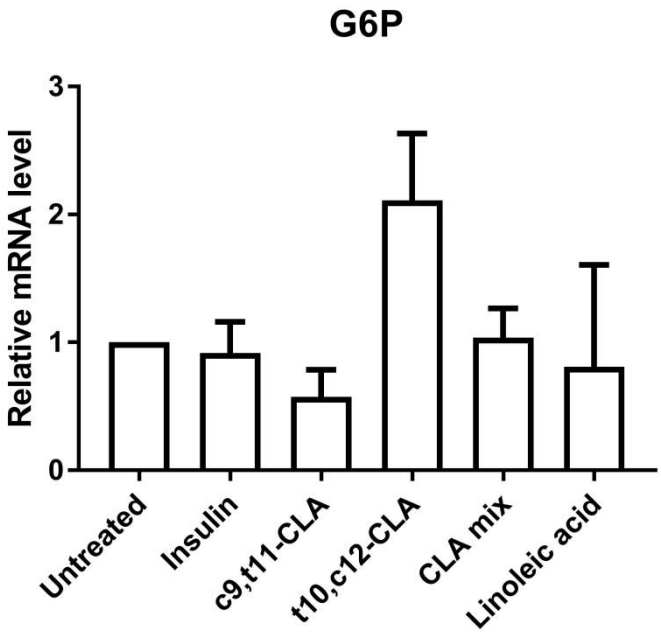


Figure 3.6: Expression of G6P in HepG2 cells treated with fatty acids. Concentrations of the treatments were insulin 100 nM; c9,t11-CLA 20 µM; t10,c12-CLA 20 µM; CLA mix consisted of c9,t11 10 µM and t10,c12 10 µM; linoleic acid 20 µM.

The HepG2 cells exposed to 100 nM insulin underwent 82.47% reduction of PEPCK expression ($p < 0.05$, Figure 3.5) but not G6P (Figure 3.6) compared to control. Likewise, the reduction of gluconeogenesis in c9,t11-CLA administration was accompanied by 87.7% reduction in PEPCK expression ($P<0.05$, Figure 3.5) and 38% reduction in G6P ($p > 0.05$, Figure 3.6). Conversely, the null effect of t10,c12-CLA is accompanied by no change in PEPCK expression ($p < 0.05$, Figure 3.5) and a non-significant 2.1-fold increase in G6P expression ($p > 0.05$, Figure 3.6). Of note, the combined administration of CLA isomers led to 90.6% reduction in PEPCK ($p < 0.05$, Figure 3.5) but no change in G6P ($p > 0.05$, Figure 3.6). The effect of 20 µM of linoleic acid on both PEPCK and G6P was found to be insignificant ($p > 0.05$, Figure 3.5 and 3.6).

3.4 Effect of PPAR agonist or antagonist on HGP

It is known that the action of insulin sensitisers to treat T2DM is dependent on the activation of PPARγ. CLA isomers have been shown to be agonists of PPARγ in adipocytes[110,111]. To understand whether the PPARγ activation or inhibition has any influence on the effects of CLA isomers on hepatic gluconeogenesis, the effect of conventional PPAR agonist or antagonist in the presence or absence of CLA isomers was examined. To justify the use of PPARγ agonist rosiglitazone, we first ensured that PPARγ is expressed in HepG2 (Figure 3.7).

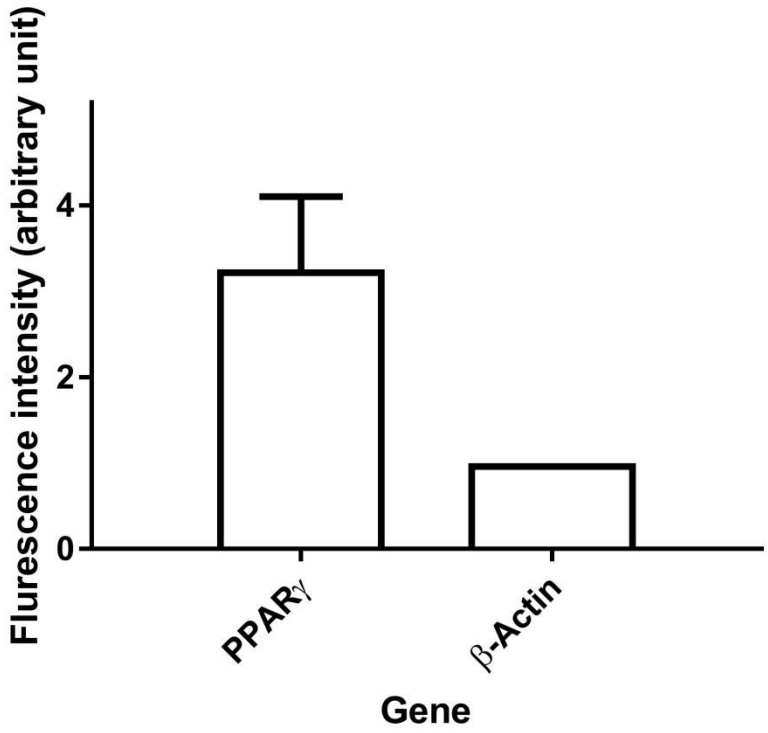


Figure 3.7: Basal expression of PPARγ in HepG2.

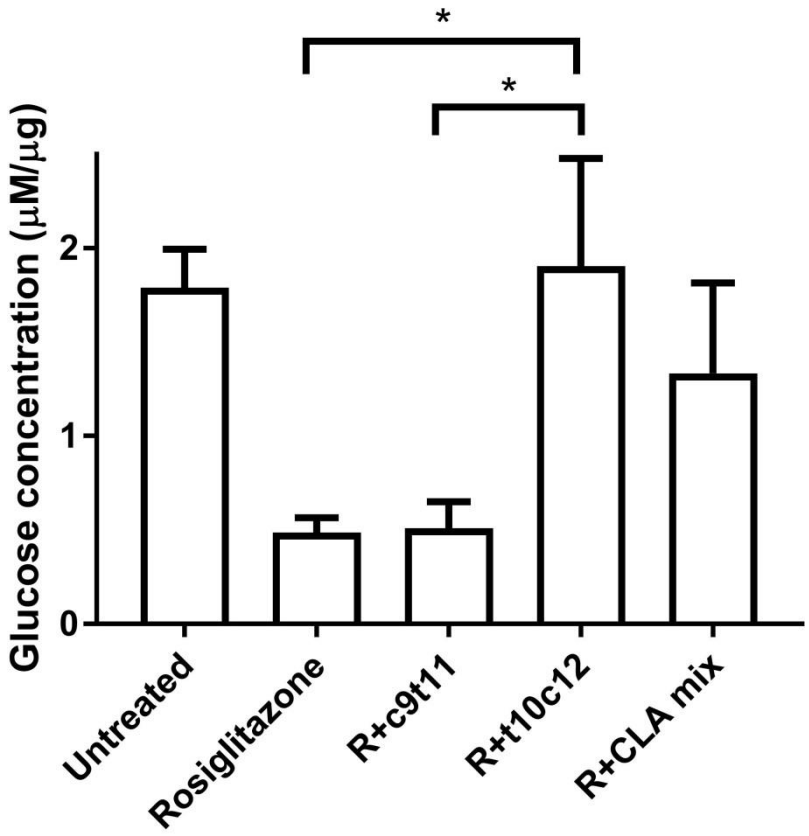


Figure 3.8: Glucose production of HepG2 treated with combinations of rosiglitazone. Concentrations of the treatments were: rosiglitazone , 10 μM; c9,t11-CLA 20 μM; t10,c12-CLA 20 μM; CLA mix consists of c9,t11 10 μM and t10,c12 10 μM. * $p < 0.05$

The concentration of 10 μM was chosen for rosiglitazone as this concentration is able to elicit biologically significant effects with HepG2 cells[139]. The exposure of HepG2 cells to 10 μM rosiglitazone, a conventional PPARγ agonist led to 72.9% reduction of glucose production ($p = 0.07$ vs. Untreated, Figure 3.8). However, rosiglitazone combined with CLA isomers either individually or mix had mixed responses. The HGP in the combined c9,t11-CLA and rosiglitazone had 75% reduced compared to control ($p = 0.08$ vs. Untreated, Figure 3.8). Conversely, the presence of t10,12-CLA or CLA mix abrogated the suppressive effects of rosiglitazone on hepatic gluconeogenesis ($p > 0.05$ vs. Untreated, Figure 3.8).

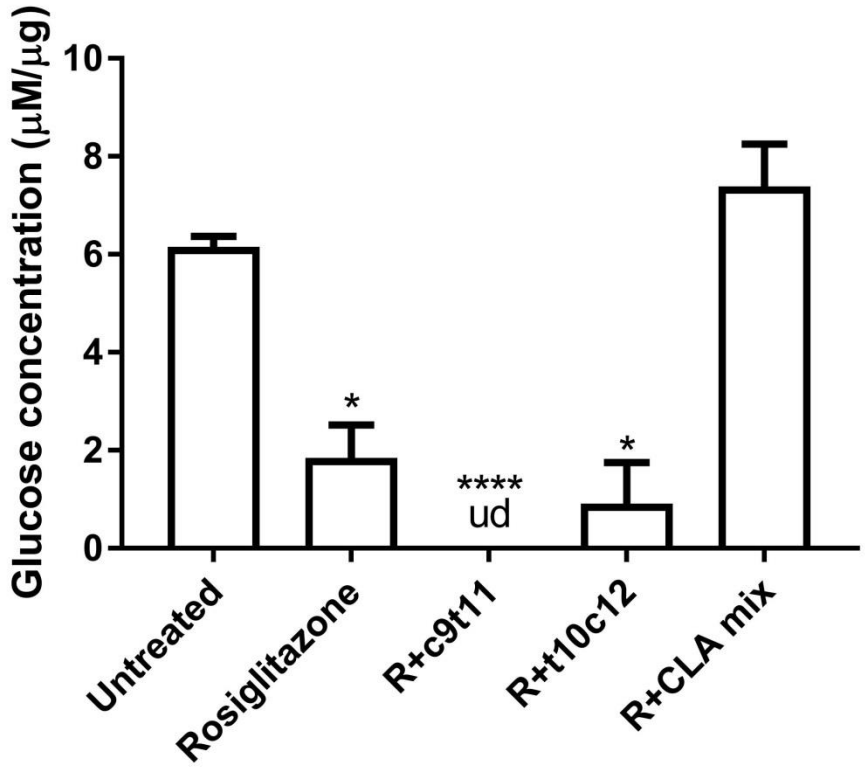


Figure 3.9: Glucose production of H4IIE treated with combinations of rosliglitazone. Concentrations of the treatments were: rosiglitazone, 10 μM; c9,t11-CLA 20 μM; t10,c12-CLA 20 μM; CLA mix consists of c9,t11 10 μM and t10,c12 10 μM. * $p < 0.05$ vs. Untreated.

Using H4IIE, a rat hepatic carcinoma cell line, it was found that rosiglitazone led to 70% reduction (Figure 3.9, $p < 0.05$ vs. Untreated). Identically with HepG2, administration of t10,c12-CLA led to no change in glucose production. Co-administration of c9,t11-CLA and rosiglitazone led to undetectable glucose levels, meanwhile t10,c12-CLA did not affect the ability of rosiglitazone to inhibit glucose production (85% reduction,; Figure 3.9, $p < 0.05$ vs. Untreated). The combination of rosiglitazone, c9,t11 and t10,c12 made no change in glucose production compared to untreated cells (Figure 3.9).

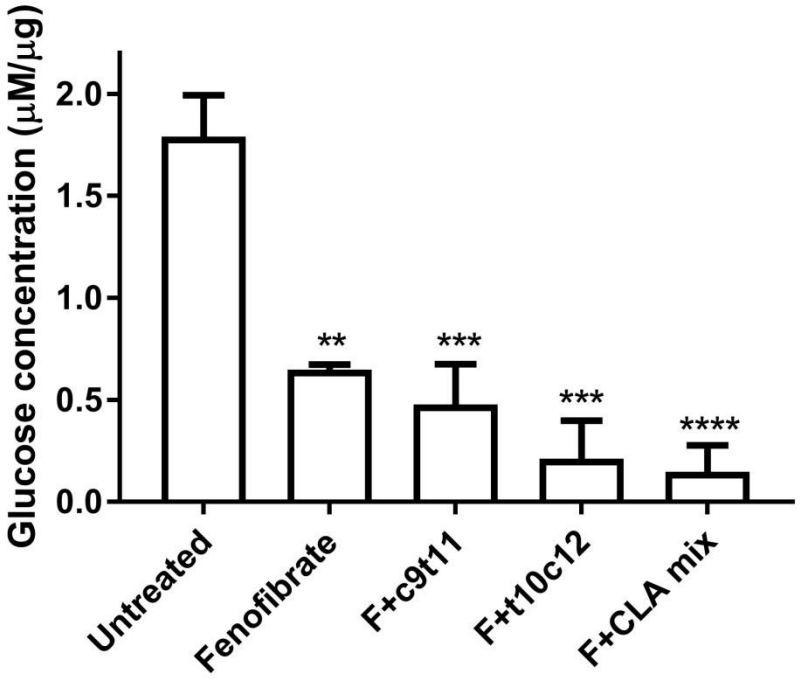


Figure 3.10: Glucose production of HepG2 treated with combinations of fenofibrate and CLA. Concentrations of the treatments are: fenofibrate, 10 μM; c9,t11-CLA 20 μM; t10,c12-CLA 20 μM; CLA mix consists of c9,t11 10 μM and t10,c12 10 μM. ** $p < 0.01$ vs. Untreated; *** $p < 0.001$ vs. Untreated; **** $p < 0.0001$ vs. Untreated.

Likewise, the concentration of 10 μM was chosen for PPARα agonist, fenofibrate. Generally, administration of fenofibrate with combinations of CLA led to reduction of glucose production in HepG2 cells. Single administration of fenofibrate led to 63.8% reduction compared to untreated control (Figure 3.10, $p < 0.05$). The addition of 20 μM c9,t11-CLA led to 73.4% reduction (Figure 3.10, $p < 0.01$). The combination of fenofibrate and 20 μM t10,c12-CLA led to 88.16% reduction (Figure 3.10, $p < 0.01$). Fenofibrate with CLA at respective isomer concentration of 10 μM led to 91.8% reduction of hepatic glucose production (Figure 3.10, $p < 0.0001$).

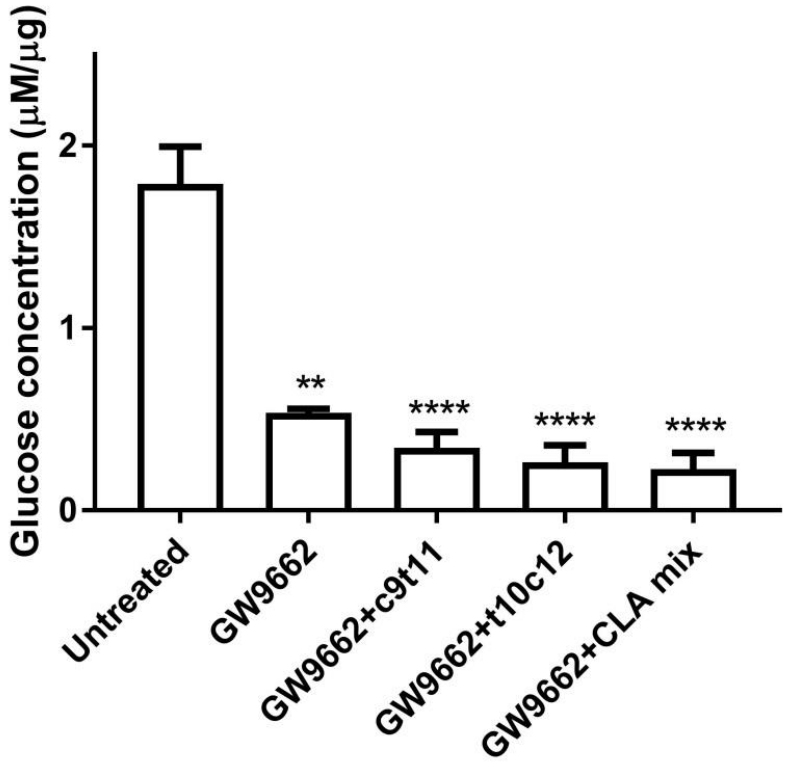


Figure 3.11: Glucose production of HepG2 treated with combinations of GW 9662 and CLA. Concentrations of the treatments are: GW 9662, 10 μM; c9,t11-CLA 20 μM; t10,c12-CLA 20 μM; CLA mix consists of c9,t11 10 μM and t10,c12 10 μM. ** $p < 0.01$ vs. Untreated; **** $p < 0.0001$ vs. Untreated.

GW 9662 is an antagonist of PPARγ. The concentration of 10 μM was chosen based on a previous study[140]. At this concentration, it led to 70.2% reduction in hepatic gluconeogenesis, compared to control ($p < 0.005$, Figure 3.11). GW 9662 was found to further decrease HGP when combined with either individual CLA isomers, c9,t11 (80.9% reduction), t10,c12 (85.2% reduction) or CLA mix (87.4% reduction) (all were $p < 0.0001$, Figure 3.11).

3.5 Effect of PPAR agonist or antagonist on PEPCK and G6P expression in CLA isomers treated human hepatocarcinoma cells (HepG2)

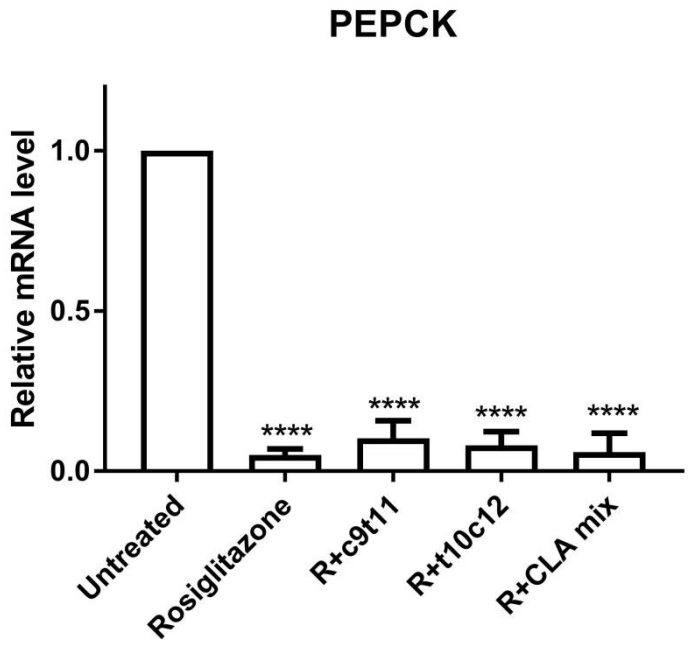


Figure 3.12: PEPCK expression of HepG2 treated with combinations involving rosiglitazone and CLA. Concentrations of the treatments are: rosiglitazone, 10 µM; c9,t11-CLA 20 µM; t10,c12-CLA 20 µM; CLA mix consists of c9,t11 10 µM and t10,c12 10 µM. **** $p < 0.0005$ vs. Untreated.

The expression of PEPCK was reduced by 95.0% upon exposure to rosiglitazone alone ($p < 0.0001$, Figure 3.12). The combination of c9,t11-CLA, t10,c12-CLA or CLA mix with rosiglitazone led to 89.8% ($p < 0.0001$), 92.0% ($p < 0.0001$) and 94.% ($p < 0.0001$) lowered expression of PEPCK, respectively (Figure 3.12).

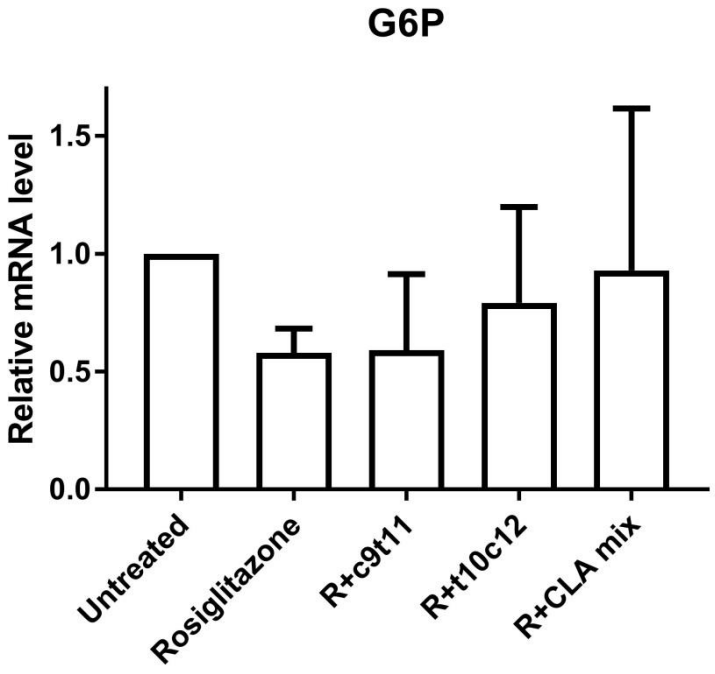


Figure 3.13: G6P expression of HepG2 treated with combinations involving rosiglitazone and CLA. Concentrations of the treatments are: rosiglitazone, 10 µM; c9,t11-CLA 20 µM; t10,c12-CLA 20 µM; CLA mix consists of c9,t11 10 µM and t10,c12 10 µM.

In contrast, the expression of G6P did not differ irrespective of any combinations involving rosiglitazone ($p > 0.05$, Figure 3.13).

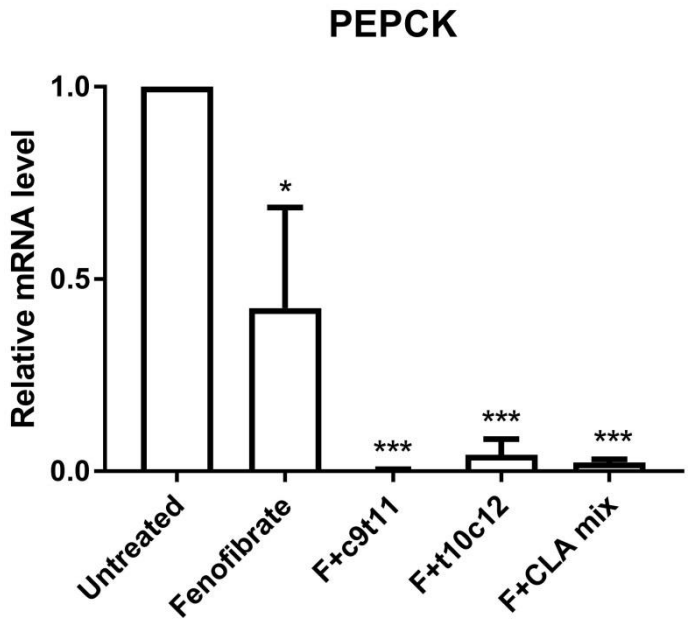


Figure 3.14: PEPCK expression of HepG2 treated with combinations involving fenofibrate and CLA. Concentrations of the treatments are: fenofibrate, 10 µM; c9,t11-CLA 20 µM; t10,c12-CLA 20 µM; CLA mix consists of c9,t11 10 µM and t10,c12 10 µM. * $p < 0.05$ vs. Untreated; *** $p < 0.001$ vs. Untreated.

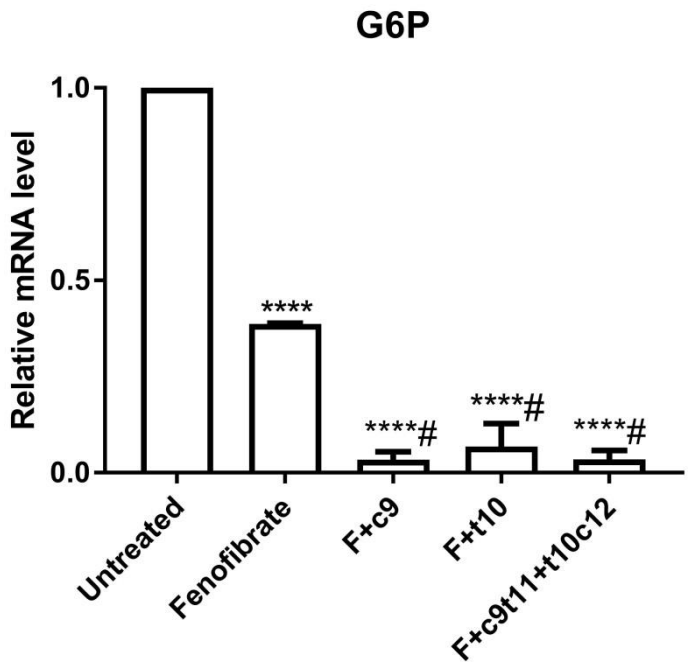


Figure 3.15: G6P expression of HepG2 cells treated with combinations of fenofibrate. . Concentrations of the treatments are: fenofibrate, 10 µM; c9,t11-CLA 20 µM; t10,c12-CLA 20 µM; CLA mix consists of c9,t11 10 µM and t10,c12 10 µM.**** $p < 0.0001$ vs. Untreated ; #: $p < 0.001$ vs. Fenofibrate

The administration of 10 µM fenofibrate led to 58% reduction in PEPCK (Figure 3.14, $p < 0.05$) and 61.3% reduction in G6P expression (Figure 3.15, $p < 0.0001$) compared to untreated control. The addition of CLA to fenofibrate treatment led to more than 90% reduction of PEPCK and G6P expression (Figure 3.14 and Figure 3.15).

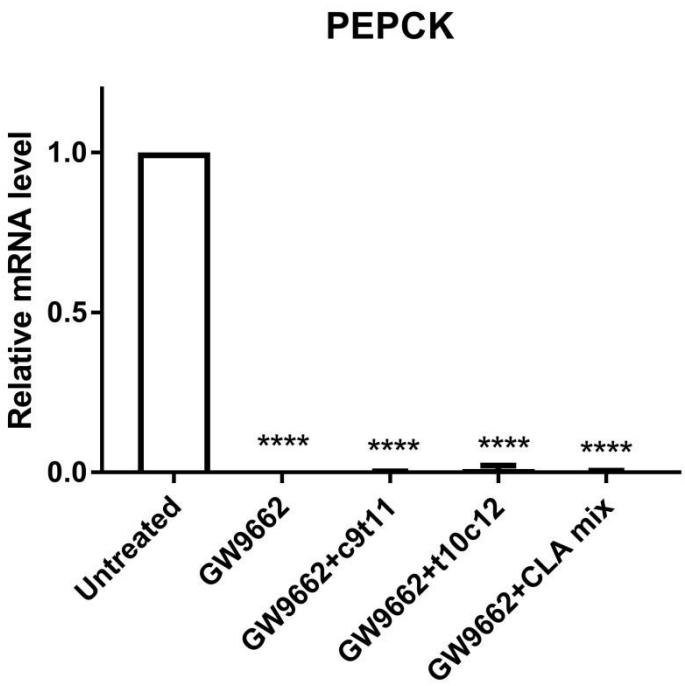


Figure 3.16: PEPCK expression of HepG2 treated with GW 9662 and combinations of CLA. Concentrations of the treatments are: GW 9662, 10 µM; c9,t11-CLA 20 µM; t10,c12-CLA 20 µM; CLA mix consists of c9,t11 10 µM and t10,c12 10 µM. **** $p < 0.0001$ vs Untreated

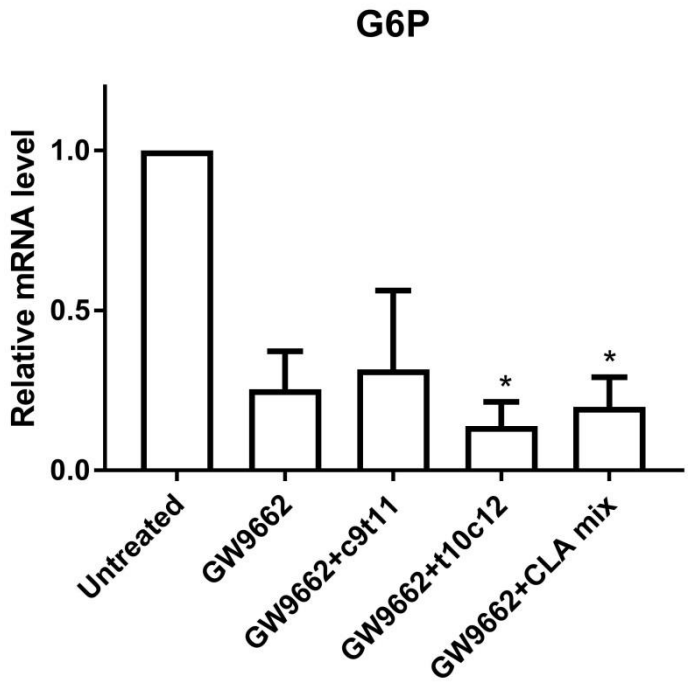


Figure 3.17: G6P expression in HepG2 cells treated with combinations of GW 9662. Concentrations of the treatments are: GW 9662, 10 µM; c9,t11-CLA 20 µM; t10,c12-CLA 20 µM; CLA mix consists of c9,t11 10 µM and t10,c12 10 µM. * $p < 0.05$ vs. Untreated.

As shown in Figure 3.16, the administration of 10 µM GW 9662 led to near undetectable expression of PEPCK either in the presence or absence of CLA, compared to untreated control ($p < 0.0001$). However, the G6P mRNA level was found to be 86% downregulated with co-treatment of GW 9662 and t10,c12-CLA (Figure 3.17, $p < 0.05$).

Information on sample quality of mRNA extraction and synthesized cDNA is shown in Table S1 and S2 in Supplementary Data.

In vivo results

3.6 Animals

Of 10 wild type and 45 ApoE null mice purchased, two animals were sacrificed from wild type, ApoE, WD and ApoE, WD+CLA(e) at Week 12 to check for disease progress. Remaining mice were further allocated into groups. Number of mice that were terminated at Week 20 were five from wild type, ND; five from ApoE, WD; seven from ApoE, WD+CLA(e); seven from ApoE, WD+CLA(l); five from ApoE, WD+Rosi and five from ApoE, WD+CLA(e)+Rosi.

3.7 Body weight and energy intake

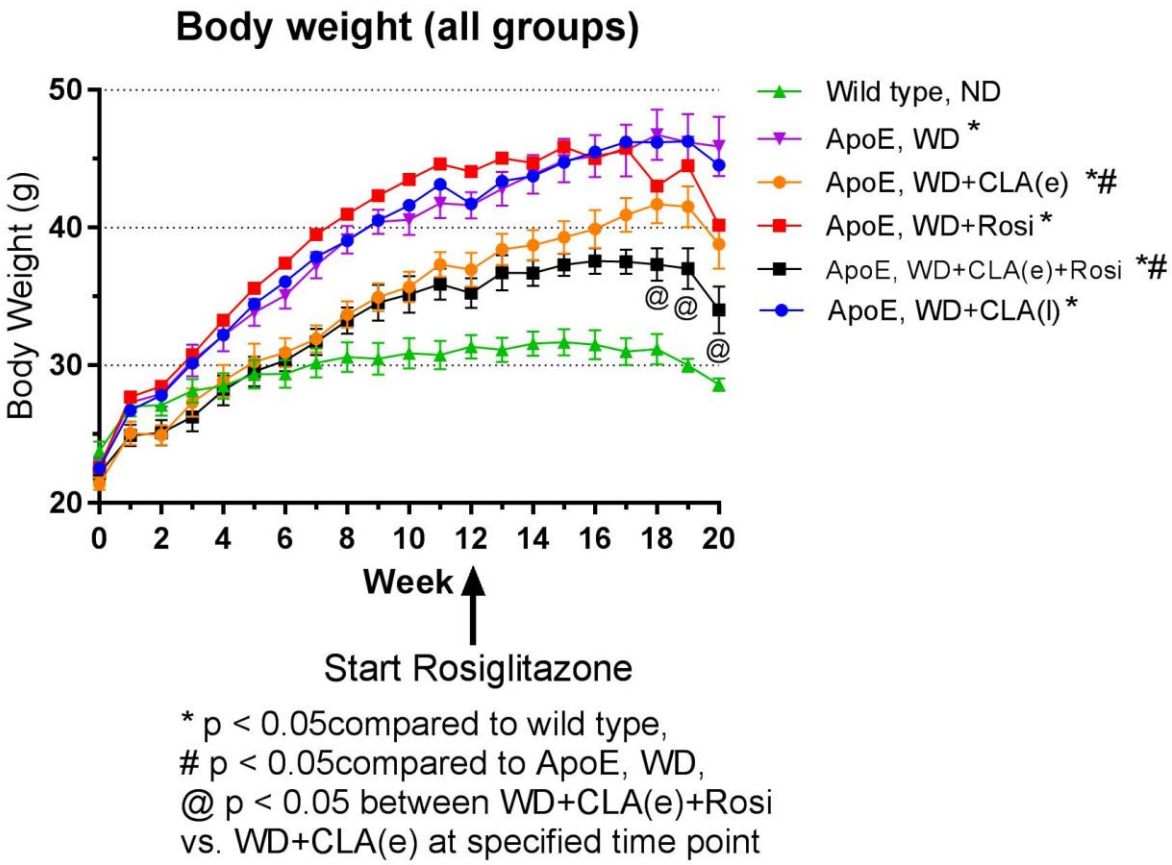


Figure 3.18a: Body weight of WT and ApoE mice across all treatment groups throughout *in vivo* study from Week 0 to Week 20.

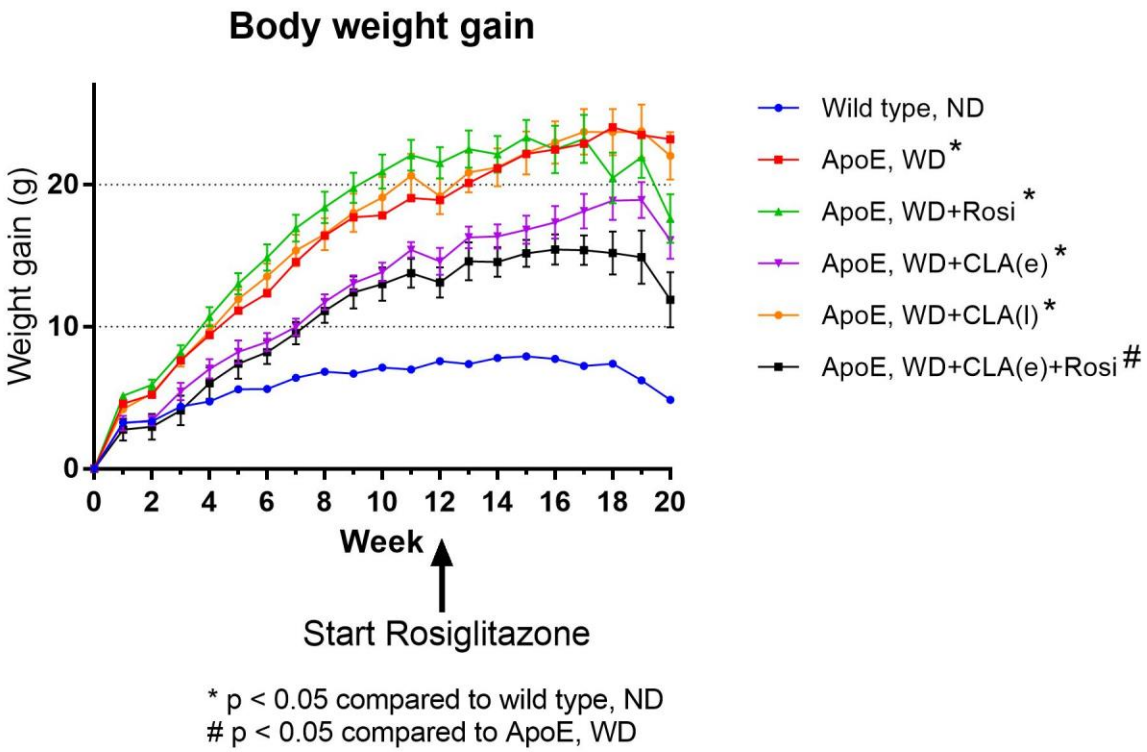


Figure 3.18b: Body weight gain, compared to Week 0 of study, of wild type and ApoE mice across all treatment groups throughout *in vivo* study.

Body weight of all mice with respect to time is shown in Figure 3.18a and body weight difference compared to Week 0 is shown is Figure 3.18b. The body weight of ApoE null mice were approximately 2 grams lower than their wild type counterparts (data not shown). At the end of the study, wild type mice hovered at 28.62g (Figure 3.18a). ApoE+WD mice increased the mean by 1.6-fold at 45.92g (Figure 3.18a). Early administration of CLA slowed body weight gain effective from Week 1. Administering CLA mixture from the beginning and treatment with rosiglitazone from Week 12 onwards [ApoE, CLA(e)+Rosi] caused a 25.9% reduction of body weight compared to ApoE null, WD fed mice (Figure 3.18a, $p < 0.0001$). Body weight reduction among ApoE, CLA(e) and ApoE, CLA(e)+Rosi is indicative of lipoatrophy caused by t10,c12-CLA.

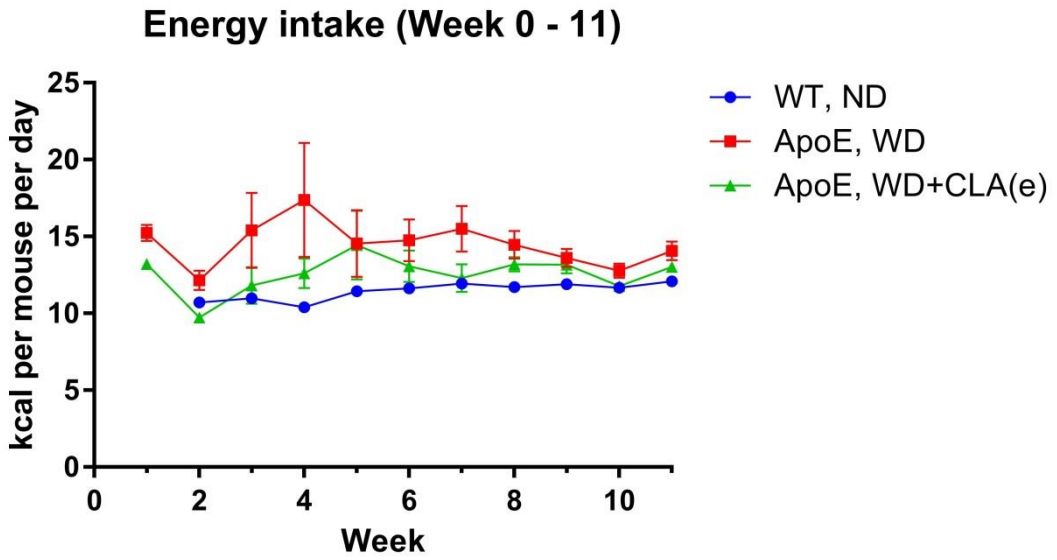


Figure 3.19a: Energy intake of mice before Week 12.

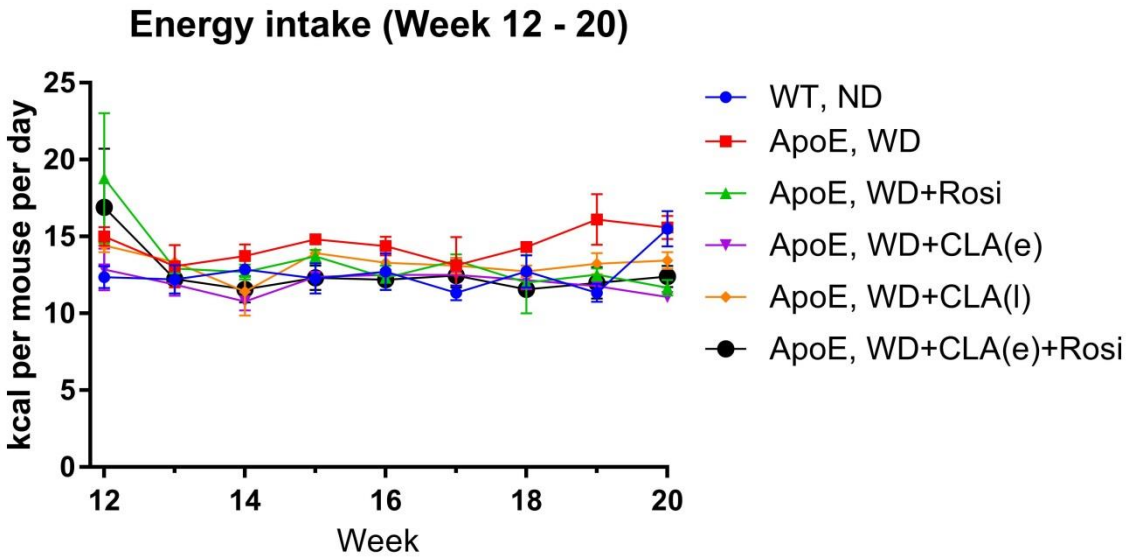


Figure 3.19b: Energy intake of mice after Week 12.

Energy intake was divided into two phases, before Week 12 (Figure 3.19a) and after Week 12 (Figure 3.19b). Before Week 12, energy intake differed significantly between wild type and ApoE, WD ($p < 0.01$); and between ApoE, WD and ApoE, WD+CLA(e) ($p < 0.05$). After Week 12, only ApoE, WD and ApoE, WD+CLA(e) differed in energy intake ($p < 0.05$).

Table 3.1: Absolute organ weights of mice sacrificed at Week 12, n = 2.

	Wild type, ND	ApoE, WD	ApoE, WD+CLA(e)
Liver	1.064	3.108	1.850
Epididymal fat	0.231	2.374	2.031
Perirenal fat	0	1.099	0.486
Mesenteric fat	0	1.081	0.527
Pancreas	0.166	0.245	0.151
Kidney	0.421	0.430	0.404
Spleen	0.073	0.137	0.107

Table 3.2: Absolute organ weights of mice sacrificed at Week 20. * $p < 0.05$ vs. WT, ND; *** $p < 0.001$ vs. WT, ND; *** $p < 0.0001$ vs. WT, ND.

	Wild type, ND	ApoE, WD	ApoE, WD+Rosi	ApoE, WD+CLA(l)	ApoE, WD+CLA(e)	ApoE, WD+CLA(e)+Rosi
Liver	1.339±0.092	2.608±0.193	3.063±0.425	2.478±0.275	1.929±0.203	2.34±0.305
Epididymal fat	0.347±0.064	2.487±0.227 ****	2.247±0.216 ***	2.442±0.207 ****	2.068±0.264 ***	1.471±0.333 *
Perirenal fat	0.806±0.275	1.261±0.188	0.911±0.171	1.185±0.130	0.739±0.098	0.440±0.077
Mescenteric fat	0.133±0.022	0.485±0.084	0.372±0.062	0.540±0.143	0.464±0.042	0.240±0.032
Pancreas	0.181±0.012	0.651±0.429	0.125±0.018	0.176±0.012	0.156±0.016	0.136±0.018
Kidney	0.409±0.011	0.414±0.018	0.413±0.021	0.399±0.017	0.373±0.006	0.433±0.014
Spleen	0.093±0.029	0.152±0.037	0.159±0.026	0.124±0.011	0.167±0.021	0.131±0.008

3.7 Liver weight

Feeding WD diet to ApoE null mice led to hepatomegaly, apparent as early as Week 12 ($p < 0.01$, Table 3.1); however it can be noted that the increase in liver weight was compensated by increased body weight. Administration of rosiglitazone (ApoE, WD+Rosi and ApoE, WD+CLA(e)+Rosi) led to increased liver weight compared to wild type mice fed ND (Table 3.2) and also increased liver to body weight ratio (not shown). Administration of early CLA [ApoE, WD+CLA(e)] attenuated hepatomegaly caused by WD without significant change in body weight throughout the study, as shown on Week 12 and Week 20 (Table 3.1 and 3.2).

3.8 Adipose weight

The effect of feeding WD was apparent as shown by increased epididymal, perirenal and mesenteric fat pads as early as Week 12 (Table 3.1) and continued throughout the study up to Week 20 (Table 3.2). Fat pad size was attenuated by early administration of CLA as early in Week 12 (Table 3.1); up to Week 20 only for epididymal fat (Table 3.2). Late administration of CLA had no effect on reducing fat pad size (Table 3.2). The combined administration of early CLA and rosiglitazone had the most effect on reducing fat pad size caused by WD feeding (Table 3.2).

3.9 Fasting and random blood glucose

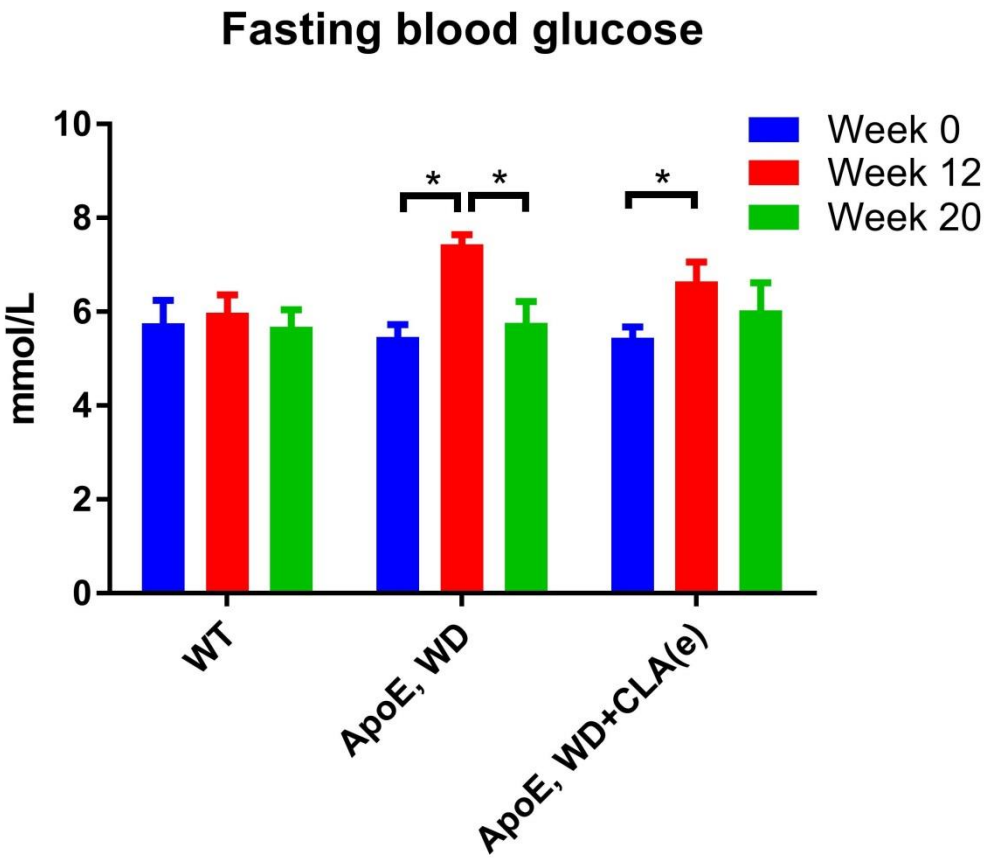


Figure 3.20: Fasting blood glucose of WT and ApoE mice. Blood glucose was taken with the tail prick method at Week 0, 12 and 20 of study.

* $p < 0.05$, difference detected by t-test

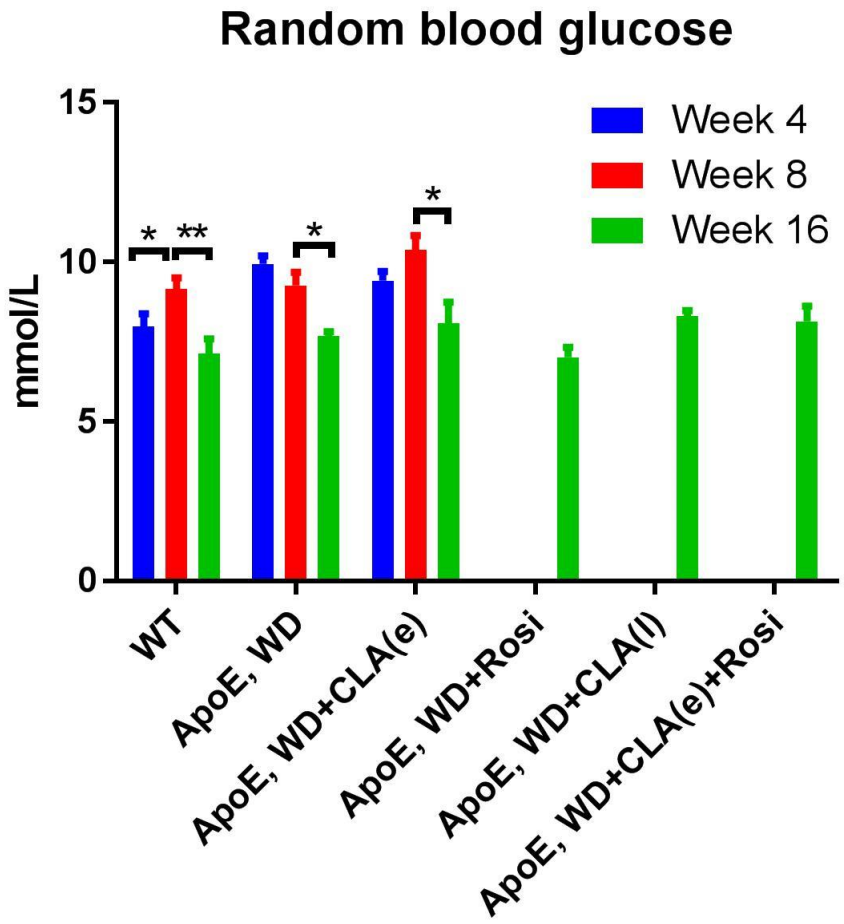


Figure 3.21: Random blood glucose of WT and ApoE mice. Blood glucose was taken with the tail prick method at Week 4, 8 and 16 of study.

* $p < 0.05$; ** $p < 0.01$, difference detected by t-test

Initial fasting blood glucose level did not differ between groups (Figure 3.20). At Week 12, a difference was detected between wild type mice and ApoE, WD+CLA(l) mice (Figure 3.20); and between ApoE, WD+CLA(e) and ApoE, WD+CLA(l) mice (Figure 3.20) at the significance level of 0.05. No difference in fasting blood glucose at Week 20 was detected (Figure 3.20). In random blood glucose, (Figure 3.21), no difference was detected between groups at the same time point.

3.10 Oral glucose tolerance test

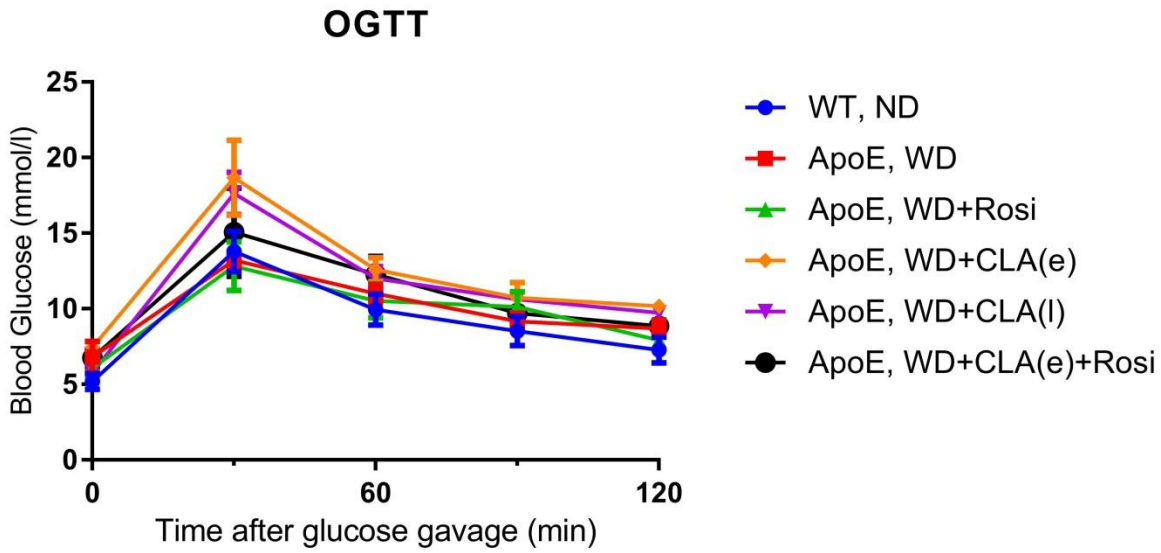


Figure 3.22: Oral glucose tolerance test performed on WT and ApoE mice at Week 19.

Although it was observed that ApoE, WD+CLA(e) has the greatest AUC for OGTT curve, no statistically significance was detected among treatment groups for oral glucose tolerance (Figure 3.22).

3.11 Hormone levels

3.11.1 Insulin

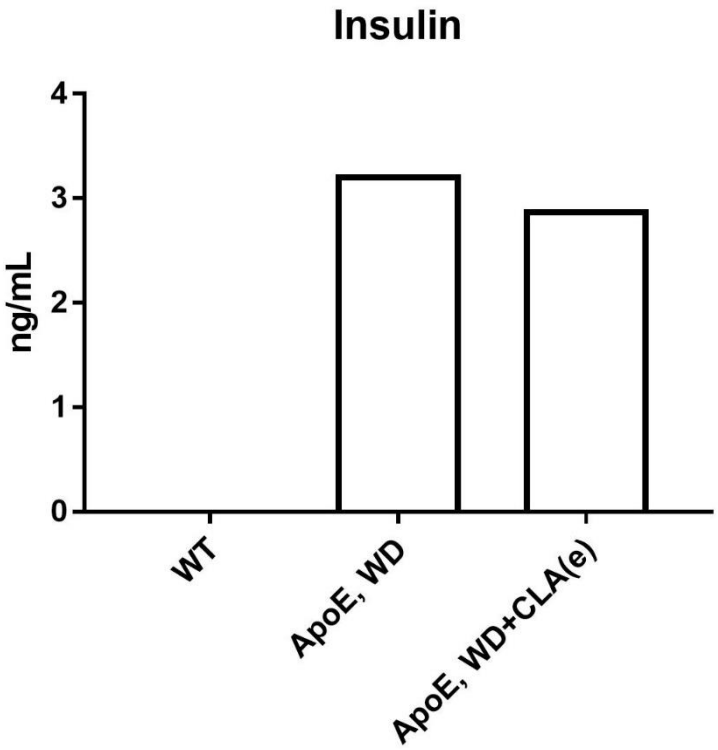


Figure 3.23: Serum insulin level at Week 12. (n = 2)

At Week 12, feeding WD to ApoE mice, irrespective of early administration of CLA mixture, led to hyperinsulinemia (Figure 3.23).

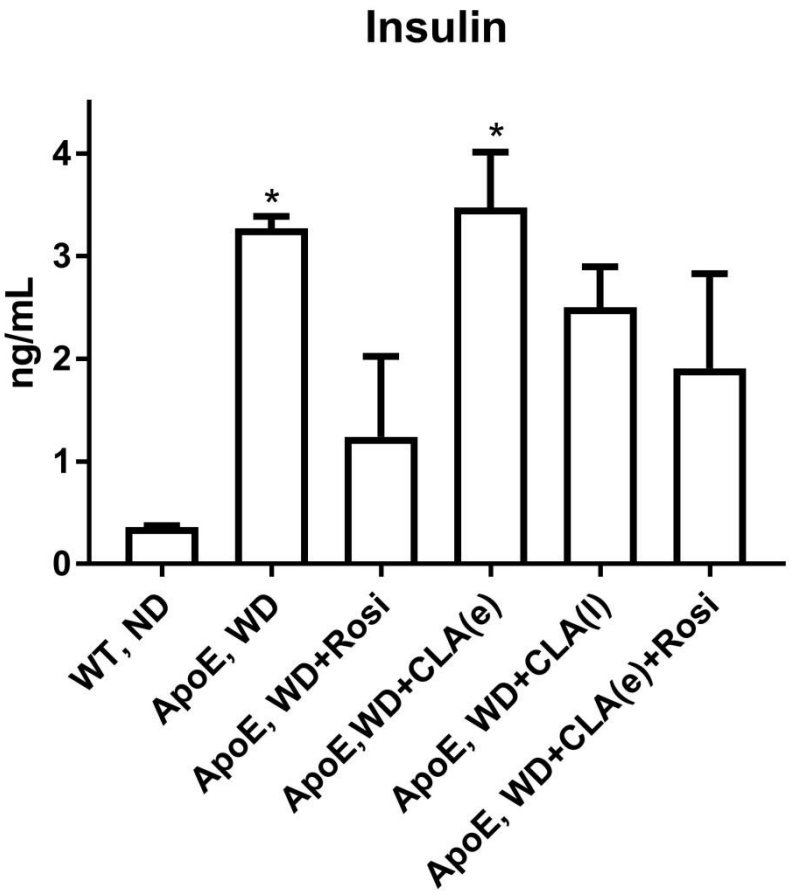


Figure 3.24: Serum insulin level at Week 20. Feeding WD led to increased insulin level and administration of rosiglitazone reduces it.

The condition of hyperinsulinemia among ApoE, WD mice persisted to Week 20 (Figure 3.24). The difference between ApoE, WD and WT was a 9.1-fold increase in insulin level (Figure 3.24, $p < 0.05$). Treatment with rosiglitazone from Week 12 onwards relieved hyperinsulinemia caused by WD, which 62% reduction for ApoE, WD+Rosi and 41.8% reduction for ApoE, WD+CLA(e)+Rosi (Figure 3.24, $p > 0.05$).

3.11.2 Adiponectin

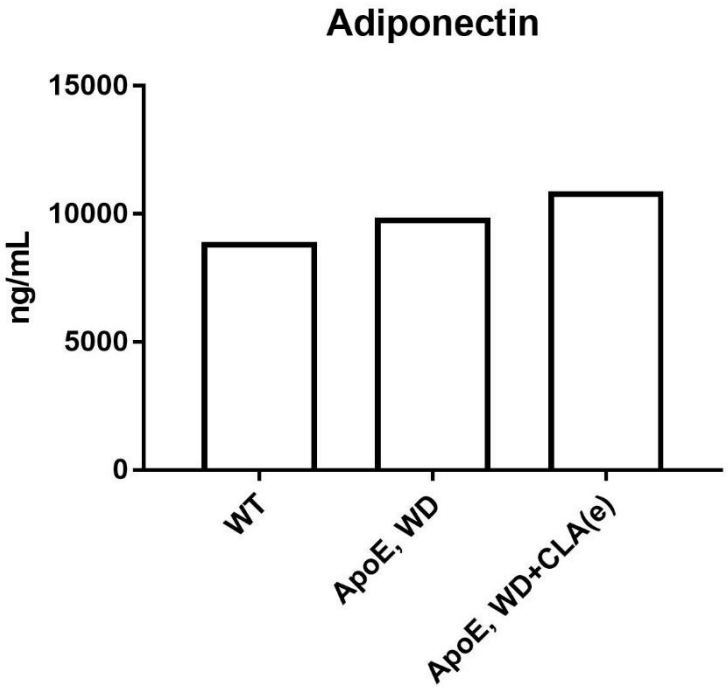


Figure 3.25: Adiponectin level at Week 12 in WT and ApoE null mice. (n = 2)

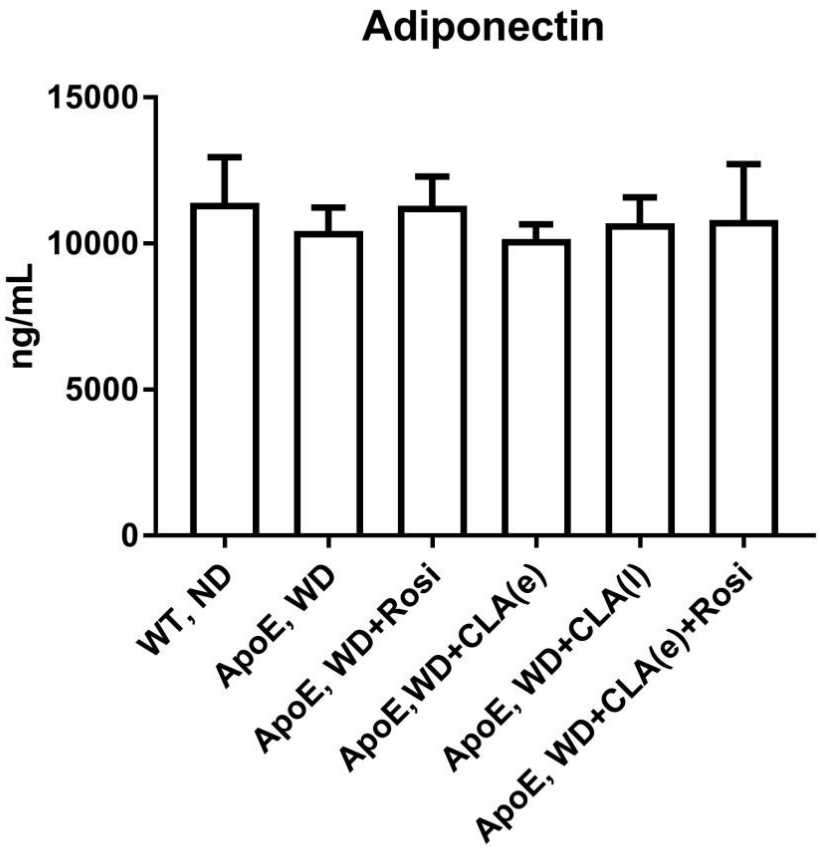


Figure 3.26: Adiponectin level at Week 20 in WT and ApoE null mice.

No difference was detected in adiponectin levels across all groups at Week 12 and Week 20 (Figure 3.25 and Figure 3.26).

3.11.3 Leptin

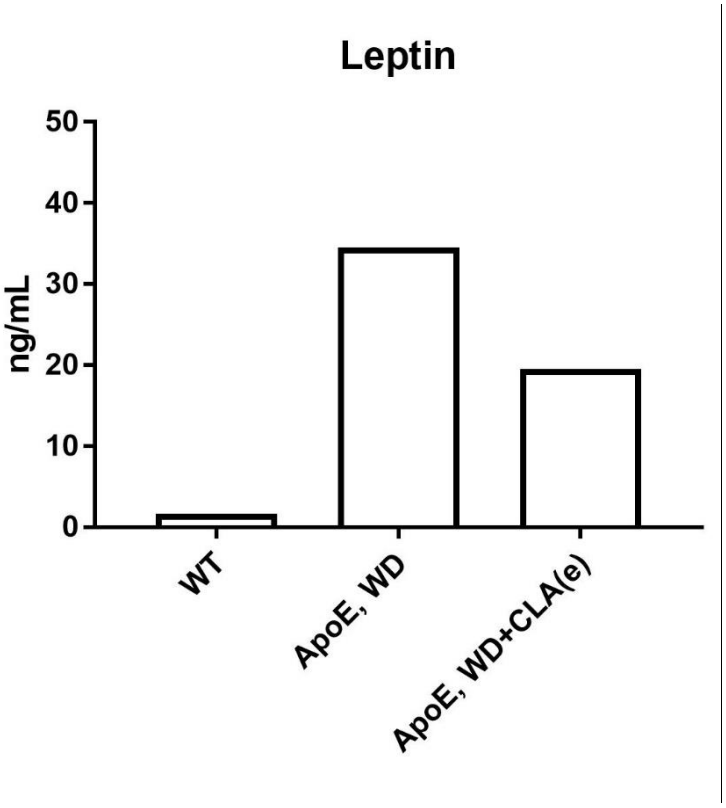


Figure 3.27: Leptin level at Week 12 in WT and ApoE null mice. Feeding WD led to increased leptin level, while early administration of CLA reduces it. (n = 2)

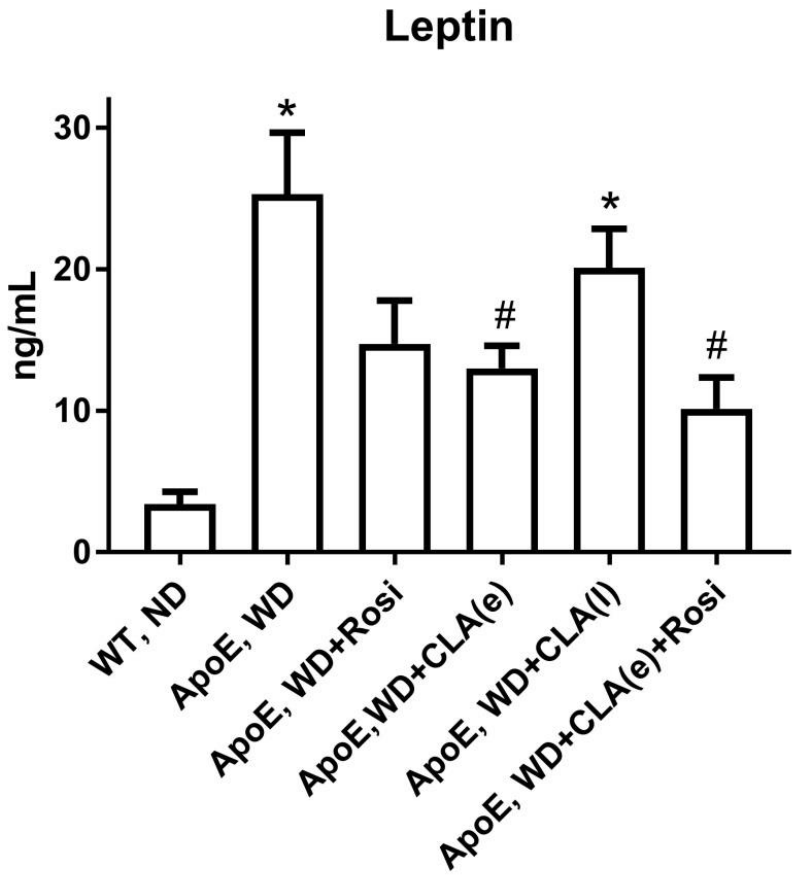


Figure 3.28: Leptin level at Week 20 in WT and ApoE null mice. Feeding WD led to hyperleptinemia and administration of rosiglitazone and CLA led to reduction in various degrees. * $p < 0.05$ vs. WT, ND; # $p < 0.05$ vs. ApoE, WD

At Week 12, hyperleptinemia was detected in ApoE, WD group, early administration of CLA mixture [ApoE, WD+CLA(e)] partially alleviated hyperleptinemia (Figure 3.27). Hyperleptinemia persisted in ApoE, WD mice, a 7.46-fold increase compared to wild type mice (Figure 3.28, $p < 0.05$). Administering CLA early or rosiglitazone after Week 12 (in ApoE, WD+CLA(e); ApoE, WD+Rosi and ApoE, WD+CLA(e)+Rosi) alleviated hyperleptinemia (Figure 3.28). Administration of CLA after Week 12 after obese pathology has developed [ApoE, WD+CLA(l)] had no effect on hyperleptinemia (Figure 3.28).

3.12 Lipid levels

3.12.1 Total cholesterol

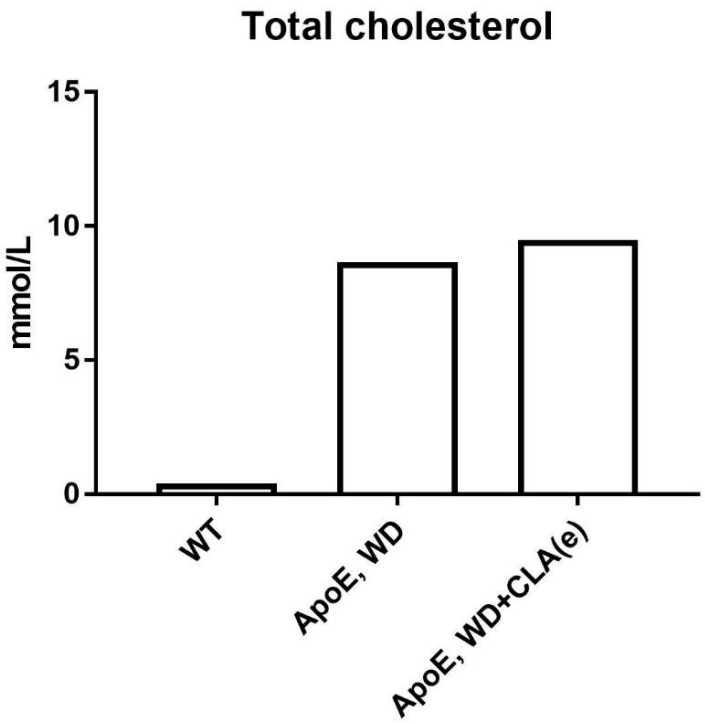


Figure 3.29: Total cholesterol level at Week 12 in WT and ApoE null mice. Feeding WD led to increased total cholesterol and CLA administration had no effect.

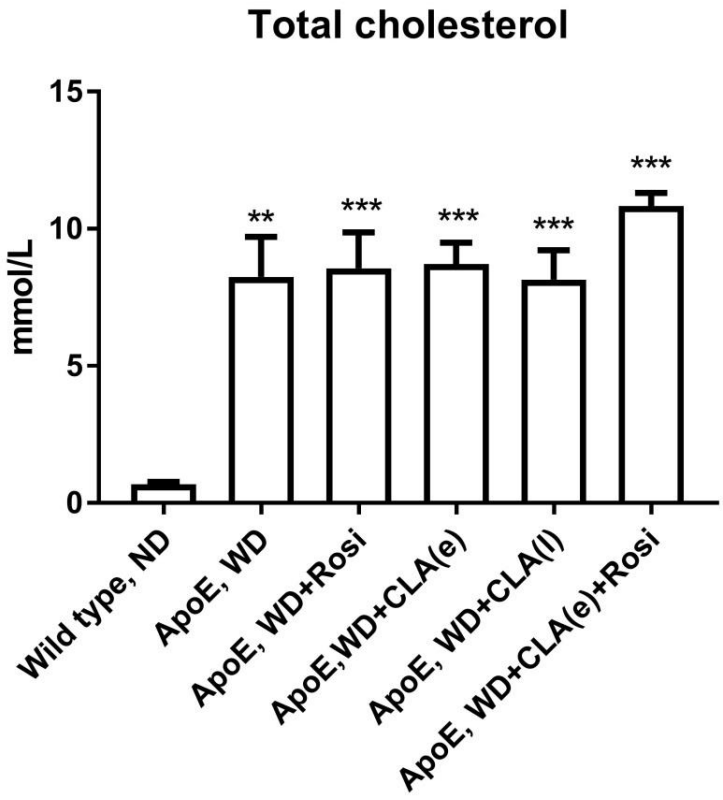


Figure 3.30: Total cholesterol at Week 20 in WT and ApoE null mice. Consumption of WD led to hypercholesterolemia that is not reduced by administration of rosiglitazone and CLA. Simultaneous administration of early CLA and rosiglitazone exacerbated hypercholesterolemia.

** $p < 0.01$ vs. WT, ND, *** $p < 0.001$ vs. WT, ND

At Week 12, feeding WD to ApoE mice, regardless of CLA treatment, led to 20-fold increase in total cholesterol compared to WT mice (Figure 3.29). At Week 20, feeding Western diet to ApoE null mice led to marked increase of 12.1-fold in total plasma cholesterol compared to wild type mice as expected (Figure 3.30, $p < 0.01$ to $p < 0.001$). Administering CLA early in the study caused a further 5.7% increase in total plasma cholesterol compared to ApoE, WD (Figure 3.30). Simultaneous administration of CLA and rosiglitazone led to 31% increase in total cholesterol compared to ApoE, WD mice (Figure 3.30).

3.12.2 LDL cholesterol

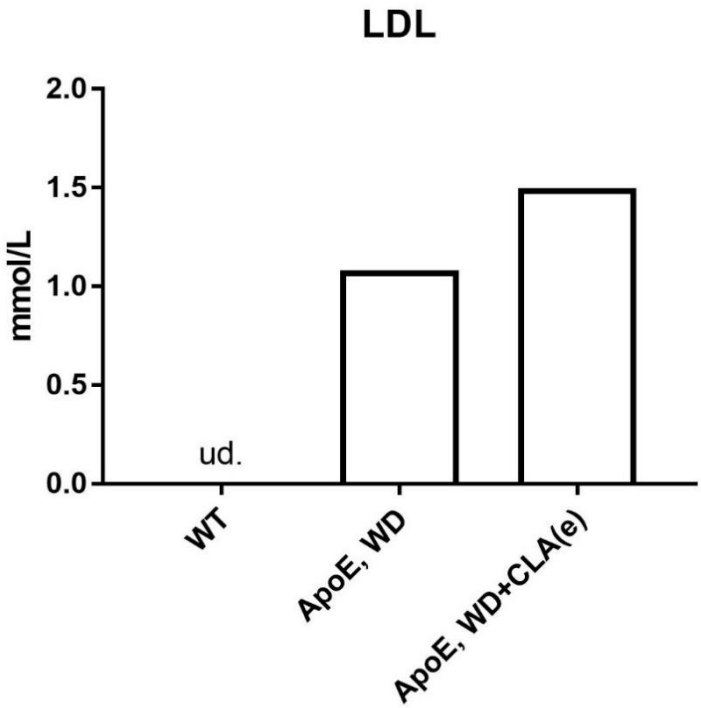


Figure 3.31: LDL level at Week 12 in WT and ApoE null mice. LDL was undetectable in WT mice, while feeding WD led to increased LDL. (n = 2)

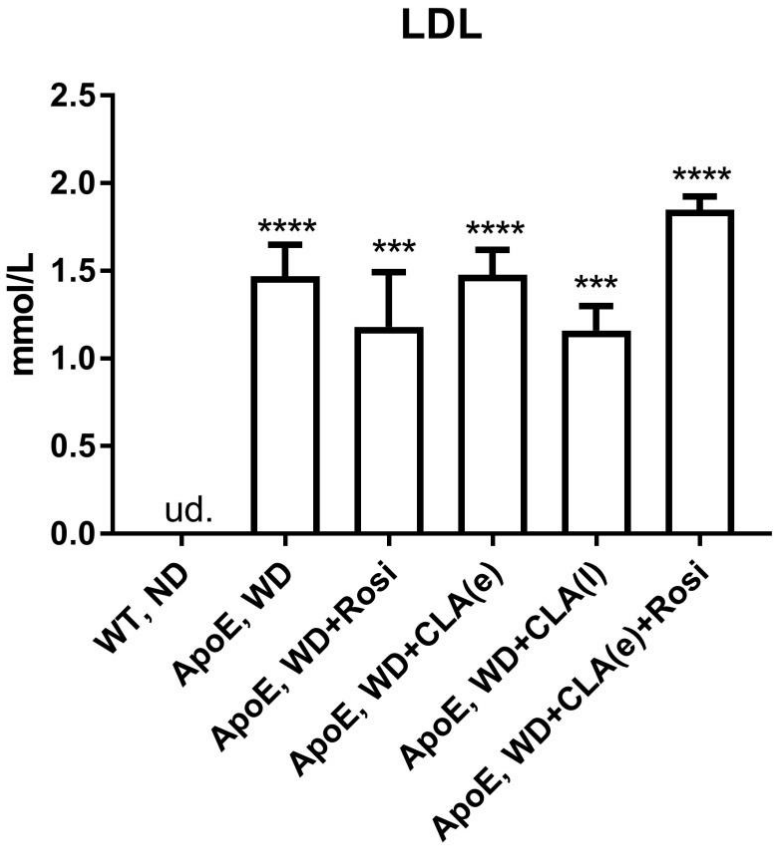


Figure 3.32: LDL level at Week 20 in WT and ApoE null mice. LDL was undetectable in WT mice. Feeding WD led to increased LDL.

*** $p < 0.001$, **** $p < 0.0001$

At Week 12, ApoE null mice fed WD regardless of treatment showed increased LDL cholesterol (Figure 3.31). LDL was close to undetectable in WT mice both at Week 12 and Week 20 (Figure 3.31 and Figure 3.32). At both Week 20, all ApoE null mice fed WD has markedly increased LDL with significance level between $p < 0.001$ to $p < 0.0001$ compared to WT mice (Figure 3.32). Particularly, for ApoE, WD+CLA(e)+Rosi, the increase in LDL was the greatest ($p < 0.0001$ vs. WT, ND).

3.12.3 HDL cholesterol

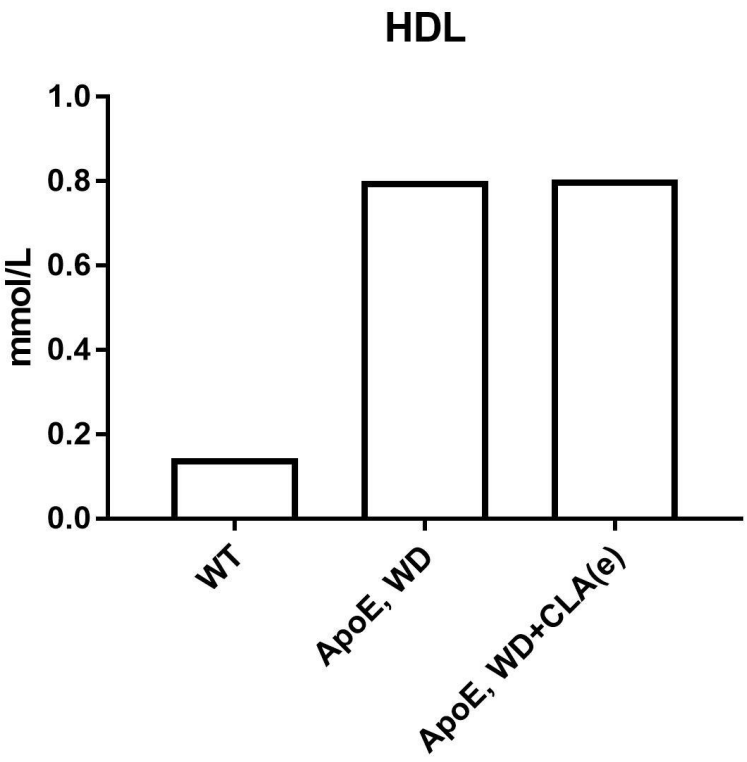


Figure 3.33: HDL level at Week 12 in WT and ApoE null mice. Feeding WD led to increased HDL. (n = 2)

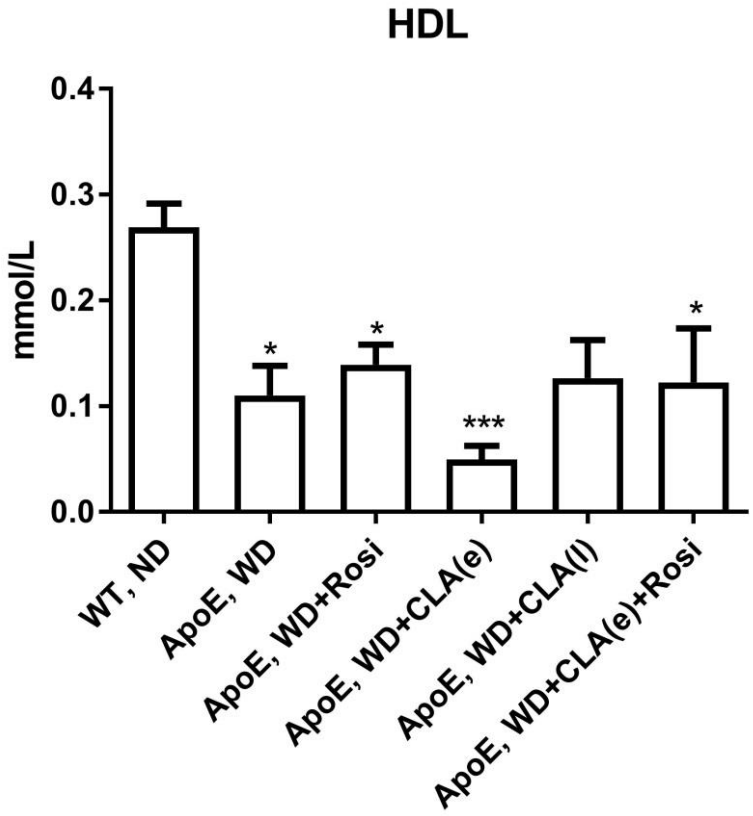


Figure 3.34: HDL level at Week 20 in WT and ApoE null mice. At Week 20, feeding WD led to decrease in HDL.

* $p < 0.05$, *** $p < 0.001$

Feeding WD to ApoE null mice led to marked increase in HDL that was detectable at Week 12 (Figure 3.34). Over time, at Week 20, HDL level decreased by an average of 54% across all ApoE null mice fed WD (Figure 3.34). Particularly, ApoE fed WD and treated with early CLA had the lowest HDL level, which was a reduction of 81.6% ($p < 0.001$) compared to WT mice (Figure 3.34).

3.12.4 Triglycerides

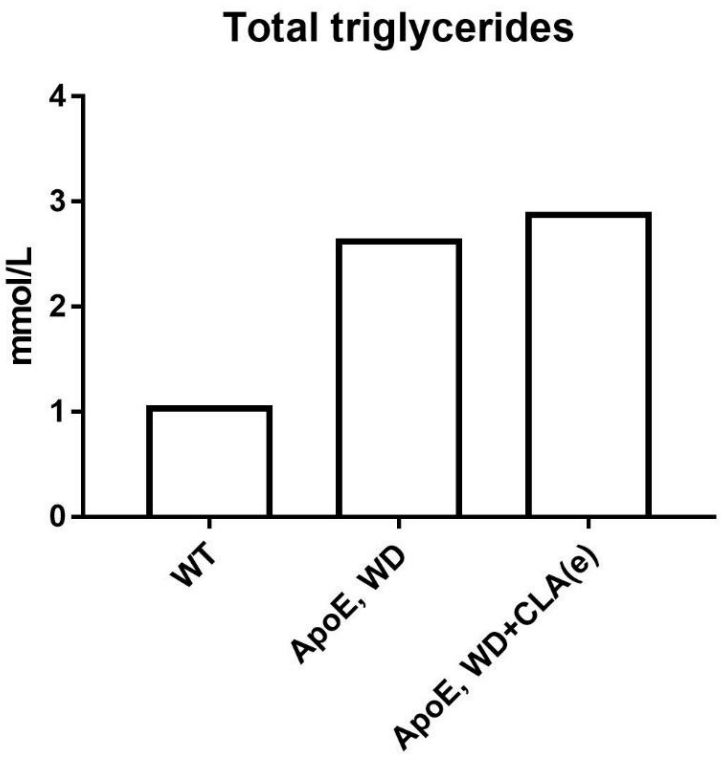


Figure 3.35: Total triglyceride level in WT and ApoE null mice at Week 12. Feeding WD led to increase in total triglyceride level. (n = 2)

Feeding WD led to marked increase in total triglycerides detectable at Week 12 (Figure 3.35).

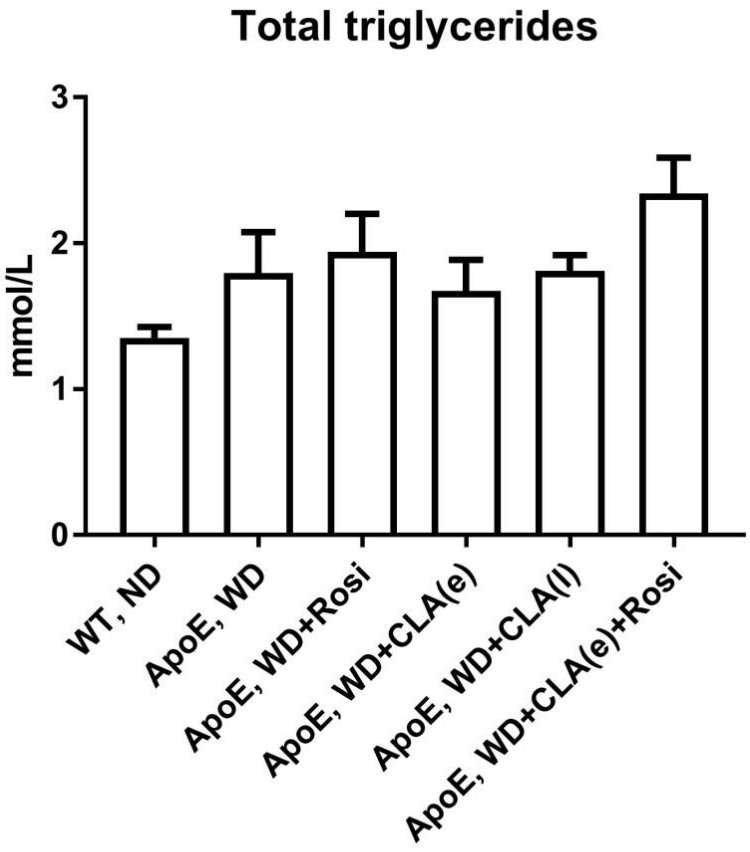


Figure 3.36: Total triglyceride level at Week 20 in WT and ApoE null mice.

Triglyceride level for ApoE, WD+CLA(e)+Rosi was the highest among all treatment groups, but none of the treatment group was found to have any statistically significant difference with each other at Week 20 (Figure 3.36).

3.12.5 Free fatty acids

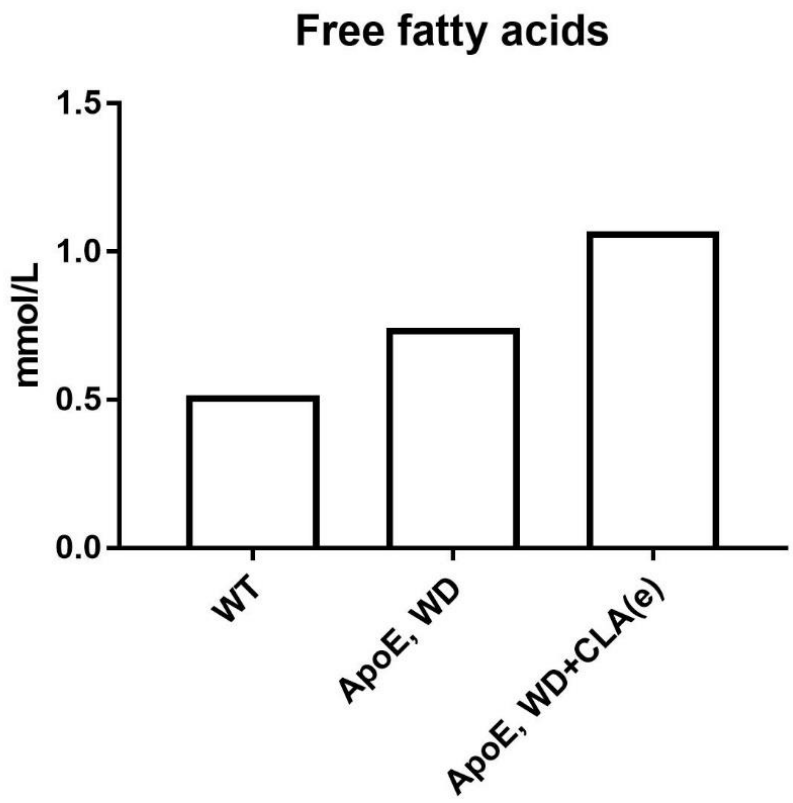


Figure 3.37: Free fatty acid level in WT and ApoE null mice at Week 12. Generally, feeding WD led to increase in free fatty acid level. (n = 2)

Feeding WD led to increase in free fatty acids, and early administration of CLA increased FFA further (Figure 3.37).

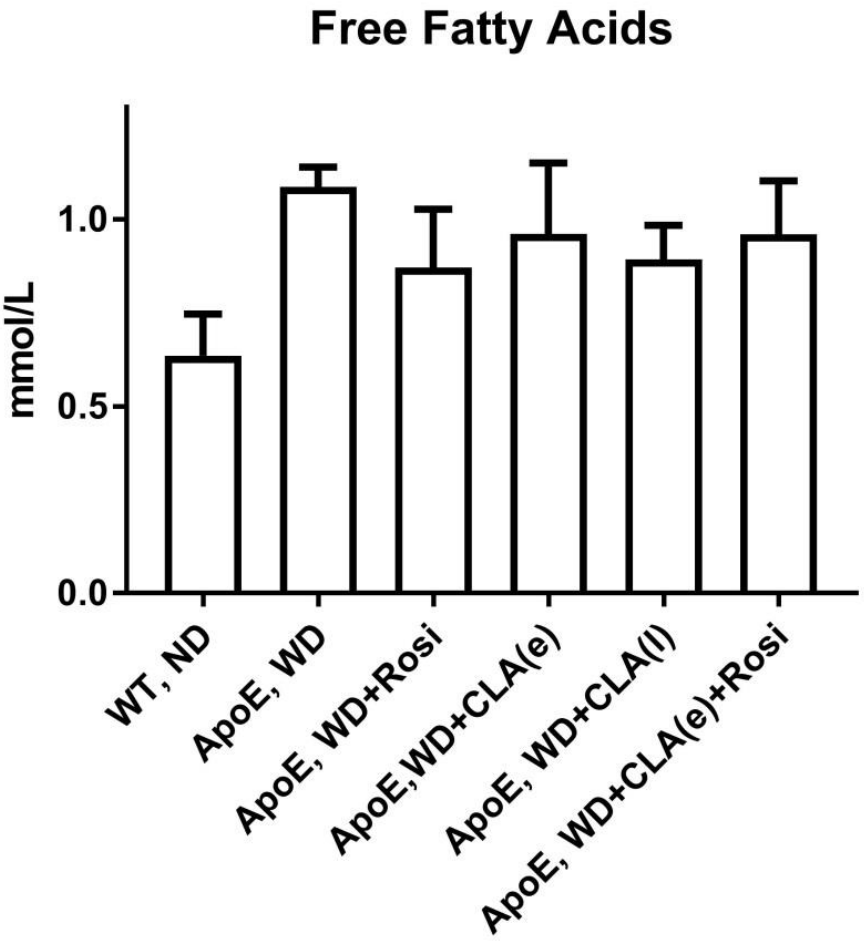


Figure 3.38: Free fatty acid level in WT and ApoE null mice at Week 20. Generally, feeding WD led to increase in free fatty acid level.

There was no significant difference in free fatty acids (FFA) among all treatment groups at Week 20 (Figure 3.38).

3.13 Insulin resistance indices

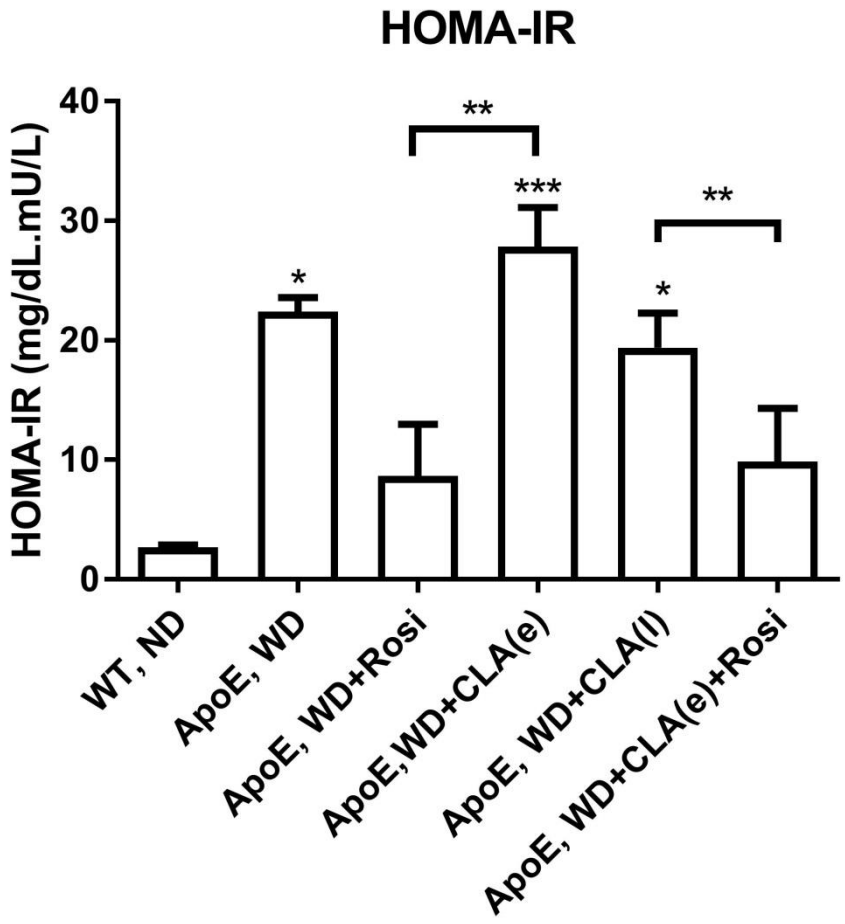


Figure 3.39: Homeostatic model of insulin resistance (HOMA-IR) in WT and ApoE null mice at Week 20. Feeding WD and administration of CLA mixture either early or late led to increase in insulin resistance, whereas administration of rosiglitazone led to attenuated increase in insulin resistance.

* $p < 0.05$; ** $p < 0.01$; *** $p < 0.001$

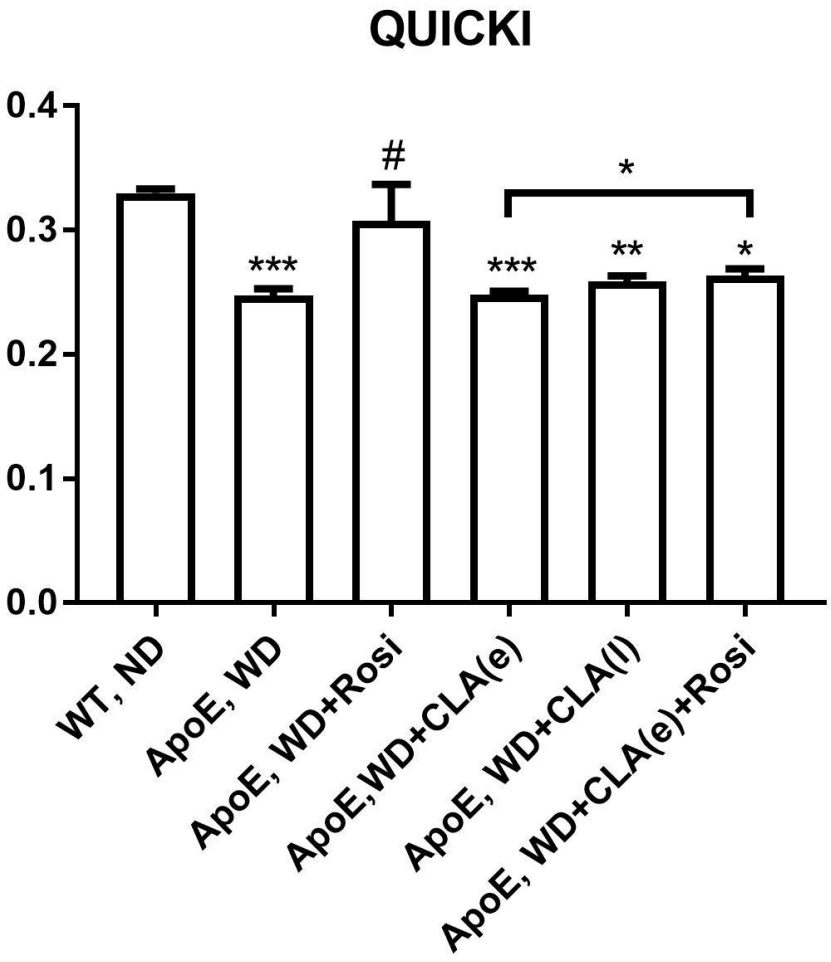


Figure 3.40: Quantitative Insulin Sensitivity Check Index (QUICKI) of WT and ApoE null mice at Week 20. Feeding WD to ApoE null mice led to increase in insulin resistance, which is indicated by decreased QUICKI. Administration of rosiglitazone alone rescued QUICKI to WT level, however CLA has no effect in conferring improvement in insulin resistance and antagonised rosiglitazone.

* $p < 0.05$; ** $p < 0.01$; *** $p < 0.001$; # $p < 0.05$ vs. ApoE, WD

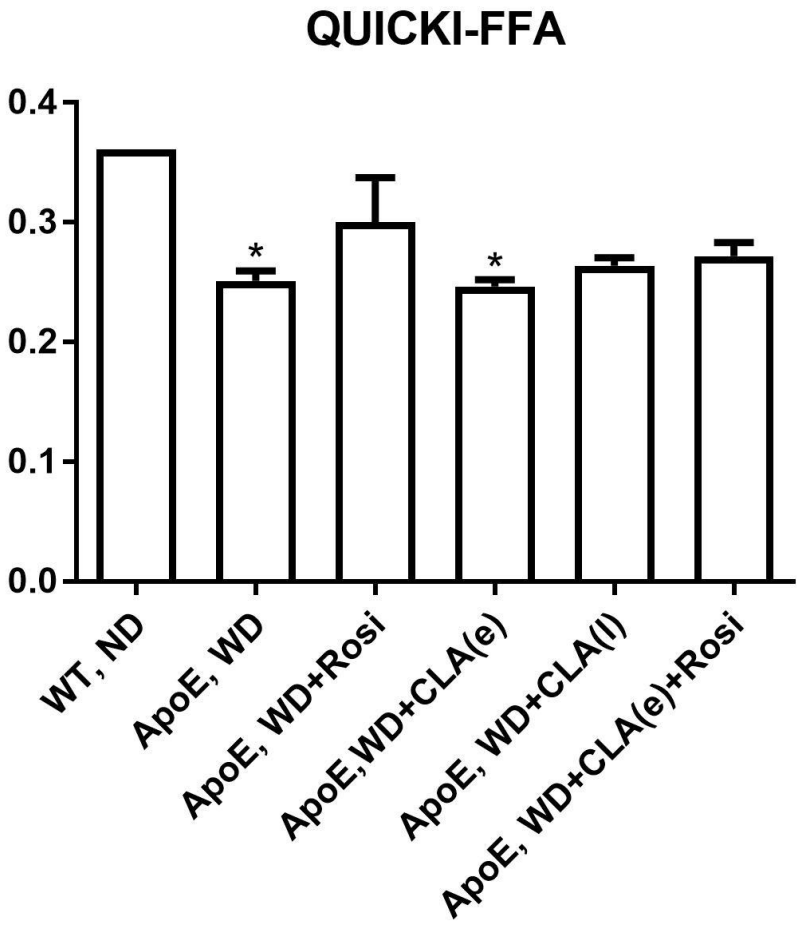


Figure 3.41: Revised Quantitative Insulin Sensitivity Check Index (QUICKI-FFA) of WT and ApoE null mice at Week 20. Feeding WD to ApoE null mice led to increase in insulin resistance, which is indicated by decreased QUICKI-FFA.

** $p < 0.01$; *** $p < 0.001$

Insulin resistance indices were tabulated as HOMA-IR (Figure 3.39), QUICKI (Figure 3.40) and QUICKI-FFA (Figure 3.41), respectively. QUICKI is derived using the same information used to calculate HOMA-IR, which is the reciprocal of the sum of the logarithm of HOMA and logarithm of a constant. QUICKI-FFA incorporates an additional parameter of free fatty acid. QUICKI-FFA is suggested to be better correlated with insulin sensitivity measured by euglycemic hyperinsulinemic clamp in a variety of insulin resistant states[141], owing to the fact

that insulin inhibits lipolysis in adipocytes[142,143] and the presence of free fatty acids leads to insulin resistance[144]. HOMA-IR, QUICKI and QUICKI-FFA showed increase in insulin resistance in all WD fed mice regardless of treatment compared to wild type mice. Feeding high fat diet in ApoE, WD led to 8.3-fold increase in HOMA-IR (Figure 3.39, $p < 0.05$) and 30% decrease in QUICKI-FFA (Figure 3.40, $p < 0.001$). ApoE, WD+CLA(e) was the most insulin resistant of all groups, that has 9.4-fold increase in HOMA-IR (Figure 3.39, $p < 0.001$) and 31.7% decrease in QUICKI-FFA (Figure 3.40, $p < 0.001$). The increase in insulin resistance in ApoE, WD+CLA(l) was also notable with an increase in HOMA-IR at 7.2 fold (Figure 3.39, $p < 0.05$) and decrease in QUICKI-FFA at 26.9% (Figure 3.40, $p < 0.01$). Administration of rosiglitazone in ApoE, WD+Rosi and ApoE, WD+CLA(e)+Rosi groups attenuated increase in insulin resistance, albeit with an approximately 25.7% reduction in QUICKI-FFA (Figure 3.40).

CHAPTER 4

Discussion

As rosiglitazone has led to non-negligible side effects especially on the cardiovascular system, we sought to ameliorate its side effects without abandoning the usage of this potent PPARγ ligand. We hypothesized that side effects may be ameliorated by any of the three strategies: substituting rosiglitazone with alternative PPAR agonists, concurrent activation of PPAR isotypes or administering competitive ligands. We have chosen CLA, since they have been demonstrated to confer health benefits in diabetes and cardiovascular diseases. CLA are known to be agonists of PPARα and PPARγ that binds to their receptor with lower affinity than pharmacological agonists[109,110]. The success of ameliorating the side effects of rosiglitazone would probably consider a step forward in management of MetS and T2DM.

4.1 *In vitro* findings

Our findings established that c9,t11-CLA is able to act directly on liver cells to reduce gluconeogenesis by suppressing the PEPCK and this effect was comparable to rosiglitazone, a PPAR agonist. However, the exposure of t10,c12 CLA on liver cells has modulated neither the HGP nor the levels of gluconeogenic enzymes. Of note, t10,c12 CLA had abrogated the effects of rosiglitazone on HGP. Taken together, our findings suggest the isomer-specific effects of CLA and the possibilities of dairy food constituents interacting with PPAR activation or inhibition to bring about health benefits, which fall into the category of functional foods. Functional food is defined as “any food or food ingredient that provides health benefit beyond its traditional nutritional value” by the Institute of Medicine Food and Nutrition Board[145]. Unfortunately, recent clinical studies on the effect of CLA in glucose homeostasis has been inconsistent and beneficial effects may not be apparent in low dose and short term (<16 weeks), but well tolerated across subjects in terms of safety[146].

In T2DM, the increase in hepatic gluconeogenesis is due to elevated basal gluconeogenesis[147]. Hepatic gluconeogenesis contributes to 75% of hepatic glucose output in T2DM, with the rest contributed by glycogenolysis and glycogen cycling[148]. It was established that hepatic gluconeogenesis is less sensitive to inhibition by insulin compared to glycogenolysis[149]. Basal gluconeogenesis is unaffected by insulin[150,151]. The primacy of gluconeogenesis in T2DM is demonstrated by the overexpression of PEPCK in animal models, which developed T2DM-like state with selective hepatic insulin resistance[152,153]. Alternatively, persistent activation of gluconeogenic transcription factors leads to hepatic insulin resistance[154]. Although hepatic gluconeogenesis may not be the primary contributor to hyperglycemia, it is thought to contribute to a feedback loop that worsens insulin resistance over time. The improvement of metabolic profile in diabetic rats can be achieved by knocking down PEPCK[155]. Therefore, inhibition of hepatic gluconeogenesis is a viable strategy to alleviate hyperglycemia and other symptoms of T2DM. Since insulin is unable to reduce basal gluconeogenesis, compounds able to exert reduction in basal gluconeogenesis will be an area of interest, taken that CLA is able to reduce the activity of gluconeogenic enzymes at the transcriptional level. It is worth noting that the lowest concentration of CLA in Canwell *et al.* is equivalent to 17.8 μM, but significant reduction in gluconeogenesis was only observed at the equivalent of 71 μM[156]; whilst we managed to show the efficacy of CLA at 20 μM.

Rosiglitazone is an anti-diabetic drug belonging to a class of insulin sensitisers known as thiazolidinediones. Administration of rosiglitazone has been shown to inhibit hepatic gluconeogenesis[157]. Our experimental results demonstrated that the reduction in the rate of hepatic gluconeogenesis when the cells were treated with rosiglitazone and CLA corresponded to the expression level of PEPCK and G6P mRNA, except for the combination of rosiglitazone and c9,t11-CLA. Our observation for rosiglitazone is at odds with a previous

observation that reported no change in PEPCK mRNA levels[158]. PEPCK activity is controlled by the abundance of PEPCK protein in the liver, as the enzyme is neither regulated by allosteric binding nor phosphorylation/dephosphorylation[159].

It has been reviewed that PPARγ activity has an inverted U-shaped relationship with gluconeogenesis[160]; moreover the PPARγ antagonist GW 9662 has recently been shown to inhibit PEPCK expression in vivo[161]. GW 9662 binds to PPARγ at an IC50 of 3.3 nM[162], therefore the reduction of hepatic glucose production in the presence of GW 9662 is attributed to inhibition of PPARγ instead of CLA activation.

In spite of our result that centered on the dependence of PPARγ, the long held paradigm of activating PPAR as the key to treating metabolic diseases is now being challenged by recent discoveries. Rosiglitazone has traditionally been regarded as a potent and specific agonist for PPARγ[76], whereas CLA has been regarded as a weaker agonist with an IC50 difference between 940-2176 fold[110]. Emerging evidences are pointing to thiazolidinediones exerting insulin sensitising effect independent of the PPARγ pathway[158,163], that is further proven by reports of glitazone mimetics improving insulin sensitivity despite lacking of PPAR agonist activity[164]. It is essential to take note that this PPAR independence may involve no change in basal PPAR receptor activity. Instead, the authors proposed that modulation of mitochondrial biogenesis as well as direct modulation of mitochondrial metabolism contribute to the pharmacology of thiazolidinediones. There are emerging evidences pointing to mitochondrial targets for insulin sensitizing drugs. Thiazolidinediones have been shown to target the pyruvate carrier complexes of the mitochondria[165–167]. Under a similar context, metformin has been identified as an inhibitor of mitochondrial glycerophosphate dehydrogenase to suppress gluconeogenesis[168]. It is suggested that these insulin sensitizing drugs, rather than acting through a linear pathway of activating downstream targets, instead alter the cellular energy state by binding to mitochondrial proteins[169]. The change in mitochondrial energy state led to

a cellular response of increasing sensitivity to insulin. Based on our observations, it will be useful to determine PPAR independence action of CLA.

The c9,t11 isomer is the most abundant CLA isomer in nature. Hence, the single administration of c9,t11 is highly applicable to the consumption of CLA from dietary sources. The t10,c12 isomer is present in low natural abundance, but high amounts in artificial preparations of CLA mixtures sold commercially. The consumption of t10,c12-CLA in high amounts is relevant in CLA supplements, as these supplements are made from artificial CLA preparations.

A myriad of studies have showed that actions of CLA is isomer dependent. While the c9,t11 isomer is associated with increase of insulin sensitivity[98,170–174], the sole consumption of t10,c12 isomer is associated with adverse effects such as insulin resistance[102], lipoatrophy, hepatic steatosis and hyperinsulinemia[101,106,175] and adipose tissue inflammation[103]. In vivo, consumption of a mixture of c9,t11- and t10,c12-CLA increased serum HDL cholesterol, but led to insulin resistance in Wistar rats, leading to authors' suggestion that CLA supplement should be approached with caution for weight management[176]. Likewise, we have shown that combination of CLA mixture and rosiglitazone decreased insulin resistance but increased atherogenicity by virtue of serum non-HDL to HDL ratio in Sprague-Dawley rats[177]. In vitro, 1:1 CLA has been shown to inhibit glucose uptake in cultured primary rat adipocytes[178]. In order to account for our observations, t10,c12-CLA must either inhibit the ability of c9,t11-CLA and thiazolidinediones to bind to their mitochondrial targets, or antagonize the activity of PPARγ. While there are no publication describing the effect of t10,c12-CLA in modulating mitochondrial metabolism, evidences are emerging for t10,c12-CLA antagonism of activated PPARγ activity[179,180]. Since c9,t11- and t10,c12-CLA are equally as efficient in activating PPARγ [179], the outcome cannot be attributed to binding of CLA isomers to PPARγ per se, but

alternative pathways activated by CLA[101]. The pathways leading to direct suppression of hepatic gluconeogenesis is a subject of future investigation.

In summary, we have demonstrated that c9,t11-CLA is able to exert an insulin-like effect directly on the liver to bring about reduction in hepatic gluconeogenesis, that is mediated by reduction in PEPCK and G6P expression. In contrast, t10,c12-CLA increases hepatic gluconeogenesis by increasing G6P expression at the transcriptional level.

4.2 *In vivo* discussion

After establishing that c9,t11-CLA is effective in reducing hepatic glucose production and mutual non-interference between c9,t11-CLA and rosiglitazone, the utility of combining both agents was tested *in vivo*. The ApoE null mouse was utilized since it is a good model for diabetic dyslipidemia. In humans, much cholesterol circulates in LDL rather than HDL; hence human beings are prone to dyslipidemia and atherosclerosis especially under conditions of metabolic syndrome and T2DM. In contrast, mice have higher HDL level than LDL in circulation, rendering them generally resistant to atherosclerosis[127]. ApoE null mice develop severe hypercholesterolemia when fed high fat or Western diet[127,132]. In wild type mice, feeding Western diet also led to increase in plasma cholesterol and triglycerides, albeit milder than ApoE null mice[127].

ApoE null mice are leaner than wild type mice when fed a normal diet[130], due to increased sequestration of lipid in LDL particles and decreased efficiency in incorporating lipids into the subcutaneous tissue. Nevertheless, they develop obesity when fed a fat rich diet. For the purpose of our study, we used male mice because they were more susceptible to insulin resistance when fed high fat diet[181].

The cardiovascular safety of combining rosiglitazone and CLA supplements was assessed by examining serum parameters. The conferral of CLA health benefits has been known to be isomer dependent. In a study using C57Bl/6J mice, c9,t11-CLA did not lead to insulin resistance, but t10,c12-CLA and 1:1 CLA mix led to insulin resistance[182]. In another study, 8:2 blend of c9,t11 and t10,c12-CLA led to resolution of early atherosclerosis[183], given that c9,t11 isomer is naturally abundant. A previous study using LDLr null mice fed high fat high sucrose diet found that t10,c12-CLA led to insulin resistance and slightly reduced plasma cholesterol[184]. The same group found that rosiglitazone was able to alleviate insulin resistance caused by t10,c12-CLA, but abrogated slight suppression of plasma cholesterol by t10,c12-CLA, and causes hepatomegaly[181].

Early administration of CLA mixture [WD+CLA(e), WD+CLA(e)+Rosi] led to significant reduction in body and adipose weight compared to WD mice, which points to lipoatrophy. In agreement with a previous study[107], CLA administered as 1:1 mixture of isomers led to lipoatrophy in mice. Given that the actions of CLA is isomer specific, this CLA dependent lipoatrophy is mediated by the t10,c12 isomer[106]. In fact, the administration of t10,c12-CLA to cause adipocyte inflammation and apoptosis in mice is a model of lipoatrophy. However, CLA mixture administered in rats does not led to lipoatrophy, due to the robustness of rat compared to mouse[185]. The adverse effects of 1:1 CLA mixture is espoused in increased total cholesterol, increased LDL and reduced HDL in ApoE, WD+CLA(e) mice and further exacerbated by rosiglitazone in ApoE, WD+CLA(e)+Rosi mice, taking consideration that ApoE knockout led to less efficient incorporation of circulating lipids into the adipose tissue. Therefore, the presence of ApoE null, lipoatrophy and glitazones may represent a dangerous triad when dyslipidemia is concerned.

Leptin is an adipocytokine involved in regulation of satiety. The onset of lipoatrophy led to low leptin levels, which was observed in CLA(e) groups. It has been shown that leptin

infusion in lipoatrophy could correct insulin resistance and hepatic steatosis[186,187]; transplantation of lipatrophic mice with adipose tissue lacking leptin failed to correct insulin resistance and hepatic steatosis[188]. For reference, a case report pointed that administration of pioglitazone has little effect on serum lipoproteins and glucose metabolism in a case lipoatrophic diabetes induced by juvenile dermatomyositis[189].

ApoE null mice are known to develop severe hepatosteatitis after being fed WD for seven weeks[134], which is indicated by increased liver weight when fed WD compared to wild type. The inducement of hepatic steatosis has been documented previously for rosiglitazone[190,191] and also t10,c12-CLA[101]. T10,c12-CLA has also been shown to increase liver triglyceride content[170]. In this study, it could be observed that administration of 1:1 CLA alone led to slight reduction in liver weight, co-administering 1:1 CLA with rosiglitazone failed to alleviate hepatic steatosis caused by the latter. We reasoned that in lipoatrophy, rosiglitazone may act on liver PPARγ to bring about hepatic steatosis that led to exacerbated LDL levels.

4.3 Limitations of study

The *in vivo* study utilised wild type mice fed normal diet as the baseline group, whereas a more convincing comparison can be achieved by using ApoE null mice fed normal diet. The normal diet used for the study was found to contain significant amount of linolenic acid that may interfere with observations. At Week 12, only two mice were sacrificed per group that precluded any statistical comparisons at that time point. Due to financial constraints, only 1:1 mixture of CLA isomers could be utilised for *in vivo* study, which made it impossible to single out the individual contribution of CLA isomers towards the observation.

4.4 Conclusions

Notwithstanding the usage of 1:1 CLA mixture in the *in vivo* study, it should be noted that health benefits of CLA is isomer dependent. t10,c12-CLA is associated with adverse effects when consumed in large amounts. It has to be noted that the reduction of blood glucose with the combination of 1:1 CLA with rosiglitazone is achieved by the indirect pathway rather than via direct action on hepatocytes, but *in vivo*, exacerbation of atherogenic dyslipidemia was also observed. This observation calls for the reconsideration of combining functional foods and drug regiment for the treatment of metabolic syndrome and diabetes as far as cardiovascular safety is concerned. The usage of CLA supplementation while undergoing treatment with a glitazone should be treated with caution, given that t10,c12-CLA is abundant in artificially prepared CLA, and this isomer not only interferes with glitazones to suppress gluconeogenesis directly in the liver, but also indirectly by causing lipoatrophy.

Instead of our expected amelioration of cardiovascular side effects by combining rosiglitazone with a mild competitive ligand, we conclude that early administration of 1:1 CLA led to lipoatrophy; the co-administration of 1:1 CLA with rosiglitazone exacerbates atherogenic dyslipidemia and hepatic steatosis.

References

1. Kaur, J. A Comprehensive Review on Metabolic Syndrome. *Cardiol. Res. Pract.* **2014**, 1–21 (2014).
2. Ford, E. S., Giles, W. H. & Dietz, W. H. Prevalence of the metabolic syndrome among US adults: findings from the third National Health and Nutrition Examination Survey. *JAMA* **287**, 356–359 (2002).
3. Beltrán-Sánchez, H., Harhay, M. O., Harhay, M. M. & McElligott, S. Prevalence and Trends of Metabolic Syndrome in the Adult U.S. Population, 1999-2010. *J. Am. Coll. Cardiol.* **62**, 697–703 (2013).
4. Palaniappan, L. P., Wong, E. C., Shin, J. J., Fortmann, S. P. & Lauderdale, D. S. Asian Americans have greater prevalence of metabolic syndrome despite lower body mass index. *Int. J. Obes. (Lond).* **35**, 393–400 (2011).
5. Nestel, P. *et al.* Metabolic syndrome: recent prevalence in East and Southeast Asian populations. *Asia Pac. J. Clin. Nutr.* **16**, 362–367 (2007).
6. Tan, C.-E., Ma, S., Wai, D., Chew, S.-K. & Tai, E.-S. Can we apply the National Cholesterol Education Program Adult Treatment Panel definition of the metabolic syndrome to Asians? *Diabetes Care* **27**, 1182–1186 (2004).
7. Grundy, S. M. *et al.* Diagnosis and Management of the Metabolic Syndrome. *Circulation* **112**, 2735–2752 (2005).
8. Ranasinghe, P., Mathangasinghe, Y., Jayawardena, R., Hills, A. P. & Misra, A. Prevalence and trends of metabolic syndrome among adults in the Asia-pacific region: A systematic review. *BMC Public Health* **17**, 1–9 (2017).
9. Ramli, A. S. *et al.* JIS definition identified more malaysian adults with metabolic syndrome compared to the NCEP-ATP III and IDF criteria. *Biomed Res. Int.* **2013**, (2013).
10. Laaksonen, D. E. *et al.* Metabolic syndrome and development of diabetes mellitus: Application and validation of recently suggested definitions of the metabolic syndrome in a prospective cohort study. *Am. J. Epidemiol.* **156**, 1070–1077 (2002).
11. Guariguata, L. *et al.* Global estimates of diabetes prevalence for 2013 and projections for 2035. *Diabetes Res. Clin. Pract.* **103**, 137–149 (2014).
12. Shaw, J. E., Sicree, R. A. & Zimmet, P. Z. Global estimates of the prevalence of diabetes for 2010 and 2030. *Diabetes Res. Clin. Pract.* **87**, 4–14 (2010).
13. Urban and rural components of population growth. *World Urbanization Prospects: The 2005 Revision* (2006).
14. Boudreau, D. M. *et al.* Health care utilization and costs by metabolic syndrome risk factors. *Metab. Syndr. Relat. Disord.* **7**, 305–314 (2009).
15. Nichols, G. A. & Moler, E. J. Metabolic syndrome components are associated with future medical costs independent of cardiovascular hospitalization and incident diabetes. *Metab. Syndr. Relat. Disord.* **9**, 127–133 (2011).
16. Rui, L. Energy Metabolism in the Liver. in *Comprehensive Physiology* vol. 141 177–197 (John Wiley & Sons, Inc., 2014).
17. Rosen, E. D. & Spiegelman, B. M. Adipocytes as regulators of energy balance and

glucose homeostasis. *Nature* **444**, 847–853 (2006).

18. Woods, S. C. Signals That Regulate Food Intake and Energy Homeostasis. *Science (80-.).* **280**, 1378–1383 (1998).
19. Zhang, J. & Liu, F. Tissue-specific insulin signaling in the regulation of metabolism and aging. *IUBMB Life* (2014) doi:10.1002/iub.1293.
20. Saltiel, A. R. & Kahn, C. R. Insulin signalling and the regulation of glucose and lipid metabolism. *Nature* **414**, 799–806 (2001).
21. Iynedjian, P. B., Jotterand, D., Nouspikel, T., Asfari, M. & Pilot, P. R. Transcriptional induction of glucokinase gene by insulin in cultured liver cells and its repression by the glucagon-cAMP system. *J. Biol. Chem.* **264**, 21824–21829 (1989).
22. Nouspikel, T. & Iynedjian, P. B. Insulin signalling and regulation of glucokinase gene expression in cultured hepatocytes. *Eur. J. Biochem.* **210**, 365–373 (1992).
23. Taniguchi, C. M., Emanuelli, B. & Kahn, C. R. Critical nodes in signalling pathways: insights into insulin action. *Nat. Rev. Mol. Cell Biol.* **7**, 85–96 (2006).
24. Oh, K.-J., Han, H.-S., Kim, M.-J. & Koo, S.-H. CREB and FoxO1: two transcription factors for the regulation of hepatic gluconeogenesis. *BMB Rep.* **46**, 567–74 (2013).
25. Jazet, I. M., Pijl, H. & Meinders, A. E. Adipose tissue as an endocrine organ: Impact on insulin resistance. *Neth. J. Med.* **61**, 194–212 (2003).
26. Coelho, M., Oliveira, T. & Fernandes, R. Biochemistry of adipose tissue: An endocrine organ. *Arch. Med. Sci.* **9**, 191–200 (2013).
27. Vekic, J., Zeljkovic, A., Stefanovic, A., Jelic-Ivanovic, Z. & Spasojevic-Kalimanovska, V. Obesity and dyslipidemia. *Metabolism* #pagerange# (2018) doi:10.1016/j.metabol.2018.11.005.
28. Brufau, G., Groen, A. K. & Kuipers, F. Reverse cholesterol transport revisited: Contribution of biliary versus intestinal cholesterol excretion. *Arterioscler. Thromb. Vasc. Biol.* **31**, 1726–1733 (2011).
29. Lewis, G. F. & Rader, D. J. New insights into the regulation of HDL metabolism and reverse cholesterol transport. *Circ. Res.* **96**, 1221–1232 (2005).
30. Drew, B. G., Rye, K.-A., Duffy, S. J., Barter, P. & Kingwell, B. A. The emerging role of HDL in glucose metabolism. *Nat. Rev. Endocrinol.* **8**, 237–245 (2012).
31. Lebovitz, H. Insulin resistance: definition and consequences. *Exp. Clin. Endocrinol. Diabetes* **109**, S135–S148 (2001).
32. Acheson, K. J. *et al.* Glycogen storage capacity and de novo lipogenesis during massive carbohydrate overfeeding in man. *Am. J. Clin. Nutr.* **48**, 240–247 (1988).
33. Chavez, J. A. & Summers, S. A. Lipid oversupply, selective insulin resistance, and lipotoxicity: molecular mechanisms. *Biochim. Biophys. Acta* **1801**, 252–65 (2010).
34. Choe, S. S., Huh, J. Y., Hwang, I. J., Kim, J. I. & Kim, J. B. Adipose tissue remodeling: Its role in energy metabolism and metabolic disorders. *Front. Endocrinol. (Lausanne).* **7**, 1–16 (2016).
35. Weisberg, S. P. *et al.* Obesity is associated with macrophage accumulation in adipose tissue. *J. Clin. Invest.* **112**, 1796–1808 (2003).
36. Guilherme, A., Virbasius, J. V, Puri, V. & Czech, M. P. Adipocyte dysfunctions linking obesity to insulin resistance and type 2 diabetes. *Nat. Rev. Mol. Cell Biol.* **9**,

367–77 (2008).

37. Tilg, H. & Moschen, A. R. Adipocytokines: mediators linking adipose tissue, inflammation and immunity. *Nat. Rev. Immunol.* **6**, 772–83 (2006).

38. Ouchi, N., Parker, J. L., Lugus, J. J. & Walsh, K. Adipokines in inflammation and metabolic disease. *Nat. Rev. Immunol.* **11**, 85–97 (2011).

39. Petersen, K. F. *et al.* The role of skeletal muscle insulin resistance in the pathogenesis of the metabolic syndrome. *Proc. Natl. Acad. Sci. U. S. A.* **104**, 12587–12594 (2007).

40. Skovsø, S. Modeling type 2 diabetes in rats using high fat diet and streptozotocin. *J. Diabetes Investig.* **5**, 349–358 (2014).

41. Snoek, F. J. Breaking the barriers to optimal glycaemic control--what physicians need to know from patients' perspectives. *Int. J. Clin. Pract. Suppl.* 80–84 (2002).

42. Malpass, A., Andrews, R. & Turner, K. M. Patients with Type 2 Diabetes experiences of making multiple lifestyle changes: A qualitative study. *Patient Educ. Couns.* **74**, 258–263 (2009).

43. Barlow, J. H., Bancroft, G. V & Turner, A. P. Self-management training for people with chronic disease: a shared learning experience. *J. Health Psychol.* **10**, 863–872 (2005).

44. Pernicova, I. & Korbonits, M. Metformin--mode of action and clinical implications for diabetes and cancer. *Nat. Rev. Endocrinol.* **10**, 143–56 (2014).

45. Proks, P., Reimann, F., Green, N., Gribble, F. & Ashcroft, F. Sulfonylurea Stimulation of Insulin Secretion. *Diabetes* **51**, S368–S376 (2002).

46. Sola, D. *et al.* Sulfonylureas and their use in clinical practice. *Arch. Med. Sci.* **11**, 840–848 (2015).

47. Soccio, R. E., Chen, E. R. & Lazar, M. A. Thiazolidinediones and the Promise of Insulin Sensitization in Type 2 Diabetes. *Cell Metab.* **20**, 573–591 (2014).

48. Kahn, C. R., Chen, L. & Cohen, S. E. Unraveling the mechanism of action of thiazolidinediones. *J. Clin. Invest.* **106**, 1305–1307 (2000).

49. Cronet, P. *et al.* Structure of the PPARα and -γ ligand binding domain in complex with AZ 242; ligand selectivity and agonist activation in the PPAR family. *Structure* **9**, 699–706 (2001).

50. Klinge, C. M. Estrogen receptor interaction with co-activators and co-repressors☆. *Steroids* **65**, 227–251 (2000).

51. Kumar, R. & Thompson, E. B. The structure of the nuclear hormone receptors. *Steroids* **64**, 310–319 (1999).

52. Nettles, K. W. Insights into PPARγ from structures with endogenous and covalently bound ligands. *Nat. Struct. & Mol. Biol.* **15**, 893–895 (2008).

53. Nolte, R. T. *et al.* Ligand binding and co-activator assembly of the peroxisome proliferator-activated receptor-gamma. *Nature* **395**, 137–143 (1998).

54. Wang, Y.-X. PPARs: diverse regulators in energy metabolism and metabolic diseases. *Cell Res.* **20**, 124–137 (2010).

55. Contreras, A. V, Torres, N. & Tovar, A. R. PPAR-α as a key nutritional and environmental sensor for metabolic adaptation. *Adv. Nutr.* **4**, 439–52 (2013).

56. Ahmadian, M. *et al.* PPARγ signaling and metabolism: the good, the bad and the

future. *Nat. Med.* **99**, 557–566 (2013).

57. Berger, J. & Moller, D. E. The mechanisms of action of PPARs. *Annu. Rev. Med.* **53**, 409–435 (2002).

58. Goldberg, R. B. *et al.* A comparison of lipid and glycemic effects of pioglitazone and rosiglitazone in patients with type 2 diabetes and dyslipidemia. *Diabetes Care* **28**, 1547–1554 (2005).

59. Camp, H. S. *et al.* Differential activation of peroxisome proliferator-activated receptor-gamma by troglitazone and rosiglitazone. *Diabetes* **49**, 539–547 (2000).

60. Chandra, V. *et al.* Structure of the intact PPAR-gamma-RXR- nuclear receptor complex on DNA. *Nature* **456**, 350–356 (2008).

61. Varga, T., Czimmerer, Z. & Nagy, L. PPARs are a unique set of fatty acid regulated transcription factors controlling both lipid metabolism and inflammation. *Biochim. Biophys. Acta* **1812**, 1007–22 (2011).

62. Rosen, E. D. *et al.* PPARγ is required for the differentiation of adipose tissue in vivo and in vitro. *Mol. Cell* **4**, 611–617 (1999).

63. Barak, Y. *et al.* PPARγ is required for placental, cardiac, and adipose tissue development. *Mol. Cell* **4**, 585–595 (1999).

64. He, W. *et al.* Adipose-specific peroxisome proliferator-activated receptor gamma knockout causes insulin resistance in fat and liver but not in muscle. *Proc. Natl. Acad. Sci. U. S. A.* **100**, 15712–15717 (2003).

65. Imai, T. *et al.* Peroxisome proliferator-activated receptor gamma is required in mature white and brown adipocytes for their survival in the mouse. *Proc. Natl. Acad. Sci. U. S. A.* **101**, 4543–4547 (2004).

66. Sugii, S. *et al.* PPARgamma activation in adipocytes is sufficient for systemic insulin sensitization. *Proc. Natl. Acad. Sci. U. S. A.* **106**, 22504–22509 (2009).

67. Gavrilova, O. *et al.* Liver peroxisome proliferator-activated receptor gamma contributes to hepatic steatosis, triglyceride clearance, and regulation of body fat mass. *J. Biol. Chem.* **278**, 34268–34276 (2003).

68. Hevener, A. L. *et al.* Muscle-specific Pparg deletion causes insulin resistance. *Nat. Med.* **9**, 1491–1497 (2003).

69. Chen, L. *et al.* Muscle-specific PPARgamma deficient mice develop insulin resistance but respond normally to thiazolidinediones. *J. Clin. Invest.* **112**, 608–618 (2003).

70. Kersten, S. Integrated physiology and systems biology of PPARα. *Mol. Metab.* **3**, 354–71 (2014).

71. Duval, C., Müller, M. & Kersten, S. PPARα and dyslipidemia. *Biochim. Biophys. Acta - Mol. Cell Biol. Lipids* **1771**, 961–971 (2007).

72. Guerre-Millo, M. *et al.* Peroxisome proliferator-activated receptor α activators improve insulin sensitivity and reduce adiposity. *J. Biol. Chem.* **275**, 16638–16642 (2000).

73. Ye, J. M. *et al.* Peroxisome proliferator-activated receptor (PPAR)-alpha activation lowers muscle lipids and improves insulin sensitivity in high fat-fed rats: comparison with PPAR-gamma activation. *Diabetes* **50**, 411–417 (2001).

74. Haluzík, M. M. & Haluzík, M. PPAR-alpha and insulin sensitivity. *Physiol. Res.* **55**, 115–122 (2006).

75. Holden, P. R. & Tugwood, J. D. Peroxisome proliferator-activated receptor alpha: Role in rodent liver cancer and species differences. *J. Mol. Endocrinol.* **22**, 1–8 (1999).

76. Edvardsson, U. *et al.* Rosiglitazone (BRL49653), a PPARgamma-selective agonist, causes peroxisome proliferator-like liver effects in obese mice. *J. Lipid Res.* **40**, 1177–84 (1999).

77. Nissen, S. E. & Wolski, K. Rosiglitazone Revisited. *Arch. Intern. Med.* **170**, 1191–1201 (2010).

78. Nissen, S. E. & Wolski, K. Effect of rosiglitazone on the risk of myocardial infarction and death from cardiovascular causes. *N. Engl. J. Med.* **356**, 2457–2471 (2007).

79. Wilson, K. D. *et al.* Transcriptome alteration in the diabetic heart by rosiglitazone: Implications for cardiovascular mortality. *PLoS One* **3**, (2008).

80. U.S. Food and Drug Administration. FDA Drug Safety Communication: FDA requires removal of some prescribing and dispensing restrictions for rosiglitazone-containing diabetes medicines.

81. McGuire, D. K. & Inzucchi, S. E. New drugs for the treatment of diabetes mellitus - Part I: Thiazolidinediones and their evolving cardiovascular implications. *Circulation* **117**, 440–449 (2008).

82. Berneis, K. *et al.* Comparative effects of rosiglitazone and pioglitazone on fasting and postprandial low-density lipoprotein size and subclasses in patients with Type 2 diabetes. *Expert Opin. Pharmacother.* **9**, 343–349 (2008).

83. Holtcamp, W. Obesogens: An Environmental Link to Obesity. *Environmental Health Perspectives* vol. 120 (2012).

84. MacLean, C. D., Littenberg, B. & Kennedy, A. G. Limitations of diabetes pharmacotherapy: results from the Vermont Diabetes Information System study. *BMC Fam. Pract.* **7**, 50 (2006).

85. Southwell, A. & Eckland, D. Limitations of treatments available for the management of Type 2 diabetes: Results from an international survey of physicians. *Pr. Diabetes Int.* **15**, 112–116 (1998).

86. Banni, S. Conjugated linoleic acid metabolism. *Curr. Opin. Lipidol.* **13**, 261–266 (2002).

87. Pariza, M. W., Park, Y. & Cook, M. E. The biologically active isomers of conjugated linoleic acid. *Prog. Lipid Res.* **40**, 283–298 (2001).

88. Churruca, I., Fernández-Quintela, A. & Portillo, M. P. Conjugated linoleic acid isomers: differences in metabolism and biological effects. *Biofactors* **35**, 105–11 (2008).

89. Belury, M. a. Dietary conjugated linoleic acid in health: physiological effects and mechanisms of action. *Annu. Rev. Nutr.* **22**, 505–531 (2002).

90. Bhattacharya, A., Banu, J., Rahman, M., Causey, J. & Fernandes, G. Biological effects of conjugated linoleic acids in health and disease. *J. Nutr. Biochem.* **17**, 789–810 (2006).

91. Rodrigues Silva, R., Oliveira Rodrigues, L. B., de Melo Lisboa, M., Silva Pereira, M. M. & de Souza, S. O. Conjugated Linoleic Acid (CLA): A Review. *Int. J. Appl. Sci. Technol.* **4**, 154–170 (2014).

92. Ritzenthaler, K. L. *et al.* Estimation of conjugated linoleic acid intake by written

dietary assessment methodologies underestimates actual intake evaluated by food duplicate methodology. *J. Nutr.* **131**, 1548–1554 (2001).

93. Benjamin, S. & Spener, F. Conjugated linoleic acids as functional food: an insight into their health benefits. *Nutr. Metab. (Lond).* **6**, 36 (2009).

94. Kramer, J. K. *et al.* Analysis of conjugated linoleic acid and trans 18:1 isomers in synthetic and animal products. *Am. J. Clin. Nutr.* **79**, 1137S-1145S (2004).

95. Schmid, a., Collomb, M., Sieber, R. & Bee, G. Conjugated linoleic acid in meat and meat products: A review. *Meat Sci.* **73**, 29–41 (2006).

96. Chin, S. F., Liu, W., Storkson, J. M., Ha, Y. L. & Pariza, M. W. Dietary sources of conjugated dienoic isomers of linoleic acid, a newly recognized class of anticarcinogens. *J. Food Compos. Anal.* **5**, 185–197 (1992).

97. Pariza, M. W., Park, Y. & Cook, M. E. Conjugated linoleic acid and the control of cancer and obesity. *Toxicol. Sci.* **52**, 107–110 (1999).

98. Moloney, F. *et al.* Antidiabetic effects of cis-9, trans-11-conjugated linoleic acid may be mediated via anti-inflammatory effects in white adipose tissue. *Diabetes* **56**, 574–582 (2007).

99. Mollica, M. P. *et al.* c9,t11-Conjugated linoleic acid ameliorates steatosis by modulating mitochondrial uncoupling and Nrf2 pathway. *J. Lipid Res.* **55**, 837–849 (2014).

100. Nestel, P., Fujii, A. & Allen, T. The cis-9,trans-11 isomer of conjugated linoleic acid (CLA) lowers plasma triglyceride and raises HDL cholesterol concentrations but does not suppress aortic atherosclerosis in diabetic apoE-deficient mice. *Atherosclerosis* **189**, 282–287 (2006).

101. Clément, L. *et al.* Dietary trans-10,cis-12 conjugated linoleic acid induces hyperinsulinemia and fatty liver in the mouse. *J. Lipid Res.* **43**, 1400–1409 (2002).

102. Risérus, U., Arner, P., Brismar, K. & Vessby, B. Treatment with dietary trans10cis12 conjugated linoleic acid causes isomer-specific insulin resistance in obese men with the metabolic syndrome. *Diabetes Care* **25**, 1516–1521 (2002).

103. Poirier, H., Shapiro, J. S., Kim, R. J. & Lazar, M. a. Nutritional supplementation with trans-10, cis-12-conjugated linoleic acid induces inflammation of white adipose tissue. *Diabetes* **55**, 1634–1641 (2006).

104. Degrace, P. *et al.* Association of liver steatosis with lipid oversecretion and hypotriglyceridaemia in C57BL/6j mice fed trans-10,cis-12-linoleic acid. *FEBS Lett.* **546**, 335–339 (2003).

105. Wendel, A. a, Purushotham, A., Liu, L.-F. & Belury, M. a. Conjugated linoleic acid fails to worsen insulin resistance but induces hepatic steatosis in the presence of leptin in ob/ob mice. *J. Lipid Res.* **49**, 98–106 (2008).

106. Poirier, H., Niot, I., Clément, L., Guerre-Millo, M. & Besnard, P. Development of conjugated linoleic acid (CLA)-mediated lipoatrophic syndrome in the mouse. *Biochimie* **87**, 73–79 (2005).

107. Tsuboyama-Kasaoka, N. *et al.* Conjugated linoleic acid supplementation reduces adipose tissue by apoptosis and develops lipodystrophy in mice. *Diabetes* **49**, 1534–1542 (2000).

108. Tricon, S. *et al. Opposing effects of cis-9,trans-11 and trans-10,cis-12 conjugated*

linoleic acid on blood lipids in healthy humans. The American journal of clinical nutrition vol. 80 (2004).

109. Moya-Camarena, S. Y., Vanden Heuvel, J. P., Blanchard, S. G., Leesnitzer, L. A. & Belury, M. A. Conjugated linoleic acid is a potent naturally occurring ligand and activator of PPARalpha. *J. Lipid Res.* **40**, 1426–33 (1999).

110. Belury, M., Moya-Camarena, S. & Lu, M. Conjugated linoleic acid is an activator and ligand for peroxisome proliferator-activated receptor-gamma (PPARγ). *Nutr. Res.* **22**, 817–824 (2002).

111. Benjamin, S., Hanhoff, T., Börchers, T. & Spener, F. An improved molecular test system for the screening of human PPAR transactivation by conjugated linoleic acid isomers and their precursor fatty acids. *Eur. J. Lipid Sci. Technol.* **107**, 706–715 (2005).

112. Brown, J. M. *et al.* Isomer-specific regulation of metabolism and PPARgamma signaling by CLA in human preadipocytes. *J. Lipid Res.* **44**, 1287–1300 (2003).

113. Sakuma, S. *et al.* cis9, trans11-Conjugated Linoleic Acid Differentiates Mouse 3T3-L1 Preadipocytes into Mature Small Adipocytes through Induction of Peroxisome Proliferator-activated Receptor γ. *J. Clin. Biochem. Nutr.* **47**, 167–173 (2010).

114. Kennedy, A., Chung, S., LaPoint, K., Fabiyi, O. & McIntosh, M. K. Trans-10, cis-12 conjugated linoleic acid antagonizes ligand-dependent PPARgamma activity in primary cultures of human adipocytes. *J. Nutr.* **138**, 455–461 (2008).

115. Yu, J., Yu, B., Jiang, H. & Chen, D. Conjugated linoleic acid induces hepatic expression of fibroblast growth factor 21 through PPAR-α. *British Journal of Nutrition* vol. 107 461–465 (2012).

116. Kim, Y. il *et al.* Potent PPARα activator derived from tomato juice, 13-oxo-9,11-octadecadienoic acid, decreases plasma and hepatic triglyceride in obese diabetic mice. *PLoS One* **7**, 1–8 (2012).

117. Morgan, D. M. L. Tetrazolium (MTT) Assay for Cellular Viability and Activity. in *Polyamine Protocols* 179–184 (Humana Press, 1998). doi:10.1385/0-89603-448-8:179.

118. Matsumoto, M. & Sakai, M. Glucose Production Assay in Primary Mouse Hepatocytes. *Bio-Protocol* **2**, 5–8 (2012).

119. NP-40 cell lysis buffer. *Cold Spring Harb. Protoc.* **2007**, pdb.rec11188 (2007).

120. Kruger, N. J. The Bradford Method for Protein Quantitation. in *Protein Protocols Handbook, The* (ed. Walker, J. M.) 15–22 (Humana Press, 2002). doi:10.1385/1-59259-169-8:15.

121. Tachibana, K. *et al.* Gene expression profiling of potential peroxisome proliferator-activated receptor (PPAR) target genes in human hepatoblastoma cell lines inducibly expressing PPAR isoforms. *Nucl. Recept.* **3**, 1–17 (2005).

122. Kim, H.-J., Jee, H. J. & Yun, J. DNA damage induces down-regulation of PEPCK and G6P gene expression through degradation of PGC-1α. *Acta Biochim. Biophys. Sin. (Shanghai).* **43**, 589–594 (2011).

123. Akamine, R. *et al.* Usefulness of the 5′ region of the cDNA encoding acidic ribosomal phosphoprotein P0 conserved among rats, mice, and humans as a standard probe for gene expression analysis in different tissues and animal species. *J. Biochem. Biophys. Methods* **70**, 481–486 (2007).

124. Yoon, J. C. *et al.* Control of hepatic gluconeogenesis through the transcriptional coactivator PGC-1. *Nature* **413**, 131–138 (2001).

125. Akamine, R. *et al.* Usefulness of the 5′ region of the cDNA encoding acidic ribosomal phosphoprotein P0 conserved among rats, mice, and humans as a standard probe for gene expression analysis in different tissues and animal species. *J. Biochem. Biophys. Methods* **70**, 481–486 (2007).

126. Schmittgen, T. D. & Livak, K. J. Analyzing real-time PCR data by the comparative CT method. *Nat. Protoc.* **3**, 1101–1108 (2008).

127. Plump, A. S. *et al.* Severe hypercholesterolemia and atherosclerosis in apolipoprotein E-deficient mice created by homologous recombination in ES cells. *Cell* **71**, 343–353 (1992).

128. Piedrahita, J. A., Zhang, S. H., Hagaman, J. R., Oliver, P. M. & Maeda, N. Generation of mice carrying a mutant apolipoprotein E gene inactivated by gene targeting in embryonic stem cells. *Proc. Natl. Acad. Sci.* **89**, 4471–4475 (1992).

129. van Ree, J. H. *et al.* Diet-induced hypercholesterolemia and atherosclerosis in heterozygous apolipoprotein E-deficient mice. *Atherosclerosis* **111**, 25–37 (1994).

130. Schreyer, S. A., Lystig, T. C., Vick, C. M. & LeBoeuf, R. C. Mice deficient in apolipoprotein E but not LDL receptors are resistant to accelerated atherosclerosis associated with obesity. *Atherosclerosis* **171**, 49–55 (2003).

131. Zhang, S. H., Reddick, R. L., Piedrahita, J. A. & Maeda, N. Spontaneous hypercholesterolemia and arterial lesions in mice lacking apolipoprotein E. *Science (80-.).* **258**, 468–471 (1992).

132. Nakashima, Y., Plump, A. S., Raines, E. W., Breslow, J. L. & Ross, R. ApoE-deficient mice develop lesions of all phases of atherosclerosis throughout the arterial tree. *Arterioscler. Thromb. Vasc. Biol.* **14**, 133–140 (1994).

133. Reddick, R. L., Zhang, S. H. & Maeda, N. Atherosclerosis in mice lacking apo E. Evaluation of lesional development and progression. *Arterioscler. Thromb.* **14**, 141–147 (1994).

134. Schierwagen, R. *et al.* Seven weeks of Western diet in apolipoprotein-E-deficient mice induce metabolic syndrome and non-alcoholic steatohepatitis with liver fibrosis. *Sci. Rep.* **5**, 1–14 (2015).

135. Mohankumar, S. K. *et al.* Dietary supplementation of trans-11-vaccenic acid reduces adipocyte size but neither aggravates nor attenuates obesity-mediated metabolic abnormalities in fa/fa Zucker rats. *Br. J. Nutr.* 1–9 (2012) doi:10.1017/S000711451200339X.

136. Hřebíček, J., Janout, V., Malinčíková, J., Horáková, D. & Čížek, L. Detection of Insulin Resistance by Simple Quantitative Insulin Sensitivity Check Index QUICKI for Epidemiological Assessment and Prevention. *J. Clin. Endocrinol. Metab.* **87**, 144–144 (2002).

137. Perseghin, G. Incorporation of the Fasting Plasma FFA Concentration into QUICKI Improves Its Association with Insulin Sensitivity in Nonobese Individuals. *J. Clin. Endocrinol. Metab.* **86**, 4776–4781 (2001).

138. Hatting, M., Tavares, C. D. J., Sharabi, K., Rines, A. K. & Puigserver, P. Insulin regulation of gluconeogenesis. *Ann. N. Y. Acad. Sci.* **1411**, 21–35 (2018).

139. Yang, S. *et al.* Rosiglitazone Inhibits Expression and Secretion of PEDF in Adipose

Tissue and Liver of Male SD Rats Via a PPAR-γ Independent Mechanism. *Endocrinology* **155**, 941–950 (2014).

140. Tan, X.-W., Xia, H., Xu, J.-H. & Cao, J.-G. Induction of apoptosis in human liver carcinoma HepG2 cell line by 5-allyl-7-gen-difluoromethylenechrysin. *World J. Gastroenterol.* **15**, 2234 (2009).

141. Rabasa-Lhoret, R. *et al.* Modified Quantitative Insulin Sensitivity Check Index Is Better Correlated to Hyperinsulinemic Glucose Clamp than Other Fasting-Based Index of Insulin Sensitivity in Different Insulin-Resistant States. *J. Clin. Endocrinol. Metab.* **88**, 4917–4923 (2003).

142. Rahn, T. *et al.* Essential role of phosphatidylinositol 3-kinase in insulin-induced activation and phosphorylation of the cGMP-inhibited cAMP phosphodiesterase in rat adipocytes studies using the selective inhibitor wortmannin. *FEBS Lett.* **350**, 314–318 (1994).

143. Morimoto, C., Tsujita, T. & Okuda, H. Antilipolytic actions of insulin on basal and hormone-induced lipolysis in rat adipocytes. *J Lipid Res* **39**, 957–962 (1998).

144. Sears, B. & Perry, M. The role of fatty acids in insulin resistance. *Lipids Health Dis.* **14**, 1–9 (2015).

145. Institute of Medicine. Enhancing the Food Supply. in *Opportunities in the Nutrition and Food Sciences* (eds. Thomas, P. R. & Earl, R.) 109 (National Academies Press, 1994). doi:10.17226/2133.

146. Kim, J. H., Kim, Y. Y. J., Kim, Y. Y. J. & Park, Y. Conjugated Linoleic Acid: Potential Health Benefits as a Functional Food Ingredient. *Annu. Rev. Food Sci. Technol.* **7**, 221–244 (2016).

147. Erion, D. M. *et al.* SirT1 knockdown in liver decreases basal hepatic glucose production and increases hepatic insulin responsiveness in diabetic rats. *Proc. Natl. Acad. Sci. U. S. A.* **106**, 11288–93 (2009).

148. Hundal, R. S. *et al.* Mechanism by which metformin reduces glucose production in type 2 diabetes. *Diabetes* **49**, 2063–2069 (2000).

149. Girard, J. The Inhibitory Effects of Insulin on Hepatic Glucose Production Are Both Direct and Indirect. *Diabetes* **55**, S65–S69 (2006).

150. He, L. *et al.* Transcriptional Co-activator p300 maintains basal hepatic gluconeogenesis. *J. Biol. Chem.* **287**, 32069–32077 (2012).

151. He, L. *et al.* Activation of basal gluconeogenesis by coactivator p300 maintains hepatic glycogen storage. *Mol. Endocrinol.* **27**, 1322–32 (2013).

152. Sun, Y. *et al.* Phosphoenolpyruvate carboxykinase overexpression selectively attenuates insulin signaling and hepatic insulin sensitivity in transgenic mice. *J. Biol. Chem.* **277**, 23301–23307 (2002).

153. Valera, A., Pujol, A., Pelegrin, M. & Bosch, F. Transgenic mice overexpressing phosphoenolpyruvate carboxykinase develop non-insulin-dependent diabetes mellitus. *Proc. Natl. Acad. Sci. U. S. A.* **91**, 9151–4 (1994).

154. Hogan, M. F. *et al.* Hepatic Insulin Resistance Following Chronic Activation of the CREB Coactivator CRTC2. *J. Biol. Chem.* **290**, 25997–26006 (2015).

155. Gómez-Valadés, A. G. *et al.* Overcoming diabetes-induced hyperglycemia through inhibition of hepatic phosphoenolpyruvate carboxykinase (GTP) with RNAi. *Mol.*

Ther. **13**, 401–410 (2006).

156. Cantwell, H., Devery, R., O'Shea, M. & Stanton, C. The effect of conjugated linoleic acid on the antioxidant enzyme defense system in rat hepatocytes. *Lipids* **34**, 833–839 (1999).

157. Gastaldelli, A. *et al.* The effect of rosiglitazone on the liver: Decreased gluconeogenesis in patients with type 2 diabetes. *J. Clin. Endocrinol. Metab.* **91**, 806–812 (2006).

158. Davies, G. F., Khandelwal, R. L., Wu, L., Juurlink, B. H. J. & Roesler, W. J. Inhibition of phosphoenolpyruvate carboxykinase (PEPCK) gene expression by troglitazone: a peroxisome proliferator-activated receptor-γ (PPARγ)-independent, antioxidant-related mechanism. *Biochem. Pharmacol.* **62**, 1071–1079 (2001).

159. Scott, D. K. *et al.* The Repression of Hormone-activated PEPCK Gene Expression by Glucose Is Insulin-independent but Requires Glucose Metabolism The Repression of Hormone-activated PEPCK Gene Expression by Glucose Is Insulin-independent but Requires Glucose Metabolism. *J. Biol. Chem.* **273**, 24145–24151 (1998).

160. Picard, F. & Auwerx, J. PPARγ and glucose homeostasis. *Annu. Rev. Nutr.* **22**, 167–197 (2002).

161. Kim, K. *et al.* RORα controls hepatic lipid homeostasis via negative regulation of PPARγ transcriptional network. *Nat. Commun.* **8**, 162 (2017).

162. Leesnitzer, L. M. *et al.* Functional Consequences of Cysteine Modification in the Ligand Binding Sites of Peroxisome Proliferator Activated Receptors by GW9662. *Biochemistry* **41**, 6640–6650 (2002).

163. Derlacz, R. A. *et al.* PPAR-gamma-independent inhibitory effect of rosiglitazone on glucose synthesis in primary cultured rabbit kidney-cortex tubules. *Biochem. Cell Biol.* **86**, 396–404 (2008).

164. Bolten, C. W. *et al.* Insulin sensitizing pharmacology of thiazolidinediones correlates with mitochondrial gene expression rather than activation of PPAR gamma. *Gene Regul. Syst. Biol.* **1**, 73–82 (2007).

165. Divakaruni, A. S. *et al.* Thiazolidinediones are acute, specific inhibitors of the mitochondrial pyruvate carrier. *Proc. Natl. Acad. Sci.* **110**, 5422–5427 (2013).

166. Colca, J. R. *et al.* Identification of a Mitochondrial Target of Thiazolidinedione Insulin Sensitizers (mTOT)-Relationship to Newly Identified Mitochondrial Pyruvate Carrier Proteins. *PLoS One* **8**, 1–10 (2013).

167. Wright, M. B., Bortolini, M., Tadayyon, M. & Bopst, M. Minireview: Challenges and opportunities in development of PPAR agonists. *Mol. Endocrinol.* **28**, 1756–68 (2014).

168. Madiraju, A. K. *et al.* Metformin suppresses gluconeogenesis by inhibiting mitochondrial glycerophosphate dehydrogenase. *Nature* **510**, 542–546 (2014).

169. Colca, J. R., Mcdonald, W. G. & Kletzien, R. F. Mitochondrial target of thiazolidinediones. *Diabetes, Obes. Metab.* **16**, 1048–1054 (2014).

170. Kelley, D. S. *et al.* Contrasting effects of t10,c12- and c9,t11-conjugated linoleic acid isomers on the fatty acid profiles of mouse liver lipids. *Lipids* **39**, 135–141 (2004).

171. Bissonauth, V. *et al.* The effects of t10,c12 CLA isomer compared with c9,t11 CLA isomer on lipid metabolism and body composition in hamsters. *J. Nutr. Biochem.* **17**, 597–603 (2006).

172. Choi, J. S., Koh, I.-U., Jung, M. H. & Song, J. Effects of three different conjugated linoleic acid preparations on insulin signalling, fat oxidation and mitochondrial function in rats fed a high-fat diet. *Br. J. Nutr.* **98**, 264–275 (2007).

173. Choi, J. S., Jung, M. H., Park, H. S. & Song, J. Effect of conjugated linoleic acid isomers on insulin resistance and mRNA levels of genes regulating energy metabolism in high-fat-fed rats. *Nutrition* **20**, 1008–1017 (2004).

174. de Almeida, M. M. *et al.* Butter naturally enriched in cis-9, trans-11 CLA prevents hyperinsulinemia and increases both serum HDL cholesterol and triacylglycerol levels in rats. *Lipids Health Dis.* **13**, 200 (2014).

175. Kennedy, A. *et al.* Inflammation and insulin resistance induced by trans-10, cis-12 conjugated linoleic acid depend on intracellular calcium levels in primary cultures of human adipocytes. *J. Lipid Res.* **51**, 1906–17 (2010).

176. Almeida, M. M. De *et al. Cis*-9, *trans*-11 and *trans*-10, *cis*-12 CLA Mixture does not Change Body Composition, Induces Insulin Resistance and Increases Serum HDL Cholesterol Level in Rats. *J. Oleo Sci.* **64**, 539–551 (2015).

177. Chai, B. K. *et al.* Co-administration of conjugated linoleic acid and rosiglitazone increases atherogenic co-efficicient and alters isoprenaline-induced vasodilatation in rats fed high fat diet. *Physiol. Res.* **in press**, (2018).

178. Pérez-Matute, P. *et al.* Conjugated linoleic acid inhibits glucose metabolism, leptin and adiponectin secretion in primary cultured rat adipocytes. *Mol. Cell. Endocrinol.* **268**, 50–58 (2007).

179. Granlund, L., Juvet, L. K., Pedersen, J. I. & Nebb, H. I. Trans10, cis12-conjugated linoleic acid prevents triacylglycerol accumulation in adipocytes by acting as a PPARgamma modulator. *J. Lipid Res.* **44**, 1441–1452 (2003).

180. Yeganeh, A., Taylor, C. G., Poole, J., Tworek, L. & Zahradka, P. Trans10, cis12 conjugated linoleic acid inhibits 3T3-L1 adipocyte adipogenesis by elevating β-catenin levels. *Biochim. Biophys. Acta - Mol. Cell Biol. Lipids* **1861**, 363–370 (2016).

181. Wang, S., Goodspeed, L., Turk, K. E., Houston, B. & Den Hartigh, L. J. Rosiglitazone improves insulin resistance mediated by 10,12 conjugated linoleic acid in a male mouse model of metabolic syndrome. *Endocrinology* **158**, 2848–2859 (2017).

182. Halade, G. V, Rahman, M. & Fernandes, G. Differential effects of conjugated linoleic acid isomers in insulin-resistant female. *J. Nutr. Biochem.* **21**, 332–337 (2010).

183. Toomey, S., Harhen, B., Roche, H. M., Fitzgerald, D. & Belton, O. Profound resolution of early atherosclerosis with conjugated linoleic acid. *Atherosclerosis* **187**, 40–9 (2006).

184. Den Hartigh, L. J. *et al.* Metabolically distinct weight loss by 10,12 CLA and caloric restriction highlight the importance of subcutaneous white adipose tissue for glucose homeostasis in mice. *PLoS One* **12**, 1–25 (2017).

185. Noto, A. *et al.* Conjugated linoleic acid reduces hepatic steatosis, improves liver function, and favorably modifies lipid metabolism in obese insulin-resistant rats. *Lipids* **41**, 179–188 (2006).

186. Shimomura, I., Hammer, R. E., Ikemoto, S., Brown, M. S. & Goldstein, J. L. Leptin reverses insulin resistance and diabetes mellitus in mice with congenital lipodystrophy. *Nature* **401**, 73–76 (1999).

187. Petersen, K. F. *et al.* Leptin reverses insulin resistance and hepatic steatosis in patients

with severe lipodystrophy. *J. Clin. Invest.* **109**, 1345–1350 (2002).

188. Colombo, C. *et al.* Transplantation of adipose tissue lacking leptin is unable to reverse the metabolic abnormalities associated with lipoatrophy. *Diabetes* **51**, 2727–2733 (2002).

189. Lawson, M. A. Lipoatrophic Diabetes: A Case Report with a Brief Review of the Literature. *J. Adolesc. Heal.* **44**, 94–95 (2009).

190. García-Ruiz, I. *et al.* Effects of rosiglitazone on the liver histology and mitochondrial function in ob/ob mice. *Hepatology* **46**, 414–423 (2007).

191. Hemmeryckx, B., Gaekens, M., Gallacher, D. J., Lu, H. R. & Lijnen, H. R. Effect of rosiglitazone on liver structure and function in genetically diabetic Akita Mice. *Basic Clin. Pharmacol. Toxicol.* **113**, 353–360 (2013).

192. Amplex® Red Glucose/Glucose Oxidase Assay Kit. https://assets.thermofisher.com/TFS-Assets/LSG/manuals/mp22189.pdf.

Supplementary Data

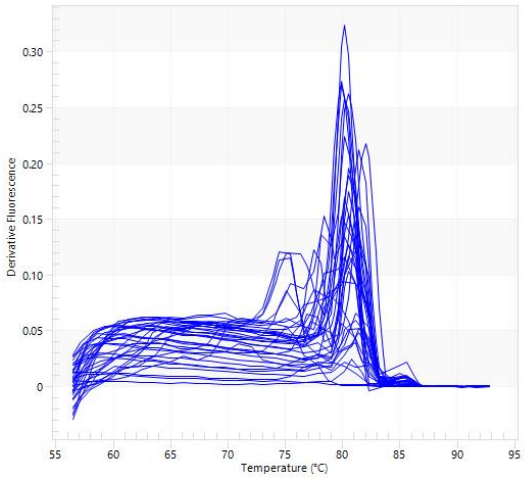
Table S1: HepG2 RNA concentration after treatment. During measurement, each sample were measured in duplicates for each attempt on a nanodrop machine. The readings were average of duplicates as recorded in the laboratory notebook.

Treatment	Concentration 1 (ng/µL)	Concentration 2 (ng/µL)
Untreated	634.0000	430.2692
Insulin 100 nM	338.4615	538.3462
Forskolin 10 µM	244.6154	436.1923
Rosiglitazone 10 µM	508.5385	457.1923
Fenofibrate 10 µM	65	74.1154
c9,t11-CLA 20 µM	317	437.2692
t10,c12-CLA 20 µM	350.8077	457.7308
Linoleic acid 20 µM	358.6538	439.1923
Rosiglitazone 10 µM + c9,t11-CLA 20 µM	389.2692	375.6538
Rosiglitazone 10 µM + t10,c12-CLA 20 µM	423.8077	402.0385
Rosiglitazone 10 µM + c9,t11-CLA 10 µM + t10,c12-CLA 10 µM	255.6538	317.2692
c9,t11-CLA 10 µM + t10,c12-CLA 10 µM	191.6538	313.2692

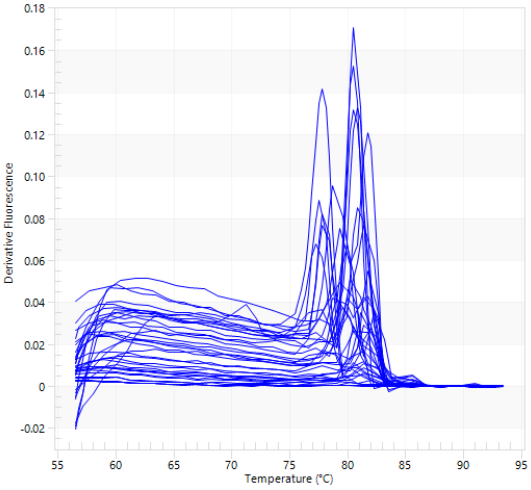
Table S2: HepG2 cDNA concentration. cDNA was synthesised based on the RNA concentration tabulated in Table S1, and have their concentration measured on a nanodrop machine. Samples were measured in duplicates, and have their average taken and recorded in the laboratory notebook.

Treatment	Concentration 1 (ng/µL)	Concentration 2 (ng/µL)
Untreated	537.1635	513
Insulin 100 nM	619.5673	462
Forskolin 10 µM	534.7596	519
Rosiglitazone 10 µM	517.9327	523
Fenofibrate 10 µM	-	-
c9,t11-CLA 20 µM	534.7596	362
t10,c12-CLA 20 µM	517.9327	366
Linoleic acid 20 µM	640.7692	454
Rosiglitazone 10 µM + c9,t11-CLA 20 µM	656.5385	536
Rosiglitazone 10 µM + t10,c12-CLA 20 µM	723.0769	530
Rosiglitazone 10 µM + c9,t11-CLA 10 µM + t10,c12-CLA 10 µM	458.5577	529
c9,t11-CLA 10 µM + t10,c12-CLA 10 µM	398.0769	534

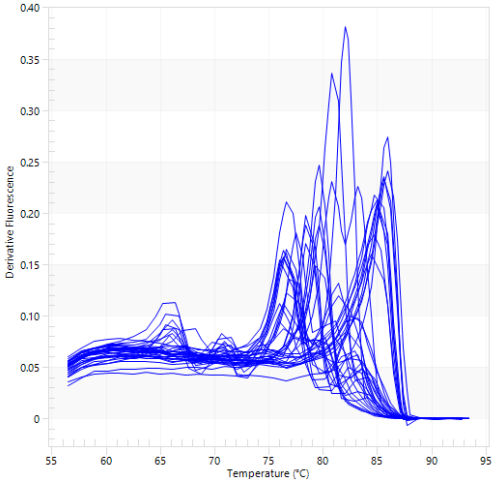
Figure S1: RT-qPCR melting curve of HepG2 RNA. Melting curves were generated after each qPCR run on Illumina Eco machine.



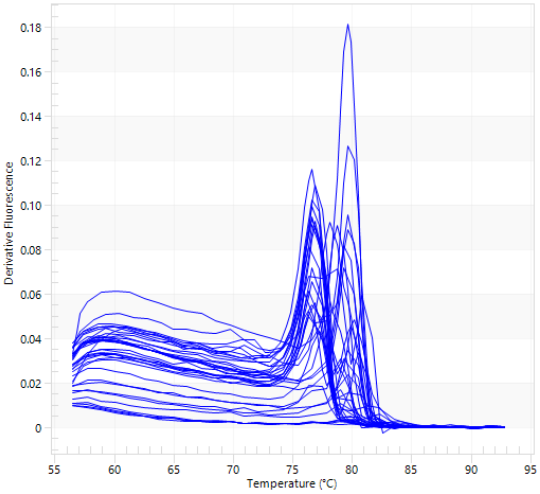
HepG2 PEPCK 1



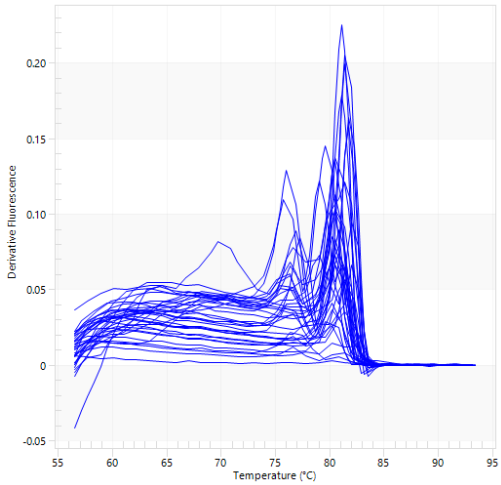
HepG2 PEPCK 2



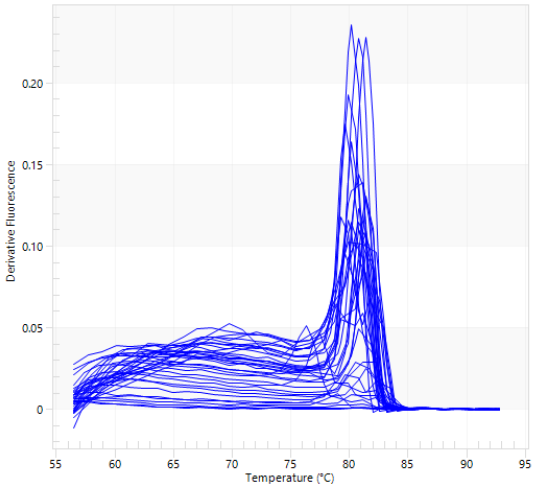
HepG2 G6P 1



HepG2 G6P 2



HepG2 36B4 1



HepG2 36B4 2

Appendices

Appendix 1 - Scientific principles behind the assays

Amplex Red Glucose Assay

In this assay, glucose oxidase reacts with glucose to form gluconolactone and hydrogen peroxide. In the presence of horseradish peroxidase, hydrogen peroxide reacts with Amplex Red to generate a red fluorescent oxidation product, resorufin. Resorufin has an absorbance maximum at 560 nm. Further details can be referred from manufacturer's documentation[192].

Bradford Assay

Bradford assay is based on non-covalent binding of Commassie Brilliant Blue G-250 to tertiary structures of proteins. Briefly, the Bradford reagent contains the dye in its anionic form, which is brown in colour. Interaction of the dye with the protein carboxyl groups, amino groups and hydrophobic regions stabilizes the cationic form of the dye, which is coloured blue.

100 µL of NP-40 was added to remaining HepG2 cells in a 12-well plate to obtain the respective protein extract. 5 µL was utilized for Bradford assay using the 96-well plate format. In each well, 250 µL Bradford reagent was added and mixed for 30 seconds and incubated at room temperature for 5 – 45 minutes. Absorbance was measured at 595 nm.

Reverse transcription quantitative polymerase chain reaction (RT-qPCR)

RT-qPCR is a method to detect gene expression. Briefly, extracted RNA was reverse transcribed with a reverse transcription kit into complementary DNA (cDNA), the kit used was Bioline Tetro cDNA synthesis kit (BLN#BIO-65042, Bioline, UK). This cDNA was then copied with DNA polymerase. The amplification product was detected using a dye, SYBR Green I that binds to double stranded DNA found in KAPA SYBR Fast qPCR Master Mix

(KAPA-KK4600, KAPA Biosystems, USA). The double stranded DNA is amplification product. Bound SYBR Green I emits green light at a wavelength of 520 nm.

The thermal profile for cDNA synthesis was

1. Incubate samples at 45°C for 30 minutes
2. Terminate reaction at 85°C for 5 minutes, chill products by switching to 4°C.

The thermal profile for RT-qPCR was

1. Initial incubation at 50°C for 2 minutes
2. Polymerase activation at 95°C for 3 minutes
3. Double strand separation at 95°C for 3 seconds
4. Strand elongation at 60°C for 25 seconds

Step 3 and 4 were repeated for 40 cycles.

The number of copies of DNA increases exponentially with each amplification cycle. The cycle number which amplification starts to become exponential is named the threshold cycle (Cq). High initial amount of cDNA gave a lower Cq. RT-qPCR result was calculated using the double delta T method as previously described[126].

LDL, HDL and total cholesterol assay

The assay kit utilizes cholesterol oxidase to generate products having absorbance at wavelength of 570 nm.

Triglyceride assay

The assay kit utilizes the action of lipase and oxidation of glycerol. First, triglycerides are hydrolysed into free fatty acids and glycerol. The resulting glycerol was oxidized to generate a product having an absorbance at wavelength of 570 nm.

Free fatty acid assay

The kit is based on the generation of coenzyme A derivatives of fatty acid and subsequent oxidation of fatty acid-coA to product products having absorbance of 570 nm.

Insulin, leptin and adiponectin assays

The assays to quantitate serum insulin, leptin and adiponectin are based on the principle of enzyme linked immunosorbent assay (ELISA). Briefly, extracted serum was placed in a pre-coated plate and washed. Then, primary antibody conjugated to biotin was incubated with hormone already bound to the plate. After washing, horseradish peroxidase conjugated to streptavidin was incubated. The enzyme activity was monitored in the presence of substrate 3,3',5,5'-tetramethylbenzidine, in which a blue colour product will be formed. Acidification turns the product yellow. The enzyme activity is measured by the increased absorbance at 450 nm subtracted by absorbance at 590 nm.

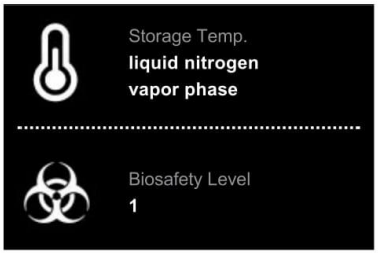
Appendix 2 – HepG2 Cell Line Data Sheet

ATCC

Product Sheet

Hep G2 [HEPG2] (ATCC® HB-8065™)

Please read this FIRST



Intended Use

This product is intended for research use only. It is not intended for any animal or human therapeutic or diagnostic use.

Complete Growth Medium

The base medium for this cell line is ATCC-formulated Eagle's Minimum Essential Medium, Catalog No. 30-2003. To make the complete growth medium, add the following components to the base medium: fetal bovine serum to a final concentration of 10%.

Citation of Strain

If use of this culture results in a scientific publication, it should be cited in that manuscript in the following manner: Hep G2 [HEPG2] (ATCC® HB-8065™)

American Type Culture Collection
PO Box 1549
Manassas, VA 20108 USA
www.atcc.org

800.638.6597 or 703.365.2700
Fax: 703.365.2750
Email: Tech@atcc.org

Or contact your local distributor

Description

Organism: *Homo sapiens*, human
Tissue: liver
Disease: hepatocellular carcinoma
Age: 15 years adolescent
Gender: male
Morphology: epithelial
Growth Properties: adherent
DNA Profile:
Amelogenin: X,Y
CSF1PO: 10,11
D13S317: 9,13
D16S539: 12,13
D5S818: 11,12
D7S820: 10
THO1: 9
TPOX: 8,9
vWA: 17
Cytogenetic Analysis: modal number = 55 (range = 50 to 60); has a rearranged chromosome 1

Batch-Specific Information

Refer to the Certificate of Analysis for batch-specific test results.

SAFETY PRECAUTION

ATCC highly recommends that protective gloves and clothing always be used and a full face mask always be worn when handling frozen vials. It is important to note that some vials leak when submersed in liquid nitrogen and will slowly fill with liquid nitrogen. Upon thawing, the conversion of the liquid nitrogen back to its gas phase may result in the vessel exploding or blowing off its cap with dangerous force creating flying debris.

Unpacking & Storage Instructions

1. Check all containers for leakage or breakage.
2. Remove the frozen cells from the dry ice packaging and immediately place the cells at a temperature below -130°C, preferably in liquid nitrogen vapor, until ready for use.

Handling Procedure for Frozen Cells

To insure the highest level of viability, thaw the vial and initiate the culture as soon as possible upon receipt. If upon arrival, continued storage of the frozen culture is necessary, it should be stored in liquid nitrogen vapor phase and not at -70°C. Storage at -70°C will result in loss of viability.

1. Thaw the vial by gentle agitation in a 37°C water bath. To reduce the possibility of contamination, keep the O-ring and cap out of the water. Thawing should be rapid (approximately 2 minutes).
2. Remove the vial from the water bath as soon as the contents are thawed, and decontaminate by dipping in or spraying with 70% ethanol. All of the operations from this point on should be carried out under strict aseptic conditions.
3. Transfer the vial contents to a centrifuge tube containing 9.0 mL complete culture medium. and spin at approximately 125 x g for 5 to7 minutes.
4. Resuspend cell pellet with the recommended complete medium (see the specific batch information for the culture recommended dilution ratio). and dispense into a 75 cm^2 culture flask. Recommended use of Corning® T-75 flasks (catalog #430641). It is important to avoid excessive alkalinity of the medium during recovery of the cells. It is suggested that, prior to the addition of the vial contents, the culture vessel containing the complete growth medium be placed into the incubator for at least 15 minutes to allow the medium to reach its normal pH (7.0 to 7.6). pH (7.0 to 7.6).
5. Incubate the culture at 37°C in a suitable incubator. A 5% CO_2 in air atmosphere is recommended if using the medium described on this product sheet.

Handling Procedure for Flask Cultures

The flask was seeded with cells (see specific batch information) grown and completely filled with medium at ATCC to prevent loss of cells during shipping.

1. Upon receipt visually examine the culture for macroscopic evidence of any microbial contamination.

ATCC

Product Sheet

Hep G2 [HEPG2] (ATCC® HB-8065™)

Please read this FIRST



Storage Temp.
liquid nitrogen vapor phase



Biosafety Level
1

Intended Use

This product is intended for research use only. It is not intended for any animal or human therapeutic or diagnostic use.

Complete Growth Medium

The base medium for this cell line is ATCC-formulated Eagle's Minimum Essential Medium, Catalog No. 30-2003. To make the complete growth medium, add the following components to the base medium: fetal bovine serum to a final concentration of 10%.

Citation of Strain

If use of this culture results in a scientific publication, it should be cited in that manuscript in the following manner: Hep G2 [HEPG2] (ATCC® HB-8065™)

American Type Culture Collection
PO Box 1549
Manassas, VA 20108 USA
www.atcc.org

800.638.6597 or 703.365.2700
Fax: 703.365.2750
Email: Tech@atcc.org

Or contact your local distributor

Using an inverted microscope (preferably equipped with phase-contrast optics), carefully check for any evidence of microbial contamination. Also check to determine if the majority of cells are still attached to the bottom of the flask; during shipping the cultures are sometimes handled roughly and many of the cells often detach and become suspended in the culture medium (but are still viable).

2. **If the cells are still attached,** aseptically remove all but 5 to 10 mL of the shipping medium. The shipping medium can be saved for reuse. Incubate the cells at 37°C in a 5% CO_2 in air atmosphere until they are ready to be subcultured.
3. **If the cells are not attached,** aseptically remove the entire contents of the flask and centrifuge at 125 x g for 5 to 10 minutes. Remove shipping medium and save. Resuspend the pelleted cells in 10 mL of this medium and add to 75 cm^2 flask. Recommended use of Corning® T-75 flasks (catalog #430641). Incubate at 37°C in a 5% CO_2 in air atmosphere until cells are ready to be subcultured.

Subculturing Procedure

Volumes are given for a 75 cm^2 flask. Corning® T-75 flasks (catalog #430641) are recommended for subculturing this product. Increase or decrease the amount of dissociation medium needed proportionally for culture vessels of other sizes.

1. Remove and discard culture medium.
2. Briefly rinse the cell layer with 0.25% (w/v) Trypsin- 0.53 mM EDTA solution to remove all traces of serum that contains trypsin inhibitor.
3. Add 2.0 to 3.0 mL of Trypsin-EDTA solution to flask and observe cells under an inverted microscope until cell layer is dispersed (usually within 5 to 15 minutes).
   Note: To avoid clumping do not agitate the cells by hitting or shaking the flask while waiting for the cells to detach. Cells that are difficult to detach may be placed at 37°C to facilitate dispersal.
4. Add 6.0 to 8.0 mL of complete growth medium and aspirate cells by gently pipetting.
5. Add appropriate aliquots of the cell suspension to new culture vessels.
6. Incubate cultures at 37°C.

Subcultivation Ratio: A subcultivation ratio of 1:4 to 1:6 is recommended
Medium Renewal: Twice per week

Cryopreservation Medium

Complete growth medium described above supplemented with 5% (v/v) DMSO. Cell culture tested DMSO is available as ATCC Catalog No. 4-X.

Comments

The cells express 3-hydroxy-3-methylglutaryl-CoA reductase and hepatic triglyceride lipase activities.
The cells demonstrate decreased expression of apoA-I mRNA and increased expression of catalase mRNA in response to gramoxone (oxidative stress).
There is no evidence of a Hepatitis B virus genome in this cell line.
In addition to the hepatocellular carcinoma or hepatoma cell line based on the original publication (PubMed: 6248960), HepG2 is also referred as hepatoblastoma cell line (PubMed: 19751877).

References

References and other information relating to this product are available online at www.atcc.org.

Biosafety Level: 1

Appropriate safety procedures should always be used with this material. Laboratory safety is discussed in the current publication of the *Biosafety in Microbiological and Biomedical Laboratories* from the U.S. Department of Health and Human Services Centers for Disease Control and Prevention and National Institutes for Health.

ATCC Warranty

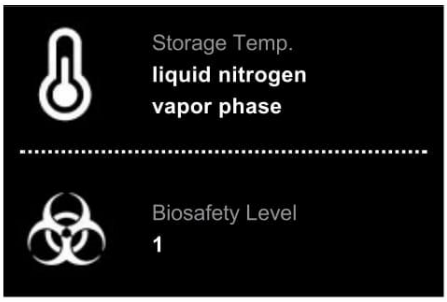
ATCC® products are warranted for 30 days from the date of shipment, and this warranty is valid only if the product is stored and handled according to the information included on this product information sheet. If the ATCC® product is a living cell or microorganism, ATCC lists the media formulation that has been found to be effective for this product. While other, unspecified media may also produce satisfactory results, a change in media or the absence of an additive from the ATCC recommended media may affect recovery, growth and/or function of this product. If an alternative medium formulation is used, the ATCC warranty for viability is no longer valid.

ATCC

Product Sheet

Hep G2 [HEPG2] (ATCC® HB-8065™)

Please read this FIRST



Intended Use

This product is intended for research use only. It is not intended for any animal or human therapeutic or diagnostic use.

Complete Growth Medium

The base medium for this cell line is ATCC-formulated Eagle's Minimum Essential Medium, Catalog No. 30-2003. To make the complete growth medium, add the following components to the base medium: fetal bovine serum to a final concentration of 10%.

Citation of Strain

If use of this culture results in a scientific publication, it should be cited in that manuscript in the following manner: Hep G2 [HEPG2] (ATCC® HB-8065™)

Disclaimers

This product is intended for laboratory research purposes only. It is not intended for use in humans.
While ATCC uses reasonable efforts to include accurate and up-to-date information on this product sheet, ATCC makes no warranties or representations as to its accuracy. Citations from scientific literature and patents are provided for informational purposes only. ATCC does not warrant that such information has been confirmed to be accurate.
This product is sent with the condition that you are responsible for its safe storage, handling, and use. ATCC is not liable for any damages or injuries arising from receipt and/or use of this product. While reasonable effort is made to insure authenticity and reliability of materials on deposit, ATCC is not liable for damages arising from the misidentification or misrepresentation of such materials.
Please see the enclosed Material Transfer Agreement (MTA) for further details regarding the use of this product. The MTA is also available on our Web site at www.atcc.org

Additional information on this culture is available on the ATCC web site at www.atcc.org.
© ATCC 2018. All rights reserved. ATCC is a registered trademark of the American Type Culture Collection. [08/17]

American Type Culture Collection
PO Box 1549
Manassas, VA 20108 USA
www.atcc.org

800.638.6597 or 703.365.2700
Fax: 703.365.2750
Email: Tech@atcc.org

Or contact your local distributor

Appendix 3 – H4IIE Cell Line Data Sheet

ATCC

Product Sheet

H-4-II-E (ATCC® CRL-1548™)

Please read this FIRST



Intended Use

This product is intended for research use only. It is not intended for any animal or human therapeutic or diagnostic use.

Complete Growth Medium

The base medium for this cell line is ATCC-formulated Eagle's Minimum Essential Medium, Catalog No. 30-2003. To make the complete growth medium, add the following components to the base medium: fetal bovine serum to a final concentration of 10%.

Citation of Strain

If use of this culture results in a scientific publication, it should be cited in that manuscript in the following manner: H-4-II-E (ATCC® CRL-1548™)

American Type Culture Collection
PO Box 1549
Manassas, VA 20108 USA
www.atcc.org

800.638.6597 or 703.365.2700
Fax: 703.365.2750
Email: Tech@atcc.org

Or contact your local distributor

Description

Organism: *Rattus norvegicus*, rat
Tissue: liver
Disease: hepatoma
Morphology: epithelial
Growth Properties: adherent

Batch-Specific Information

Refer to the Certificate of Analysis for batch-specific test results.

SAFETY PRECAUTION

ATCC highly recommends that protective gloves and clothing always be used and a full face mask always be worn when handling frozen vials. It is important to note that some vials leak when submersed in liquid nitrogen and will slowly fill with liquid nitrogen. Upon thawing, the conversion of the liquid nitrogen back to its gas phase may result in the vessel exploding or blowing off its cap with dangerous force creating flying debris.

Unpacking & Storage Instructions

1. Check all containers for leakage or breakage.
2. Remove the frozen cells from the dry ice packaging and immediately place the cells at a temperature below -130°C, preferably in liquid nitrogen vapor, until ready for use.

Handling Procedure for Frozen Cells

To insure the highest level of viability, thaw the vial and initiate the culture as soon as possible upon receipt. If upon arrival, continued storage of the frozen culture is necessary, it should be stored in liquid nitrogen vapor phase and not at -70°C. Storage at -70°C will result in loss of viability.

1. Thaw the vial by gentle agitation in a 37°C water bath. To reduce the possibility of contamination, keep the O-ring and cap out of the water. Thawing should be rapid (approximately 2 minutes).
2. Remove the vial from the water bath as soon as the contents are thawed, and decontaminate by dipping in or spraying with 70% ethanol. All of the operations from this point on should be carried out under strict aseptic conditions
3. It is recommended that the cryoprotective agent be removed immediately. Centrifuge the cell suspension at approximately 125 x g for 5 to 10 minutes. Discard the supernatant and resuspend the cell pellet in an appropriate amount of fresh growth medium.
4. Transfer the cell pellet to an appropriate size vessel. It is important to avoid excessive alkalinity of the medium during recovery of the cells. It is suggested that, prior to the addition of the vial contents, the culture vessel containing the growth medium be placed into the incubator for at least 15 minutes to allow the medium to reach its normal pH (7.0 to 7.6).
5. Incubate the culture at 37°C in a suitable incubator. A 5% CO_2 in air atmosphere is recommended if using the medium described on this product sheet.

Handling Procedure for Flask Cultures

The flask was seeded with cells (see specific batch information) grown and completely filled with medium at ATCC to prevent loss of cells during shipping.

1. Upon receipt visually examine the culture for macroscopic evidence of any microbial contamination. Using an inverted microscope (preferably equipped with phase-contrast optics), carefully check for any evidence of microbial contamination. Also check to determine if the majority of cells are still attached to the bottom of the flask; during shipping the cultures are sometimes handled roughly and many of the cells often detach and become suspended in the culture medium (but are still viable).
2. **If the cells are still attached,** aseptically remove all but 5 to 10 mL of the shipping medium. The shipping medium can be saved for reuse. Incubate the cells at 37°C in a 5% CO_2 in air atmosphere until they are ready to be subcultured.
3. **If the cells are not attached,** aseptically remove the entire contents of the flask and centrifuge at 125 x g for 5 to 10 minutes. Remove shipping medium and save. Resuspend the pelleted cells in 10 mL of this medium and add to 25 cm^2 flask. Incubate at 37°C in a 5% CO_2 in air atmosphere until cells are ready to be subcultured.

Subculturing Procedure

ATCC

Product Sheet

H-4-II-E (ATCC® CRL-1548™)

Please read this FIRST

Biosafety Level
1

Intended Use

This product is intended for research use only. It is not intended for any animal or human therapeutic or diagnostic use.

Complete Growth Medium

The base medium for this cell line is ATCC-formulated Eagle's Minimum Essential Medium, Catalog No. 30-2003. To make the complete growth medium, add the following components to the base medium: fetal bovine serum to a final concentration of 10%.

Citation of Strain

If use of this culture results in a scientific publication, it should be cited in that manuscript in the following manner: H-4-II-E (ATCC® CRL-1548™)

Remove medium, and rinse with 0.25% trypsin, 0.03% EDTA solution. Remove the solution and add an additional 1 to 2 mL of trypsin-EDTA solution. Allow the flask to sit at room temperature (or at 37°C) until the cells detach. Add fresh culture medium, aspirate and dispense into new culture flasks.
Subcultivation Ratio: A subcultivation ratio of 1:2 to 1:4 is recommended
Medium Renewal: Every 2 to 3 days

Cryopreservation Medium

Complete growth medium described above supplemented with 5% (v/v) DMSO.
Cell culture tested DMSO is available as ATCC Catalog No. 4-X.

Comments

The line has been cured of Mycoplasma arginini contamination.

References

References and other information relating to this product are available online at www.atcc.org.

Biosafety Level: 1

Appropriate safety procedures should always be used with this material. Laboratory safety is discussed in the current publication of the *Biosafety in Microbiological and Biomedical Laboratories* from the U.S. Department of Health and Human Services Centers for Disease Control and Prevention and National Institutes for Health.

ATCC Warranty

ATCC® products are warranted for 30 days from the date of shipment, and this warranty is valid only if the product is stored and handled according to the information included on this product information sheet. If the ATCC® product is a living cell or microorganism, ATCC lists the media formulation that has been found to be effective for this product. While other, unspecified media may also produce satisfactory results, a change in media or the absence of an additive from the ATCC recommended media may affect recovery, growth and/or function of this product. If an alternative medium formulation is used, the ATCC warranty for viability is no longer valid.

Disclaimers

This product is intended for laboratory research purposes only. It is not intended for use in humans.
While ATCC uses reasonable efforts to include accurate and up-to-date information on this product sheet, ATCC makes no warranties or representations as to its accuracy. Citations from scientific literature and patents are provided for informational purposes only. ATCC does not warrant that such information has been confirmed to be accurate.
This product is sent with the condition that you are responsible for its safe storage, handling, and use. ATCC is not liable for any damages or injuries arising from receipt and/or use of this product. While reasonable effort is made to insure authenticity and reliability of materials on deposit, ATCC is not liable for damages arising from the misidentification or misrepresentation of such materials.
Please see the enclosed Material Transfer Agreement (MTA) for further details regarding the use of this product. The MTA is also available on our Web site at www.atcc.org

Additional information on this culture is available on the ATCC web site at www.atcc.org.
© ATCC 2018. All rights reserved. ATCC is a registered trademark of the American Type Culture Collection. [08/17]

American Type Culture Collection
PO Box 1549
Manassas, VA 20108 USA
www.atcc.org

800.638.6597 or 703.365.2700
Fax: 703.365.2750
Email: Tech@atcc.org

Or contact your local distributor

Appendix 4 – Amplex Red Glucose/Glucose Oxidase Assay Kit Data Sheet

invitrogen™

Molecular Probes™
invitrogen detection technologies

Amplex® Red Glucose/Glucose Oxidase Assay Kit

Table 1. Contents and storage information.

Material	Amount	Concentration	Storage	Stability
Amplex® Red reagent (Component A, blue cap, MW = 257)	5 vials, 154 µg of reagent each	NA	• ≤–20°C • Desiccate • Protect from light	When stored as directed, kit components should remain stable for at least 6 months.
DMSO, anhydrous (Component B, green cap)	700 µL	NA		
5X reaction buffer (Component C, white cap)	28 mL	0.25 M sodium phosphate, pH 7.4		
Horseradish peroxidase (Component D, yellow cap)	10 U *	NA		
Glucose oxidase (Component E, orange cap)	100 U †	NA		
D-Glucose (Component F, black cap, MW = 180)	~1 g	NA		
Hydrogen peroxide (H_2O_2) (Component G, red cap)	200 µL	In a stabilized ~3% solution ††		

* 1 unit (U) is defined as the amount of enzyme that will form 1.0 mg purpurogallin from pyrogallol in 20 seconds at pH 6.0 at 20°C. † 1 unit (U) is defined as the amount that will oxidase 1.0 µmole of β-D-glucose to D-gluconolactone and H_2O_2 per minute at pH 5.1 and 30°C. †† The actual concentration is indicated on the label.

Number of labelings: Each kit provide sufficient reagents for approximately 500 assays using either a fluorescence or absorbance microplate reader and reaction volumes of 100 µL per assay.

Approximate fluorescence excitation/emission maxima: 571/585 nm for reaction product

Introduction

The Amplex® Red Glucose/Glucose Oxidase Assay Kit A22189) provides a sensitive one-step method for detecting glucose or glucose oxidase. The Amplex® Red reagent (10-acetyl-3,7-dihydroxyphenoxazine) is a colorless, stable, and extremely versatile peroxidase substrate. Because peroxidase- and glucose oxidase–mediated reactions can be coupled,[1,2] it is possible to measure glucose oxidase activity or the release of glucose by any glucosidase enzyme—for instance, β-glucosidase and glucocerebrosidase—in either a continuous or discontinuous assay. This assay should also be very useful for quantitation of glucose levels in foods, fermentation media, and bodily fluids.

Revised: 22–May–2006 | MP 22189

In the assay, glucose oxidase reacts with D-glucose to form D-gluconolactone and H_2O_2. In the presence of horseradish peroxidase (HRP), the H_2O_2 then reacts with the Amplex® Red reagent in a 1:1 stoichiometry to generate the red-fluorescent oxidation product, resorufin.[3] Resorufin has fluorescence excitation and emission maxima of approximately 571 nm and 585 nm, respectively (Figure 1), and because the extinction coefficient is high (54,000 $cm^{-1}M^{-1}$), the assay can be performed either fluorometrically or spectrophotometrically. Furthermore, at these long wavelengths, there is little interference from autofluorescence found in most biological samples. With the Amplex® Red Glucose/Glucose Oxidase Assay Kit, we have detected as little as 3 µM D-glucose (Figure 2) and 0.05 mU/mL glucose oxidase (Figure 3).

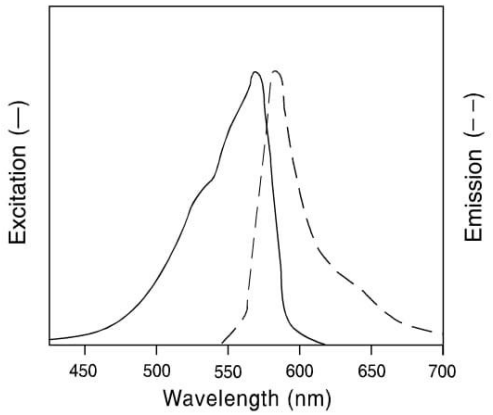


Figure 1. Normalized fluorescence excitation and emission spectra of resorufin, the product of the Amplex® Red reaction.

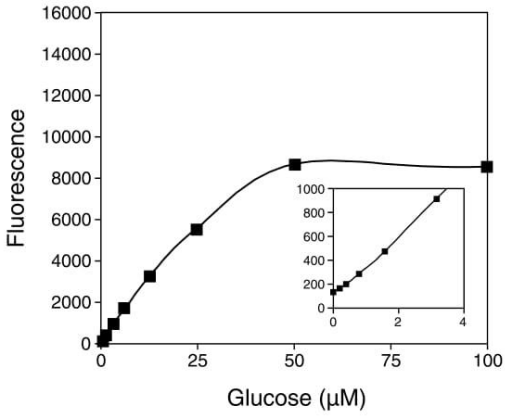


Figure 2. Detection of glucose using the Amplex® Red Glucose/Glucose Oxidase Assay Kit (A22189). Reactions containing 50 µM Amplex® Red reagent, 0.1 U/mL HRP, 1 U/mL glucose oxidase and the indicated amount of glucose in 50 mM sodium phosphate buffer, pH 7.4, were incubated for 37°C. Fluorescence was then measured with a fluorescence microplate reader using excitation at 530 ± 12.5 nm and fluorescence detection at 590 ± 17.5 nm. Background fluorescence (201 arbitrary units), determined for a no–glucose control reaction, has been subtracted from each value. The inset shows the sensitivity and linearity of the assay at low levels of glucose.

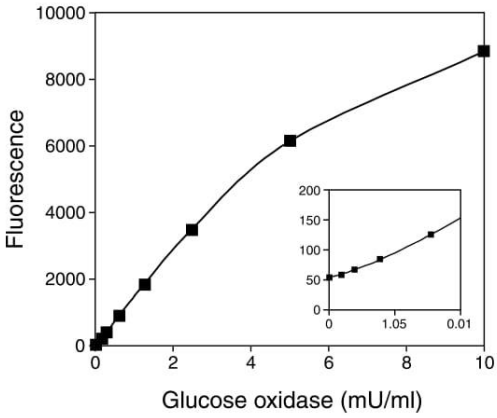


Figure 3. Detection of glucose oxidase using the Amplex® Red Glucose/Glucose Oxidase Assay Kit (A22189). Reactions containing 50 µM Amplex® Red reagent, 0.1 U/mL HRP, 10 mM glucose and the indicated amount of glucose oxidase in 50 mM sodium phosphate buffer, pH 7.4, were incubated for 30 minutes at 37°C. Fluorescence was measured with a fluorescence microplate reader using excitation at 530 ± 12.5 nm and fluorescence detection at 590 ± 17.5 nm. Background fluorescence (19 arbitrary units), determined for a no–glucose oxidase control reaction, has been subtracted from each value. The inset shows the assay's sensitivity at low levels of glucose oxidase.

Before You Begin

Allow reagents to warm to room temperature before opening vials. The Amplex® Red reagent is somewhat air sensitive. Once a vial of Amplex® Red reagent is opened, the reagent should be used promptly. PROTECT THE AMPLEX® RED REAGENT FROM LIGHT

Amplex® Red Reagent Restrictions

Please note the following restrictions on the use of the Amplex® Red reagent. The Amplex® Red reagent is unstable in the presence of thiols such as dithiothreitol (DTT) and 2-mercaptoethanol. The final concentration of DTT or 2-mercaptoethanol in the reaction should be no higher than 10 µM. The Amplex® Red reagent is also unstable at high pH (>8.5). Furthermore, the absorption and fluorescence of the reaction product, resorufin, are pH-dependent. Below the pK_a (~6.0), the absorption maximum shifts to ~480 nm and the fluorescence quantum yield is markedly lower. For these reasons, the reactions should be performed at pH 7–8. The provided reaction buffer, pH 7.4, is recommended.

Preparing the Stock Solutions

1.1 Prepare a 10 mM stock solution of Amplex® Red reagent. Allow one vial of Amplex® Red reagent (Component A, blue cap) and DMSO (Component B, green cap) to warm to room temperature. Just prior to use, dissolve the contents of the vial of Amplex® Red reagent in 60 µL of DMSO. Each vial of Amplex® Red reagent is sufficient for approximately 100 assays, with a final reaction volume of 100 µL per assay.

1.2 Prepare 1X Reaction Buffer. Add 4 mL of 5X Reaction Buffer (Component C, white cap) to 16 mL of deionized water (dH_2O). This 20 mL volume of 1X Reaction Buffer is sufficient for approximately 100 assays of 100 µL each with a 10 mL excess for making stock solutions.

1.3 Prepare a 10 U/mL stock solution of horseradish peroxidase (HRP). Dissolve the contents of the vial of HRP (Component D, yellow cap) in 1 mL of 1X Reaction Buffer. After the assay, any remaining unused solution should be divided into single-use aliquots and stored frozen at ≤–20°C.

1.4 Prepare a 100 U/mL glucose oxidase stock solution. Dissolve the contents of the vial of glucose oxidase (Component E, orange cap) in 1.0 mL of 1X Reaction Buffer. This stock solution should be stored frozen at ≤–20°C.

1.5 Prepare a 400 mM (72 mg/mL) glucose stock solution. Weigh out a portion of glucose (Component F, black cap), and dissolve it in the appropriate amount of 1X Reaction Buffer

1.6 Prepare a 20 mM H_2O_2 working solution. Dilute the ~3% H_2O_2 stock solution (Component G, red cap) into the appropriate volume of 1X Reaction Buffer. The actual concentration of H_2O_2 is indicated on the label. For instance, a 20 mM H_2O_2 working solution can be prepared from a 3.0% (0.88 M) H_2O_2 stock solution by diluting 22.7 µL of 3.0% H_2O_2 into 977 µL of 1X Reaction Buffer.

Note: Although the ~3% H_2O_2 stock solution has been stabilized to slow degradation, the 20 mM H_2O_2 working solution prepared in this step will be less stable and should be used promptly.

Experimental Protocol

The following procedure is designed for use with a fluorescence or absorbance microplate reader. For use with a standard fluorometer, volumes must be increased accordingly.

Glucose Assay

The following protocol describes the assay of glucose in a total volume of 100 µL per microplate well. The volumes recommended here are sufficient for ~100 assays. The kit provides sufficient material for ~500 assays.

2.1 Prepare a glucose standard curve. Dilute the appropriate amount of the 400 mM glucose stock solution (prepared in step 1.5) into 1X Reaction Buffer to produce glucose concentrations of 0 to 200 µM, each in a volume of 50 µL. Be sure to include a no-glucose control. Final glucose concentrations will be twofold lower (e.g., 0 to 100 µM).

2.2 If no standard curve is to be used, prepare positive and negative controls. For a glucose-positive control, dilute the 400 mM glucose stock solution (prepared in step 1.5) to 200 µM in 1X Reaction Buffer. For an H_2O_2-positive control, dilute the 20 mM H_2O_2 working solution (prepared in step 1.6) to 10 µM in 1X Reaction Buffer. For a negative control, use 1X Reaction Buffer without H_2O_2.

2.3 Dilute the glucose-containing samples in 1X Reaction Buffer. A volume of 50 µL will be used for each reaction. A variable dilution will be required depending on the total glucose present in the sample. In the first trial the samples should be serially diluted to determine the optimal amount of sample for the assay.

Note: Extremely high levels of glucose (e.g., 500 µM, final concentration) can produce lower fluorescence than moderately high levels (e.g., 100 µM), because excess H_2O_2 resulting from the reaction of glucose with glucose oxidase can oxidize the reaction product, resorufin, to nonfluorescent resazurin.

2.4 Load the samples. Pipet 50 µL of the standard curve samples, controls, and experimental samples into individual wells of a microplate.

2.5 Prepare a working solution of 100 µM Amplex® Red reagent, 0.2 U/mL HRP and 2 U/mL glucose oxidase. Mix the following:

- 50 µL of 10 mM Amplex® Red reagent stock solution (prepared in step 1.1)
- 100 µL of 10 U/mL HRP stock solution (prepared in step 1.3)
- 100 µL of 100 U/mL glucose oxidase stock solution (prepared in step 1.4)
- 4.75 mL of 1X Reaction Buffer

This 5 mL volume is sufficient for ~100 assays. Note that the final concentration of each component will be twofold lower in the final reaction volume.

2.6 Begin the reactions. Add 50 µL of the Amplex® Red reagent/HRP/glucose oxidase working solution to each microplate well containing the standards, controls, and samples.

2.7 Incubate the reactions. Incubate at room temperature for 30 minutes, protected from light. Because the assay is continuous (not terminated), fluorescence or absorbance may be measured at multiple time points to follow the kinetics of the reactions.

2.8 Measure the fluorescence or absorbance. Use a microplate reader equipped for excitation in the range of 530–560 nm and fluorescence emission detection at ~590 nm, or for absorbance at ~560 nm (see Figure 1).

2.9 Correct for background fluorescence or absorbance. For each point, subtract the value derived from the no-glucose control.

Glucose Oxidase Assay

The following protocol describes the assay of glucose oxidase in a total volume of 100 µL per microplate well. The volumes here are sufficient for ~100 assays. The kit provides sufficient material for ~500 assays.

3.1 Prepare a glucose oxidase standard curve. Dilute the appropriate amount of 100 U/mL glucose oxidase stock solution (prepared in step 1.4) into 1X Reaction Buffer (prepared in step 1.2) to produce glucose oxidase concentrations of approximately 0 to 10 mU/mL glucose oxidase, each in a volume of 50 µL. Be sure to include a no–glucose oxidase control. Please note that final glucose oxidase concentrations will be twofold lower (e.g., 0 to 5 mU/mL).

3.2 If no standard curve is to be used, prepare positive and negative controls. For a glucose oxidase–positive control, dilute the 100 U/mL glucose oxidase stock solution (prepared in step 1.4) to 10 mU/mL in 1X Reaction Buffer. For an H_2O_2 positive control, dilute the 20 mM H_2O_2 working solution to 10 µM in 1X Reaction Buffer. For a negative control, use 1X Reaction Buffer without H_2O_2.

3.3 Dilute the glucose oxidase–containing samples in 1X Reaction Buffer. A volume of 50 µL will be used for each reaction. A variable dilution will be required depending on the total glucose oxidase present in the sample. In the first trial, the samples should be serially diluted to determine the optimal amount of sample for the assay. Note that extremely high levels of glucose oxidase (e.g., 50 mU/mL, final concentration) can produce lower fluorescence than moderately high levels (e.g., 10 mU/mL), because excess H_2O_2 resulting from the reaction of glucose with glucose oxidase can oxidize the reaction product, resorufin, to nonfluorescent resazurin.

3.4 Load the samples. Pipet 50 µL of the standard curve samples, controls and experimental samples into individual wells of a microplate.

3.5 Prepare a working solution of 100 µM Amplex® Red reagent, 0.2 U/mL HRP, and 100 mM glucose. Mix the following:

- 50 µL of 10 mM Amplex® Red reagent stock solution (prepared in step 1.1)
- 100 µL of 10 U/mL HRP stock solution (prepared in step 1.3)
- 1.25 mL of 400 mM glucose stock solution (prepared in step 1.5)
- 3.60 mL of 1X Reaction Buffer

This 5 mL volume is sufficient for ~100 assays. Note that the final concentration of each component will be twofold lower in the final reaction volume.

3.6 Begin the reactions. Add 50 µL of the Amplex® Red reagent/HRP/glucose working solution to each microplate well containing the standards, controls, and samples.

3.7 Incubate the reactions. Incubate at room temperature for 30 minutes, protected from light. Because the assay is continuous (not terminated), fluorescence or absorbance may be measured at multiple time points to follow the kinetics of the reactions.

3.8 Measure the fluorescence or absorbance. Use a microplate reader equipped for excitation in the range of 530–560 nm and fluorescence emission detection at ~590 nm (see Figure 1), or for absorbance at ~560 nm.

3.9 Correct for background fluorescence or absorbance. For each point, subtract the value derived from the no–glucose oxidase control.

References

1. Proc SPIE-Intl Soc Opt Eng 3606, 119 (1999); **2.** Anal Biochem 253, 162-168 (1997); **3.** J Immunol Methods 202, 133 (1997).

Product List **Current prices may be obtained from our website or from our Customer Service Department.**

Cat #	Product Name	Unit Size
A22189	Amplex® Red Glucose/Glucose Oxidase Assay Kit *500 assays*	1 kit
A12222	Amplex® Red reagent	5 mg
A22177	Amplex® Red reagent *packaged for high-throughput screening*	10 x 10 mg
A36006	Amplex® UltraRed reagent	5 x 1 mg
R363	resorufin, sodium salt *reference standard*	100 mg

Appendix 5 – Bioline TRIsure RNA Lysis Kit Data Sheet

TRIsure™

Catalog Numbers

TRIsure	BIO-38032	100ml
TRIsure	BIO-38033	200ml

Batch No.: See vial

BIOLINE
A Meridian Life Science® Company

Store at +4°C

Storage and Stability:
TRIsure is shipped at room temperature. For optimal performance, we recommend to store at +4°C.

Expiry:
When stored under the recommended conditions and handled correctly, full activity is retained until the expiry date on the outer box label.

Safety Precautions:
Toxic in contact with skin. Toxic if swallowed. Causes burns. Please refer to the material safety data sheet for information regarding hazards and safe handling practice.



Signal word : DANGER

Notes:
Research Use Only.

Features

- Quick isolation of high-quality total RNA DNA and/or and protein from a single sample
- Performs well with large or small amounts of tissue or cells
- Ready-to-use solution

Applications

- Purified RNA is ideal for any downstream application such as RT-PCR, *in vitro* translation, Northern blotting, RNase protection assays or dot blot hybridization
- Purified DNA can be used for PCR and Southern blotting
- Purified protein can be used for Western blotting

Description

TRIsure™ is a complete, ready-to-use reagent for the isolation of total RNA DNA and protein from cells and tissues. Using TRIsure a biological sample is homogenized or lysed before being separated into three phases: an aqueous phase (upper), an organic phase (lower) and an interphase. The RNA is extracted from the aqueous phase by isopropyl alcohol precipitation. The highly effective RNase inhibitory property of TRIsure protects the integrity of the RNA during lysis and results in the isolation of high-quality material. DNA is precipitated from the organic layer with ethanol. Protein is precipitated from the phenol-ethanol supernatant by isopropyl alcohol precipitation.

1ml of TRIsure is sufficient to isolate RNA and DNA from 1 x 10^7 cells or 100mg of tissue. The table below presents typical yields of RNA and DNA from various starting materials.

Starting material	Quantity	RNA	DNA
Mouse liver	1mg	2-5µg	3-4µg
Mouse kidney	1mg	5-10µg	3-4µg
epithelial cells	1 x 10^6 cells	8-15µg	5-7µg
cell fibroblasts	1 x 10^6 cells	20-25µg	5-7µg

Protocol for the isolation of RNA using TRIsure

Reagents required (not supplied):

- Chloroform
- Isopropyl alcohol (chilled)
- 75% ethanol (in DEPC-treated water)
- DEPC-treated water (BIO-38030) or PCR water (BIO-37080)

1. Homogenization

Tissue:
Homogenize tissue samples in 1 ml of TRIsure per 50-100mg of tissue. For small quantities of tissue (1-10mg), add 800µl of TRIsure. For samples of fat tissue, a layer of fat may accumulate at the top, which should be removed.

Plant tissue
Following homogenization, insoluble material is removed by centrifugation at 12,000 x g for 10 minutes at 4°C. Transfer the cleared homogenate to a fresh tube.

Cells Grown on Monolayer:
Lyse cells directly in a culture dish or flask by adding 1ml of TRIsure per 10cm^2 growth area, pipette the cell lysate several times to ensure sufficient cell disruption.

Cells Grown in Suspension:
Pellet cells at 200 x g for 5 minutes at room temperature. Lyse cells with 1 ml of TRIsure per 5 x 10^6 cells and pass the lysate several times through a pipette tip. For small quantities of cells (10^2 -10^6), lyse cells in 800µl of TRIsure.

Note: At this stage, samples can be stored for at least one month at -70°C.

2. Phase Separation
Incubate samples for 5 minutes at room temperature. Add 0.2 ml of chloroform per 1 ml of TRIsure used. Cap tubes securely and shake vigorously by hand for 15 seconds.

Incubate samples for 3 minutes at room temperature. Centrifuge samples at 12,000 x g for 15 minutes (or 2600 x g for 30 minutes) at 4°C. The sample will separate into a pale green, organic phase, an interphase and a colorless upper aqueous phase that contains the RNA.

The aqueous phase is removed for RNA extraction.

3. RNA Precipitation
Transfer the aqueous phase very carefully, without disturbing the interphase to another tube. Precipitate the RNA by mixing with cold isopropyl alcohol. Use 0.5 ml of isopropyl alcohol per 1 ml of TRIsure used. Incubate samples for 10 minutes at room temperature then centrifuge at 12,000 x g for 10 minutes (or 2600 x g for 30 minutes) at 4°C.

Note: For small quantities of cells, RNase-free Co-precipitant Pink (BIO-37075) can be added to the aqueous phase before addition of isopropyl alcohol to aid RNA precipitation. Add 5-10µg of Co-precipitant per 800µl of TRIsure.

4. RNA Wash
Remove the supernatant. Wash the pellet once with 75% ethanol, adding at least 1 ml of ethanol per 1 ml of TRIsure used. Vortex samples and centrifuge at 7500 x g for 5 minutes at 4°C.

Note: At this stage, samples can be stored for one week at 4°C, or 12 months at -20°C.

5. Re-dissolving the RNA
Air-dry the pellet and dissolve in PCR water or DEPC-treated water by pipetting the solution up and down. Incubate for 10 minutes at 60°C if necessary. Store RNA at -70°C.

Protocol for the isolation of DNA using TRIsure

Reagents required (not supplied):

- 100% ethanol
- 0.1M sodium citrate in 10% ethanol
- 75% ethanol
- 8mM NaOH
- DEPC-treated water or PCR water

After homogenization and phase separation the upper aqueous phase is removed for optional RNA precipitation, leaving the interphase and the organic phase for subsequent isolation of DNA and protein.

Note: The interphase and organic phase can be stored overnight at 4°C.

1. DNA Precipitation

Remove any remaining aqueous phase overlying the interphase (step 3 of the RNA isolation protocol). Add 0.3ml of 100% Ethanol per 1ml or TRIsure used, and mix samples by inversion. Leave samples at room temperature for 3 minutes, then centrifuge at 2000 x g for 5 minutes at 4°C.

Note: At this stage, samples can be stored for at least one month at 4°C.

2. DNA Wash
Remove the supernatant to waste or retain for protein isolation. Wash the DNA pellet, with 1ml of 0.1M sodium citrate in 10% ethanol per 1ml of TRIsure used and mix for 30 minutes at room temperature. Centrifuge samples at 2000 x g for 5 minutes at 4°C. Two washes are usually sufficient, however for large pellets containing >200µg of DNA an additional wash may be necessary.

Following the washing, adding 1.5ml of 75% ethanol per 1ml of TRIsure used. Mix for 20 minutes at room temperature, then centrifuge samples at 2000 x g for 5 minutes at 4°C.

3. Re-dissolving the DNA
Air-dry the pellet for 15 minutes. Resuspend the pellet in 8mM NaOH Remove any insoluble material by centrifugation at 12000 x g for 10 minutes and then transfer the supernatant to another tube.

Note: Samples dissolved in 8mM NaOH can be stored overnight at 4°C. For long-term storage, adjust the pH to 7.5 and adjust the EDTA concentration to 1mM. Store at -20°C.

Protocol for the isolation of protein using TRIsure

Reagents required (not supplied):

- Isopropyl alcohol
- 0.3M Guanidine hydrochloride in 95% ethanol
- Ethanol
- 1% SDS

1. Protein Precipitation
To the retained supernatant (step 2 of the DNA isolation protocol) add 1.5ml of isopropyl alcohol per 1ml of TRIsure used. Mix samples for 10 minutes at room temperature the centrifuge at 12000 x g for 10 minutes at 4°C.

2. Protein Wash
Remove supernatant and wash the protein pellet twice. To wash the protein pellet add 2ml of 0.3M guanidine hydrochloride in 95% ethanol per 1ml of TRIsure used. Mix for 20 minutes at room temperature then centrifuge at 7500 x g for 5 minutes at 4°C.

Note: At this stage, samples can be stored for at least one month at 4°C, or 12 months at -20°C.

Following the washing steps, add 2ml of ethanol and vortex. Mix for 20 minutes at room temperature then centrifuge at 7500 x g for 5 minutes at 4°C.

Note: At this stage, samples can be stored for at least one month at 4°C, or 12 months at -20°C.

3. Re-dissolving the Protein
Vacuum dry the protein pellet for 5-10 minutes. Dissolve in 1% SDS by pipetting up and down. For difficult samples incubate at 50°C. Remove any insoluble material by centrifugation at 10000 x g for 10 minutes at 4°C and then transfer the supernatant to another tube. Store protein at -20°C.

References:
Chomczynski, P. and Sacchi, N. *Anal. Biochem. 162,* 156. (1987)
Chomczynski, P. *Biotechniques 15,* 532. (1993)

Troubleshooting Guide

Problem	Possible Cause	Recommendation
DNA contamination or RNA contamination	Interphase/organic phase pipetted up with aqueous phase	Do not attempt to draw off the entire aqueous layer after phase separation.
	Insufficient removal of the aqueous phase from the organic phase	Remove remnants of the aqueous phase prior to DNA precipitation.
	Insufficiently wash of the DNA pellet	Make sure pellet is washed with 0.1 M sodium citrate in 10% ethanol.
Low RNA yield	Insufficient homogenisation or lysis of samples	Decrease the amount of starting material. Mince tissues into smaller pieces and make sure it is completely immersed in TRIsure for optimal lysis.
	Insufficient solubilization of RNA, DNA or protein pellet	Increase the solubilization rate by pipetting the sample repeatedly, heat the sample to 60°C.
	Loss of pellet	If starting sample is small, the pellet may not be easily visualized after precipitation, so care must be taken when removing the supernatant from the pellet.
RNA is degraded, DNA is degraded, or protein is degraded.	Samples were not immediately processed or frozen after collection	Sample must be processed or frozen immediately after collection.
	Isolated RNA, DNA or protein preparations were stored at the incorrect temperature	Store RNA samples at –80°C. Store DNA and protein samples at –20°C.
	RNase contamination	Protocol must be carried out carefully in a DNA-free, RNase-free environment. Addition of RNase Inhibitor to the extracted RNA sample can help prevent degradation of the sample.
Low $A_{260/280}$ for RNA	Insufficient volume of TRIsure	Ensure that 1 ml TRIsure per 10cm^2 area of cells or 5 x 10^6 cells is used. If problem persists, increase TRIsure volume by 1.5 x.
	Contamination of interphase layer during separation of the RNA-containing aqueous layer	Pipette off the aqueous phase very carefully. It is important that none of the white interphase is transferred into your RNA sample, so we recommend that you leave the lower part of the aqueous phase intact.
Low $A_{260/280}$ for DNA	Phenol was not sufficiently removed from the DNA preparation	Wash the DNA pellet one additional time in 0.1 M sodium citrate in 10% ethanol.

Technical Support

If the troubleshooting guide does not solve the difficulty you are experiencing, please contact Technical Support with details of the procedure and relevant data.

Email: tech@bioline.com

Associated Products

Product Name	Pack Size	Cat No.
SensiFAST™ cDNA Synthesis Kit	50 Reactions	BIO-65053
MyTaq™ HS Mix	200 Reactions	BIO-25045
SensiFAST™ SYBR® No-ROX One-Step Kit	100 Reactions	BIO-72001

Trademarks

TRIsure, MyTaq and SensiFAST are trademarks of Bioline

Bioline Reagents Ltd
UNITED KINGDOM
Tel: +44 (0)20 8830 5300
Fax: +44 (0)20 8452 2822

Bioline USA Inc.
USA
Tel: +1 508 880 8990
Fax: +1 508 880 8993

Bioline GmbH
GERMANY
Tel: +49 (0)337 168 1229
Fax: +49 (0)3371 68 1244

Bioline (Aust) Pty. Ltd
AUSTRALIA
Tel: +61 (0)2 9209 4180
Fax: +61 (0)2 9209 4763

Bioline France
FRANCE
Tel: +33 (0)1 42 56 04 40
Fax: +33 (0)9 70 06 62 10

Meridian Bioscience Asia Pte Ltd
SINGAPORE
Tel: +65 6774 7196
Fax: +65 6774 6441

Website: www.bioline.com email: info@bioline.com

Appendix 6 – Bioline Tetro cDNA Synthesis Kit Data Sheet

Tetro cDNA Synthesis Kit

Shipping: On Dry/Blue Ice

Catalog numbers

BIO-65042 : 30 reactions

Batch No.: See vial

BIO-65043 : 100 reactions

BIOLINE
A Meridian Life Science® Company

Store at –20°C

Storage and stability:
Tetro cDNA Synthesis Kit is shipped on dry/blue ice. All kit components should be stored at -20°C upon receipt. Excessive freeze/thawing is not recommended.
Expiry:
When stored under the recommended conditions and handled correctly, full activity of the kit is retained until the expiry date on the outer box label.
Quality Control:
Tetro cDNA Synthesis Kit and its components are extensively tested for activity, processivity, efficiency, sensitivity, absence of nuclease contamination and absence of nucleic acid contamination.
Unit definitions:
Reverse Transcriptase: One unit catalyzes the incorporation of 1nmole of dTTP into acid-insoluble material in 10 minutes at 37°C in 50 mM Tris-HCl, pH 8.6, 40mM KCl, 1mM $MnSO_4$, 1mM DTT, and 0.5mM [3H]TTP, using 200µM oligo$(dT)_{12\text{-}18}$-primed poly$(A)_n$ as template.
RNase Inhibitor: One unit inhibits 5ng of RNase A by 50%.
Safety precautions:
Harmful if swallowed. Irritating to eyes, respiratory system and skin. Please refer to the material safety data sheet for information regarding hazards and safe handling practice.

Signal word: WARNING

Notes:
For research use only.

Description

The Tetro cDNA Synthesis Kit contains all the necessary components to generate cDNA from an RNA template. The generated cDNA is suitable for PCR with gene-specific primers or for other downstream applications. The kit contains MMLV Reverse Transcriptase and is suitable for first strand cDNA synthesis, cDNA library construction, and the production of templates for RT-PCR amplification.

The Tetro cDNA Synthesis Kit is optimized for RT reactions using a wide range of total RNA amounts (100pg-2µg), such that long and low abundance cDNAs can be detected by amplification after cDNA synthesis. The Kit contains oligo $(dT)_{18}$ and random hexamer primers. The dNTPs included in the kit are manufactured by Bioline and are 99% pure.

Components

Product Name	30 reactions	100 reactions
5x RT Buffer	120µl	400µl
(200u/µl) Reverse Transcriptase	30µl	100µl
(10u/µl) RNase Inhibitor	30µl	100µl
dNTP Mix 10mM Total	30µl	100µl
Oligo $(dT)_{18}$ Primer Mix	30µl	100µl
Random Hexamer Primer Mix	30µl	100µl
DEPC-treated Water	1.8ml	1.8ml

Tetro cDNA Synthesis Kit Reaction Guidelines

Template Quality

- Intact, high-quality RNA is essential for the reverse-transcription reaction.
- All reagents for use with RNA must be prepared using DEPC-treated water (BIO-38030).
- The inclusion of an RNase Inhibitor protein can reduce template degradation and increase yield of PCR product.
- Low-copy-number genes may require an increase in starting material.
- Use a suitable RNA extraction reagent e.g. TRIsure™ (BIO-38032) or ISOLATE II RNA Mini Kit (BIO-52072).

Primer Design and Concentration

There are three methods for priming cDNA synthesis:

- **Oligo dT Primers**
  Oligo dT priming uses the poly-A tail found on the 3' end of most eukaryotic mRNAs. This ensures that the 3' end of mRNAs are represented, although long mRNAs can have their 5' ends under-represented in the subsequent cDNA pool.
- **Random Hexamers**
  Random priming gives random coverage to all regions of the RNA to generate a cDNA pool containing various lengths of cDNA. Random priming is unable to distinguish between mRNA and other RNA species present in the reaction.
- **Gene Specific Primers (GSP)**
  Gene specific primers are designed to generate cDNA for a specific gene of interest. It is a widely used method for performing One-Step RT-PCR when only 1 gene is under investigation. It can be useful when RNA concentrations are low (use at 0.4µM/reaction).

A combination of Oligo dT and Random Hexamers primers can improve the reverse transcription efficiency of some mRNA templates.

Reaction Recommendations and Optimization

- The use of RNase-free plasticware and tips is essential.
- We recommend using a final volume of 20µl.
- Prepare all reactions on ice.
- Efficient reverse-transcription can be achieved at temperatures of 37°C to 45°C for 30-60 min.
- The use of higher incubation temperatures up to 48°C may increase the yield of cDNA synthesized in cases of complex RNA secondary structure. However, the yield of the majority of RNA molecules will be reduced.

Tetro cDNA Synthesis Kit Protocol

1. Vortex solutions and centrifuge briefly before use.
2. Prepare the priming premix on ice in an RNase-free reaction tube:

Total RNA (up to 5µg) or mRNA (up to 5µg)	*n*µl
Primer: Oligo $(dT)_{18}$ *or* Random Hexamer (*or* GSP)	1µl
10mM dNTP mix	1µl
5x RT Buffer	4µl
RiboSafe RNase Inhibitor	1µl
Tetro Reverse Transcriptase (200u/µl)	1µl
DEPC-treated water*	to 20µl

*

Available separately (see Associated Products)

3. Mix gently by pipetting.
4. Incubate samples at 45°C for 30 min. If using random hexamers, incubate at 10 min at 25°C followed by 45°C for 30 min.
5. Terminate reaction by incubating at 85°C for 5 min, chill on ice.
6. Store reaction at –20°C for long term storage, or proceed to PCR immediately.

This protocol is intended for use as a guide only; conditions will vary from reaction to reaction and may need optimization.

Troubleshooting

Problem	Possible Cause	Recommendation
No cDNA synthesis	RNA degraded	Analyze RNA on a denaturing gel to verify integrity. Ensure that all reagents are RNase-free.
	RNA contained an RT inhibitor	The presence of inhibitors can be determined by mixing a control RNA with some of the sample and comparing the yield with that of the original amplification. Remove inhibitors such as SDS, EDTA, formamide and pyrophosphate, by ethanol precipitation of RNA, including a 70% ethanol wash step.
	Reaction temperature not optimal	Perform a temperature-gradient experiment ranging from 37-48°C.
	Not enough starting RNA	Increase the amount of starting RNA, this can be an important factor when amplifying low-copy genes from total RNA.
	RNA had high secondary structure	Prior to reaction set-up, denature RNA with primers. Raise the temperature of the RT step, up to a maximum of 48°C (for short amplicons).
	Insufficient product	Increase reverse transcription step to 60 minutes
Poor Specificity in PCR	Non-specific annealing of primers to template	Use gene-specific primers rather than Oligo dT or random hexamers in RT reaction. Increase the annealing temperature in PCR. Check for presence of pseudogenes. Set up reactions on ice.
	Primer dimers	Redesign primers to prevent self-annealing.
	Genomic DNA contamination	Treat RNA with DNase I and re-purify. If possible, use intron-spanning primers in PCR.
Product in no-RTase control	Template contaminated with DNA	Treat samples with DNase I.

Technical Support:

If the troubleshooting guide does not solve the difficulty you are experiencing, please contact Technical Support with details of reaction setup, cycling conditions and relevant data.

Email: tech@bioline.com

Associated products:

Product Name	Cat. No.
SensiFAST™ SYBR No-ROX Kit	BIO-98002
ISOLATE II RNA Mini Kit	BIO-52072
TRIsure™	BIO-38032
HyperLadder™ 1kb	BIO-33025
DEPC-treated Water	BIO-38030
Agarose, Molecular Grade	BIO-41026

Product Citations:

1. Green, T. J. *et al. Fish & Shellfish Immunol.* **36(1):** 151-157 (2014).
2. Skarratt, K. K. *et al. J. Microbiol. Methods* **96:** 99-100 (2014).
3. Liying, C. *et al. Leukemia* **27(4):** 813-822 (2013).
4. Ahmadimoghaddam, D., *et al. Biol. Reprod.* **88(3):** 1-10 (2013).
5. Zhao, Y. G., et al. J. Immunol. 189(9): 4417-4425 (2012).
6. Bałkowiec-Iskra, E., *et al. Neurosci.* **180:** 322-333 (2011).
7. Szczepanek, K., *et al. J. Biol. Chem.* **286:** 29610-29620 (2011).
8. Gowen, C.M. & Fong, S.S., *Biotechnol. J.* **7:** 759-767 (2010).
9. Hsieh, H.Y., *et al. J. Neurosci. Res.* **88(6):** 1285-1297 (2010).
10. Liu, X., *et al. Plant Physiol.* **152:** 985-999 (2010).
11. Vermehren-Schmaedick, A., *et al. Genetics* **186:** 183-196 (2010).
12. Giordani, L., *et al. J. Leukoc. Biol.* **86:** 261-271 (2009).

Bioline Reagents Ltd
UNITED KINGDOM

Tel: +44 (0)20 8830 5300
Fax: +44 (0)20 8452 2822

Bioline USA Inc.
USA

Tel: +1 508 880 8990
Fax: +1 508 880 8993

Bioline GmbH
GERMANY

Tel: +49 (0)33 7168 1229
Fax: +49 (0)337168 1244

Bioline (Aust) Pty. Ltd
AUSTRALIA

Tel: +61 (0)2 9209 4180
Fax: +61 (0)2 9209 4763

Appendix 7 – KAPA Biosystems SYBR Fast qPCR Master Mix (2x) Data Sheet

KAPABIOSYSTEMS

Technical Data Sheet

KAPA SYBR® FAST qPCR Kit Master Mix (2X) Universal

KR0389 – v9.13

Product Description

KAPA SYBR® FAST qPCR Master Mix is designed for high performance real-time PCR. The kit contains a novel DNA polymerase engineered via a process of molecular evolution. The result is a unique enzyme, specifically designed for qPCR using SYBR® Green I dye chemistry.

KAPA SYBR® DNA Polymerase has been engineered to perform optimally in stringent real-time quantitative PCR (qPCR) reaction conditions, exhibiting dramatic improvements in signal-to-noise ratio (fluorescence), quantification cycle (C_q), linearity, and sensitivity. The KAPA SYBR® DNA Polymerase and proprietary buffer system improves the amplification efficiency of difficult targets, including both GC- and AT-rich templates.

KAPA SYBR® FAST qPCR Master Mix (2X) Universal is a ready-to-use cocktail containing all components except primers and template, for the amplification and detection of DNA in qPCR. The KAPA SYBR® FAST qPCR Kit is supplied as a 2X Master Mix with integrated antibody-mediated hot start, SYBR® Green I fluorescent dye, $MgCl_2$, dNTPs and stabilizers. ROX reference dye is not included in the 2X Master Mix but is supplied separately.

Product Applications

KAPA SYBR® FAST qPCR Kits are ideally suited for:

- Gene expression analysis
- Low copy gene detection
- Absolute quantification of NGS libraries.

Product Specifications

Shipping and Storage

Upon arrival, store kit components protected from light at -20 °C in a constant-temperature freezer. When stored under these conditions and handled correctly, the Master Mix (2X) will retain full activity until the expiry date indicated on the kit label.

Handling

Minimize exposure of the Master Mix (2X) to direct light. Exposure to direct light for an extended period of time may result in loss of fluorescent signal intensity. Always ensure that the product has been fully thawed and mixed before use.

Quality Control

KAPA SYBR® FAST qPCR Master Mix (2X) is free of contaminating DNase and RNase. It is functionally tested by generating a standard curve with human genomic DNA as template, with a dynamic range of 5 orders of magnitude, a reaction efficiency of 90 – 110% and a correlation coefficient >0.99.

Kit Codes and Components	
KK4600 100 x 20 µl reactions	**KAPA SYBR® FAST Master Mix (2X) Universal** qPCR Master Mix (2X) – 1 x 1 ml ROX Reference Dye High (50X) – 1 x 200 µl ROX Reference Dye Low (50X) – 1 x 200 µl
KK4601 500 x 20 µl reactions	**KAPA SYBR® FAST Master Mix (2X) Universal** qPCR Master Mix (2X) – 1 x 5 ml ROX Reference Dye High (50X) – 1 x 200 µl ROX Reference Dye Low (50X) – 1 x 200 µl
KK4602 1000 x 20 µl reactions	**KAPA SYBR® FAST Master Mix (2X) Universal** qPCR Master Mix (2X) – 2 x 5 ml ROX Reference Dye High (50X) – 2 x 200 µl ROX Reference Dye Low (50X) – 2 x 200 µl

Quick Notes

- This kit contains an engineered enzyme optimized for qPCR using SYBR® Green I dye chemistry.
- The 2X Master Mix contains a proprietary buffer. Together with the novel enzyme, this improves amplification efficiency of both GC- and AT-rich targets.
- 20 sec initial denaturation at 95 °C is sufficient for enzyme activation. When working with complex templates, an initial denaturation of 3 min is recommended.
- For two-step cycling, use 20 sec combined annealing/extension/data acquisition.
- Do not exceed 25 µl reaction volumes.

Instrument	ROX Reference Dye
Applied Biosystems® 5700, 7000, 7300, 7700, 7900HT, StepOne™, and StepOnePlus™	ROX High
Applied Biosystems® 7500, ViiA™7, QuantStudio™ 12K Flex, Agilent Mx3000P™, Mx3005P™, and Mx4000™	ROX Low
Rotor-Gene™, DNA Engine Opticon™, Opticon™ 2, Chromo 4™ Real-Time Detector, Mastercycler® ep realplex, Smart Cycler®, Roche LightCycler® 480, Roche LightCycler® Nano, Bio-Rad CFX96, and Illumina Eco™	No ROX

KAPA SYBR® FAST qPCR Protocol

Any existing qPCR assay performed efficiently using standard cycling conditions may be converted to a fast qPCR assay with KAPA SYBR® FAST qPCR Kits. Typically, minimal re-optimization of reaction parameters is required.

Step 1: Prepare the qPCR master mix

- Ensure all reaction components are properly thawed and mixed.
- Prepare a PCR master mix containing the appropriate volume of all reaction components common to all or a subset of reactions to be performed.
- Calculate the required volume of each component based on the following table:

Component	20 µl rxn[1]	Final conc.
PCR-grade water	Up to 20 µl	N/A
2X KAPA SYBR® FAST qPCR Master Mix[2] Universal	10 µl	1X
10 µM Forward Primer	0.4 µl	200 nM
10 µM Reverse Primer	0.4 µl	200 nM
Template DNA[3]	As required	<20 ng
50X ROX High/Low (As required)[4]	0.4 µl	1X

[1] Reaction volumes may be adjusted between 5 – 25 µl. Reaction volumes >25 µl are not recommended.

[2] KAPA SYBR® FAST qPCR Master Mix contains $MgCl_2$ at a final concentration of 2.5 mM.

[3] Do not exceed 20 ng per 20 µl reaction. For more information, refer to Important Parameters: Template.

[4] The use of ROX dye is necessary for all Applied Biosystems® instruments and is optional for the Agilent Mx3000P™, Mx3005P™, and Mx4000™ cyclers. Bio-Rad/MJ Research, Cepheid, Corbett/Qiagen, Eppendorf, Illumina and Roche instruments do not require ROX dye.

Step 2: Set up individual reactions

- Transfer the appropriate volumes of qPCR master mix, template and primers to each well of a PCR tube/plate.
- Cap or seal the reaction tube/plate and centrifuge briefly.

Step 3: Run the qPCR

- If applicable, select fast mode on the instrument.
- Confirm that qPCR protocol to be used conforms to the following parameters:

Step	Temperature	Duration	Cycles
Enzyme activation	95 °C	3 min[1]	Hold
Denaturation	95 °C	1 – 3 sec	40
Annealing/ extension/ data acquisition[3]	60 °C	≥ 20 sec[2]	
Dissociation	According to instrument guidelines		

[1] 20 sec at 95 °C is sufficient time for enzyme activation; however, optimal denaturation of complex targets may require up to 3 min denaturation.

[2] Select shortest time possible for instrument, but not less than 20 sec.

[3] For 3-step cycling protocols, anneal at optimal annealing temperature for 20 sec followed by the minimum time required for data acquisition at 72 °C according to instrument guidelines.

Note: The above cycling parameters are not optimal for qPCR-based quantification of next-generation sequencing libraries. Please refer to the protocol in the KAPA Library Quantification Kit Technical Data Sheet.

Step 4: Analyze the results

- Melt curve analysis should be performed to identify the presence of primer-dimers and analyze the specificity of the reaction. Program your thermocycler according to the instrument guidelines.
- Data analysis is dependent on experimental design. Refer to your instrument guidelines for more information on how to perform the appropriate data analysis.

Important Parameters

Template

High concentrations of template may increase background fluorescence and reduce linearity of standard curves. For optimal quantitative results, use up to 20 ng of genomic DNA or plasmid DNA per 20 µl reaction (for smaller volumes, the amount of template should be decreased proportionally). For two-step RT-PCR, use either undiluted or diluted cDNA generated from up to 1 µg of total RNA. The volume of the cDNA (reverse transcription reaction product) should not exceed 10% of the final PCR volume (e.g. for a 20 µl qPCR reaction, use up to 2.0 µl of undiluted cDNA).

Important Parameters (continued)

Primers

Careful primer design and purification (HPLC-purified primers are recommended) will minimize loss in sensitivity due to nonspecific amplification. This effect becomes more prominent at low target concentrations. To maximize the sensitivity of the assay, use the lowest primer concentration determined not to compromise reaction efficiency (50 – 400 nM of each primer). For optimal results, design primers that amplify PCR products 60 – 400 bp in length. Use appropriate primer design software to design primers with a melting temperature (T_m) of approximately 60 °C, to take advantage of two-step cycling. If performing qRT-PCR, we recommend designing primers specifically for amplification of cDNA derived from mRNA. This prevents amplification of contaminating genomic DNA and inaccurate quantification of mRNA.

KAPA SYBR® DNA Polymerase

KAPA SYBR® DNA Polymerase is an engineered version of *Taq* DNA polymerase, designed specifically for real-time PCR using SYBR Green I chemistry. KAPA SYBR® DNA Polymerase displays no enzymatic activity at ambient temperature. This prevents the formation of misprimed products and primer-dimers during reaction setup, prior to the first denaturation step, and results in high PCR specificity and accurate quantification. The enzyme is activated during the initial denaturation step of the PCR. The activation of the enzyme is complete after 20 sec; however, complex targets may require up to 3 min for optimal denaturation. The hot start feature obviates the need to cool reactions during setup.

ROX Reference Dye

For certain real-time cyclers, the presence of ROX reference dye compensates for non-PCR-related variations in fluorescence detection. The fluorescence level of ROX reference dye does not change significantly during the course of real-time PCR, but provides a stable baseline against which PCR-related fluorescent signals are normalized. Thus, ROX dye compensates for differences in fluorescence detection between wells due to slight variations in reaction volume or differences in well position. The presence of ROX dye in the master mix does not interfere with real-time PCR on any instrument, since the dye is not involved in the reaction and has an emission spectrum different from that of SYBR® Green I.

SYBR® Green I

KAPA SYBR® FAST qPCR Master Mix (2X) contains an elevated, optimized concentration of the fluorescent dye, SYBR® Green I. High signal intensities are achieved as a result of increased tolerance to high concentrations of SYBR® Green I by the engineered KAPA SYBR® DNA Polymerase. SYBR® Green I binds all double-stranded DNA molecules, emitting a fluorescent signal on binding.

Magnesium chloride

The KAPA SYBR® FAST qPCR Master Mix contains an optimized $MgCl_2$ concentration. It is highly unlikely that additional $MgCl_2$ will improve reaction efficiency or specificity.

Note to Purchaser: Limited License

Certain applications of this product are covered by patents issued to parties other than Kapa Biosystems and applicable in certain countries. Purchase of this product does not include a license to perform any such applications. Users of this product may therefore be required to obtain a patent license depending upon the particular application and country in which the product is used.

Use of this product is covered by one or more of the following US patents and corresponding patent claims outside the US: 5,994,056, 6,171,785, and 5,928,907 (claim numbers 12-24, 27-28). The purchase of this product includes a limited, non-transferable immunity from suit under the foregoing patent claims for using only this amount of product for the purchaser's own internal research. No right under any other patent claim (such as apparatus or system claims in US Patent No. 6,814,934) and no right to perform commercial services of any kind, including without limitation reporting the results of purchaser's activities for a fee or other commercial consideration, is conveyed expressly, by implication, or by estoppel. This product is for research use only. Diagnostic uses under Roche patents require a separate license from Roche. Further information on purchasing licenses may be obtained by contacting the Director of Licensing, Applied Biosystems, 850 Lincoln Centre Drive, Foster City, California 94404, USA.

This product is provided under an agreement between Life Technologies Corporation. and Kapa Biosystems Inc., and the manufacture, use, sale or import of this product is subject to one or more of U.S. Patent Nos. 5,436,134; 5,658,751 and corresponding international equivalents, owned by Life Technologies Corporation. The purchase of this product conveys to the buyer the non-transferable right to use the purchased amount of the product and components of the product in research conducted by the buyer, where such research does not include testing, analysis or screening services for any third party in return for compensation on a per test basis. The buyer cannot sell or otherwise transfer (a) this product (b) its components or (c) materials made using this product or its components to a third party or otherwise use this product or its components or materials made using this product or its components for Commercial Purposes. Commercial Purposes means any activity by a party for consideration and may include, but is not limited to: (1) use of the product or its components in manufacturing; (2) use of the product or its components to provide a service, information, or data; (3) use of the product or its components for therapeutic, diagnostic or prophylactic purposes; or (4) resale of the product or its components, whether or not such product or its components are resold for use in research. For information on purchasing a license to this product for purposes other than research, contact Life Technologies Corporation, 5791 Van Allen Way, Carlsbad, CA 92008 USA or outlicensing@lifetech.com.

Licensed under U.S. Patent nos. 5,338,671 and 5,587,287 and corresponding patents in other countries.

The purchase of this product includes a limited, non-transferable license under specific claims of U.S. Patent Nos. 6,174,670, 6,569,627 and 5,871,908, owned by the University of Utah Research Foundation or Evotec Biosystems GmbH and licensed to Idaho Technology, Inc. and Roche Diagnostics GmbH, to use only the enclosed amount of product according to the specified protocols. No right is conveyed, expressly, by implication, or by estoppel, to use any instrument or system under any claim of U.S. Patent Nos. 6,174,670, 6,569,627 and 5,871,908, other than for the amount of product contained herein.

Applied Biosystems®, SYBR®, PRISM®, GeneAmp®, ViiA™, QuantStudio™, StepOne™, and StepOnePlus™ are trademarks or registered trademarks of Life Technologies Corporation. iCycler®, Mx3000P™, Mx3005™, Mx4000™, Rotor-Gene™, DNA Engine Opticon™, Chromo 4™, LightCycler®, Smart Cycler®, and Eco™ are trademarks or registered trademarks of their respective companies.

Troubleshooting

Symptoms	Possible Causes	Solutions
Positive signal in no-template control (NTC) Presence of secondary, nonspecific peak in melt curve of sample	Reasons for a positive signal in a NTC and/or nonspecific amplifcation are often due to multiple factors that include: 1. Contamination 2. Primer-dimer formation due to: • Incorrect cycling protocol • Sub-optimal primer annealing temperature (often due to differences between qPCR systems) • Primer and/or template degradation. Primers should be stored and diluted in 10 mM Tris-HCl (pH 8.0 – 8.5), not in PCR-grade water) • Sub-optimal primer synthesis • Sub-optimal primer design	Perform melt curve analysis (or run qPCR products on a gel) to determine if the product is specific or nonspecific (primer-dimer). If the NTC contains a specific product, the assay is contaminated: • Discard all reagents, clean all pipettes and surfaces and prepare fresh stocks of primer, etc. Note: The increased sensitivity of KAPA SYBR® FAST qPCR Kits may result in the detection of low levels of contamination in assays considered contaminant-free when using competitor kits containing wild-type *Taq* DNA polymerase. If the NTC and/or sample contains nonspecific product, assay optimization may be required: • 30 sec combined annealing/extension time is recommended for most assays. Longer times may result in nonspecific amplification. • Increase the combined annealing/extension temperature in increments of 3 °C. • Decrease primer concentration. • Resynthesize or redesign primers. HPLC purified primers are recommended for low copy number detection, and often results in reduced primer-dimer formation.
Low fluorescence intensity	Incorrect handling Incorrect concentration of ROX reference dye	SYBR® Green I dye is light sensitive; avoid exposure to light and repeated freeze-thaw cycles. Always thaw and mix solutions thoroughly before use. If the incorrect concentration of ROX reference dye is added to the master mix, the normalized signal may be lower than expected (if too much ROX has been added), or higher than expected (if too little ROX has been added). If using ABI instrumentation, analysis of the raw signal can always be performed with the ROX filter switched off.
Melting temperature of specific product is different from competitor kit	Differences in the buffer composition (e.g. salt concentration) of qPCR master mixes	Differences in master mix formulation may affect the melting temperature of the product slightly. A particular DNA fragment will melt at a higher temperature in a reaction buffer containing a higher salt concentration.

For technical support please contact:
support@kapabiosystems.com

Boston, Massachusetts, United States
Int. Tel: +1 781 497 2933 Tel: +1 855 KAPA BIO
Fax: +1 781 497 2934
Email: sales@kapabiosystems.com

Cape Town, South Africa
Tel: +27 21 448 8200 Fax: +27 21 448 6503
Email: sales@kapabiosystems.com

altromin

1320 M - product data sheet

1320 M

Maintenance diet for mice

Available as

1321 M - Powder 1324 M - 10mm pellets 1328 M - Hybridpellet

Product variations

The 1320 M formula is optionally also available in one or a combination of the following variants.

Variant P
deficient in phytoestrogens
Variant Fortified
autoclavable, increased vitamin content, coated on request
Variant Irradiated
irradiated with 5 to 50kGy
The contents may vary for these variants.

Metabolized energy

Content		Value	unit
Fat	496	(15%)	kcal/kg
Protein	823	(24%)	kcal/kg
Carbonhydrates	2,067	(61%)	kcal/kg

crude nutrients and moisture

Content		Value	unit
Moisture	111,756	(11.2%)	mg/kg
Crude Ash	58,708	(5.9%)	mg/kg
Crude Fibre	40,304	(4.0%)	mg/kg
Crude Fat	55,116	(5.5%)	mg/kg
Crude Protein	205,829	(20.6%)	mg/kg
Nitrogenfree extractives	528,287	(52.8%)	mg/kg

Carbonhydrates

Content	Value	unit
Monosaccharides	0	mg/kg
Disaccharides	51,201	mg/kg
Polysaccharides	374,856	mg/kg

Altromin Spezialfutter GmbH & Co. KG
Im Seelenkamp 20, 32791 Lage, Germany
info@altromin.de - www.altromin.com

Minerals

Content	Value	unit
Calcium	7,063	mg/kg
Potassium	9,503	mg/kg
Magnesium	2,151	mg/kg
Sodium	2,133	mg/kg
Phosphorus	5,054	mg/kg

Trace elements

Content	Value	unit
Aluminium	85.94	mg/kg
Chlorine	3,471.79	mg/kg
Iron	191.82	mg/kg
Flourine	3.07	mg/kg
Iodine	1.60	mg/kg
Cobalt	0.44	mg/kg
Copper	13.60	mg/kg
Manganese	87.49	mg/kg
Molybdenum	1.29	mg/kg
Sulfur	1,181.92	mg/kg
Selenium	0.26	mg/kg
Zinc	92.72	mg/kg

Altromin Spezialfutter GmbH & Co. KG
Im Seelenkamp 20, 32791 Lage, Germany
info@altromin.de - www.altromin.com

Added vitamins

Content	Standard	Fortified	unit
Vitamin A	15,000	26,250	IU/kg
Vitamin D3	600	1,050	IU/kg
Vitamin E	78	134	mg/kg
Vitamin K3	3	5	mg/kg
Vitamin B1	18	32	mg/kg
Vitamin B2	12	21	mg/kg
Vitamin B6	9	16	mg/kg
Vitamin B12	24	42	µg/kg
Nicotinic acid	36	63	mg/kg
Pantothenic acid	21	37	mg/kg
Folic acid	2	4	mg/kg
Biotin	260	297	µg/kg
Choline chloride	690	1,140	mg/kg
Vitamin C	36	63	mg/kg

Amino acids

Content	Value	unit
Alanine	9,061	mg/kg
Arginine	12,898	mg/kg
Aspartic acid	18,224	mg/kg
Cystine	3,289	mg/kg
Glutaminc acid	42,392	mg/kg
Glycine	8,810	mg/kg
Histidine	4,894	mg/kg
Isoleucine	8,528	mg/kg
Leucine	14,926	mg/kg
Lysine	9,601	mg/kg
Methionine	3,332	mg/kg
Phenylalanine	9,403	mg/kg
Proline	13,536	mg/kg
Serine	10,129	mg/kg
Threonine	7,267	mg/kg
Tryptophan	2,667	mg/kg
Tyrosine	6,632	mg/kg
Valine	9,696	mg/kg

Altromin Spezialfutter GmbH & Co. KG
Im Seelenkamp 20, 32791 Lage, Germany
info@altromin.de - www.altromin.com

Fatty acid

Content	Value	unit
Arachidic acid C-20:0	179	mg/kg
Eicosanoic acid C-20:1	224	mg/kg
Alpha-Linolenic acid C-18:3	3,393	mg/kg
Linolenic acid C-18:2	24,731	mg/kg
Palmitic acid C-16:0	6,014	mg/kg
Stearic acid C-18:0	1,816	mg/kg
Oleic acid C-18:1	10,442	mg/kg

Altromin Spezialfutter GmbH & Co. KG
Im Seelenkamp 20, 32791 Lage, Germany
info@altromin.de - www.altromin.com

Appendix 9 – Research Diets #D12079B Data Sheet (Western Diet)

Open formula purified diets for lab animals



OpenSource DIETS®

Report ▶ Repeat ▶ Revise

Product Data - D12079B

Description
RD Western Diet

Used in Research
Obesity
Diabetes
Osteoporosis
Hypertension
Atherosclerosis
Metabolic Syndrome

Packaging
Product is packed in 12.5 kg box. Each box is identified with the product name, description, lot number and expiration date.

Lead Time
5-7 business days.

Gamma-Irradiation
Yes. Add 10 days to delivery time.

Form
Pellet, Powder, Liquid

Shelf Life
Most diets require storage in a cool dry environment. Stored correctly they should last 6 months.

Control Diets
Custom diets available on request.

Formula

Product # D12079B		gm%	kcal%
Protein		20	17
Carbohydrate		50	43
Fat		21	41
	Total		100
	kcal/gm	4.7	

Ingredient	gm	kcal
Casein, 80 Mesh	195	780
DL-Methionine	3	12
Corn Starch	50	200
Maltodextrin 10	100	400
Sucrose	341	1364
Cellulose	50	0
Milk Fat, Anhydrous*	200	1800
Corn Oil	10	90
Mineral Mix S10001	35	0
Calcium Carbonate	4	0
Vitamin Mix V10001	10	40
Choline Bitartrate	2	0
Cholesterol, USP*	1.5	0
Ethoxyquin	0.04	0
Total	**1001.54**	**4686**

*Anhydrous milk fat typically contains approximately 0.3% cholesterol. On this basis, D12079B contains approximately 0.21% cholesterol.
Formulated by E. A. Ulman, Ph.D., Research Diets, Inc., October 12, 1995.
Diet formulated to match Teklad Western Diet #TD88137, except that 1% Corn Oil replaces 1% Butter Fat.

RESEARCH DIETS INC.
www.ResearchDiets.com
Where NutriPhenomics Begins

Research Diets, Inc.
20 Jules Lane
New Brunswick, NJ 08901 USA
Tel: 732.247.2390
Fax: 732.247.2340
info@researchdiets.com

© 2006 Research Diets, Inc. All rights reserved. D12079B--6-12



OpenSource DIETS®

Report ▶ Repeat ▶ Revise

References - D12079B

1. Beigneux, A.P., et al. ATP-Citrate lyase deficiency in the mouse. Journal of Biological Chemistry. 279:9557-9564, 2004.
2. Bhat, B.G. et al. Inhibition of ileal bile acid transport and reduced atherosclerosis in apoE-/- mice by SC-435. Journal of Lipid Research. 44:1614-1621, 2003.
3. Collins, A.R. et al. Troglitazone inhibits formation of early atherosclerotic lesions in diabetic and nondiabetic low density lipoprotein receptor-deficient mice. Arterioscler Thromb. Vasc. Biol. 21:365-371, 2001.
4. Davis, H.R., et al. Ezetimibe, a potent cholesterol absorption inhibitor, inhibit the development of atherosclerosis in ApoE knockout mice. Arterioscler Thromb. Vasc. Biol. 21:2032-2038, 2001.
5. Lemaître, V., et al. Increased medial degradation with pseudo-aneurysm formation in apolipoprotein E-knockout mice deficient in tissue inhibitor of metalloproteinases-1. Circulation. 107:333-338, 2003.
6. Lemaître, V. et al. ApoE knockout mice expressing human matrix metalloproteinase-1 macrophages have less advanced atherosclerosis. Journal of Clinical Investigation. 107:1227-1234, 2001.
7. Ogus, S. et al. Hyperleptinemia precipitates diet-induced obesity in transgenic mice overexpressing leptin. Endocrinology. 144:2865-2869, 2003.
8. Park, Tae-Sik, et al. Inhibition of sphingomyelin synthesis reduces atherogeneesis in apolipoprotein E-knockout mice. Circulation. 110:3465-3471, 2004.
9. Seli, E., et al. Estradiol suppresses vascular monocyte chemotactic protein-1 expression during early atherogenesis. Am. J. Obstet. Gynecol. 187:1544-1549, 2002.

Research Diets, Inc.
20 Jules Lane
New Brunswick, NJ 08901 USA
Tel: 732.247.2390
Fax: 732.247.2340
info@researchdiets.com

© 2006 Research Diets, Inc. All rights reserved. D12079B--6-12

Appendix 10 – Mouse Leptin ELISA Kit Data Sheet

MOUSE LEPTIN ELISA KIT
96-Well Plate (Cat.# EZML-82K)

I. INTENDED USE

This kit is used for the non-radioactive quantification of leptin in mouse sera. Plasma samples may also be used but application to samples of other biological fluids may need validation by the user. One kit is sufficient to measure 37 unknown samples in duplicate.

For Research Use Only. Not for Use in Diagnostic Procedures.

II. PRINCIPLES OF PROCEDURE

This assay is a Sandwich ELISA based, sequentially, on: 1) binding of leptin in the sample by a pre-titered antiserum and immobilization of the resulting complexes in the wells of a microtiter plate, 2) after washing purified biotinylated detection antibody is allowed to bind to the immobilized leptin, 3) binding of horseradish peroxidase to the immobilized biotinylated antibodies after free detection antibodies are washed off, 4) wash away of free enzyme conjugates, and 5) quantification of immobilized antibody-enzyme conjugates by monitoring horseradish peroxidase activities in the presence of the substrate 3,3',5,5'-tetramethylbenzidine. The enzyme activity is measured spectrophotometrically by the increased absorbency at 450 nm, corrected from the absorbency at 590nm, after acidification of formed products. Since the increase in absorbency is directly proportional to the amount of captured leptin in the unknown sample, the latter can be derived by interpolation from a reference curve generated in the same assay with reference standards of known concentrations of mouse leptin.

III. REAGENTS SUPPLIED

Each kit is sufficient to run one 96-well plate and contains the following reagents:

A. Rat/Mouse Leptin Microtiter Plate
Coated with pre-titered capture antibodies
Quantity: 1 plate
Preparation: Ready to use.
Note: Unused strips should be resealed in the foil pouch with the desiccant provided and stored at 2-8°C.

B. Adhesive Plate Sealer
Quantity: 2 sheets
Preparation: Ready to use.

C. Rat/Mouse Leptin Antiserum
Pre-titered anti-rodent leptin serum
Quantity: 6 mL
Preparation: Ready to use.

III. REAGENTS SUPPLIED (continued)

D. 10X HRP Wash Buffer Concentrate
10X concentrate of 50 mM Tris Buffered Saline containing Tween-20.
Quantity: Two bottles containing 50 mL each
Preparation: Dilute 1:10 with distilled or de-ionized water.

E. Mouse Leptin ELISA Standard
Mouse leptin in buffer: 30 ng/mL.
Quantity: 0.5 mL/vial
Preparation: Serial dilution is required

Note: The standard(s) in this kit have been calibrated to an International Reference standard, NIBSC code # 97/626.

F. Quality Controls 1 and 2
Various peptides including leptin in QC buffer.
Quantity: 0.5 mL/vial
Preparation: Ready to use.

G. Rat/Mouse Leptin Matrix Solution
Matrix containing 0.08% Sodium Azide
Quantity: 0.5 mL/vial
Preparation: Ready to use.

H. Assay Buffer
0.05 M phosphosaline, pH 7.4, containing 0.025 M EDTA, 0.08% sodium azide, 0.05% Triton X-100 and 1% BSA.
Quantity: 40 mL/vial
Preparation: Ready to use.

I. Rat/Mouse Leptin Detection Antibody
Pre-titered biotinylated anti-mouse leptin antibody.
Quantity: 12 mL/vial
Preparation: Ready to use.

J. Enzyme Solution
Pre-titered streptavidin-horseradish peroxidase conjugate in buffer.
Quantity: 12 mL/vial
Preparation: Ready to use.

K. Substrate (Light Sensitive: avoid unnecessary exposure to light)
3, 3',5,5'-tetramethylbenzidine in buffer.
Quantity: 12 mL/vial
Preparation: Ready to use.

L. Stop Solution (Caution: Corrosive Solution)
0.3 M HCl
Quantity: 12 mL/vial
Preparation: Ready to use.

IV. STORAGE AND STABILITY

Recommended storage for kit components is 2 - 8°C.

All components are shipped and stored at 2-8°C. Once opened, liquid standards and controls can be stored up to 30 days at 2-8°C. Refer to expiration dates on all reagents prior to use. Do not mix reagents from different kits unless they have the same lot numbers.

V. REAGENT PRECAUTIONS

A. Sodium Azide

Sodium Azide has been added to certain reagents as a preservative at a concentration of 0.08%. Although it is at a minimum concentration, Sodium Azide may react with lead and copper plumbing to form explosive metal azides. Dispose of unused contents and waste in accordance with international, federal, state, and local regulations.

B. Hydrochloric Acid

Hydrochloric Acid is corrosive and can cause eye and skin burns. It is harmful if swallowed and can cause respiratory and digestive tract burns. Avoid contact with skin and eye. Do not swallow or ingest.

Note: See Full Labels of Hazardous components on next page.

Full Labels of Hazardous components:

Ingredient, Cat #		Full Label	
Rat Leptin Detection Antibody	E1083		**Warning.** Causes serious eye irritation. IF IN EYES: Rinse cautiously with water for several minutes. Remove contact lenses, if present and easy to do. Continue rinsing.
Mouse Leptin Quality Control 1 & 2	E6082-K		**Warning.** Causes serious eye irritation. IF IN EYES: Rinse cautiously with water for several minutes. Remove contact lenses, if present and easy to do. Continue rinsing.
Mouse Leptin Standards	E8082-K		**Warning.** Causes serious eye irritation. IF IN EYES: Rinse cautiously with water for several minutes. Remove contact lenses, if present and easy to do. Continue rinsing.
Antiserum	EAS83		**Warning.** Causes serious eye irritation. IF IN EYES: Rinse cautiously with water for several minutes. Remove contact lenses, if present and easy to do. Continue rinsing.
Wash Buffer Concentrate	EWB-HRP		**Warning.** May cause an allergic skin reaction. Wear protective gloves. IF ON SKIN: Wash with plenty of soap and water.
Stop Solution	ET-TMB		**Warning. May be corrosive to metals.**

VI. MATERIALS REQUIRED BUT NOT PROVIDED

1. Pipettes and pipette tips: 10 µL ~ 20 µL and 20 µL ~ 100 µL
2. Multi-channel Pipettes and pipette tips: 0 ~ 50 µL and 50 ~ 300 µL
3. Buffer and Reagent Reservoirs
4. Vortex Mixer
5. De-ionized Water
6. Microtiter Plate Reader capable of reading absorbency at 450 nm and 590nm
7. Orbital Microtiter Plate Shaker
8. Absorbent Paper or Cloth

VII. SAMPLE COLLECTION AND STORAGE

1. To prepare serum samples, whole blood is directly drawn into a centrifuge tube that contains no anti-coagulant. Let blood clot at room temperature for 30 min.

2. Promptly centrifuge the clotted blood at 2,000 to 3,000 x g for 15 minutes at 4 ± 2°C.

3. Transfer and store serum samples in separate tubes. Date and identify each sample.

4. Use freshly prepared serum or aliquot and store samples at -20°C for later use. Avoid multiple (> 3) freeze/thaw cycles.

5. To prepare plasma sample, whole blood should be collected into centrifuge tubes containing enough K_3EDTA to achieve a final concentration of 1.735 mg/mL and centrifuge immediately after collection. Observe the same precautions in the preparation of serum samples.

6. If heparin is to be used as anti-coagulant, the effect on the assay outcome at the dose of heparin used should be pre-determined.

7. Avoid using samples with gross hemolysis or lip.

VIII. STANDARD PREPARATION

1. Use care in opening the Standard vial.

2. Label seven tubes 1, 2, 3, 4, 5, 6 and 7. Add 0.20 mL Assay Buffer to each of the seven tubes. Prepare serial dilutions by adding 0.20 mL of the 30ng/mL standard to tube 1, mix well and transfer 0.20 mL of tube 1 to tube 2, mix well and transfer 0.20 mL of tube 2 to tube 3, mix well and transfer 0.20 mL of tube 3 to tube 4, mix well and transfer 0.20 mL of tube 4 to tube 5, mix well and transfer 0.20 mL of tube 5 to tube 6, mix well and transfer 0.20 mL of tube 6 to tube 7 and mix well.

Note: Do not use a Repeater pipette. Change tip for every dilution. Wet tip with standard before dispensing. Unused portions of standard should be stored at ≤ -20°C. Avoid multiple freeze/thaw cycles.

	Volume of Assay Buffer to Add	Volume of Standard to Add	Standard Concentration (ng/mL)
1.		0.5 mL of 30 ng/mL	30.00
2.	0.20 mL	0.2 mL of Tube 1	15.00
3.	0.20 mL	0.2 mL of Tube 2	7.50
4.	0.20 mL	0.2 mL of Tube 3	3.75
5.	0.20 mL	0.2 mL of Tube 4	1.88
6.	0.20 mL	0.2 mL of Tube 5	0.94
7.	0.20 mL	0.2 mL of Tube 6	0.47
8.	0.20 mL	0.2 mL of Tube 7	0.23

IX. ASSAY PROCEDURE

Pre-warm all reagents to room temperature immediately before setting up the assay.

1. Dilute the 10X concentrated HRP Wash Buffer 10 fold by mixing the entire contents of both buffer bottles with 900 mL de-ionized or distilled water.

2. Remove the required number of strips from the Microtiter Assay Plate. Unused strips should be resealed in the foil pouch and stored at 2-8°C. Assemble strips in an empty plate holder and wash each well 3 times with 300 µl of diluted Wash Buffer per wash. Decant Wash Buffer and remove the residual amount from all wells by inverting the plate and tapping it smartly onto absorbent towels several times. **Do not let wells dry before proceeding to the next step. If automated machine is used for assay, follow the manufacturer's instructions for all washing steps described in this protocol.**
3. Add 30 µL Assay Buffer to Background wells, Standard wells, and QC1 and QC2 wells. Add 40 µL Assay Buffer to sample wells.

4. If samples to be assayed are serum or plasma, add 10 µL Matrix Solution to the Background wells, Standard wells, and QC1 and QC2 wells. If samples are free of significant serum matrix components, add 10 µL Assay Buffer instead.

5. Add 10 µL Assay Buffer to the Background wells and add in duplicates 10 µL Mouse Leptin Standards in the order of ascending concentration to the appropriate wells.

6. Add 10 µL QC1 and 10 µL QC2 to the appropriate wells.

7. Add sequentially 10 µL of the unknown samples in duplicate to the remaining wells.

8. Transfer Antiserum Solution to a reagent reservoir and add 50 µL of this solution to each well with a multi-channel pipette. Cover the plate with plate sealer and incubate at room temperature for 2 hours on an orbital microtiter plate shaker set to rotate at moderate speed, about 400 to 500 rpm.

9. Remove plate sealer and decant solutions from the plate. Tap as before to remove residual solutions in well.

10. Wash wells 3 times with diluted Wash Buffer, 300 µl per well per wash. Decant and tap after each wash to remove residual buffer.

11. Add 100 µl Detection Antibody to each well. Cover plate with sealer and incubate with moderate shaking at room temperature for 1 hour on an orbital microtiter plate shaker set to rotate at moderate speed, approximately 400-500 rpm.

12. Remove plate sealer and decant solutions from the plate. Tap as before to remove residual solutions in well.

13. Wash wells 3 times with diluted Wash Buffer, 300 µL per well per wash. Decant and tap after each wash to remove residual buffer.

IX. ASSAY PROCEDURE (continued)

14. Add 100 µL Enzyme Solution to each well. Cover plate with sealer and incubate with moderate shaking at room temperature for 30 minutes on the micro-titer plate shaker.

15. Remove plate sealer and decant solutions from the plate. Tap as before to remove residual solutions in well.

16. Wash wells 6 times with diluted Wash Buffer, 300 µL per well per wash. Decant and tap after each wash to remove residual buffer.

17. Add 100 µL of Substrate solution to each well, cover plate with sealer and shake in the plate shaker for approximately 5 to 20 minutes. Blue color should be formed in wells of leptin standards with intensity proportional to increasing concentrations of leptin.

    NOTE: Please be aware that the color may develop more quickly or more slowly than the recommended incubation time depending on the localized room temperature. Please visually monitor the color development to optimize the incubation time. One can monitor color development using 370 nm filter, if available on the spectrophotometer. When the absorbance is between 1.2 and 1.8 at 370 nm, the stop solution can be added to terminate the color development.

18. Remove sealer and add 100 µL Stop Solution **[CAUTION: CORROSIVE SOLUTION]** and shake plate by hand to ensure complete mixing of solution in all wells. The blue color should turn into yellow after acidification. Wipe the bottom of the ELISA plate before reading absorbance at 450 nm and 590 nm in a plate reader. Plate should be read within 5 minutes to ensure that there are no air bubbles in any well. Record the difference of absorbance units.

Assay Procedure for Intact Mouse Leptin ELISA kit (Cat. # EZML-82K)

	Step 1	Step 2	Step 3	Step 4	Step 5-7	Step 8	Step 9-10	Step 11	Step 12-13	Step 14	Step 15-16	Step 17		Step 18	
Well #	Dilute both bottles of 10X Wash Buffer with 900mL Deionized Water.	Wash plate 3X with 300 µL Wash Buffer. Remove residual buffer by tapping smartly on absorbent towels.	Assay Buffer	Matrix*	Standards/ Controls/ Samples	Antiserum	Seal, Agitate, Incubate 2 hours at Room Temperature. Wash 3X with 300 µL Wash Buffer	Detection Antibody	Seal, Agitate, Incubate 1 hour at Room Temperature. Remove residual buffer by tapping smartly on absorbent towels. Wash 3X with 300 µL Wash Buffer	Enzyme Solution	Seal, Agitate, Incubate 30 minutes at Room Temperature . Wash 6X with 300 µL Wash Buffer	Substrate	Seal, Agitate, Incubate 10-15 minutes at Room Temperature.	Stop Solution	Shake by hand. Read Absorbance at 450 nm and 590 nm within 5 minutes.
A1, B1			40 µL	10 µL	---------	50 µL		100 µL		100 µL		100 µL		100 µL	
C1, D1			30 µL	10 µL	10 µL of 0.23 ng/mL Standard	50 µL									
E1, F1			30 µL	10 µL	10 µL of 00.47 ng/mL Standard	50 µL									
G1, H1			30 µL	10 µL	10 µL of 0.94 ng/mL Standard	50 µL									
A2, B2			30 µL	10 µL	10 µL of 1.88 ng/mL Standard	50 µL									
C2, D2			30 µL	10 µL	10 µL of 3.75 ng/mL Standard	50 µL									
E2, F2			30 µL	10 µL	10 µL of 7.5 ng/mL Standard	50 µL									
G2, H2			30 µL	10 µL	10 µL of 15 ng/mL Standard	50 µL									
A3, B3			30 µL	10 µL	10 µL of 30 ng/mL Standard	50 µL									
C3, D3			30 µL	10 µL	10 µL of QC 1	50 µL									
E3, F3			30 µL	10 µL	10 µL of QC 2	50 µL									
G3, H3			40 µL	---------	10 µL of Sample	50 µL									
A4, B4…			40 µL	---------	10 µL of Sample	50 µL									

* See Section VIII. Assay Procedure Step 4: If samples are free of significant matrix components, add 10 µL assay buffer instead.

XI. CALCULATIONS

Graph a reference curve by plotting the absorbance unit of 450nm, less unit at 590nm, on the Y-axis against the concentrations of mouse leptin standard on the X-axis. The dose-response curve of this assay fits best to a sigmoidal 4- or 5-parameter logistic equation. The results of unknown samples can be calculated with any computer program having a 4- or 5-parameter logistic function.

Note: When sample volumes assayed differ from 10 µL, an appropriate mathematical adjustment must be made to accommodate for the dilution factor (e.g., if 5 µL of sample is used, then calculated data must be multiplied by 2). When sample volume assayed is less than 10 µL, compensate the volume deficit with either matrix solution or assay buffer, whichever is appropriate.

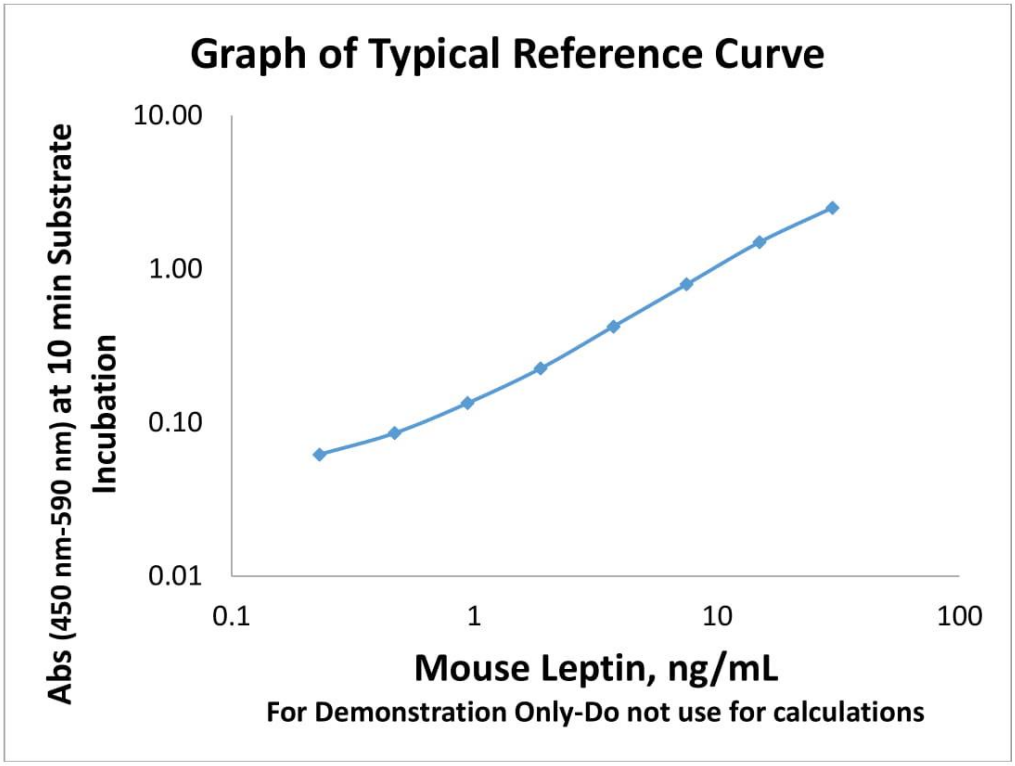
XII INTERPRETATION

1. If the difference between duplicate results of a sample is >15% CV, repeat the sample.

2. The limit of sensitivity of this assay is 0.05 ng/mL (~3.13 pM) leptin (10 µL sample size).

3. The appropriate range of this assay is 0.23 ng/mL to 30 ng/mL leptin (10 µL sample size). Any result greater than 30 ng/mL in a 10 µL sample assayed should be repeated on dilution using either matrix solution or assay buffer, whichever is appropriate, as diluent until it falls within range.

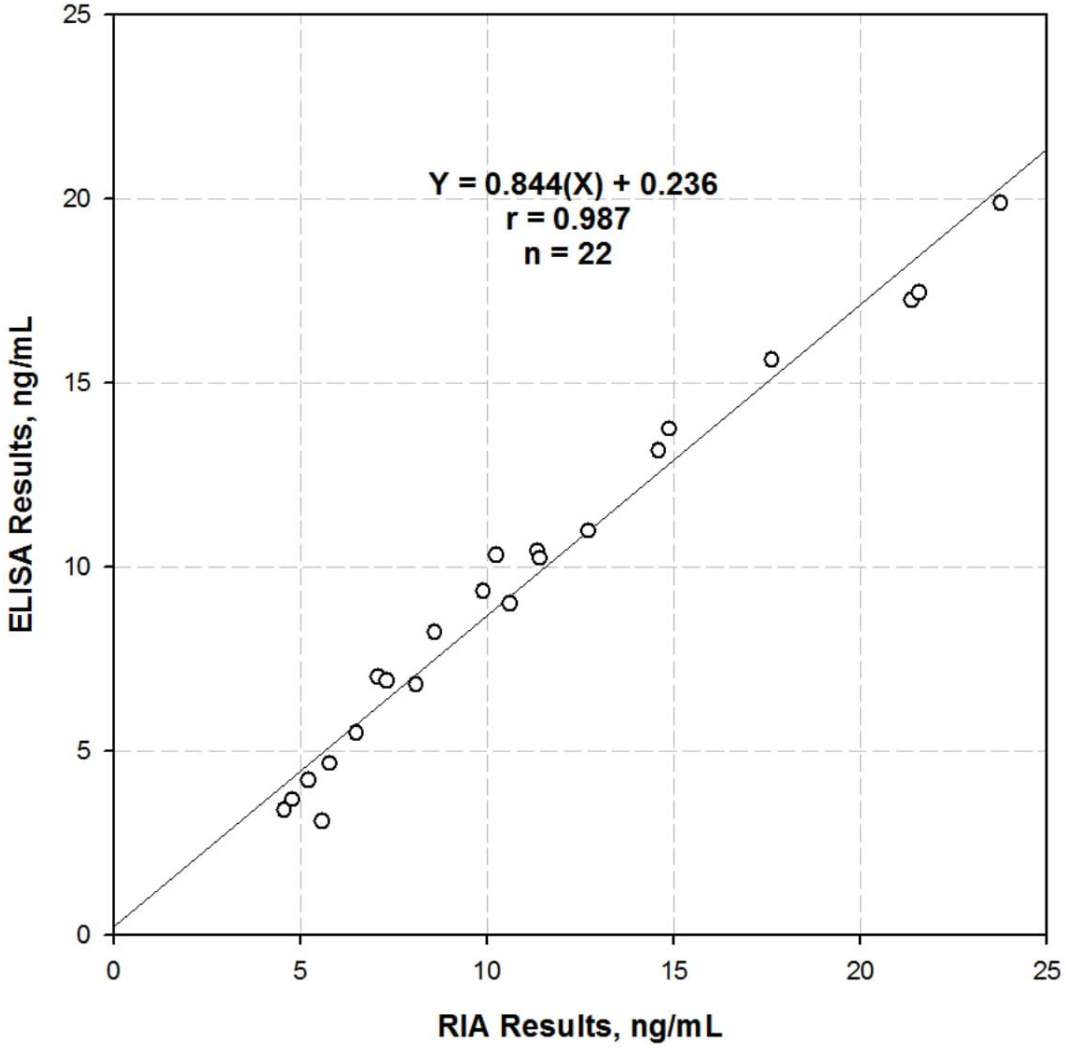
XIII Graph of Typical Reference Curve



XIV Correlation

Mouse leptin Assays:

Correlation of Results by RIA and ELISA Methods



Serum samples from 22 mice were assayed for Leptin using Millipore Mouse RIA Kit (Cat# ML-82K) and Mouse Leptin ELISA Kit (Cat# EZML-82K). Correlation of the two kits are derived by linear regression analysis of paired results from each sample.

XV. ASSAY CHARACTERISTICS

A. Sensitivity

The lowest level of mouse leptin that can be detected by this assay is 0.05 ng/mL using a 10 µL sample size.

B. Specificity

The specificity (also known as selectivity) of the analytical test is its ability to selectively measure the analytes in the presence of other like components in the sample matrix.

Mouse Leptin	100%
Rat Leptin	70%
Human Leptin	9%
Porcine Leptin	< 0.05%
Ovine Leptin	< 0.05%
Chicken Leptin	< 0.05%
Rat Insulin	0%
Rat C-peptide	0%
Human Proinsulin	0%
Bovine Proinsulin	0%
Porcine Proinsulin	0%
Glucagon	0%
Human Ghrelin	0%

C. Precision

Sample Number	Mean Leptin Level (ng/mL)	Assay Variation (CV)	
		Intra-assay	Inter-assay
1	1.66	1.06%	4.59%
2	5.78	1.64%	3.96%
3	17.60	1.76%	3.01%

The assay variations of EMD Millipore Mouse Leptin ELISA kit were studied on three mouse serum samples with varying concentrations of spiked analyte. The intra-assay variations are calculated from eight duplicate determinations in an assay. The inter-assay variations are calculated from results of 6 separate assays with duplicate samples in each assay.

XV. ASSAY CHARACTERISTICS (continued)

D. Recovery

Spike and Recovery of Mouse Leptin in Mouse Serum

Serum Sample #	Mouse Leptin		Recovery (%) of Spiked Insulin
	Added (ng/mL)	Observed (ng/mL)	
Mouse Serum # 1	0	1.33	--
	0.5	1.83	100
	2.0	3.14	91
	10.0	10.04	87
Mouse Serum # 2	0	1.76	--
	0.5	2.24	96
	2.0	3.49	87
	10.0	10.48	87

Mouse leptin at indicated levels was added to two pooled mouse serum samples and the resulting leptin content of each sample was assayed by ELISA. The % of recovery = [(observed leptin level after spike - observed leptin level before spike) / spiked level of leptin] x 100%. Mean recovery rate at spiked leptin level of 0.5, 2, and 10 ng/mL is 98%, 89%, and 87%, respectively.

E. Linearity

Effect of Serum Dilution

Serum Sample #	Dilution Factor	Leptin Level		
		Observed (ng/mL)	Expected (ng/mL)	% Of Expected
Mouse Serum # 1	--	16.43	16.43	**100**
	2x	16.42		100
	5x	16.60		101
	10x	17.50		107
	20x	17.20		105
Mouse Serum # 2	--	16.44	16.44	**100**
	2x	16.56		101
	5x	17.60		107
	10x	17.70		108
	20x	18.20		111

Two leptin-spiked pooled mouse serum samples are diluted each with matrix solution to various degrees as indicated and assayed for leptin levels along with neat samples of each serum. Measured leptin levels are corrected for dilution factors and reported as observed leptin level.

XVI. QUALITY CONTROLS

The ranges for each Quality Control 1 and 2 are provided on the card insert or can be located at the EMD MILLIPORE website www.emdmillipore.com using the catalog number as the keyword.

XVII. TROUBLESHOOTING GUIDE

1. To obtain reliable and reproducible results the operator should carefully read this manual and fully understand all aspects of each assay step before attempting to run the assay.
2. Throughout the assay the operator should adhere strictly to the procedures with good laboratory practice.
3. Have all necessary reagents and equipment ready on hand before starting. Once the assay has been started all steps should be completed with precise timing and without interruption.
4. Avoid cross contamination of any reagents or samples to be used in the assay.
5. Make sure that all reagents and samples are added to the bottom of each well.
6. Careful and complete mixing of solutions in the well is critical. Poor assay precision will result from incomplete mixing or cross well contamination due to inappropriate mixing.
7. Remove any air bubble formed in the well after acidification of substrate solution because bubbles interfere with spectrophotometric readings.
8. Do not let the absorbance reading of the highest standard fall beyond the limit of your microtiterplate reader's capacity. Adjust the length of substrate incubation time accordingly.
9. High absorbance in background or blank wells could be due to 1) cross well contamination by standard solution or sample and 2) inadequate washing of wells with wash buffer.

XVIII. REPLACEMENT REAGENTS

Reagents	Cat#
Rat/Mouse Leptin Microtiter Plate	EP83
Rat/Mouse Leptin Antiserum	EAS83
10X HRP Wash Buffer Concentrate	EWB-HRP
Mouse Leptin ELISA Standards	E8082-K
Quality Controls 1 and 2	E6082-K
Rat/Mouse Leptin Matrix Solution	EPS0016
Assay Buffer	EAB-PTR
Rat/Mouse Leptin Detection Antibody	E1083
Enzyme Solution	EHRP-4
Substrate	ESS-TMB2
Stop Solution	ET-TMB
10-pack of Mouse Leptin ELISA kits	EZML-82BK

Appendix 11 – Mouse Adiponectin ELISA Kit Data Sheet

MOUSE ADIPONECTIN ELISA KIT
96-Well Plate (Cat. # EZMADP-60K)

I. INTENDED USE

This Mouse Adiponectin (ACRP30) ELISA kit is used for the non-radioactive quantification of Mouse Adiponectin in serum, plasma, and adipocyte extracts or cell culture media samples. This kit has 100% cross reactivity to Mouse Adiponectin. There is no binding to Mouse Adiponectin globular domain, or to Rat Adiponectin. One kit is sufficient to measure 38 unknown samples in duplicate. ***For Research Use Only. Not for Use in Diagnostic Procedures.***

II. PRINCIPLES OF PROCEDURE

This assay is a Sandwich ELISA based, sequentially, on: 1) concurrent capture of Mouse Adiponectin molecules from samples to the wells of a microtiter plate coated by a pre-titered amount of anti- mouse adiponectin monoclonal antibodies, and binding of a second biotinylated anti- mouse polyclonal antibody to the captured molecules, 2) wash away of unbound materials from samples, 3) conjugation of horseradish peroxidase to the immobilized biotinylated antibodies, 4) wash away of free enzyme conjugates, and 5) quantification of immobilized antibody-enzyme conjugates by monitoring horseradish peroxidase activities in the presence of the substrate 3,3',5,5'-tetramethylbenzidine. The enzyme activity is measured spectrophotometrically by the increased absorbency at 450 nm, corrected from the absorbency at 590nm, after acidification of formed products. Since the increase in absorbency is directly proportional to the amount of captured Mouse Adiponectin in the unknown sample, the latter can be derived by interpolation from a reference curve generated in the same assay with reference standards of known concentrations of Mouse Adiponectin.

III. REAGENTS SUPPLIED

Each kit is sufficient to run one 96-well plate and contains the following reagents:

A. Mouse Adiponectin ELISA Plate
Coated with Rat Monoclonal anti-Mouse Adiponectin Antibodies
Quantity: 1 plate
Preparation: Ready to Use
Note: Unused strips should be resealed in the foil pouch with the desiccant provided and stored at 2-8°C.

B. Adhesive Plate Sealer
Quantity: 1 sheet
Preparation: Ready to Use

III. REAGENTS SUPPLIED (continued)

C. 10X HRP Wash Buffer Concentrate
10X concentrate of 50mM Tris Buffered Saline containing Tween-20.
Quantity: Two bottles containing 50 mL each
Preparation: Dilute 1:10 with distilled or deionized water.

D. Mouse Adiponectin Standard
Mouse Adiponectin, lyophilized.
Quantity: 1mL upon hydration
Preparation: Contents Lyophilized. Reconstitute with 1 mL distilled or deionized water. The actual concentration of Mouse Adiponectin present in the vial will be lot dependent. Please refer to the analysis sheet for exact concentration present in a specific lot.

E. Quality Controls 1 and 2
Purified Recombinant Mouse Adiponectin in Assay Buffer, lyophilized.
Quantity: 1mL/vial upon hydration
Preparation: Contents Lyophilized. Reconstitute with 1 mL distilled or deionized water.

F. 10X Assay Buffer
Quantity: 50 mL
Preparation: Dilute 1:10 with distilled or deionized water to make 1X assay buffer (0.05M Phosphosaline containing 0.025M EDTA, 0.08% Sodium Azide, 1% BSA).

Note: Use 1X Assay Buffer to dilute samples (Section VIII, SAMPLE PREPARATION) and Standard Curve (SECTION IX, STANDARD AND QUALITY CONTROL PREPARATION) and in Assay Procedure (SECTION X, ASSAY PROCEDURE).

G. Mouse Adiponectin Detection Antibody
Pre-titered Biotinylated Goat anti-Mouse Adiponectin Polyclonal Antibody
Quantity: 3.0 mL
Preparation: Ready to Use

H. Enzyme Solution
Pre-titered Streptavidin-Horseradish Peroxidase Conjugate in Buffer
Quantity: 12 mL
Preparation: Ready to Use

I. Substrate (Light sensitive, avoid unnecessary exposure to light)
3, 3', 5, 5'-tetramethylbenzidine in buffer
Quantity: 12 mL
Preparation: Ready to Use.

III. REAGENTS SUPPLIED (continued)

J. Stop Solution (Caution: Corrosive Solution)

0.3 M HCl
Quantity: 12 mL
Preparation: Ready to Use

IV. STORAGE AND STABILITY

Recommended storage for kit components is 2-8°C.

All components are shipped and stored at 2-8°C. Reconstituted standards and quality controls can be frozen for future use, but repeated freeze thaws should be avoided. Refer to expiration dates on all reagents prior to use. Do not mix reagents from different kits unless they have the same lot numbers

V. REAGENT PRECAUTIONS

A. Sodium Azide

Sodium Azide or Proclin has been added to some reagents as a preservative. Although the concentrations are low, Sodium Azide and Proclin may react with lead and copper plumbing to form highly explosive metal azides. Dispose of unused contents and waste in accordance with international, federal, state, and local regulations

B. Hydrochloric Acid

Hydrochloric Acid is corrosive and can cause eye and skin burns. It is harmful if swallowed and can cause respiratory and digestive tract burns. Avoid contact with skin and eyes. Do not swallow or ingest.

Note: See Full Labels of Hazardous components on next page.

Full Hazardous Labeling for components in this kit:

Ingredient, Cat #		Full Label	
Mouse Adiponectin Quality Controls 1 & 2	E6300-K		**Danger.** Toxic if swallowed. Toxic to aquatic life with long lasting effects. Avoid release to the environment. IF exposed or concerned: immediately call a POISON CENTER or doctor/ physician.
Mouse Adiponectin Standards	E8060-K		**Danger.** Toxic if swallowed. Toxic to aquatic life with long lasting effects. Avoid release to the environment. IF exposed or concerned: immediately call a POISON CENTER or doctor/ physician.
Stop Solution	ET-TMB		**Warning.** May be corrosive to metals.
10X HRP Wash Buffer Concentrate	EWB-HRP		**Warning.** May cause an allergic skin reaction. Wear protective gloves. IF ON SKIN: Wash with plenty of soap and water.

VI. MATERIALS REQUIRED BUT NOT PROVIDED

1. Pipettes and Pipette Tips: 10µL - 20 µL or 20µL - 100 µL
2. Multi-Channel Pipettes and Pipette Tips: 5 ~ 50 µL and 50 ~ 300 µL
3. Buffer and Reagent Reservoirs
4. Vortex Mixer
5. Deionized Water
6. Microtiter Plate Reader capable of reading absorbency at 450 nm
7. Orbital Microtiter Plate Shaker
8. Absorbent Paper or Cloth

VII. SAMPLE COLLECTION AND STORAGE

1. To prepare serum samples, whole blood is directly drawn into a centrifuge tube that contains no anti-coagulant. Let blood clot at room temperature for 30 min.

   Promptly centrifuge the clotted blood at 2,000 to 3,000 x g for 15 minutes at 4 ± 2°C.

   Transfer and store serum samples in separate tubes. Date and identify each sample.

   Use freshly prepared serum or aliquot and store samples at ≤ –20°C for later use. For long-term storage, keep at -70°C. Avoid freeze/thaw cycles.

2. To prepare plasma samples, whole blood should be collected into centrifuge tubes containing enough K_3EDTA to achieve a final concentration of 1.735 mg/mL and centrifuged immediately after collection. Observe the same precautions in the preparation of serum samples.

3. If heparin is to be used as an anticoagulant, the effect on the assay outcome at the dose of heparin used should be pre-determined.

4. Avoid using samples with gross hemolysis or lipemia.

VIII. SAMPLE PREPARATION

1. Allow all the reagents to come to room temperature.

2. Dilute serum or plasma samples 1:1000 in 1X Assay Buffer (See Section III, F). Cellular extract and culture media dilutions will vary.

   a. Make Dilution A by adding 10 µL sample to 990 µL Assay Buffer and vortex.

   b. Make Dilution B by adding 100 µL of Dilution A to 900 µL Assay Buffer and vortexing. Use Dilution B (1:1000) for the assay procedure.

IX. STANDARD AND QUALITY CONTROLS PREPARATION

A. Mouse Adiponectin Standard Preparation

1. Use care in opening the lyophilized Standard vial. Using a pipette, reconstitute the Mouse Adiponectin Standard with 1.0 mL distilled or deionized water into the vial to give a concentration prescribed in the analysis sheet. Invert and mix gently, let sit for 5 minutes then mix well.

2. Label seven tubes 1, 2, 3, 4, 5, 6, and 7. Add 0.5 mL Assay Buffer to each of the seven tubes. Prepare serial dilutions by adding 0.5 mL of the reconstituted standard to tube 1, mix well and transfer 0.5 mL of tube 1 to tube 2, mix well and transfer 0.5 mL of tube 2 to tube 3, mix well and transfer 0.5 mL of tube 3 to tube 4, mix well and transfer 0.5 mL of tube 4 to tube 5, mix well and transfer 0.5 mL of tube 5 to tube 6, mix well and transfer 0.5 mL of tube 6 to tube 7 and mix well.

Note: Do not use a Repeater pipette. Change tip for every dilution. Wet tip with Standard before dispensing. Unused portions of reconstituted standard should be stored at ≤ -20°C. Avoid multiple freeze/thaw cycles.

Volume of Deionized Water to Add	Volume of Standard to Add	Standard Concentration ng/mL
1 mL	0	X (Refer to analysis sheet for exact concentration)

Tube #	Volume of Assay Buffer to Add	Volume of Standard to Add	Standard Concentration ng/mL
1	0.5 mL	0.5 mL of reconstituted standard	X/2
2	0.5 mL	0.5 mL of tube 1	X/4
3	0.5 mL	0.5 mL of tube 2	X/8
4	0.5 mL	0.5 mL of tube 3	X/16
5	0.5 mL	0.5 mL of tube 4	X/32
6	0.5 mL	0.5 mL of tube 5	X/64
7	0.5 mL	0.5 mL of tube 6	X/128

B. Mouse Adiponectin Quality Control 1 and 2 Preparation

1. Use care in opening the lyophilized Quality Control vials. Using a pipette, reconstitute each of the Mouse Adiponectin Quality Control 1 and Quality Control 2 with 1 mL distilled or deionized water into the vials. Invert and mix gently, let sit for 5 minutes then mix well.

X. ASSAY PROCEDURE

Pre-warm all reagents to room temperature prior to setting up the assay.

Note: Since the standard concentration may vary from lot to lot, please make sure to change the standard concentration in the template while reading absorbance in the spectrophotometer.

1. Dilute the 10X Wash Buffer concentrate 10 fold by mixing the entire content of each bottle of Wash Buffer with 450 mL deionized water (dilute both bottles with 900 mL deionized water).

2. Remove the required number of strips from the Microtiter Assay Plate. Unused strips should be resealed in the foil pouch and stored at 2-8°C. Assemble the strips in an empty plate holder and wash each well 3 times with 300 µL of diluted Wash Buffer per wash. Decant Wash Buffer and remove the residual amount from all wells by inverting the plate and tapping it smartly onto absorbent towels several times. **Do not let wells dry before proceeding to the next step. If an automated machine is used for the assay, use a gentle wash program for all washing steps described in this protocol.**

3. Add 60 µL Assay Buffer to all wells.

4. Add in duplicate 20 µL Assay Buffer to the blank wells.

5. Add in duplicate 20 µL Mouse Adiponectin Standards in the order of ascending concentration to the appropriate wells. Add in duplicate 20 µL QC1 and 20 µL QC2 to the appropriate wells. Add sequentially 20 µL of the unknown samples in duplicate to the remaining wells

6. Add 20 µL Detection Antibody to all wells. **For best result all additions should be completed within one hour.** Cover the plate with plate sealer and incubate at room temperature for 2 hours on an orbital microtiter plate shaker set to rotate at moderate speed, approximately 400 to 500 rpm.

7. Remove plate sealer and decant solutions from the plate. Tap as before to remove residual solutions in the wells.

8. Wash wells 5 times with diluted Wash Buffer, 300 µL per well per wash. Decant and tap firmly after each wash to remove residual buffer.

9. Add 100 µL Enzyme Solution to each well. Cover plate with sealer and incubate with moderate shaking at room temperature for 30 minutes on the microtiter plate shaker.

10. Remove sealer, decant solutions from the plate, and tap plate to remove the residual fluid.

X. ASSAY PROCEDURE (continued)

11. Wash wells 5 times with diluted Wash Buffer, 300 µl per well per wash. Decant and tap firmly after each wash to remove residual buffer.

12. Add 100 µL of Substrate Solution to each well, cover plate with sealer and shake on the plate shaker for **approximately** 5 to 20 minutes. Blue color should be formed in wells of Adiponectin standards with intensity proportional to increasing concentrations of Adiponectin.

    NOTE: Please be aware that the color may develop more quickly or more slowly than the recommended incubation time depending on the localized room temperature. Please visually monitor the color development to optimize the incubation time. One can monitor color development using 370 nm filter, if available on the spectrophotometer. When the absorbance is between 1.2 and 1.8 at 370 nm, the stop solution can be added to terminate the color development.

13. Remove sealer and add 100 µl Stop Solution **[CAUTION: CORROSIVE SOLUTION]** and shake plate by hand to ensure complete mixing of solution in all wells. The blue color should turn to yellow after acidification. Wipe the bottom of the microtiter plate to remove any residue prior to reading on plate reader. Read absorbance at 450 nm and 590nm in a plate reader within 5 minutes and ensure that there are no air bubbles in any well. Record the difference of absorbance units. The absorbance of highest Adiponectin standard should be approximately 2.2-2.8 or not to exceed the capability of the plate reader used.

Assay Procedure for Mouse Adiponectin ELISA kit (Cat. # EZMADP-60K)

	Step 1	Step 2	Step 3-4	Step 5	Step 6	Step 6-8	Step 9	Step 10-11	Step 12	Step 12	Step 13	Step 13
Well #	Dilute each bottle of 10X Wash Buffer with 450mL Deionized Water.	Wash plate 3X with 300 µL Wash Buffer. Remove residual buffer by tapping smartly on absorbent towels	Assay Buffer	Standards/ Controls/ Samples	Detection Ab	Seal, Agitate, Incubate 2 hours at Room Temperature. Wash 5X with 300 µL Wash Buffer	Enzyme Solution	Seal, Agitate, Incubate 30 minutes at Room Temperature . Wash 5X with 300 µL Wash Buffer	Substrate	Seal, Agitate, Incubate 5 - 20 minutes at Room Temperature.	Stop Solution	Read Absorbance at 450 nm and 590 nm.
A1, B1			80 µL		20 µL		100 µL		100 µL		100 µL	
C1, D1			60 µL	20 µL of Tube 7								
E1, F1			60 µL	20 µL of Tube 6								
G1, H1			60 µL	20 µL of Tube 5								
A2, B2			60 µL	20 µL of Tube 4								
C2, D2			60 µL	20 µL of Tube 3								
E2, F2			60 µL	20 µL of Tube 2								
G2, H2			60 µL	20 µL of Tube 1								
A3, B3			60 µL	20 µL of QC I								
C3, D3			60 µL	20 µL of QC II								
E3, F3			60 µL	20 µL of Sample								
G3, H3			60 µL	20 µL of Sample								
A4, B4 ↓			60 µL	20 µL of Sample								

XII. CALCULATIONS

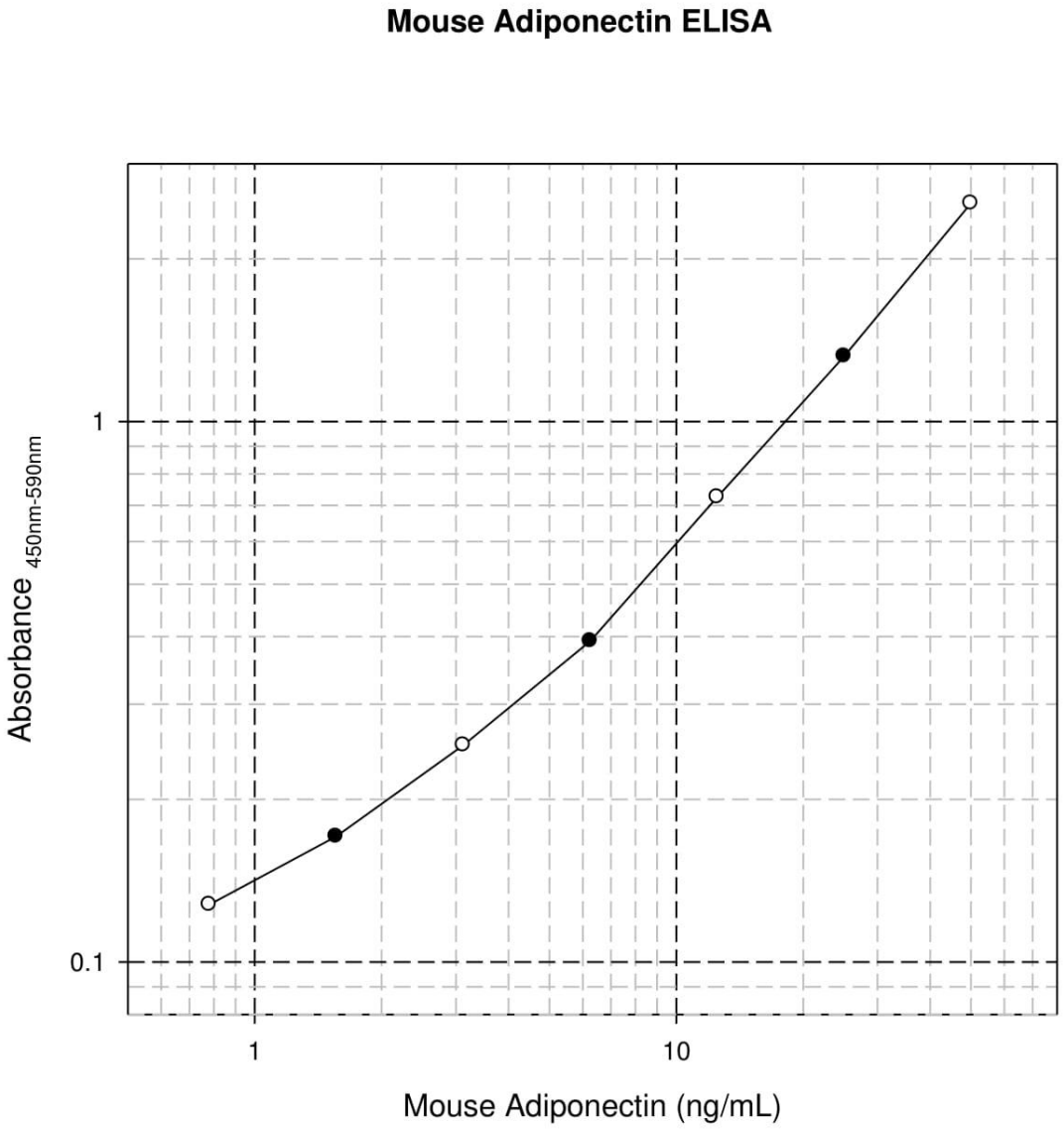
The dose-response curve of this assay fits best to a sigmoidal 4- or 5-parameter logistic equation. The results of unknown samples can be calculated with any computer program having a 4- or 5-parameter logistic function. Final results should be multiplied by a 1000 dilution factor.

Note: When sample volumes assayed differ from 20 µL, an appropriate mathematical adjustment must be made to accommodate for the dilution factor (e.g., if 10 µL of sample is used, then calculated data must be multiplied by 2). When sample volume assayed is less than 20 µL, compensate the volume deficit with assay buffer.

XIII. INTERPRETATION - Acceptance Criteria

1. The assay will be considered accepted when all Quality Control values fall within the calculated Quality Control Range. If any QC's fall outside the control range, review results with a supervisor.
2. If the difference between duplicate results of a sample is >15% CV, repeat the sample.
3. The limit of sensitivity of this assay is 0.2 ng/mL mouse Adiponectin (20 µL sample size).
4. The approximate dynamic range of this assay is 1 - 50 ng/mL mouse Adiponectin (20 µl sample size). Any result greater than 50 ng/mL in a 20 µL sample should be diluted using 1X assay buffer, and the assay repeated until the results fall within range.

XIV. STANDARD CURVE



Typical Standard Curve, not to be used to calculate results.

XV. ASSAY CHARACTERISTICS

A. Sensitivity

The lowest level of Adiponectin that can be detected by this assay is 0.2 ng/mL when using a 20 µL sample size.

B. Specificity

The antibody pair used in this assay is specific to mouse adiponectin and does not significantly cross-react with human adiponectin, globular domain of mouse adiponectin, and other cytokine or hormone molecules tested, as shown in the following table.

Analyte	Max. Conc.	Cross Reactivity
Human Adiponectin	200ng/mL	< 2%
Mouse gAcrp	1000ng/mL	n.d.
Mouse Endocrines:		
Insulin	10nM	n.d.
Amylin	10nM	n.d.
Leptin	10nM	n.d.
Glucagon	10nM	n.d.
GLP-1	10nM	n.d.
Mouse Cytokines:		
IL-1ß	10nM	n.d.
IL-2	10nM	n.d.
IL-4	10nM	n.d.
IL-5	10nM	n.d.
IL-6	10nM	n.d.
IL-9	10nM	n.d.
IL-10	10nM	n.d.
IL-12	10nM	n.d.
IL-13	10nM	n.d.
IFN-γ	10nM	n.d.
TNF-α	10nM	n.d.
GMCSF	10nM	n.d.
MIP-1α	10nM	n.d.
KC	10nM	n.d.
RANTES	10nM	n.d.
MCP-1	10nM	n.d.

n.d. = not detectable
No cross reactivity to rat serum or plasma samples.

XV. ASSAY CHARACTERISTICS (continued)

C. Precision

Within and Between Assay Variation

Sample No.	Mean Adiponectin Levels (ng/mL)	Within% CV	Between% CV
1	9.18	3.8	6.8
2	13.74	5.4	1.4
3	6.89	8.2	4.9
4	7.23	5.6	10.8

The assay variations of EMD Millipore Mouse Adiponectin ELISA kits were studied on four mouse serum samples with varying concentrations of endogenous Adiponectin. The mean within variation was calculated from results of six duplicate determinations in each assay of the indicated samples. The mean between variations of each sample was calculated from results of four separate assays with duplicate samples in each assay.

D. Recovery

Spike & Recovery of Mouse Adiponectin in Serum

Sample No.	Adiponectin Added (ng/mL)	Expected (ng/mL)	Observed (ng/mL)	% of Recovery
1	0	7.1	7.1	100
	5	12.1	12.6	104
	10	17.1	17	99
	20	27.1	26.7	99
2	0	7.2	7.2	100
	5	12.2	13.7	112
	10	17.5	17.8	103
	20	27.2	28.9	106
3	0	10.49	10.49	100
	5	15.49	15.76	102
	10	20.49	22.17	108
	20	30.49	31.07	102

Varying amounts of mouse Adiponectin were added to three mouse serum samples and the Adiponectin content was determined in three separate assays. The % of recovery = observed Adiponectin concentrations/expected Adiponectin concentrations x 100%.

XV. ASSAY CHARACTERISTICS (continued)

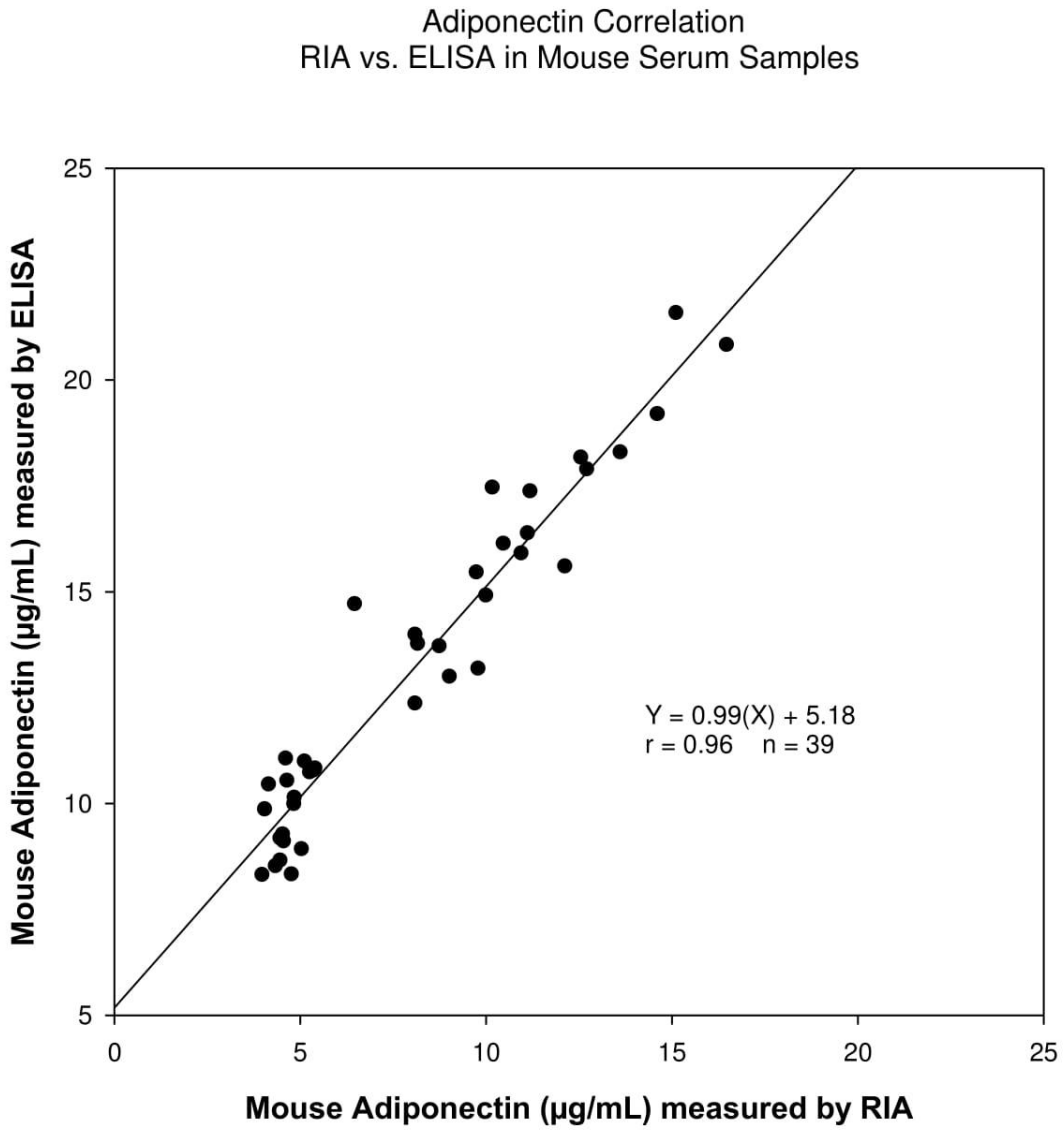
E. Linearity

Effect of Serum Dilution

Sample No.	Volume Sampled (µL)	Expected (ng/mL)	Observed (ng/mL)	% Of Expected
1	20	14.3	14.3	100
	10	7.15	7.3	102
	5	3.6	4.1	114
	3.33	2.4	2.9	121
2	20	14.99	14.99	100
	10	7.49	7.23	96
	5	3.75	4.37	116
	3.33	2.5	2.81	112
3	20	14.43	14.43	100
	10	7.2	7.17	99
	5	3.61	4.16	115
	3.33	2.41	2.58	107

Three mouse serum samples with the indicated sample volumes were assayed in three separate experiments. Required amounts of assay buffer were added to compensate for lost volumes below 20 µL. The resulting dilution factors of 1.0, 2.0, 4.0, and 6.0 representing 20 µL, 10 µL, 5 µL, and 3.3 µL sample volumes assayed, respectively, were applied in the calculation of observed Adiponectin concentrations. % expected = observed/expected x 100%.

XVI. CORRELATION GRAPH



Serum samples obtained from 39 mouse subjects were assayed for Adiponectin content using both EMD Millipore Mouse Adiponectin RIA Kit (Catalogue #MADP-60HK) and Mouse Adiponectin ELISA Kit (Catalogue EZMADP-60K). Correlation of the two kits is derived by linear regression analysis of paired results from each sample.

XVII. QUALITY CONTROLS

The ranges for Quality Control 1 and 2 are provided on the card insert or can be located at the EMD MILLIPORE website www.emdmillipore.com using the catalog number as the keyword.

.

XVIII. TROUBLESHOOTING GUIDE

1. To obtain reliable and reproducible results the operator should carefully read this manual and fully understand all aspects of each assay step before attempting to run the assay.
2. Throughout the assay the operator should adhere strictly to the procedures with good laboratory practice.
3. Have all necessary reagents and equipment ready on hand before starting. Once the assay has been started all steps should be completed with precise timing and without interruption.
4. Avoid cross contamination of any reagents or samples to be used in the assay.
5. Make sure all reagents and samples are added to the bottom of each well.
6. Careful and complete mixing of solutions in the well is critical. Poor assay precision will result from incomplete mixing or cross well contamination due to inappropriate mixing.
7. Remove any air bubble formed in the well after acidification of substrate solution because bubbles interfere with spectrophotometric readings.
8. Do not let the absorbency reading of the highest standard reach 3.0 units or higher after acidification.
9. High absorbance in background or blank wells could be due to 1) cross well contamination by standard solution or sample or 2) inadequate washing of wells with HRP Wash Buffer or 3) overexposure to light after substrate has been added.

XIX. REPLACEMENT REAGENTS

Reagents	Cat. #
Mouse Adiponectin ELISA Plate	EP60
10X HRP Wash Buffer Concentrate (50 mL)	EWB-HRP
Mouse Adiponectin Standards	E8060-K
Quality Controls 1 and 2	E6300-K
Assay Buffer (10X)	EAB-10XP
Mouse Adiponectin Detection Antibody	E1060
Enzyme Solution	EHRP-3
Substrate	ESS-TMB
Stop Solution	ET-TMB
10-pack of Mouse Adiponectin (ACRP30) ELISA kits	EZMADP-60BK

Appendix 12 – Mouse Insulin ELISA Data Sheet

Rat / Mouse Insulin ELISA Kit
96-Well Plate (Cat. # EZRMI-13K)

I. INTENDED USE

This Rat / Mouse Insulin ELISA kit is used for the non-radioactive quantification of insulin in mouse and rat sera. Plasma samples may also be used but application to samples of other biological fluids may need validation by the user. One kit is sufficient to measure 39 unknown samples in duplicate. ***This kit is for Research Use Only. Not for Use in Diagnostic Procedures.***

II. PRINCIPLES OF PROCEDURE

This assay is a Sandwich ELISA based, sequentially, on: 1) capture of insulin molecules from samples to the wells of a microtiter plate coated by pre-titered amount of a monoclonal mouse anti-rat insulin antibodies and the binding of biotinylated polyclonal antibodies to the captured insulin, 2) wash away of unbound materials from samples, 3) binding of horseradish peroxidase to the immobilized biotinylated antibodies, 4) wash away of free enzyme conjugates, and 5) quantification of immobilized antibody-enzyme conjugates by monitoring horseradish peroxidase activities in the presence of the substrate 3,3',5,5'-tetramethylbenzidine. The enzyme activity is measured spectrophotometrically by the increased absorbency at 450 nm, corrected from the absorbency at 590 nm, after acidification of formed products. Since the increase in absorbency is directly proportional to the amount of captured insulin in the unknown sample, the latter can be derived by interpolation from a reference curve generated in the same assay with reference standards of known concentrations of rat insulin.

III. REAGENTS SUPPLIED

Each kit is sufficient to run one 96-well plate including, in duplicates, background, 6 rat insulin standards, 2 quality controls and 39 unknown samples.

A. Rat/Mouse Insulin ELISA Plate
Coated with mouse monoclonal anti-rat insulin antibodies.
Quantity: 1 plate
Preparation: Ready to use.
Note: Unused strips should be resealed in the foil pouch with the desiccant provided and stored at 2-8°C.

B. Adhesive Plate Sealer
Quantity: 1 sheet
Preparation: Ready to use.

C. 10X HRP Wash Buffer Concentrate
10X concentrate of 50 mM Tris Buffered Saline containing Tween-20.
Quantity: Two bottles containing 50 mL each
Preparation: Dilute 10 times with de-ionized water.

III. REAGENTS SUPPLIED (continued)

D. Rat/Mouse Insulin Standards
Rat insulin in Assay Buffer: 0.2, 0.5, 1, 2, 5 and 10 ng/mL.
Quantity: 0.25 mL/vial
Preparation: Ready to use.

E. Rat/Mouse Insulin Quality Controls 1 and 2
Rat insulin in QC buffer.
Quantity: 0.25 mL/vial
Preparation: Ready to use.

F. Matrix Solution
Charcoal stripped pooled mouse serum
Quantity: 0.5 mL
Preparation: Ready to use.

G. Assay Buffer
0.05 M phosphosaline, pH 7.4, containing 0.025 M EDTA, 0.08% sodium azide, and 1% BSA.
Quantity: 20 mL
Preparation: Ready to use.

H. Rat/Mouse Insulin Detection Antibody
Pre-titered biotinylated anti-insulin antibody.
Quantity: 10 mL
Preparation: Ready to use.

I. Enzyme Solution
Pre-titered streptavidin-horseradish peroxidase conjugate in buffer.
Quantity: 12 mL
Preparation: Ready to use.

J. Substrate (Light sensitive, avoid unnecessary exposure to light)
3, 3', 5, 5'-tetramethylbenzidine in buffer.
Quantity: 12 mL
Preparation: Ready to use.

K. Stop Solution
0.3 M HCl
Quantity: 12 mL
Preparation: Ready to use.

IV. STORAGE AND STABILITY

- Recommended storage for kit components is 2-8°C.
- All components are shipped and stored at 2-8°C. Reconstituted standards and controls can be frozen for future use but repeated freeze/thaw cycles should be avoided. Refer to expiration dates on all reagents prior to use. Do not mix reagents from different kits unless they have the same lot numbers.

V. REAGENT PRECAUTIONS

A. Sodium Azide

Sodium Azide or Proclin has been added to some reagents as a preservative. Although the concentrations are low, Sodium Azide and Proclin may react with lead and copper plumbing to form highly explosive metal azides. Dispose of unused contents and waste in accordance with international, federal, state, and local regulations.

B. Hydrochloric Acid

Hydrochloric Acid is corrosive and can cause eye and skin burns. It is harmful if swallowed and can cause respiratory and digestive tract burns. Avoid contact with skin and eye. Do not swallow or ingest.

Full Hazardous Component Labels:

Ingredient, Cat #		Full Label	
Rat/Mouse Insulin ELISA Plate	EP13		**Warning.** Causes skin irritation. May cause an allergic skin reaction. Causes serious eye irritation. Harmful to aquatic life with long lasting effects. Avoid release to the environment. Wear protective gloves. IF ON SKIN: Wash with plenty of soap and water. IF IN EYES: Rinse cautiously with water for several minutes. Remove contact lenses, if present and easy to do. Continue rinsing. Get medical advice/ attention. .
Stop Solution	ET-TMB		**Warning.** May be corrosive to metals.
10X HRP Wash Buffer Concentrate	EWB-HRP		**Warning.** May cause an allergic skin reaction. Wear protective gloves. IF ON SKIN: Wash with plenty of soap and water.

VI. MATERIALS REQUIRED BUT NOT PROVIDED

1. Pipette with tips, 10 µL - 100 µL.
2. Multi-channel Pipette: 50 µL ~ 300 µL
3. Reagent Reservoirs
4. Vortex Mixer
5. Refrigerator
6. De-ionized Water
7. Microtiter Plate Reader capable of reading absorbency at 450 nm and 590 nm
8. Orbital Microtiter Plate Shaker
9. Absorbent Paper or Cloth

VII. SAMPLE COLLECTION AND STORAGE

A. To prepare serum, whole blood is directly drawn into a centrifuge tube that contains no anti-coagulant. Let blood clot at room temperature for 30 min.

B. Promptly centrifuge the clotted blood at 2,000 to 3,000 x g for 15 minutes at 4 ± 2°C.

C. Transfer and store serum samples in separate tubes. Date and identify each sample.

D. Use freshly prepared serum or aliquot and store samples at –20 ± 5°C for later use. For long-term storage, keep at -70 °C. Avoid freeze/thaw cycles.

E. To prepare plasma sample, whole blood should be collected into centrifuge tubes containing enough K_3EDTA to achieve a final concentration of 1.735 mg/mL and centrifuged immediately after collection. Observe same precautions in the preparation of serum samples.

F. If heparin is to be used as anti-coagulant, the effect on the assay outcome at the dose of heparin used should be pre-determined.

G. Avoid using samples with gross hemolysis or lipemia.

VIII. ASSAY PROCEDURE

Pre-warm all reagents to room temperature prior to setting up assay.

1. Dilute the 10X Wash Buffer concentrate 10 fold by mixing the entire content of each bottle of Wash Buffer with 450mL de-ionized water. (dilute both bottles with 900 mL deionized water)

2. Remove the required number of strips from the Microtiter Assay Plate. Unused strips should be resealed in the foil pouch and stored at 2-8°C. Assemble strips in an empty plate holder and wash each well 3 times with 300 µL of diluted Wash Buffer per wash. Decant Wash Buffer and remove the residual amount from all wells by inverting the plate and tapping it smartly onto absorbent towels several times. **Do not let wells dry before proceeding to the next step.** If automated machine is used for assay, follow the manufacturer's instructions for all washing steps described in this protocol.

3. Add 10 µL Assay Buffer to each of the Blank and sample wells. Refer to Section IX for suggested well orientations.

VIII. ASSAY PROCEDURE (continued)

4. If samples to be assayed are serum or plasma, add 10 µL Matrix Solution to the Blank, Standard and Control wells (Option A). If samples are free of significant serum matrix components, add 10 µL Assay Buffer instead (Option B).

5. Add in duplicate 10 µL Rat Insulin Standards in the order of ascending concentration to the appropriate wells.

6. Add 10 µL QC1 and 10 µL QC2 to the appropriate wells.

7. Add sequentially 10 µL samples of the unknown samples in duplicates to the remaining wells.

8. Add 80 µL Detection Antibody to all wells. **For best result all additions should be completed within one hour.** Cover the plate with plate sealer and incubate at room temperature for 2 hours on a orbital microtiter plate shaker set to rotate at moderate speed, about 400 to 500 rpm.

9. Remove plate sealer and decant solutions from the plate. Tap as before to remove residual solutions in well.

10. Wash wells 3 times with diluted Wash Buffer, 300 µL per well per wash. Decant and tap after each wash to remove residual buffer.

11. Add 100 µL Enzyme Solution to each well. Cover plate with sealer and incubate with moderate shaking at room temperature for 30 min on the microtiter plate shaker.

12. Remove sealer, decant solutions from the plate and tap plate to remove the residual fluid.

13. Wash wells 6 times with diluted Wash Buffer, 300 µL per well per wash. Decant and tap after each wash to remove residual buffer.

14. Add 100 µL of Substrate Solution to each well, cover plate with sealer and shake in the plate shaker for **approximately** 5 to 20 minutes. Blue color should be formed in wells of Insulin Standards with intensity proportional to increasing concentrations of insulin.

NOTE: Please be aware that the color may develop more quickly or more slowly than the recommended incubation time depending on the localized room temperature. Please visually monitor the color development to optimize the incubation time. One can measure the color development using 370 nm filter, if available on the spectrophotometer. When absorbance is between 1.2 and 1.8 at 370 nm, the stop solution can be added to terminate color development.

15. Remove sealer and add 100 µL Stop Solution **[CAUTION: CORROSIVE SOLUTION]** and shake plate by hand to ensure complete mixing of solution in all wells. The blue color should turn into yellow after acidification. Wipe the bottom of the microtiter plate to remove any residue prior to reading on plate reader. Read absorbance at 450 nm and 590 nm in a plate reader within 5 minutes and ensure that there is no air bubbles in any well. Record the difference of absorbance units.

Assay Procedure for Rat / Mouse Insulin ELISA kit (Cat. # EZRMI-13K)

Option A: For Samples with significant Serum Matrix Effect

	Step 1	Step 2	Step 3	Step 4	Step 5-7	Step 8	Step 8-10	Step 11	Step 11-13	Step 14	Step 14	Step 15	St
Well #	Dilute each bottle 10X Wash Buffer with 450mL Deionized Water.	Wash plate 3X with 300 µL Wash Buffer. Remove residual buffer by tapping smartly on absorbent towels	Assay Buffer	Matrix Solution	Standards/ Controls/ Samples	Detection Ab	Seal, Agitate, Incubate 2 hours at Room Temperature. Wash 3X with 300 µL Wash Buffer	Enzyme Solution	Seal, Agitate, Incubate 30 minutes at Room Temperature. Wash 6X with 300 µL Wash Buffer	Substrate	Seal, Agitate, Incubate 15 minutes at Room Temperature.	Stop Solution	Read Absorbance at 450 nm and 590 nm.
A1, B1			10 µL	10 µL	----------	80 µL		100 µL		100 µL		100 µL	
C1, D1			------	10 µL	10 µL of 0.2 ng/mL Standard	80 µL		100 µL		100 µL		100 µL	
E1, F1			------	10 µL	10 µL of 0.5 ng/mL Standard	80 µL		100 µL		100 µL		100 µL	
G1, H1			------	10 µL	10 µL of 1 ng/mL Standard	80 µL		100 µL		100 µL		100 µL	
A2, B2			------	10 µL	10 µL of 2 ng/mL Standard	80 µL		100 µL		100 µL		100 µL	
C2, D2			------	10 µL	10 µL of 5 ng/mL Standard	80 µL		100 µL		100 µL		100 µL	
E2, F2			------	10 µL	10 µL of 10 ng/mL Standard	80 µL		100 µL		100 µL		100 µL	
G2, H2			------	10 µL	10 µL of QC I	80 µL		100 µL		100 µL		100 µL	
A3, B3			------	10 µL	10 µL of QC II	80 µL		100 µL		100 µL		100 µL	
C3, D3 ↓			10 µL	------	10 µL of Sample	80 µL		100 µL		100 µL		100 µL	

Assay Procedure for Rat / Mouse Insulin ELISA kit (Cat. # EZRMI-13K)

Option B: For Samples without significant Serum Matrix Effect

	Step 1	Step 2	Step 3-4	Step 5-7	Step 8	Step 8-10	Step 11	Step 11-13	Step 14	Step 14	Step 15	Step 15
Well #	Dilute each bottle 10X Wash Buffer with 450mL Deionized Water.	Wash plate 3X with 300 µL Wash Buffer. Remove residual buffer by tapping smartly on absorbent towels	Assay Buffer	Standards/ Controls/ Samples	Detection Ab	Seal, Agitate, Incubate 2 hours at Room Temperature. Wash 3X with 300 µL Wash Buffer	Enzyme Solution	Seal, Agitate, Incubate 30 minutes at Room Temperature. Wash 6X with 300 µL Wash Buffer	Substrate	Seal, Agitate, Incubate 15 minutes at Room Temperature.	Stop Solution	Read Absorbance at 450 nm and 590 nm.
A1, B1			20 µL	----------	80 µL		100 µL		100 µL		100 µL	
C1, D1			10 µL	10 µL of 0.2 ng/mL Standard	80 µL		100 µL		100 µL		100 µL	
E1, F1			10 µL	10 µL of 0.5 ng/mL Standard	80 µL		100 µL		100 µL		100 µL	
G1, H1			10 µL	10 µL of 1 ng/mL Standard	80 µL		100 µL		100 µL		100 µL	
A2, B2			10 µL	10 µL of 2 ng/mL Standard	80 µL		100 µL		100 µL		100 µL	
C2, D2			10 µL	10 µL of 5 ng/mL Standard	80 µL		100 µL		100 µL		100 µL	
E2, F2			10 µL	10 µL of 10 ng/mL Standard	80 µL		100 µL		100 µL		100 µL	
G2, H2			10 µL	10 µL of QC I	80 µL		100 µL		100 µL		100 µL	
A3, B3			10 µL	10 µL of QC II	80 µL		100 µL		100 µL		100 µL	
C3, D3 ↓			10 µL	10 µL of Sample	80 µL		100 µL		100 µL		100 µL	

X. CALCULATIONS

The dose-response curve of this assay fits best to a sigmoidal 4- or 5-parameter logistic equation. The results of unknown samples can be calculated with any computer program having a 4- or 5-parameter logistic function. Graph the reference curve for sample interpretation by plotting the absorbance unit of 450 nm, less that of 590 nm, on the Y-axis against the concentration of rat insulin standards on the X-axis.

Note: When sample volumes assayed differ from 10 µL, an appropriate mathematical adjustment must be made to accommodate for the dilution factor (e.g., if 5 µL of sample is used, then calculated data must be multiplied by 2). When sample volume assayed is less than 10 µL, compensate the volume deficit with either matrix solution or assay buffer, whichever is appropriate.

XI. INTERPRETATION

A. Acceptance Criteria

1. The assay will be considered accepted when all Quality Control values fall within the calculated Quality Control Range. If any QC's fall outside the control range, review results with a supervisor.

2. If the difference between duplicate results of a sample is >15% CV, repeat the sample.

3. The limit of sensitivity of this assay is 0.1 ng/mL (17.5 pM) insulin (10 µL sample size).

4. The appropriate range of this assay is 0.1 ng/mL to 10 ng/mL insulin (10 µL sample size). Any result greater than 10 ng/mL in a 10 µL sample assayed should be repeated on dilution using either matrix solution or assay buffer, whichever is appropriate, as diluent until it falls within range.

XII. ASSAY CHARACTERISTICS

A. Sensitivity

The lowest level of Insulin that can be detected by this assay is 0.1 ng/mL (17.5 pM) insulin when using a 10 µL sample size.

B. Specificity

The specificity (also known as selectivity) of the analytical test is its ability to selectively measure the analytes in the presence of other like components in the sample matrix.

Rat Insulin	100% [ED(50) = 1.57 nM]
Porcine Insulin	102%
Bovine Insulin	78%
Ovine Insulin	106%
Human Insulin	106%
Human Proinsulin	52%
Des(64,65) Human Proinsulin	101%
Des(31,32) Human Proinsulin	69%
Porcine Proinsulin	57%
Bovine Proinsulin	56%
Human IGF-I	n.d.*
Human IGF-II	n.d.*
Porcine Glucagon	n.d.*
Human C-peptide	n.d.*
Rat C-peptide	n.d.*
Rat Leptin	n.d.*
Mouse Leptin	n.d.*

n.d.*: not detectable at concentrations up to 120 nM

C. Precision:

Sample Number	Mean Insulin Level (ng/mL)	Mean Assay Variation (% CV)	
		Intra-assay	Inter-assay
Mouse serum #1	0.32	8.35	17.9
Mouse serum #2	1.69	0.92	6.03
Mouse serum #3	3.45	1.92	7.64
Rat serum #1	1.15	3.22	6.95
Rat serum #2	2.32	1.33	6.71
Rat serum #3	3.65	1.17	9.23

The assay variations of EMD Millipore Mouse/Rat Insulin ELISA kit were studied on three mouse and three rat serum samples with varying concentrations of endogenous analyte. The intra-assay variations are calculated from six duplicate determinations in an assay. The inter-assay variations are calculated from results of 5 separate assays with duplicate samples in each assay.

XII. ASSAY CHARACTERISTICS (continued)

D. Dilutional Linearity:

Serum Sample #	Dilution Factor	Insulin Level		
		Observed (ng/mL)	Expected (ng/mL)	% Of Expected
Mouse Serum # 1	--	2.06	2.06	**100**
	2x	1.84		89
	4x	2.20		107
	8x	3.12		152
Mouse Serum # 2	--	2.98	2.98	**100**
	2x	2.84		95
	4x	3.08		103
	8x	3.76		126
Mouse Serum # 3	--	2.95	2.95	**100**
	2x	2.94		100
	4x	3.08		104
	8x	3.92		133
Rat Serum # 1	--	4.22	4.22	**100**
	2x	3.80		90
	5x	3.55		84
	10x	4.70		111
Rat Serum # 2	--	3.78	3.78	**100**
	2x	3.16		84
	5x	3.00		79
	10x	3.40		90
Rat Serum # 3	--	3.42	3.42	**100**
	2x	3.12		91
	5x	3.15		92
	10x	3.90		114

Three mouse and three rat serum samples are diluted each with matrix solution to various degrees as indicated and assayed for insulin levels along with neat samples of each serum. Measured insulin levels are corrected for dilution factors and reported as observed insulin level.

XII. ASSAY CHARACTERISTICS (continued)

E. Recovery

Spike and Recovery of Insulin in Serum Samples:

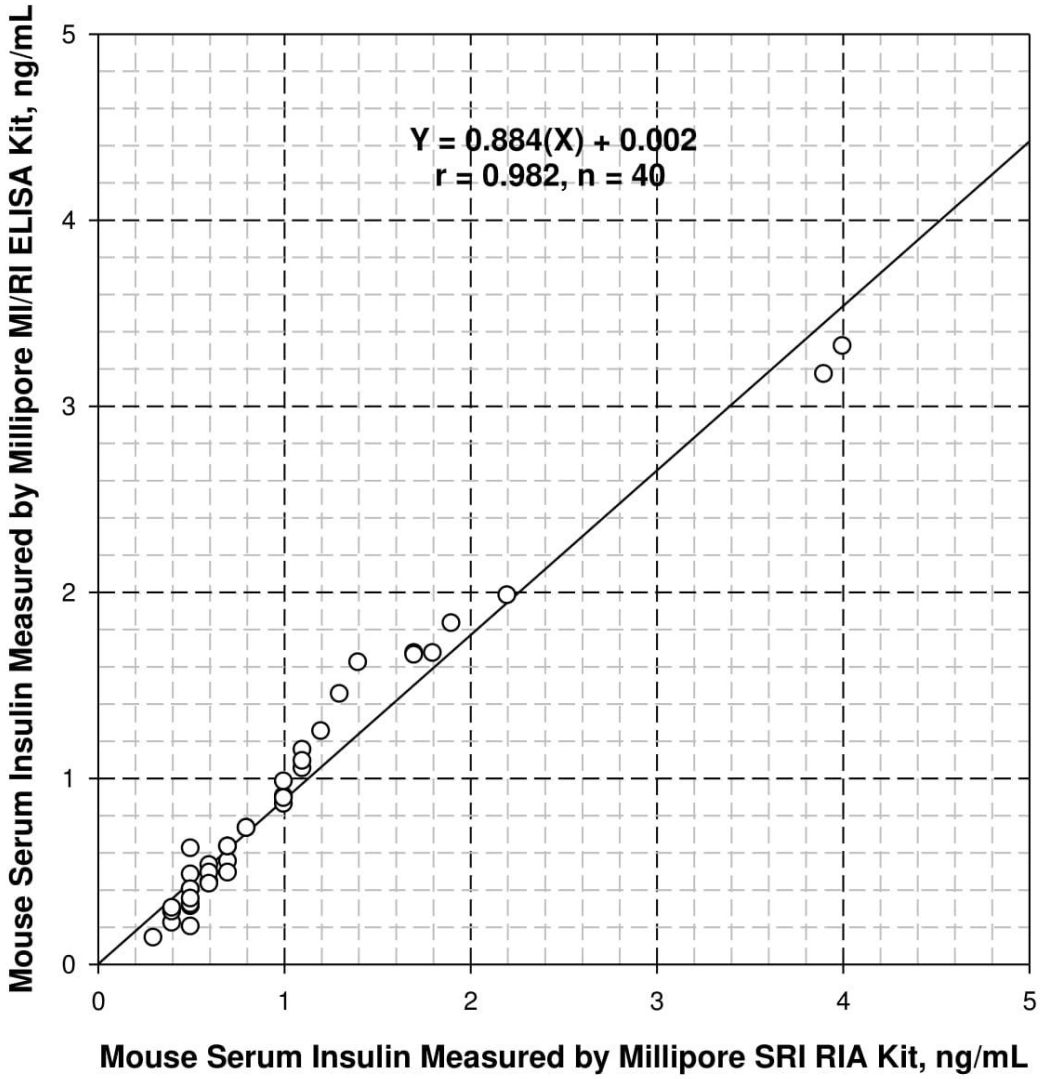
Serum Sample #	Rat Insulin		Recovery (%) of Spiked Insulin
	Added (ng/mL)	Observed (ng/mL)	
Mouse Serum # 1	0	0.33	--
	0.5	0.83	100
	2	2.15	91
	5	5.07	95
Mouse Serum # 2	0	1.78	--
	0.5	2.20	84
	2	3.43	83
	5	6.16	88
Mouse Serum # 3	0	1.01	--
	0.5	1.49	96
	2	2.91	95
	5	5.95	99
Rat Serum # 1	0	1.06	--
	0.5	1.57	102
	2	2.86	90
	5	5.88	96
Rat Serum # 2	0	1.07	--
	0.5	1.53	92
	2	2.95	94
	5	6.01	99
Rat Serum # 3	0	0.99	--
	0.5	1.45	92
	2	2.69	85
	5	5.40	88

Rat insulin at indicated levels was added to three mouse and three rat serum samples and the resulting insulin content of each sample was assayed by ELISA. The % of recovery = [(observed insulin level after spike - observed insulin level before spike) / spiked level of insulin] x 100%. Mean ± S.D. of recovery rate at spiked insulin level of 0.5, 2, and 5 ng/mL is 93 ± 8%, 90 ± 6% and 94 ± 6% in mouse serum and 95 ± 6%, 90 ± 5% and 94 ± 7% in rat serum, respectively.

XIII. CORRELATION GRAPH

Mouse Serum Insulin Assays:

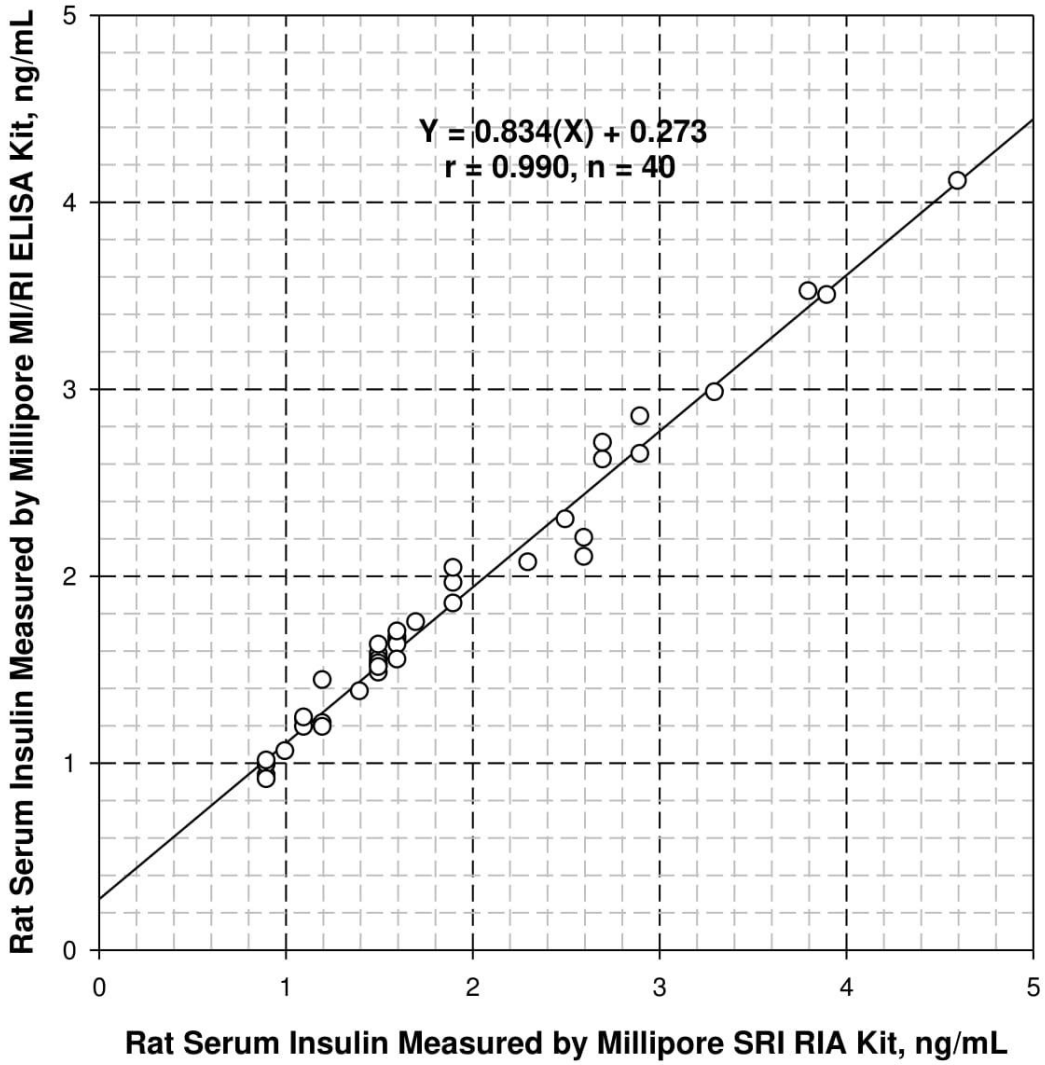
Correlation of Results by RIA and ELISA Methods



XIII. CORRELATION GRAPH (continued)

Rat Serum Insulin Assays:

Correlation of Results by RIA and ELISA Methods



XIV. QUALITY CONTROLS

The ranges for Quality Control 1 and 2 are provided on the card insert or can be located at the EMD MILLIPORE website www.emdmillipore.com using the catalog number as the keyword.

XV. TROUBLE SHOOTING GUIDE

1. To obtain reliable and reproducible results the operator should carefully read this manual and fully understand all aspects of each assay step before attempting to run the assay.
2. Throughout the assay the operator should adhere strictly to the procedures with good laboratory practice.
3. Have all necessary reagents and equipment ready on hand before starting. Once the assay has been started all steps should be completed with precise timing and without interruption.
4. Avoid cross contamination of any reagents or samples to be used in the assay.
5. Make sure that all reagents and samples are added to the bottom of each well.
6. Careful and complete mixing of solutions in the well is critical. Poor assay precision will result from incomplete mixing or cross well contamination due to inappropriate mixing.
7. Remove any air bubble formed in the well after acidification of substrate solution because bubbles interfere with spectrophotometric readings.
8. High absorbance in background or blank wells could be due to 1) cross well contamination by standard solution or sample or 2) inadequate washing of wells with TBS.

XVI. REPLACEMENT REAGENTS

REAGENTS	CAT. #
Rat/Mouse Insulin ELISA Plate	EP13
10X HRP Wash Buffer Concentrate (50 mL)	EWB-HRP
Rat/Mouse Insulin Standards	E8013-K
Rat/Mouse Insulin Quality Controls 1 and 2	E6013-K
Matrix Solution	EMTX-RMI
Assay Buffer	AB-PHK
Rat/Mouse Insulin Detection Antibody	E1013
Enzyme Solution	EHRP-5
Substrate	ESS-TMB2
Stop Solution	ET-TMB

Appendix 13 – Biovision HDL and LDL Quantitation Kit Data Sheet

BioVision

rev. 12/14

For research use only

HDL and LDL/VLDL Quantification Colorimetric/Fluorometric Kit

(Catalog # K613-100; 100 assays; Store at -20°C)

I. Introduction:

Regulation of HDL (high-density-lipoprotein)-cholesterol and LDL (low-density-lipoprotein)-cholesterol plays a central role in various disease developments. It is well known that low levels of HDL and high level of LDL are associated with an increased risk of cardiovascular events. BioVision's HDL and LDL/VLDL Cholesterol Quantification Kit provides a simple quantification method of HDL and LDL/VLDL after a convenient separation of HDL from LDL and VLDL (very low-density lipoprotein) in serum samples. In the assay, cholesterol oxidase specifically recognizes free cholesterol and produces products which react with probe to generate color (λ = 570 nm) and fluorescence (Ex/Em = 538/587 nm). Cholesterol esterase hydrolyzes cholesteryl ester into free cholesterol, therefore, cholesterol ester and free cholesterol can be detected separately in the presence and absence of cholesterol esterase in the reactions.

II. Kit Contents:

Components	Volume	Cap Code	Part No.
Cholesterol Assay Buffer	25 ml	WM	K613-100-1
2X LDL/VLDL Precipitation Buffer	10 ml	NM	K613-100-2
Cholesterol Probe (in DMSO, anhydrous)	200 µl	Red	K613-100-3A
Enzyme Mix (Lyophilized)	1 vial	Green	K613-100-5
Cholesterol Esterase (Lyophilized)	1 vial	Blue	K613-100-6
Cholesterol Standard (2 µg/µl)	100 µl	Yellow	K613-100-7

III. Reagent Preparation:

Cholesterol Probe: Ready to use as supplied. Warm to room temperature to thaw the DMSO solution. Store at –20°C, protect from light. Use within two months.

Cholesterol Esterase: Dissolve in 220 µl Cholesterol Assay Buffer prior to use. Aliquot and store at –20°C. Use within two months.

Enzyme Mix: Dissolve in 220 µl Cholesterol Assay Buffer prior to use. Aliquot and store at –20°C. Use within two months.

IV. Cholesterol Assay Protocol:

1. **Separation of HDL and LDL/VLDL:** Mix 100 µl of 2X Precipitation Buffer with 100 µl of serum sample in microcentrifuge tubes. Incubate 10 min at room temperature, centrifuge at 2000 x g (5000 rpm on bench-top microcentrifuge) for 10 min. Transfer the supernatant into new labeled tubes. This is the HDL fraction. The precipitates are the LDL/VLDL fraction. If you want to measure the LDL/VLDL level, the precipitate should be spun again, and the trace amount of HDL supernatant carefully removed. Resuspend the precipitate in 200 µl PBS (not provided). This is the LDL/VLDL fraction.

   Note A: If the supernatant is cloudy, the sample should be re-centrifuged. If the sample remains cloudy, dilute the sample 1:1 with PBS, and repeat the separation procedure. Multiply final results by two (2) due to the dilution with the 2X Precipitation Buffer.

   Note B: Precipitation time and temperature do not affect the results significantly.

2. **Standard Curve and Sample Preparations:** Dilute the Cholesterol Standard to 0.25 µg/µl by adding 20 µl of the Cholesterol Standard to 140 µl of Cholesterol Assay Buffer, mix well. Add 0, 4, 8, 12, 16, 20 µl into a series of wells in a 96-well plate. Adjust volume to 50 µl/well with Cholesterol Assay Buffer to generate 0, 1, 2, 3, 4, 5 µg/well of the Cholesterol Standard. (**Note:** Fluorometric assay is ~10 times more sensitive than the colorimetric assay, the cholesterol standards should be diluted 10 times further if using fluorometric assay).

For sample testing, using 1 to 20 µl of the HDL or LDL/VLDL fraction, adjust the total volume to 50 µl/well with Cholesterol Assay Buffer. For unknown samples, we suggest testing different volumes of sample to ensure the readings are within the linear portion of the standard curve.

3. **Reaction Mix Preparation:** Mix enough reagent for the number of assays performed. For each assay, prepare a total 50 µl Reaction Mix containing:

   44 µl Cholesterol Assay Buffer
   2 µl Cholesterol Probe[1]
   2 µl Enzyme Mix
   2 µl Cholesterol Esterase[2,3]

*Notes: 1. If using fluorometric assay, use 0.4 ul of Cholesterol Probe per reaction to reduce fluorescence background.

2. Cholesterol Esterase hydrolyzes cholesteryl ester to free cholesterol. If you want to detect free cholesterol only, omit the Cholesterol Esterase in the reaction, and substitute with 2 µl of Assay Buffer. With the addition of Cholesterol Esterase, the assay detects total cholesterol (cholesterol and cholesteryl esters). If you want to detect cholesteryl esters only, subtract the value of free cholesterol from the value of total cholesterol.

Cholesterol Esterase must be added to the reaction for standard curve to convert all the cholesterol in the standard solution.

4. Add 50 µl of the Reaction Mix to each well containing the Cholesterol Standard or test samples, mix well.
5. Incubate the reaction for 60 min at 37°C, protect from light. Measure O.D. at 570 nm or fluorescence at Ex/Em 538/587 nm in a micro-titer plate reader.
6. **Calculations:** Subtract 0 standard reading from readings. Plot the standard curve. Apply the sample readings to the standard curve to determine sample cholesterol amount in the reaction well. Sample cholesterol concentrations:

C = A/V (µg/µl)

Where: **A** is the sample cholesterol amount from the standard curve (in µg).
V is original sample volume added to the sample reaction well (in µl).
Cholesterol Molecular Weight: 386.6; 1 µg/µl = 100 mg/dL.

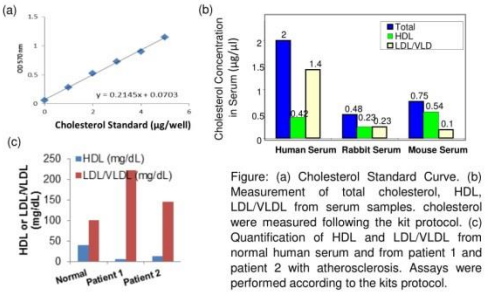


Figure: (a) Cholesterol Standard Curve. (b) Measurement of total cholesterol, HDL, LDL/VLDL from serum samples. cholesterol were measured following the kit protocol. (c) Quantification of HDL and LDL/VLDL from normal human serum and from patient 1 and patient 2 with atherosclerosis. Assays were performed according to the kits protocol.

FOR RESEARCH USE ONLY! Not to be used on humans.

BioVision Incorporated
155 S. Milpitas Boulevard, Milpitas, CA 95035 USA

Tel: 408-493-1800 | Fax: 408-493-1801
www.biovision.com | tech@biovision.com

BioVision **TROUBLESHOOTING GUIDE:**

rev. 12/14

For research use only

Problems	Cause	Solution
Assay not working	• Use of ice-cold assay buffer	• Assay buffer must be at room temperature
	• Omission of a step in the protocol	• Refer and follow the data sheet precisely
	• Plate read at incorrect wavelength	• Check the wavelength in the data sheet and the filter settings of the instrument
	• Use of a different 96-well plate	• Fluorescence: Black plates (clear bottoms) ; Luminescence: White plates ; Colorimeters: Clear plates
Samples with erratic readings	• Use of an incompatible sample type	• Refer data sheet for details about incompatible samples
	• Samples prepared in a different buffer	• Use the assay buffer provided in the kit or refer data sheet for instructions
	• Samples were not deproteinized (if indicated in datasheet)	• Use the 10 kDa spin cut-off filter or PCA precipitation as indicated
	• Cell/ tissue samples were not completely homogenized	• Use Dounce homogenizer (increase the number of strokes); observe for lysis under microscope
	• Samples used after multiple free-thaw cycles	• Aliquot and freeze samples if needed to use multiple times
	• Presence of interfering substance in the sample	• Troubleshoot if needed, deproteinize samples
	• Use of old or inappropriately stored samples	• Use fresh samples or store at correct temperatures till use
Lower/ Higher readings in Samples and Standards	• Improperly thawed components	• Thaw all components completely and mix gently before use
	• Use of expired kit or improperly stored reagents	• Always check the expiry date and store the components appropriately
	• Allowing the reagents to sit for extended times on ice	• Always thaw and prepare fresh reaction mix before use
	• Incorrect incubation times or temperatures	• Refer datasheet & verify correct incubation times and temperatures
	• Incorrect volumes used	• Use calibrated pipettes and aliquot correctly
Readings do not follow a linear pattern for Standard curve	• Use of partially thawed components	• Thaw and resuspend all components before preparing the reaction mix
	• Pipetting errors in the standard	• Avoid pipetting small volumes
	• Pipetting errors in the reaction mix	• Prepare a master reaction mix whenever possible
	• Air bubbles formed in well	• Pipette gently against the wall of the tubes
	• Standard stock is at an incorrect concentration	• Always refer the dilutions in the data sheet
	• Calculation errors	• Recheck calculations after referring the data sheet
	• Substituting reagents from older kits/ lots	• Use fresh components from the same kit
Unanticipated results	• Measured at incorrect wavelength	• Check the equipment and the filter setting
	• Samples contain interfering substances	• Troubleshoot if it interferes with the kit
	• Use of incompatible sample type	• Refer data sheet to check if sample is compatible with the kit or optimization is needed
	• Sample readings above/below the linear range	• Concentrate/ Dilute sample so as to be in the linear range

Note: The most probable list of causes is under each problem section. Causes/ Solutions may overlap with other problems.

BioVision Incorporated
155 S. Milpitas Boulevard, Milpitas, CA 95035 USA

Tel: 408-493-1800 | Fax: 408-493-1801
www.biovision.com | tech@biovision.com

Appendix 14 – Biovision Free Fatty Acid Quantitation Kit Data Sheet

BioVision

rev. 3/15

For research use only

Free Fatty Acid Quantification Colorimetric/Fluorometric Kit

(Catalog #K612-100; 100 assays; Store at -20°C)

I. Introduction:

Fatty Acids play very important roles in normal metabolism and many disease developments. They are precursors to a number of bioactive classes of compounds such as prostaglandins, leucotrienes and others, and have been implicated in diverse functions such as autism, immune system and inflammation response. BioVision's Free Fatty Acid Quantification Kit provides a convenient, sensitive enzyme-based method for detecting the long-chain free fatty acids in various biological samples, such as serum, plasma and other body fluids, food, growth media, etc. In the assay, Fatty Acids are converted to their CoA derivatives, which are subsequently oxidized with the concomitant generation of color or fluorescence. C-8 (octanoate) and longer fatty acids can then be easily quantified by either colorimetric (spectrophotometry at λ = 570 nm) or fluorometric (at Ex/Em = 535/587 nm) methods with detection limit 2 µM free fatty acid in variety samples.

II. Kit Contents:

Components	100 Assays	Cap Cod	Part Number
Fatty Acid Assay Buffer	25 ml	WM	K612-100-1
Fatty Acid Probe (in DMSO)	200 µl	Red	K612-100-2A
ACS Reagent	1 vial	Blue	K612-100-4
Enzyme Mix	1 vial	Green	K612-100-5
Enhancer	200 µl	Purple	K612-100-6
Palmitic Acid Standard (1nmol/µl)	300 µl	Yellow	K612-100-7

III. Storage and Handling:

Store kit at –20°C, protect from light. Allow Fatty Acid Assay Buffer warm to room temperature before use.

IV. Reagent Preparation:

- **Probe**: Ready to use as supplied. Warm to room temperature prior to use to melt frozen DMSO. Store at –20°C, protect from light and moisture. Use within two months.
- **Enzymes:** Dissolve ACS (Acyl-CoA Synthetase) Reagent and Enzyme Mix individually with 220 µl Assay Buffer each by pipetting up and down. Store at –20°C. Use within two months.
- **Palmitic Acid Standard:** Frozen storage may cause the Palmitic Acid Standard to separate from the aqueous phase. To re-dissolve, keep the cap tightly closed, place in a hot water bath (~80-100°C) for 1 min. or until the standard looks cloudy, vortex for 30 sec., the standard should become clear. Repeat the heat and vortex one more time. The Palmitic Acid Standard is now completely in solution, and ready to use.

V. Free Fatty Acid Assay Protocol:

The following protocol describes assays in 100 µl per microplate well.

1. **Standard Curve Preparation:**

   For the colorimetric assay, add 0, 2, 4, 6, 8, 10 µl Palmitic Acid Standard into 96-well plate individually. Adjust volume to 50 µl/well with Assay Buffer to generate 0, 2, 4, 6, 8, 10 nmol/well of the Fatty Acid Standard.

   For the fluorometric assay, dilute the Palmitic Acid Standard to 0.1 nmol/µl by adding 10 µl of the Standard to 90 µl of Assay Buffer, mix well. Add 0, 2, 4, 6, 8, 10 µl into each well individually. Adjust volume to 50 µl/well with Assay Buffer to generate 0, 0.2, 0.4, 0.6, 0.8, 1.0 nmol/well of the Fatty Acid Standard.

2. **Sample Preparation:** For testing liquid samples, different volume of samples can be directly added to each well in a 96-well plate, then bring up the volume to 50 µl/well with Assay Buffer. For unknown samples, we suggest using different doses to ensure the readings are within the standard curve range.

BioVision Incorporated
155 S. Milpitas Boulevard, Milpitas, CA 95035 USA

For testing cell or tissue samples, 10^6 cells or 10 mg tissue samples can be extracted by homogenization with 200 µl of chloroform-Triton X-100 (1% Triton X-100 in pure chloroform) in a microhomogenizer. Then spin the extract 5-10 minutes at top speed in a microcentrifuge. Collect organic phase (lower phase), air dry at 50°C to remove chloroform. Vacuum dry 30 min to remove trace chloroform. Dissolve the dried lipids (in Triton X-100) in 200 µl of Fatty Acid Assay Buffer by vortexing extensively for 5 mins (Note: The solution may be slightly turbid or opalescent, but this does not affect the assay). The extraction procedure can be proportionally scaled up if larger amount of sample is desired. Use 1- 50 µl of the extracted sample per assay.

3. **Acyl-CoA Synthesis:** Add 2 µl ACS Reagent into all the standard and sample wells. Mix well; incubate the reaction at 37°C for 30 min.
4. **Reaction Mix Preparation:** Mix enough reagents for the number of assays and standard performed: For each well, prepare a total 50 µl Reaction Mix containing:

   44 µl Assay Buffer
   2 µl Fatty Acid Probe
   2 µl Enzyme Mix
   2 µl Enhancer

   Mix well. Add 50 µl of the Reaction Mix to each well containing the Standard or test samples. Incubate the reaction for 30 min at 37°C, protect from light.
6. Measure O.D. 570 nm for colorimetric assay or fluorescence at Ex/Em = 535/590 nm in a micro-plate reader.
7. **Calculation:** Subtract background value (the 0 Control) from all standard and sample readings. Plot standard curve nmol/well vs. OD_{570nm} or fluorescence readings. Then apply the sample readings to the standard curve to obtain Fatty Acid amount in the sample wells.

   Fatty Acid Concentration = Fa/Sv (nmol/µl or mM)
   Fa is the Fatty Acid amount (nmol) in the well obtained from standard curve.
   Sv is the sample volume (µl) added to the sample well.

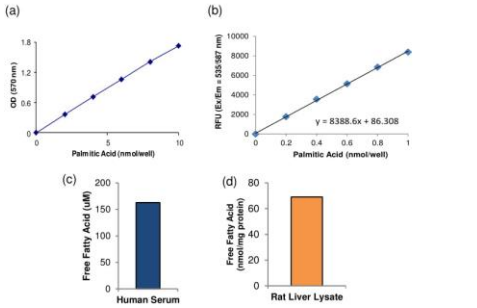


Figure: Palmitic Acid Standard Curve: Colorimetric (a), Fluorometric (b). Quantitation of free fatty acid in pooled human serum (10 µl) (c) and rat liver lysate (50 µg) (d). Assays were performed following the kit protocol.

FOR RESEARCH USE ONLY! Not to be used on humans.

Tel: 408-493-1800 | Fax: 408-493-1801
www.biovision.com | tech@biovision.com

BioVision **ESHOOTING GUIDE:**

rev. 12/14

For research use only

Problems	Cause	Solution
Assay not working	• Use of ice-cold assay buffer	• Assay buffer must be at room temperature
	• Omission of a step in the protocol	• Refer and follow the data sheet precisely
	• Plate read at incorrect wavelength	• Check the wavelength in the data sheet and the filter settings of the instrument
	• Use of a different 96-well plate	• Fluorescence: Black plates (clear bottoms) ; Luminescence: White plates ; Colorimeters: Clear plates
Samples with erratic readings	• Use of an incompatible sample type	• Refer data sheet for details about incompatible samples
	• Samples prepared in a different buffer	• Use the assay buffer provided in the kit or refer data sheet for instructions
	• Samples were not deproteinized (if indicated in datasheet)	• Use the 10 kDa spin cut-off filter or PCA precipitation as indicated
	• Cell/ tissue samples were not completely homogenized	• Use Dounce homogenizer (increase the number of strokes); observe for lysis under microscope
	• Samples used after multiple free-thaw cycles	• Aliquot and freeze samples if needed to use multiple times
	• Presence of interfering substance in the sample	• Troubleshoot if needed, deproteinize samples
	• Use of old or inappropriately stored samples	• Use fresh samples or store at correct temperatures till use
Lower/ Higher readings in Samples and Standards	• Improperly thawed components	• Thaw all components completely and mix gently before use
	• Use of expired kit or improperly stored reagents	• Always check the expiry date and store the components appropriately
	• Allowing the reagents to sit for extended times on ice	• Always thaw and prepare fresh reaction mix before use
	• Incorrect incubation times or temperatures	• Refer datasheet & verify correct incubation times and temperatures
	• Incorrect volumes used	• Use calibrated pipettes and aliquot correctly
Readings do not follow a linear pattern for Standard curve	• Use of partially thawed components	• Thaw and resuspend all components before preparing the reaction mix
	• Pipetting errors in the standard	• Avoid pipetting small volumes
	• Pipetting errors in the reaction mix	• Prepare a master reaction mix whenever possible
	• Air bubbles formed in well	• Pipette gently against the wall of the tubes
	• Standard stock is at an incorrect concentration	• Always refer the dilutions in the data sheet
	• Calculation errors	• Recheck calculations after referring the data sheet
	• Substituting reagents from older kits/ lots	• Use fresh components from the same kit
Unanticipated results	• Measured at incorrect wavelength	• Check the equipment and the filter setting
	• Samples contain interfering substances	• Troubleshoot if it interferes with the kit
	• Use of incompatible sample type	• Refer data sheet to check if sample is compatible with the kit or optimization is needed
	• Sample readings above/below the linear range	• Concentrate/ Dilute sample so as to be in the linear range

Note: The most probable list of causes is under each problem section. Causes/ Solutions may overlap with other problems.

BioVision Incorporated
155 S. Milpitas Boulevard, Milpitas, CA 95035 USA

Tel: 408-493-1800 | Fax: 408-493-1801
www.biovision.com | tech@biovision.com

Appendix 15 – Biovision Triglyceride Quantitation Kit Data Sheet

FOR RESEARCH USE ONLY!

BioVision
BioVision Incorporated

Triglyceride Quantification Colorimetric/Fluorometric Kit

rev. 8/13

(Catalog # K622-100; 100 assays; Store at -20°C)

I. Introduction:

Triglycerides (TG) are the main constituent of vegetable oil, animal fat, LDL and VLDL, and play an important role as transporters of fatty acids as well as serving as an energy source. TG are broken down into fatty acids and glycerol, after which both can serve as substrates for energy producing and metabolic pathways. High blood levels of TG are implicated in atherosclerosis, heart disease and stroke as well as in pancreatitis. The Triglyceride Quantification Kit provides a sensitive, easy assay to measure TG concentration in a variety of samples. In the assay, TG are converted to free fatty acids and glycerol. The glycerol is then oxidized to generate a product which reacts with the probe to generate color (spectrophotometry at λ = 570 nm) and fluorescence (Ex/Em = 535/587 nm). The kit can detect 2 pmol-10nmol (or 2-10000µM range) of triglyceride in various samples. The kit also detects monoglycerides and diglycerides.

II. Application:

- Measurement of triglycerides in various tissues, cells & other biological fluids
- Mechanistic study of cardiovascular diseases
- Analysis of lipid metabolism

III. Sample Type:

- Animal tissues: Liver, pancreas, heart etc.
- Cell culture: adipocytes etc.
- Biological fluids: serum, plasma etc..

IV. Kit Contents:

Components	K622-100	Cap Code	Part Number
Triglyceride Assay Buffer	25 ml	WM	K622-100-1
Triglyceride Probe (in DMSO, anhydrous)	200 µl	Red	K622-100-2A
Lipase	1 vial	Blue	K622-100-4
Triglyceride Enzyme Mix (lyophilized)	1 vial	Green	K622-100-5
Triglyceride Standard (1 mM)	0.3 ml	Yellow	K622-100-6

V. User Supplied Reagents and Equipment:

- 96-well white plate (fluorometric) or clear plate (colorimetric)
- Multi-well spectrophotometer (Absorbance/Fluorescence reader)

VI. Storage and Handling:

Store kit at –20˚C, protect from light. Warm Triglyceride Assay Buffer to room temperature before use. Briefly centrifuge small vials prior to opening.

VII. Reagent Preparation and Storage Conditions:

- **Triglyceride Standard:** Frozen storage may cause the Triglyceride Standard to separate from the aqueous phase. To re-dissolve, keep the cap tightly closed, place in a hot water bath (~80-100°C) for 1 min or until the standard looks cloudy, vortex for 30 sec., the standard should become clear. Repeat the heat and vortex one more time. The Triglyceride Standard is now completely in solution, and ready to use.
- **Triglyceride Probe:** Ready to use as supplied. Warm by placing in a 37°C bath for 1-5 min to thaw the DMSO solution before use. (**Note:** DMSO tends to be a solid after -20°C storage, even when left at room temperature- so need to melt for a few min. at 37°C). Store at –20°C, protect from light. Use within two months.
- **Triglyceride Enzyme Mix:** Dissolve in 220 µl Triglyceride Assay Buffer. Aliquot and store at -20 °C. Use within two months.
- **Lipase:** Dissolve in 220 µl Triglyceride Assay Buffer. Aliquot and store at -20 °C. Use within two months.

VIII. Triglyceride Assay Protocol:

1. **Sample Preparation:** Add 2-50 µl test samples to a 96-well plate. Adjust the volume to 50 µl/well with Triglyceride Assay Buffer. We suggest using different volumes of sample to ensure readings are within the Standard Curve range. A background control should be performed by replacing 2 µl Lipase with 2 µl Triglyceride Assay Buffer (see section 3). The background should be subtracted from all readings. Endogenous compounds in the sample may interfere with the assay, so it is suggested to spike samples with a known amount of Standard (4 nmol) to ensure accurate determinations of Triglyceride in your sample.

   Note: Serum contains 0.1-6 mM triglyceride, which can be tested directly. For tissue (~100 mg), cells (~10 million) or other non-aqueous samples, homogenize in 1 ml solution containing 5 % NP-40 in water, slowly heat the samples to 80-100 °C in a water bath for 2-5 min. or until the NP-40 becomes cloudy, then cool down to room temperature. Repeat the heating one more time to solubilize all triglyceride. Centrifuge for 2 min. (top speed using a microcentrifuge) to remove any insoluble material. Dilute 10 fold with dH_2O before the assay.
2. **Standard Curve Preparation:** For the colorimetric assay, Dilute 40 µl of the 1 mM Triglyceride into 160 µl Triglyceride Assay Buffer, mix to generate 0.2 mM Triglyceride Standard. Add 0, 10, 20, 30, 40, 50 µl of the 0.2 mM Triglyceride Standard into a series of wells. Adjust volume to 50 µl/well with Triglyceride Assay Buffer to generate 0, 2, 4, 6, 8, 10 nmol/well of Triglyceride Standard.
   For the fluorometric assay, dilute the Triglyceride Standard to 0.02 mM with the Triglyceride Assay Buffer (Detection sensitivity is 10-100 fold higher for a fluorometric than a colorimetric assay). Follow the procedure as the colorimetric assay.

3. **Lipase:** Add 2 µl of Lipase to each Standard and sample well. Mix and incubate 20 min. at room temperature to convert triglyceride to glycerol and fatty acid.

   Note: If samples contain glycerol, do a sample background control, omit the Lipase to determine glycerol background only, not triglyceride.

4. **Triglyceride Reaction Mix:** Mix enough reagent for the number of assays to be performed: For each well, prepare a total 50 µl Reaction Mix:

	Reaction Mix
Triglyceride Assay Buffer	46 µl
Triglyceride Probe*	2 µl
Triglyceride Enzyme Mix	2 µl

   Add 50 µl of the Reaction Mix to each well containing the Triglyceride Standard, samples and background control(s). Mix well. Incubate at room temperature for 30-60 min. (60 min. gives slightly better result) protect from light.

   ***Note:** For the fluorometric assay, use 0.4 µl/well of the Probe to decrease the background readings, therefore increase detection sensitivity.

5. **Measurement:** Measure absorbance at 570 nm for colorimetric assay or fluorescence at Ex/Em = 535/590 nm for fluorometric assay in a microtiter plate reader. The reaction is stable for at least two hr.

6. **Calculations:** Subtract 0 Standard reading from all readings. If sample background control reading is significant then subtract the sample background control reading from sample reading. Plot the TG Standard Curve. For unspiked samples, apply the corrected OD to the TG Standard Curve to get B nmol of TG in the sample well.

Sample TG concentration (C) = B/V X D nmol/µl or mM

Where: **B** is the amount of TG from Standard Curve (nmol)
V is the sample volume added into the reaction well (µl)
D is the sample dilution factor

Note: For spiked samples, correct for any sample interference by subtracting the sample reading from spiked sample reading.

For spiked samples, TG amount in sample well (B) = $\left(\frac{(\text{OD}_{\text{sample (corrected)}})}{(\text{OD}_{\text{sample + TG Std(corrected)}}) - (\text{OD}_{\text{sample(corrected)}})}\right) * TG\ Spike\ (\text{nmol})$

Triglyceride molecular weight: 885.4 g/mol

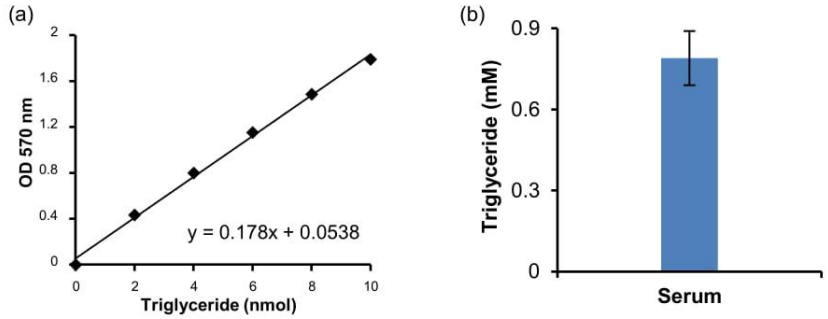


Figure: (a) Triglyceride Standard Curve. (b) Determination of Triglyceride in pooled normal human serum. Serum sample (3 µl) was spiked with a known amount of Triglyceride as internal Standard (4 nmol) and assayed according to the kit protocol. Calculated concentration of triglyceride: 0.79 ± 0.1 mM; (70 ± 8.8 mg/dl).

IX. RELATED PRODUCTS:

PicoProbe™ Triglyceride Quantification Kit (K614)
Cholesterol/Cholesteryl Ester Quantitation Kit (K603)
CETP Activity Fluorometric Assay Kit (K601)
PLTP Activity Fluorometric Assay Kit (K604)
Cholesterol/Cholesteryl Ester Quantitation Assay Kit II (K623)
HDL and LDL/VLDL Quantification Kit (K613)
CETP Inhibitor Drug Screening Kit (Fluorometric) (K602)
PLTP Inhibitor Drug Screening Kit (Fluorometric) (K605)

FOR RESEARCH USE ONLY! Not to be used on humans.

Study Outcomes

Co-Administration of Conjugated Linoleic Acid and Rosiglitazone Increases Atherogenic Co-Efficient and Alters Isoprenaline-Induced Vasodilatation in Rats Fed High Fat Diet

B. K. CHAI[1], Y. S. LAU[2], B. J. LOONG[1], M. M. RAIS[2], K. N. TING[1], D. M. DHARMANI[2], S. K. MOHANKUMAR[3]

[1]Department of Biomedical Sciences, Faculty of Science, University of Nottingham Malaysia Campus, Semenyih, Selangor, Malaysia, [2]Department of Pharmacology, Faculty of Medicine, University of Malaya, Kuala Lumpur, Malaysia, [3]TIFAC CORE in Herbal Drugs, JSS College of Pharmacy, Udhagamandalam, JSS Academy of Higher Education and Research, Mysuru, India

Received July 4, 2017
Accepted January 5, 2018
On-line May 5, 2018

Summary

The cis(c)-9, trans(t)-11 (c9,t11) and t10,c12 isomers of conjugated linoleic acid (CLA) have been reported as agonists of peroxisome proliferator-activated receptor (PPAR) and beneficial in lipidemia and glycemia. However, it is unclear whether CLA isomers enhance or antagonize effects of conventional drugs targeting PPAR. Male Sprague-Dawley rats were fed high fat diet (HFD) for 8 weeks and treated without or with CLA, rosiglitazone or both for 4 weeks. Oral glucose tolerance and surrogate markers of insulin resistance were not significantly different for all treatments compared to untreated normal diet (ND) or HFD group, except lipoprotein levels. The combination of CLA and rosiglitazone had suppressed levels of low and high density lipoproteins (46 % and 25 %, respectively), compared to HFD-alone. Conversely, the atherogenic co-efficient of the animals received HFD or HFD+rosiglitazone+CLA was 2-folds higher than ND, HFD+rosiglitazone or HFD+CLA. Isolated aortic rings from the combined CLA and rosiglitazone treated animals were less sensitive to isoprenaline-induced relaxation among endothelium-denuded aortas with a decreased efficacy and potency (R_{max}=53±4.7 %; pEC50=6±0.2) compared to endothelium-intact aortas (R_{max}=100±9.9 %; pEC50=7±0.2). Our findings illustrate that the combination of CLA and rosiglitazone precede the atherogenic state with impaired endothelium-independent vasodilatation before the onset of HFD-induced insulin resistance.

Key words

PPAR agonist • High fat diet • High density lipoprotein • Rosiglitazone • Atherogenic

Corresponding author

S. K. Mohankumar, TIFAC CORE Herbal Drugs JSS College of Pharmacy, Udhagamandalam – 643 001, Jagadguru Sri Shivrathreeshwara University, Mysuru, India. E-mail: suresh.jsscpo@jssuni.edu.in or mssureshkum@yahoo.com

Introduction

Type 2 diabetes mellitus (T2DM) is one of the major global health burdens and have reached worldwide epidemic. T2DM is accompanied by major hallmarks such as atherogenic dyslipidemia and endothelial dysfunction (Mooradian 2009, Bakker *et al.* 2009). Together, these hallmarks predispose T2DM patients to cardiovascular diseases. The current options available for treatment and management of T2DM are relatively limited, having problems with non-negligible side effects, and/or often require multiple combinations of drugs that mostly potentiate the adverse effects.

Thiazolidinediones (TZD) or glitazones are oral anti-hyperglycemic drugs commonly referred as "insulin sensitizers". The use of these glitazones, including rosiglitazone, have been cautioned for increased risk of cardiovascular diseases in T2DM patients (Hiatt *et al.*

© 2018 Institute of Physiology of the Czech Academy of Sciences, Prague, Czech Republic
Fax +420 241 062 164, e-mail: physres@fgu.cas.cz, www.biomed.cas.cz/physiolres

2013, Nissen and Wolski 2007, Nissen and Wolski 2010). This prompts the search for alternative drugs with a better clinical safety profile or suitable supplements to combat the adverse effects of TZD without altering its insulin sensitizing potential.

Conjugated linoleic acids (CLA) refer to a group of positional and geometric isomers of octadecadienoate (C18:2) with conjugated double bonds. Specifically two isomers of CLA, cis-9, trans-11 (c9,t11) and trans-10, cis-12 (t10,c12) isomers exist in abundance in dairy products and ruminant meats (Pariza *et al.* 1999) and garnered immense interest for their biological activity (Dilzer and Park 2012, Mohankumar *et al.* 2011, Shokryzadan *et al.* 2017, Taylor and Zahradka 2004). Unlike TZDs, dietary supplementation of CLA has been shown to promote weight loss in obese animals and weight gain in lean animals, prevent cardiac hypertrophy and blood pressure elevation in spontaneously hypertensive rats (Alibin *et al.* 2008, DeClercq *et al.* 2012b), and decrease LDL cholesterol in obese insulin-resistant rats and healthy human subjects (Derakhshande-Rishehri *et al.* 2015, Noone *et al.* 2002, Wanders *et al.* 2010). These distinct properties of CLA compared to TZDs suggest that there is a possibility that CLA may be used as an alternative supplement or substitute to combat the adverse effects of TZD.

In regards, a previous study conducted in mice fed a high fat diet demonstrated that supplementation with CLA prevented weight gain in rosiglitazone-treated mice without affecting the insulin sensitizing effects of rosiglitazone (Liu *et al.* 2007). However, it is not clear whether or not co-administration of CLA and TZD alter lipoproteins level and vascular functions. The present study therefore examined the effects of CLA isomers and rosiglitazone either alone or in combination on surrogate markers of insulin resistance, including lipoproteins, and on vascular contractility in rats fed high fat diet.

Methods

Chemicals

Rosiglitazone was purchased from LKT Laboratories (R5773), USA. Conjugated linoleic acid (1:1 ratio of c9,t11 and t10,c12) was purchased from Nu Chek Prep (UC-59-AX), USA. (R)-(–)-Phenylephrine hydrochloride and isoproterenol hydrochloride (isoprenaline) were purchased from Tocris Bioscience, UK.

Animals and diet

Thirty male Sprague-Dawley (SD) rats (6 weeks old) were received (Monash University Malaysia Campus, Malaysia) and acclimatized with normal rodent chow diet (Altromin, 1324, Germany) for two weeks. We selectively used male rats as they are known to be more susceptible to metabolic disorder than female rats and to avoid the estrous cycle mediated interference on metabolic parameters in female rats. The experimental protocol was approved by the Faculty of Medicine Institutional Animal Care and Use Committee, University of Malaya (Approval number: 2014-03-05/PHAR/R/DDM) and the Animal Welfare and Ethical Review Body, University of Nottingham. Food and water were provided *ad libitum*.

The rats were divided into groups fed with normal diet (ND; 4.10 % total energy from fat; 6 rats) and high fat diet (24 rats; 60 % total energy from fat; Research Diets, D12492, USA). After completion of 8 weeks of HFD feeding, rats were divided into the following groups and treated for 4 weeks: HFD control (HFD), HFD treated with rosiglitazone (HFD+RGZ), HFD treated with CLA (HFD+CLA) and HFD treated with rosiglitazone and CLA (HFD+RGZ+CLA). CLA was dissolved in 5 % w/w fat free milk and administered at 0.2 g per animal per day by oral gavage. The dose of CLA is based on the human consumption equivalent, which amounts to 1-2 % of dietary weight per day. On average, a rat consumes 20 g of food per day. With this assumption, we calculate that each rat should be given 0.2 g of CLA per day. The control rats received only 5 % w/w fat free milk. Rosiglitazone was administered daily by intraperitoneal injection at 2 mg/kg body weight and control rats received only saline injection. The dose of rosiglitazone is based on the previously published study (Zhao *et al.* 2012).

Body weight, feed intake and blood glucose (Accu-Check blood glucose monitor) were recorded weekly, except terminal blood glucose. A week before the sacrifice, rats were fasted overnight and undergone oral glucose tolerance test (OGTT) as previously described (Noto *et al.* 2006). At the end of the study, all rats were fasted overnight, asphyxiated with CO_2 and their blood and organs were collected. The blood samples were centrifuged at 2,000 rpm for 10 min and the serum separated were stored at -80 °C until further analyses. The thoracic aortas were isolated for vascular contractility studies.

Serum biochemical analysis

Terminal fasting blood samples were analyzed for glucose (Cayman, 10009582, Ann Arbor, MI, USA), total cholesterol (Cayman, 10007640, USA), total triglycerides (Zen-Bio, STG-1-NC, USA), high density lipoprotein (HDL) and LDL/vLDL (BioVision, K613-100, Milpitas, CA, USA) and insulin levels (Alpco Diagnostics, 80-INSRT-E01, Salem, NH, USA) according to manufacturer's instructions. The colorimetric and fluorimetric end points were measured in Varioskan Flash Multimode Reader (Thermo Scientific, USA).

In vitro organ bath experiments

This procedure was performed as previously described (Loong *et al.* 2015). Briefly, thoracic aortae were immediately excised and transferred into cold Krebs-Ringer bicarbonate solution upon sacrifice. In an aerated tissue bath, the aortic rings (4 mm) were left in the bath for 30 min to equilibrate before the application of 2 g weight tension. Endothelium denuded rings were prepared by gently rubbing the intimal surface using the blunt tip of stainless steel forceps. Successful denudation was confirmed if the tissue produced less than 30 % relaxation in the presence of $1x10^{-6}$ M carbachol in the pre-constricted rings. All aortic rings were pre-contracted to at least 70 % of maximal contraction with 0.1 μM phenylephrine before the addition of isoprenaline ($1x10^{-10}$ – $3x10^{-5}$ M). Maximal relaxation (R_{max}) and pEC50 values were calculated using Prism version 6.0 (GraphPad Software, USA) in which EC_{50} is the concentration of isoprenaline that produces 50 % of maximal relaxation and pEC_{50} is taken as the negative common logarithm of EC_{50}.

Calculations

Weekly energy intake was calculated with the following formula:

$$Energy\ intake\ (KJ\ g^{-1}) = \frac{Metabolisable\ energy\ per\ gram\ of\ food\ (KJ\ g^{-1}) \times Average\ food\ consumed\ per\ rat\ (g)}{Average\ body\ weight\ per\ rat\ (g)}$$

Homeostatic model assessment-insulin resistance (HOMA-IR) was calculated by taking the product of blood glucose in mg/dl and serum insulin in mU/l, divided by 405, as described previously (Mohankumar *et al.* 2013).

Lipoprotein ratios were obtained by using serum total, LDL and HDL cholesterol readings in mmol/l. Non-HDL cholesterol was calculated by subtracting HDL-cholesterol from total cholesterol (Martirosyan *et al.* 2007). Ratios of LDL:HDL, total cholesterol (TC):HDL and non-HDL:HDL were obtained.

Statistics

Results are shown as means ± standard error of the mean for the number of rats tested. Statistical analyses were performed using unpaired Student's t-test to compare two groups and one-way ANOVA with Tukey's *post hoc* tests to compare three or more groups. Repeated measure one-way ANOVA was performed for concentration-responses and time responses. Analyses were done on SPSS version 22 (IBM, USA) and graphics prepared using Prism version 6.0 (GraphPad Software, USA). A probability of less than 0.05 ($p<0.05$) was considered to be statistically significant. Diet specific differences were compared with ND and treatment specific differences were compared with HFD.

Results

Physical characteristics and energy intake

First, we analyzed the effect of diet and treatment on body weight, organ weight and food intake. From week 4 onwards, all groups fed high fat diet (HFD, HFD+RGZ, HFD+CLA, HFD+RGZ+CLA) were ~20 % heavier than normal diet (ND) (Fig. 1A). Organ weights were similar in all groups except fat pads including epididymal, perirenal and mesenteric fats, the weight of groups fed high fat diet were 1.3 to 2.7 folds higher than normal diet (Table 1). However, no treatment specific difference was observed ($p>0.05$). Energy intakes, in kilojoules measured weekly, were similar across all groups (Fig. 1B).

Blood glucose and insulin

Since hyperglycemia and insulin resistance are major hallmarks of T2DM and metabolic syndrome (Kaur 2014), we measured the fasting blood glucose and insulin levels to determine the effect of the diet and/or treatment of glycemia.

The fasting blood glucose levels were found to be similar across all groups (Fig. 2A). All rats were found to have similar glucose clearance with respect to OGTT (Fig. 2B). In addition, whilst rats belonging to

HFD+RGZ, HFD+CLA and HFD+CLA+RGZ groups geared towards improved insulin sensitivity as shown by homeostatic model assessment of insulin resistance (HOMA-IR) index (Fig. 2C), they were not statistically different from ND or HFD control groups.

Table 1. Effects of diet and treatment on organ weights.

	ND	HFD	HFD+RGZ	HFD+CLA	HFD+RGZ+CLA
Heart (g)	1.28 ± 0.07	1.47 ± 0.05	1.52 ± 0.10	1.51 ± 0.04	1.43 ± 0.04
Liver (g)	10.67 ± 0.06	10.33 ± 0.46	11.00 ± 0.11	11.19 ± 0.35	10.00 ± 0.66
Fat pads					
Epididymal fat (g)	4.24 ± 0.45	8.15 ± 0.96*	7.90 ± 0.14*	9.06 ± 0.99*	7.50 ± 0.97*
Perirenal fat (g)	3.8 ± 0.46	8.64 ± 1.4*	9.81 ± 1.16*	10.54 ± 0.89*	8.87 ± 1.20*
Mesenteric fat (g)	2.14 ± 0.26	3.39 ± 0.45*	3.78 ± 0.32*	3.60 ± 0.23*	2.92 ± 0.48*
Pancreas	1.03 ± 0.14	1.45 ± 0.18	1.30 ± 0.18	1.61 ± 0.15	1.50 ± 0.18
Kidneys					
Right kidney (g)	1.46 ± 0.11	1.54 ± 0.08	1.62 ± 0.13	1.69 ± 0.08	1.60 ± 0.06
Left kidney (g)	1.44 ± 0.11	1.50 ± 0.08	1.56 ± 0.14	1.67 ± 0.04	1.57 ± 0.08
Gastrocnemius muscle (g)	2.23 ± 0.36	2.33 ± 0.18	3.00 ± 0.50	2.21 ± 0.10	2.16 ± 0.16
Soleus muscle (g)	0.16 ± 0.01	0.20 ± 0.02	0.19 ± 0.01	0.20 ± 0.07	0.20 ± 0.02

Data were presented as mean ± SEM, n=6 for each group. *p<0.05 compared to ND.

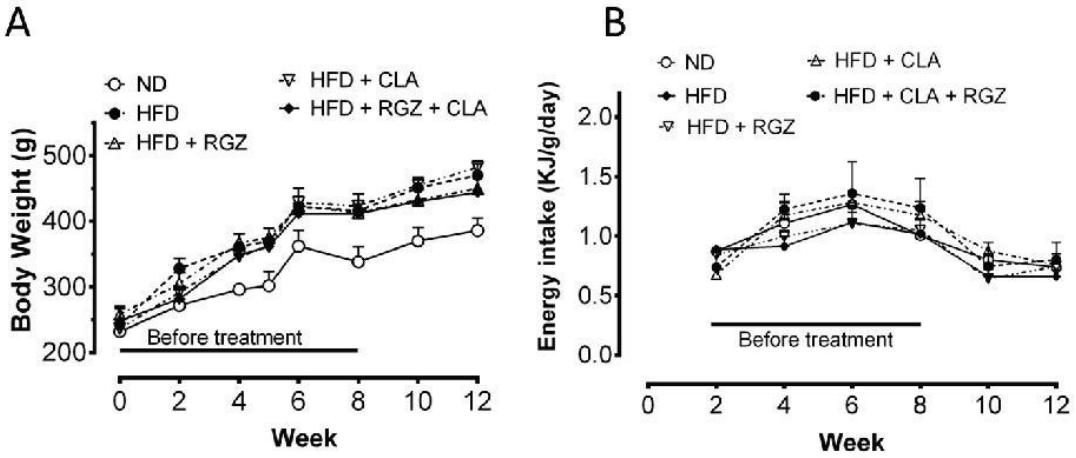


Fig. 1. Effect of diet and treatments on body weight and energy intake. (**A**) Body weight of Sprague-Dawley rats throughout the study. (**B**) Average energy intake of Sprague-Dawley rats throughout the study. Data is presented as mean ± SEM, n=6 in all groups. # p<0.05 compared to ND.

Serum lipoprotein levels and ratios

Atherogenic dyslipidemia is one of the critical metabolic characteristic of T2DM (Mooradian 2009), hence various serum lipid markers of dyslipidemia were measured. As depicted in Figures 3A and 3D, neither diet nor treatments have altered the serum TC and triglyceride levels. The serum LDL level was 46 % reduced in HFD+CLA+RGZ group in comparison to HFD alone (p<0.05, Fig. 3B). Conversely, animals from HFD, HFD+RGZ and HFD+CLA have shown 1.3 folds elevated levels of HDL compared to ND (p<0.05), whereas HFD+RGZ+CLA have 25 % suppressed serum HDL than HFD group and the level was similar to the level measured in ND group (Fig. 3C). A plethora of published studies reported that cholesterol ratios, especially LDL:HDL, TC:HDL and non-HDL:HDL ratios have been recognized as the critical markers of atherogenicity and are widely used to assess

cardiovascular risk (van Deventer *et al.* 2011, Hermans *et al.* 2007, Lu *et al.* 2003). As shown in Figures 4A and 4B, the TC:HDL and non-HDL:HDL ratios in the animals received HFD or HFD+RGZ+CLA was 2-folds higher than ND ($p<0.05$), whereas no significant changes observed for HFD+RGZ and HFD+CLA. Although the LDL:HDL ratio was lower in treatment groups (Fig. 4C), they were not significantly different compared to ND and HFD, respectively ($p>0.05$).

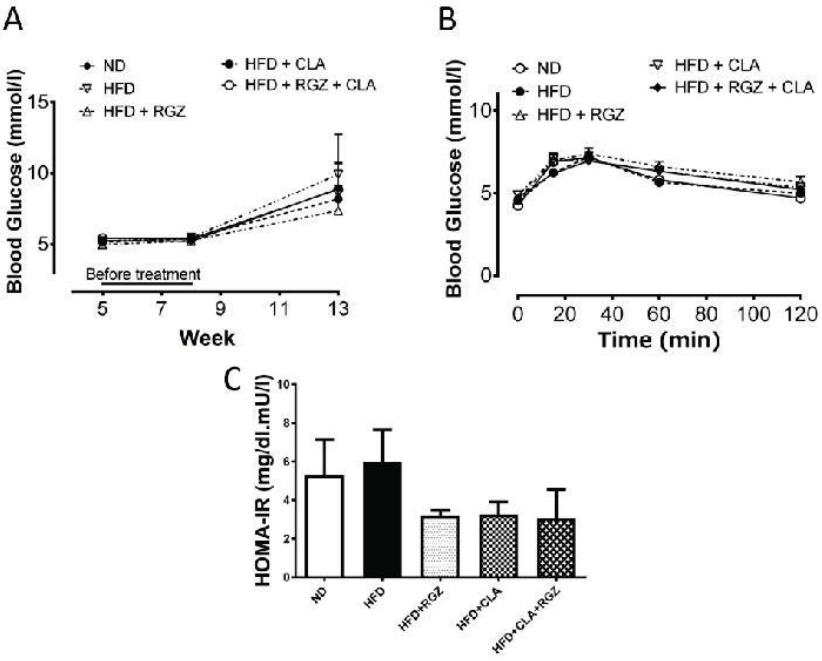


Fig. 2. Effect of diet and treatment on glycemia (**A**) Measurement of blood glucose level. Blood glucose on week 5 and week 8 measured using tail prick method; terminal blood glucose on week 13 measured using glucose assay kit. Data is presented as mean ± SEM, n=6 in all groups. (**B**) Oral glucose tolerance test (OGTT). A day before the 12 week, rats were fasted overnight before undergoing oral glucose tolerance test. (**C**) HOMA-IR of rats at termination. Data were presented as mean ± SEM, n=6 in all groups.

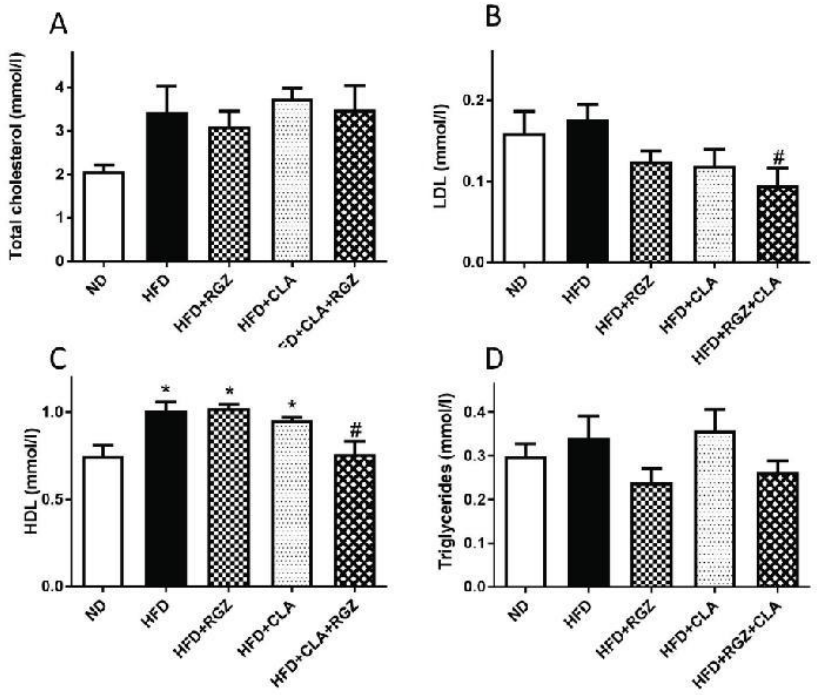


Fig. 3. Effect of diet and treatments on lipid profiles. (**A**) Total cholesterol. (**B**) LDL-cholesterol. (**C**) HDL-cholesterol. (**D**) Triglycerides. Data were presented as mean ± SEM, n=6 in all groups. * $p<0.05$ compared to ND. # $p<0.05$ compared to HFD.

Isoprenaline-induced vasorelaxation

A set of preliminary experiments were conducted to optimize the experimental conditions for isoprenaline-induced relaxation (data not shown). The degree of initial contraction induced by 0.1 μM phenylephrine for both control and treatment groups either without or with endothelium were not statistically significant ($p>0.05$; data not shown). A representative trace of isoprenaline-induced relaxation in aortic rings excised from SD rats fed normal rodent chow diet is shown in Figure 5A.

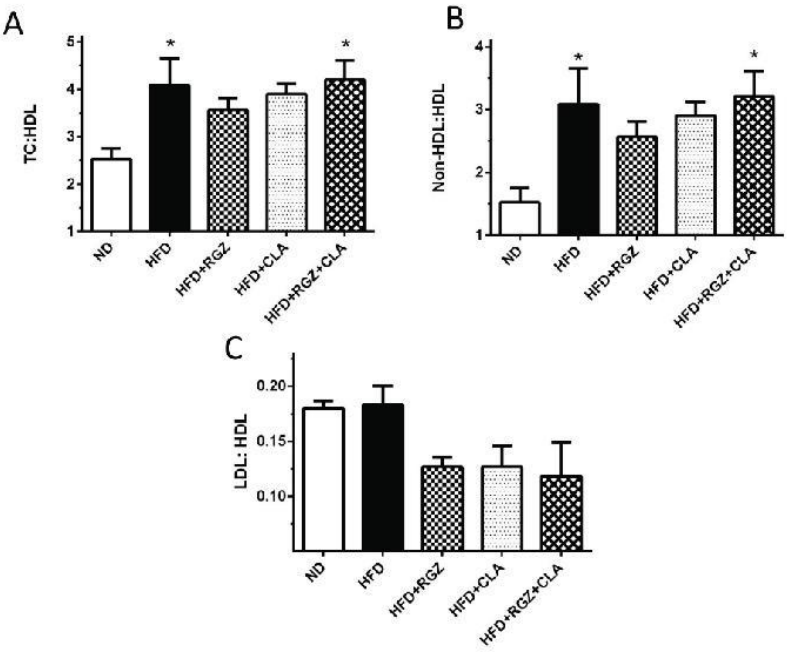


Fig. 4. Effect of diet and treatments on lipoprotein ratios. (**A**) TC:HDL ratio. (**B**) non-HDL:HDL ratio. (**C**) LDL:HDL ratio. Data were presented as mean ± SEM, n=6 for each group. *$p<0.05$ compared to ND.

The effect of diet and treatment on isoprenaline-induced vascular relaxation in isolated aortic rings excised from the rats was examined. The endothelial layer was removed on some of the aortic rings to check if the endothelium has been affected by the various treatments. All isolated aortic rings exhibited concentration-dependent vasodilatation in response to isoprenaline as the vasodilator. Repeated measures analysis indicated that the isoprenaline-induced vasorelaxation was significantly different between ND, HFD and HFD+RGZ+CLA regardless of endothelial presence (Figs 5B and 5C).

Among endothelium intact rings (Fig. 5B), all rings fed HFD, regardless of treatments were more responsive than ND. HFD+RGZ+CLA was the most responsive to isoprenaline. This was followed by HFD. The responsiveness of HFD+RGZ is intermediate of HFD and HFD+RGZ+CLA, while HFD+CLA is intermediate of HFD and ND. All groups exhibited similar pEC50 and R_{max} (Table 2 and Fig. 5B). However, the trend was reversed in endothelium denuded rings (Table 2 and Fig. 5C). Removal of endothelium worsened the isoprenaline-induced vasorelaxation in all HFD and treatment groups. The relaxation was severely affected in aortic rings obtained from HFD+RGZ+CLA treated animals (pEC50=6±0.2, R_{max}=53.6±4.7 %) compared to ND (pEC50=7±0.2, R_{max}=113±22 %). Likewise, aortic rings from both HFD and HFD+CLA had diminished response to isoprenaline compared to ND (pEC50=6.6±0.1, R_{max}=93±24.2 % and pEC50=6.4±0.4, R_{max}=77.70±22.8 %, respectively). Notably, the efficacy and potency of isoprenaline was significantly reduced in endothelium denuded aortic rings in comparison to endothelium intact aortic rings of HFD+RGZ+CLA treated rats (Endothelium intact: pEC50=7±0.2, R_{max}=100±9.9 % vs. endothelium denuded: pEC50=6±0.2, R_{max}=53±4.7 %) (Figs 5B and 5C), indicating the critical role of endothelium in protecting the PPAR agonists-mediated atherogenic risks.

Discussion

Our key findings of this study were that the co-administration of CLA and rosiglitazone to SD rats

fed HFD (60 % energy from fat) had elevated TC:HDL and non HDL:HDL ratio, suppressed LDL and HDL level, and a marked decrease in endothelium-independent aortic relaxation, suggesting that CLA and rosiglitazone precede the atherogenic state and impaired endothelium-independent vasodilatation despite the reduction of HFD-induced insulin resistance.

There have been previous efforts to examine feeding rosiglitazone and CLA alone in rodent models fed with HFD. Dietary supplementation with CLA for seven weeks, regardless of isomer composition, led to an improvement in glucose tolerance, insulin resistance and serum triglycerides (Choi *et al.* 2004). Likewise, treatment with rosiglitazone improved insulin sensitivity with a side effect of increasing serum LDL (Zhao *et al.* 2012). It is noteworthy that in this study SD rats were treated for four weeks to induce acute, instead of chronic effects as showed previously (Lessard *et al.* 2007, Murthy *et al.* 2005, Umrani *et al.* 2002). The onset of insulin resistance in animals can be influenced by a number of factors such as feeding period, type of fat in the diet and genotype of animals. We observed neither change in glucose tolerance nor obvious insulin resistance following 12 weeks of HFD. We reason that the rats used in our study possibly mimic the obesity resistant phenotype, since we did not observe significant impairments in glucose tolerance following HFD supplementation for 12 weeks, whilst rats gained marginal rise in body and fat pad weights compared to their normal diet counterparts (Dake and Oltman 2015).

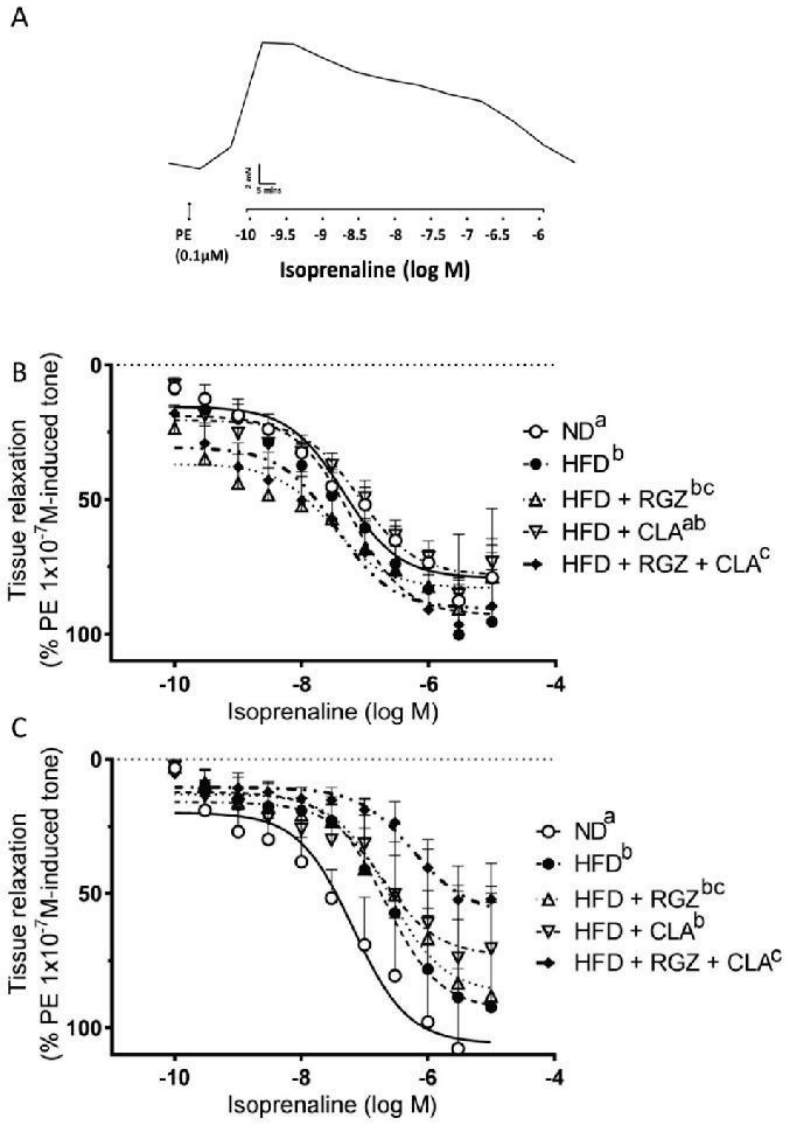


Fig. 5. Effect of diet and treatments on isoprenaline-induced aortic ring relaxation. (**A**) Representative trace of isoprenaline-induced aortic ring relaxation of normal SD rats. (**B**) Relaxation of endothelium-intact aortic rings. (**C**) Relaxation of endothelium-denuded aortic rings. Data were presented as mean ± SEM, n=4-6 for endothelium intact and n=3 for endothelium denuded. For B and C, statistical significance is indicated by letters next to the legends, groups having the same letter(s) are not significant from each other.

Table 2. pEC50 and maximal relaxation (R_{max}) of aortic rings isolated from rats.

	ND	HFD	HFD+RGZ	HFD+CLA	HFD+RGZ+CLA
pEC50 E+	7.414 ± 0.236	7.271 ± 0.239	7.979 ± 0.453	7.128 ± 0.2414	7.453 ± 0.2088
pEC50 E-	7.105 ± 0.176	6.600 ± 0.127	6.583 ± 0.375*	6.398 ± 0.3754	6.133 ± 0.231*
R_{max} E+ (% PE induced tone)	89.75 ± 6.95	102.50 ± 13.18	91.00 ± 12.02	85.93 ± 6.16	100.2 ± 9.92
R_{max} E- (% PE induced tone)	113.4 ± 22.45	93.19 ± 24.15	90.60 ± 29.71	77.70 ± 22.81	53.58 ± 4.68*

Data were presented as mean ± SEM. *p<0.05 compared to E+.

Alternatively, as observed in earlier studies (Pranprawit *et al.* 2013, Stark *et al.* 2000, Xu *et al.* 2010), the period of less than 12 weeks is too short to induce metabolic changes in obesity resistant rats. In contrast, Huang *et al.* (2004) reported reduction in glucose tolerance after 8 weeks of high fat diet feeding. It is apparent that no standardization of diet-induced obesity exists in literature despite using the common strain of SD rats. In a study that report the body weight reduction in SD rats with dietary supplementation of CLA, the animals have been fed with CLA from the beginning of the study together with HFD; moreover CLA elicits isomer-specific effects (Choi et al. 2004). Conversely, in another study dietary supplementation of CLA mixture for 6 weeks in rats showed no change in body weight (Moya-Camarena *et al.* 1999). Thus, our observation that the absence of weight reduction following oral administration of CLA mixture (0.2 g/day) for 4 weeks in SD rats pre fed with HFD for 8 weeks could be explained by the duration of CLA supplementation and isomer composition of CLA mixture.

Dyslipidemia is linked to vascular dysfunction in T2DM (Dixon *et al.* 1999). Generally, increased circulating concentration of HDL is associated with lowered risk of cardiovascular disease. HDL are lipoprotein particles that mediate reverse cholesterol transport (RCT) with apolipoprotein A as the major protein component. Beyond its role in RCT, HDL binds to scavenger receptor (SR)-B1 and SR-B2 and directly exerts vasoprotective effects on the endothelium (Calabresi 2003). As demonstrated previously by Hayek *et al.* (1993), the increase in HDL is typical in rodents fed HFD. Thus, the HDL rise in our study is possibly an adaptive response to maintain vascular tone to compensate the increased atherogenicity brought by HFD.

CLA are known to be weak PPARα agonists (Moya-Camarena *et al.* 1999). While studies of rosiglitazone and CLA are difficult to come by, our observation of HDL reduction in HFD+CLA+RGZ treated rats is in agreement with the previous observations in case reports (Im *et al.* 2010, Normen *et al.* 2004, Schwing *et al.* 2010) and a clinical trial (Linz *et al.* 2014) in which rosiglitazone and fenofibrate, a commonly prescribed PPARα agonist, were simultaneously administered to human patients. Whilst the biological actions of CLA on HDL and insulin sensitivity were complicated by isomer and composition dependence, our observation that a 1:1 mixture of c9,t11 and t10,c12-CLA increases HDL level is similar to a recent published study conducted in Wistar rats fed HFD (de Almeida *et al.* 2015). We have noted that HFD+RGZ+CLA brought about suppression of LDL and HDL without significant reduction in LDL:HDL ratio. Since fractions outside LDL and HDL are also involved in atherogenesis, we make use of the non-HDL:HDL ratio, also known as the atherogenic coefficient, that has been proposed to be better predictors of cardiovascular risks (Hermans *et al.* 2007, Kim *et al.* 2013). Another ratio, TC:HDL, is linked to non-HDL:HDL by a linear relationship. Both ratios were increased in HFD+RGZ+CLA group despite having similar HDL level with ND suggesting increased atherogenicity, that is corroborated with the decreased ability of aortic rings to respond to isoprenaline-mediated vasodilatation in HFD+RGZ+CLA treatment group.

It is well established that the changes in vascular function when fed an atherogenic diet precede the onset of insulin resistance and cardiovascular diseases. In agreement with these studies (Garcia-Prieto *et al.* 2015, Stark *et al.* 2000), we observed diminished endothelium-independent vasodilatation without significant changes in glycemia. The vascular endothelium forms the inner lining of blood vessels and plays important role in maintaining vessel physiology (Deanfield *et al.* 2007, Hadi *et al.* 2005). Under physiological conditions, blood vessels are kept quiescent and dilated by endothelial secretion such as nitric oxide (NO). However, endothelial denudation due to apoptotic loss of endothelium is known

to occur under the diabetic and insulin resistant state (Avogaro *et al.* 2011, Sena *et al.* 2013). The increased responsiveness in HFD-fed endothelium intact rings may be an acute adaptive response to high circulating lipoproteins. Similar observations were recorded in obese spontaneously hypertensive rats (Kagota *et al.* 2004).

Isoprenaline-induced vascular relaxation is dependent on β-adrenergic receptors present on both endothelium and vascular smooth muscle (VSM) (Akimoto *et al.* 2002). Endothelium independent relaxation of VSM is mediated by NO produced *in situ* (Bernhardt *et al.* 1991). Our observation of vascular impairment in rosiglitazone fed endothelium denuded rings agrees with a previous finding, which stemmed from the improvement in endothelial production of NO but impaired response of VSM in rats (Onuta *et al.* 2008). The decreased responsiveness of endothelium denuded rings can be explained by rosiglitazone, *via* PPARγ, induced upregulation of CD36 in the VSM (Ballesteros *et al.* 2014, Kleinhenz *et al.* 2015), as CD36 is responsive to LDL and lead to inhibition of cGMP synthesis in the VSM (Isenberg *et al.* 2009). Conversely, it has been reported that t10,c12-CLA increases NO formation in human endothelium (DeClercq *et al.* 2012a), nonetheless our observations warrant further studies to elucidate the precise mechanisms by which CLA modulate endothelium-independent relaxation.

The ability of aorta to constrict in obesity has been shown to be impaired due to many factors, including overnutrition of dietary fats (Stapleton *et al.* 2008). It has been previously reported that under certain environmental stressors, including HFD, the VSM cells tends to lose its contractile ability due to the remodeling of VSM into synthetic phenotype (Beamish *et al.* 2010). Watts *et al.* (2012) have demonstrated the impairments in phenylephrine-mediated contraction in aorta excised from SD rats fed HFD for 17 weeks. Conversely, we observed no differences with phenylephrine-induced contraction in both control and HFD diet groups. Whilst we reason that the differences could be due to the duration of HFD feeding, proportion of HFD and age of rats, the impairment in contractile ability of VSM in rodents fed HFD was shown to be more prominent in small mesenteric arteries than the thoracic aorta (Soares *et al.* 2017).

In summary, while glucose tolerance and HOMA-IR may be unchanged, simultaneous administration of CLA and rosiglitazone led to increase in atherogenic coefficient. The increase in atherogenicity is coupled with vascular resistance in the context of endothelial loss. This observation hints the complex interplay between nutrient-drug interactions and warrants further investigation on their molecular mechanisms. Whilst it is believed that the use of normal rodent phenotype is limited in studying lipoprotein metabolism due to higher level of circulating HDL compared to humans, our observations, the linkage of cholesterol ratios and vascular resistance in SD rats fed HFD provides a reasonable basis for revisiting the lipoprotein dynamics in rodents.

Conflict of Interest

There is no conflict of interest.

Acknowledgements

We thank Ms. Ling Wei Chih for her help with animal care. We thank Ms. Akila Raghavan for analyzing blood glucose and total cholesterol. We would like to acknowledge the generous infrastructure provided by University of Nottingham Malaysia Campus (UNMC) and University of Malaya. This research was supported by UNMC Pump Priming grant and the Fundamental Research Grant Scheme from the Ministry of Higher Education, Malaysia (grant number: 64924).

References

AKIMOTO Y, HORINOUCHI T, SHIBANO M, MATSUSHITA M, YAMASHITA Y, OKAMOTO T, YAMAKI F, TANAKA Y, KOIKE K: Nitric oxide (NO) primarily accounts for endothelium-dependent component of beta-adrenoceptor-activated smooth muscle relaxation of mouse aorta in response to isoprenaline. *J Smooth Muscle Res* **38**: 87-99, 2002.

ALIBIN CP, KOPILAS MA, ANDERSON HD: Suppression of cardiac myocyte hypertrophy by conjugated linoleic acid: role of peroxisome proliferator-activated receptors alpha and gamma. *J Biol Chem* **283**: 10707-10715, 2008.

AVOGARO A, ALBIERO M, MENEGAZZO L, DE KREUTZENBERG S, FADINI GP: Endothelial dysfunction in diabetes: The role of reparatory mechanisms. *Diabetes Care* **34** (Suppl 2): S285-S290, 2011.

BAKKER W, ERINGA EC, SIPKEMA P, VAN HINSBERGH VW: Endothelial dysfunction and diabetes: roles of hyperglycemia, impaired insulin signaling and obesity. *Cell Tissue Res* **335**: 165-189, 2009.

BALLESTEROS I, CUARTERO MI, PRADILLO JM, DE LA PARRA J, PÉREZ-RUIZ A, CORBÍ A, RICOTE M, HAMILTON J A, SOBRADO M, VIVANCOS J, NOMBELA F, LIZASOAIN I, MORO MA: Rosiglitazone-induced CD36 up-regulation resolves inflammation by PPARγ and 5-LO-dependent pathways. *J Leukoc Biol* **95**: 587-598, 2014.

BEAMISH JA, HE P, KOTTKE-MARCHANT K, MARCHANT RE: Molecular regulation of contractile smooth muscle cell phenotype: implications for vascular tissue engineering. *Tissue Eng Part B Rev* **16**: 467-491, 2010.

BERNHARDT J, TSCHUDI MR, DOHI Y, GUT I, URWYLER B, BÜHLER FR, LÜSCHER TF: Release of nitric oxide from human vascular smooth muscle cells. *Biochem Biophys Res Commun* **180**: 907-912, 1991.

CALABRESI L: Endothelial protection by high-density lipoproteins: from bench to bedside. *Arterioscler Thromb Vasc Biol* **23**: 1724-1731, 2003.

CHOI JS, JUNG MH, PARK HS, SONG J: Effect of conjugated linoleic acid isomers on insulin resistance and mRNA levels of genes regulating energy metabolism in high-fat-fed rats. *Nutrition* **20**: 1008-1017, 2004.

DAKE BL, OLTMAN CL: Cardiovascular, metabolic, and coronary dysfunction in high-fat-fed obesity-resistant/prone rats. *Obesity* **23**: 623-629, 2015.

DE ALMEIDA MM, DE SOUZA YO, DUTRA LUQUETTI SC, SABARENSE CM, DO AMARAL CORRÊA JO, DA CONCEIÇÃO EP, LISBOA PC, DE MOURA EG, ANDRADE SOARES SM, MOURA GUALBERTO AC, GAMEIRO J, DA GAMA MA, FERRAZ LOPES FC, GONZÁLEZ GARCIA RM: Cis-9, trans-11 and trans-10, cis-12 CLA mixture does not change body composition, induces insulin resistance and increases serum HDL cholesterol level in rats. *J Oleo Sci* **64**: 539-551, 2015.

DEANFIELD JE, HALCOX JP, RABELINK TJ: Endothelial function and dysfunction: testing and clinical relevance. *Circulation* **115**: 1285-1295, 2007.

DECLERCQ V, TAYLOR CG, WIGLE J, WRIGHT B, TWOREK L, ZAHRADKA P: Conjugated linoleic acid improves blood pressure by increasing adiponectin and endothelial nitric oxide synthase activity. *J Nutr Biochem* **23**: 487-493, 2012a.

DECLERCQ V, TAYLOR CG, ZAHRADKA P: Isomer-specific effects of conjugated linoleic acid on blood pressure, adipocyte size and function. *Br J Nutr* **107**: 1413-1421, 2012b.

DERAKHSHANDE-RISHEHRI SM, MANSOURIAN M, KELISHADI R, HEIDARI-BENI M: Association of foods enriched in conjugated linoleic acid (CLA) and CLA supplements with lipid profile in human studies: a systematic review and meta-analysis. *Public Health Nutr* **18**: 2041-2054, 2015.

DILZER A, PARK Y: Implication of conjugated linoleic acid (CLA) in human health. *Crit Rev Food Sci Nutr* **52**: 488-513, 2012.

DIXON JL, STOOPS JD, PARKER JL, LAUGHLIN MH, WEISMAN GA, STUREK M: Dyslipidemia and vascular dysfunction in diabetic pigs fed an atherogenic diet. *Arterioscler Thromb Vasc Biol* **19**: 2981-2992, 1999.

GARCÍA-PRIETO CF, HERNÁNDEZ-NUÑO F, RIO DD, RUIZ-HURTADO G, ARÁNGUEZ I, RUIZ-GAYO M, SOMOZA B, FERNÁNDEZ-ALFONSO MS: High-fat diet induces endothelial dysfunction through a down-regulation of the endothelial AMPK-PI3K-Akt-eNOS pathway. *Mol Nutr Food Res* **59**: 520-532, 2015.

HADI HA, CARR CS, AL SUWAIDI J: Endothelial dysfunction: cardiovascular risk factors, therapy, and outcome. *Vasc Health Risk Manag* **1**: 183-198, 2005.

HAYEK T, ITO Y, AZROLAN N, VERDERY RB, AALTO-SETÄLÄ K, WALSH A, BRESLOW JL: Dietary fat increases high density lipoprotein (HDL) levels both by increasing the transport rates and decreasing the fractional catabolic rates of HDL cholesterol ester and apolipoprotein (Apo) A-I. Presentation of a new animal model and mechanistic stud. *J Clin Invest* **91**: 1665-1671, 1993.

HERMANS MP, AHN SA, ROUSSEAU MF: The non-HDL-C/HDL-C ratio provides cardiovascular risk stratification similar to the ApoB/ApoA1 ratio in diabetics: comparison with reference lipid markers. *Diabetes Metab Syndr Clin Res Rev* **1**: 23-28, 2007.

HIATT WR, KAUL S, SMITH RJ: The cardiovascular safety of diabetes drugs--insights from the rosiglitazone experience. *N Engl J Med* **369**: 1287-1289, 2013.

HUANG BW, CHIANG MT, YAO HT, CHIANG W: The effect of high-fat and high-fructose diets on glucose tolerance and plasma lipid and leptin levels in rats. *Diabetes Obes Metab* **6**: 120-126, 2004.

IM M, KIM M, LEE JK, CHANG YH, LEE DY, HONG S-I, LEE YY, HONG YJ: HDL cholesterol reduction during rosiglitazone and fenofibrate treatment in a type 2 diabetes mellitus patient with dyslipidemia (in Korean). *Korean J Lab Med* **30**: 17-19, 2010.

ISENBERG JS, MARTIN-MANSO G, MAXHIMER JB, ROBERTS DD: Regulation of nitric oxide signalling by thrombospondin 1: implications for anti-angiogenic therapies. *Nat Rev Cancer* **9**: 182-194, 2009.

KAGOTA S, TANAKA N, KUBOTA Y, YAMAGUCHI Y, NAKAMURA K, KUNITOMO M, SHINOZUKA K: Characteristics of vasorelaxation responses in a rat model of metabolic syndrome. *Clin Exp Pharmacol Physiol* **31** (Suppl 2): S54-S56, 2004.

KAUR J: A comprehensive review on metabolic syndrome. *Cardiol Res Pract* **2014**: 943162, 2014.

KIM SW, JEE JH, KIM HJ, JIN SM, SUH S, BAE JC, KIM SW, CHUNG JH, MIN YK, LEE MS, LEE MK, KIM KW, KIM JH: Non-HDL-cholesterol/HDL-cholesterol is a better predictor of metabolic syndrome and insulin resistance than apolipoprotein B/apolipoprotein A1. *Int J Cardiol* **168**: 2678-2683, 2013.

KLEINHENZ JM, MURPHY TC, POKUTTA-PASKALEVA AP, GLEASON RL, LYLE AN, TAYLOR WR, BLOUNT MA, CHENG J, YANG Q, SUTLIFF RL, HART CM: Smooth muscle-targeted overexpression of peroxisome proliferator activated receptor-γ disrupts vascular wall structure and function. *PLoS One* **10**: 1-25, 2015.

LESSARD SJ, RIVAS DA, CHEN ZP, BONEN A, FEBBRAIO MA, REEDER DW, KEMP BE, YASPELKIS BB, HAWLEY JA: Tissue-specific effects of rosiglitazone and exercise in the treatment of lipid-induced insulin resistance. *Diabetes* **56**: 1856-1864, 2007.

LINZ PE, LOVATO LC, BYINGTON RP, O'CONNOR PJ, LEITER LA, WEISS D, FORCE RW, CROUSE JR, ISMAIL-BEIGI F, SIMMONS DL, PAPADEMETRIOU V, GINSBERG HN, ELAM MB: Paradoxical reduction in HDL-C with fenofibrate and thiazolidinedione therapy in type 2 diabetes: the ACCORD lipid trial. *Diabetes Care* **37**: 686-693, 2014.

LIU LF, PURUSHOTHAM A, WENDEL AA, BELURY MA: Combined effects of rosiglitazone and conjugated linoleic acid on adiposity, insulin sensitivity, and hepatic steatosis in high-fat-fed mice. *Am J Physiol Gastrointest Liver Physiol* **292**: G1671-G1682, 2007.

LOONG BJ, TAN JH, LIM KH, MBAKI Y, TING KN: Contractile function of smooth muscle retained after overnight storage. *Naunyn Schmiedebergs Arch Pharmacol* **388**: 1061-1067, 2015.

LU W, RESNICK HE, JABLONSKI KA, JONES KL, JAIN AK, HOWARD WJ, ROBBINS DC, HOWARD BV: Non-HDL cholesterol as a predictor of cardiovascular disease in type 2 diabetes: the strong heart study. *Diabetes Care* **26**: 16-23, 2003.

MARTIROSYAN DM, MIROSHNICHENKO LA, KULAKOVA SN, POGOJEVA AV, ZOLOEDOV VI: Amaranth oil application for coronary heart disease and hypertension. *Lipids Health Dis* **6**: 1, 2007.

MOHANKUMAR SK, ZAHRADKA P, TAYLOR C: Does conjugated linoleic acid boost or battle metabolic syndrome? *Clin Lipidol* **6**: 501-505, 2011.

MOHANKUMAR SK, HANKE D, SIEMENS L, CATTINI A, ENNS J, SHEN J, REANEY M, ZAHRADKA P, TAYLOR CG: Dietary supplementation of trans-11-vaccenic acid reduces adipocyte size but neither aggravates nor attenuates obesity-mediated metabolic abnormalities in fa/fa Zucker rats. *Br J Nutr* **109**: 1628-1636, 2013.

MOORADIAN A: Dyslipidemia in type 2 diabetes mellitus. *Nat Clin Pract Endocrinol Metab* **5**: 150-159, 2009.

MOYA-CAMARENA SY, VANDEN HEUVEL JP, BLANCHARD SG, LEESNITZER LA, BELURY MA: Conjugated linoleic acid is a potent naturally occurring ligand and activator of PPARalpha. *J Lipid Res* **40**: 1426-1433, 1999.

MURTHY SN, OBREGON DF, CHATTERGOON NN, FONSECA NA, MONDAL D, DUNNE JB, DIEZ JG, JETER JR JR, KADOWITZ PJ, AGRAWAL KC, MCNAMARA DB, FONSECA VA: Rosiglitazone reduces serum homocysteine levels, smooth muscle proliferation, and intimal hyperplasia in Sprague-Dawley rats fed a high methionine diet. *Metabolism* **54**: 645-652, 2005.

NISSEN SE, WOLSKI K: Effect of rosiglitazone on the risk of myocardial infarction and death from cardiovascular causes. *N Engl J Med* **356**: 2457-2471, 2007.

NISSEN SE, WOLSKI K: Rosiglitazone revisited: an updated meta-analysis of risk for myocardial infarction and cardiovascular mortality. *Arch Intern Med* **170**: 1191-1201, 2010.

NOONE EJ, ROCHE HM, NUGENT AP, GIBNEY MJ: The effect of dietary supplementation using isomeric blends of conjugated linoleic acid on lipid metabolism in healthy human subjects. *Br J Nutr* **88**: 243-251, 2002.

NORMEN L, FROHLICH J, MONTANER J, HARRIS M, ELLIOTT T, BONDY G: Combination therapy with fenofibrate and rosiglitazone paradoxically lowers serum HDL cholesterol. *Diabetes Care* **27**: 2241-2242, 2004.

NOTO A, ZAHRADKA P, YURKOVA N, XIE X, NITSCHMANN E, OGBORN M, TAYLOR CG: Conjugated linoleic acid reduces hepatic steatosis, improves liver function, and favorably modifies lipid metabolism in obese insulin-resistant rats. *Lipids* **41**: 179-188, 2006.

ONUTA G, HILLEBRANDS JL, RIENSTRA H, BOER MW, KLATTER FA, NAVIS G, ROZING J, ROKS AJ: Dichotomous effects of rosiglitazone in transplantation-induced systemic vasodilator dysfunction in rats. *Transplantation* **85**: 582-588, 2008.

PARIZA MW, PARK Y, COOK ME: Conjugated linoleic acid and the control of cancer and obesity. *Toxicol Sci* **52**: 107-110, 1999.

PRANPRAWIT A, WOLBER FM, HEYES JA, MOLAN AL, KRUGER MC: Short-term and long-term effects of excessive consumption of saturated fats and/or sucrose on metabolic variables in Sprague Dawley rats: a pilot study. *J Sci Food Agric* **93**: 3191-3197, 2013.

SCHWING W, HUSTAK L, TAYLOR H: Paradoxical severe decrease in high-density lipoprotein cholesterol due to rosiglitazone-fenofibrate interaction. *Endocr Pract* **16**: 382-388, 2010.

SENA CM, PEREIRA AM, SEIÇA R: Endothelial dysfunction - a major mediator of diabetic vascular disease. *Biochim Biophys Acta* **1832**: 2216-2231, 2013.

SHOKRYZADAN P, RAJION MA, MENG GY, BOO LJ, EBRAHIMI M, ROYAN M, SAHEBI M, AZIZI P, ABIRI R, JAHROMI MF: Conjugated linoleic acid: a potent fatty acid linked to animal and human health. *Crit Rev Food Sci Nutr* **57**: 2737-2748, 2017.

SOARES AG, DE CARVALHO MHC, AKAMINE E: Obesity induces artery-specific alterations: evaluation of vascular function and inflammatory and smooth muscle phenotypic markers. *Biomed Res Int* **2017**: 5038602, 2017.

STAPLETON PA, JAMES ME, GOODWILL AG, FRISBEE JC: Obesity and vascular dysfunction. *Pathophysiology* **15**: 79-89, 2008.

STARK AH, TIMAR B, MADAR Z: Adaptation of Sprague Dawley rats to long-term feeding of high fat or high fructose diets. *Eur J Nutr* **39**: 229-234, 2000.

TAYLOR CG, ZAHRADKA P: Dietary conjugated linoleic acid and insulin sensitivity and resistance in rodent models. *Am J Clin Nutr* **79** (6 Suppl): 1164S-1168S, 2004.

UMRANI DN, BANDAY AA, HUSSAIN T, LOKHANDWALA MF: Rosiglitazone treatment restores renal dopamine receptor function in obese Zucker rats. *Hypertension* **40**: 880-885, 2002.

VAN DEVENTER HE, MILLER WG, MYERS GL, SAKURABAYASHI I, BACHMANN LM, CAUDILL SP, DZIEKONSKI A, EDWARDS S, KIMBERLY MM, KORZUN WJ, LEARY ET, NAKAJIMA K, NAKAMURA M, SHAMBUREK RD, VETROVEC GW, WARNICK GR, REMALEY AT: Non-HDL cholesterol shows improved accuracy for cardiovascular risk score classification compared to direct or calculated LDL cholesterol in a dyslipidemic population. *Clin Chem* **57**: 490-501, 2011.

WANDERS AJ, BROUWER IA, SIEBELINK E, KATAN MB: Effect of a high intake of conjugated linoleic acid on lipoprotein levels in healthy human subjects. *PLoS One* **5**: e9000, 2010.

WATTS SW, MCCLAIN JL, DORRANCE AM: Perivascular fat impairs contraction in aorta from obese but not lean adult rats. *FASEB J* **26** (Suppl 1): 1115.4, 2012.

XU ZJ, FAN JG, DING XD, QIAO L, WANG GL: Characterization of high-fat, diet-induced, non-alcoholic steatohepatitis with fibrosis in rats. *Dig Dis Sci* **55**: 931-940, 2010.

ZHAO D, MCCULLY BH, BROOKS VL: Rosiglitazone improves insulin sensitivity and baroreflex gain in rats with diet-induced obesity. *J Pharmacol Exp Ther* **343**: 206-213, 2012.

Lipids (2019)
DOI 10.1002/lipd.12154

ORIGINAL ARTICLE

Cis-9, *Trans*-11 Conjugated Linoleic Acid Reduces Phosphoenolpyruvate Carboxykinase Expression and Hepatic Glucose Production in HepG2 Cells

Boon Kheng Chai[1] · Mustafa Al-Shagga[1] · Yan Pan[1] · Sue-Mian Then[1] · Kang Nee Ting[1] · Hwei-San Loh[2] · Suresh K. Mohankumar[3]

Received: 15 November 2018 / Revised: 23 April 2019 / Accepted: 24 April 2019
© 2019 AOCS

Abstract Dysregulated hepatic gluconeogenesis is a hallmark of insulin resistance and type 2 diabetes mellitus (T2DM). Although existing drugs have been proven to improve gluconeogenesis, achieving this objective with functional food is of interest, especially using conjugated linoleic acid (CLA) found in dairy products. Both *cis*-9, *trans*-11 (c9,t11) and *trans*-10, *cis*-12 (t10,c12) isomers of CLA were tested in human (HepG2) and rat (H4IIE) hepatocytes for their potential effects on gluconeogenesis. The hepatocytes exposed for 24 h with 20 μM of c9,t11-CLA had attenuated the gluconeogenesis in both HepG2 and H4IIE by 62.5% and 80.1%, respectively. In contrast, t10,c12-CLA had no effect. Of note, in HepG2 cells, the exposure of c9,t11-CLA decreased the transcription of gluconeogenic enzymes, cytosolic phosphoenolpyruvate carboxykinase (*PCK1*) by 87.7%, and glucose-6-phosphatase catalytic subunit (*G6PC*) by 38.0%, while t10,c12-CLA increased the expression of *G6PC*, suggesting the isomer-specific effects of CLA on hepatic glucose production. In HepG2, the peroxisome proliferator-activated receptor (PPAR) agonist, rosiglitazone, reduced the glucose production by 72.9%. However, co-administration of c9,t11-CLA and rosiglitazone neither exacerbated nor attenuated the efficacy of rosiglitazone to inhibit glucose production; meanwhile, t10,c12-CLA abrogated the efficacy of rosiglitazone. Paradoxically, PPARγ antagonist GW 9662 also led to 70.2% reduction of glucose production and near undetectable *PCK1* expression by abrogating CLA actions. Together, while the precise mechanisms by which CLA isomers modulate hepatic gluconeogenesis directly or *via* PPAR warrant further investigation, our findings establish that c9,t11-CLA suppresses gluconeogenesis by decreasing PEPCK on hepatocytes.

Keywords Conjugated linoleic acid · Gluconeogenesis · Glucose-6-phosphatase · Phosphoenolpyruvate carboxykinase · Rosiglitazone

Lipids (2019).

Supporting information Additional supporting information may be found online in the Supporting Information section at the end of the article.

✉ Suresh K. Mohankumar
suresh.jsscpo@jssuni.edu.in

[1] Department of Biomedical Sciences, Faculty of Science, University of Nottingham Malaysia Campus, Jalan Broga, 43500, Semenyih, Selangor Darul Ehsan, Malaysia

[2] School of Biosciences, Faculty of Science, University of Nottingham Malaysia Campus, Jalan Broga, 43500, Semenyih, Selangor Darul Ehsan, Malaysia

[3] TIFAC CORE in Herbal Drugs, Department of Pharmacognosy, JSS College of Pharmacy (Ooty), JSS Academy of Higher Education & Research, Rocklands, Udhagamandalam, 643001, Tamil Nadu, India

Abbreviations

ATCC	American Type Culture Collection
CLA	conjugated linoleic acid
DMEM	Dulbecco's modified Eagle's medium
DMSO	dimethyl sulfoxide
G6PC	glucose-6-phosphatase catalytic
HGP	hepatic glucose production
LDL	low density lipoprotein
LNA	linoleic acid
MTT	3-[4-5-dimethylthiazol-2-yl]-2-5-diphenyl tetrazolium bromide
PBS	phosphate buffer saline

PCK1	cytosolic phosphoenolpyruvate carboxykinase
PEPCK	phosphoenolpyruvate carboxykinase
PPAR	peroxisome proliferator-activated receptor
RT-qPCR	reverse-transcription quantitative polymerase chain reaction
SEM	standard error of mean
T2DM	type 2 diabetes mellitus

Introduction

Milk and dairy products are generally regarded worldwide as the key sources of vital nutrients for maintaining health (Givens, 2018). Regular consumption of dairy products has been demonstrated to lower the incidence of many chronic diseases including metabolic and vascular diseases (Rice, 2014; Shin et al., 2017). Consequently, there is spurring interest in unleashing the nutritional value and molecular mechanism by which the constituents of dairy food elicit health benefits. In this regard, one of the nutrients in the dairy product that have gained enormous attention for its beneficial effects on metabolic and vascular diseases is conjugated linoleic acid (CLA) (Benjamin and Spener, 2009; Dilzer and Park, 2012; Fuke and Nornberg, 2017; Kim et al., 2016).

CLA are conjugated octadecadienoate (18:2, n-7) with conjugated double bonds. CLA is synthesized by the action of Δ^9-desaturase in ruminants (Griinari et al., 2000; Kay et al., 2004) and can be enriched in milk by increasing the amount of linoleic acid (LNA) in animal feed (Kelly et al., 1998). The *cis-9*, *trans-11* (c9,t11) is the isomer with the highest natural abundance (Bhattacharya et al., 2006; Churruca et al., 2008), whereas the *trans-10*, *cis-12* (t10,c12) isomer occurs in low amounts (Bhattacharya et al., 2006; Dilzer and Park, 2012). Commercial preparations of CLA result in equal amounts of c9,t11 and t10,c12 isomers (Kramer et al., 2004), which are known as CLA mixture or 50:50 CLA.

CLA treatment has been shown to promote weight loss in obese animals (Houseknecht et al., 1998), prevent cardiac hypertrophy and blood pressure elevation in spontaneously hypertensive rats (Alibin et al., 2008), and decrease low-density lipoprotein (LDL) cholesterol in obese insulin-resistant rats (Noto et al., 2006) and healthy human subjects (Noone et al., 2002). These distinct properties of CLA suggest that CLA exert insulin-like effects and could modulate the central regulation glucose and lipid homeostasis. Despite the compelling evidence that indicates CLA mimics the properties of insulin in a number of tissues involved in glucose and lipid metabolism including skeletal muscle (Mohankumar et al., 2012, 2013) and adipose tissue (DeClercq et al., 2012), there is insufficient information to delineate the molecular mechanism of CLA in liver.

The liver plays a central role in blood glucose homeostasis by regulating glycogenolysis, breakdown of glycogen into glucose and gluconeogenesis, and endogenous synthesis of glucose from substrates including lactate, pyruvate, glycerol, and alanine.

Gluconeogenesis is strictly regulated by insulin. The rise in glucose levels triggers an insulin response to control the blood glucose levels in the 4-10 mmol/L range. Insulin inhibits the transcription of the gene-encoding phosphoenolpyruvate carboxykinase (PEPCK), the rate-limiting step of gluconeogenesis (Girard, 2006a). In addition, insulin decreases the transcription of gene-encoding glucose-6-phosphatase (G6P/*G6PC*) but increases transcription of glycolytic enzymes such as glucokinase and pyruvate kinase (Dentin et al., 2007).

In type 2 diabetes mellitus (T2DM), the rate of gluconeogenesis is substantially elevated, which results in an excess production of glucose in liver leading to hyperglycemia (Boden et al., 2001). Currently, it is unclear whether the uncontrolled increase in hepatic glucose production (HGP) is due to the direct or indirect effects of insulin. The direct effect is caused by the interaction of hepatic sinusoidal insulin with the hepatocyte insulin receptor (Gupta, 2006), while the indirect effect is due to the insulin action on muscle and adipose tissue to decrease the availability of glucogenic precursors (Girard, 2006b). Given the hyperglycemia due to elevated glycogenolysis is negligible compared to gluconeogenesis in T2DM (Girard, 2006a; Hundal et al., 2000), therapeutic approaches focused on combating dysregulated gluconeogenesis in T2DM could have a potential role in future treatment and management of metabolic diseases (Giralt et al., 2018). Thus, it will be of great nutritional value if we could use the components from dairy food to modulate the gluconeogenesis process. Of note, published studies using CLA mixtures have shown the effectiveness in reducing hepatic gluconeogenesis (Cantwell et al., 1999; Conde-Aguilera et al., 2012). However, to our knowledge, no study has reported the direct effects and molecular dynamics of pure isomers of CLA on gluconeogenesis in hepatocytes. In this study, we tested the cellular effects of two common CLA isomers, c9,t11-CLA and t10,c12-CLA, on gluconeogenesis by hepatocytes.

Materials and Methods

Cell Culture and Treatments

The following liver cells, HepG2 (ATCC® HB 8065™) and H4IIE (ATCC®CRL1548™), were obtained from the American Type Culture Collection (ATCC, Manassas, VA 20110, USA). Cells were cultured in α-MEM (Nacalai Tesque, #21445-95, Japan) supplemented with 10% fetal

bovine serum (Sigma, SIG#F7524, USA) and 100 U/mL Penicillin–Streptomycin (Nacalai Tesque, #26253-84, Japan). The cells were grown in a 75 mL flask (SPL Life Sciences, SPL#70075, South Korea) and maintained in the incubator at 37°C, 5% CO_2 (ESCO, CCL-170B-8, Singapore). The growth media were refreshed every 2–3 days. Upon reaching 80–90% confluence, the cells were passaged. Briefly, the cultured cells were washed with 2 mL of phosphate buffer saline to remove the dead cells and serum. The cells were then incubated for 5–10 min with 2 mL of 0.5% Trypsin–EDTA (Nacalai Tesque, #35554-64, Japan). Following this, 8 mL of media was added and centrifuged at 3000 rpm for 5 min at 4°C. The harvested cells were then rinsed with phosphate buffer saline (PBS) and homogenized with growth media. The cells were counted in hemocytometer (Hirschmann Laborgerate, EM Techcolor, Germany) before subculturing or seeding experimental plates. All experiments were carried out with cells at 5–15 passage unless otherwise mentioned.

Source of the treatment agents was: Insulin (Eli Lilly, Humulin R U-100, USA), LNA (Cayman Chemicals, #90150, USA, purity: 99%), Rosiglitazone (Cayman Chemicals, #71740, USA, purity: ≥98%), GW 9662 (Tocris Bioscience, #GZ-1508, USA, purity: ≥98%), c9,t11-CLA (Cayman Chemicals, #90140, USA, purity: ≥98%), and t10,c12-CLA (Cayman Chemicals, #90145, USA, purity: ≥98%). Fatty acid-based treatments such as LNA, c9,t11-CLA, t10,c12-CLA, and insulin were prepared in 100% ethanol. Rosiglitazone and GW 9662 were dissolved in dimethyl sulfoxide (DMSO; Sigma, USA). Final concentrations of the solvents in cell culture treatments were 0.084% for insulin, 0.33% for c9,t11-CLA, 0.33% for t10,c12-CLA, 0.20% for LNA, 0.1% for rosiglitazone, and 0.1% for GW9662.

Cell Viability Assay

HepG2 and H4IIE were seeded at 1×10^4 cells per well and left to incubate for 24 h. Cells were exposed to concentrations of c9,t11-CLA and t10,c12-CLA at 0, 5, 15, 20, 30, 50, 70, and 100 μM in serum-free media for 24 h. Cell viability was determined using the 3-(4,5-dimethylthiazol-2-yl)-2,5-diphenyl tetrazolium bromide (MTT) assay (Ehrich and Sharova, 2001).

In vitro Glucose Production Assay

The glucose production assay was conducted based on a published protocol (Matsumoto and Sakai, 2012). Briefly, the cells were seeded at 2.8×10^5 per well for HepG2 and 2.0×10^5 per well for H4IIE, in a 12-well plate and incubated for 48 h. Cells were serum starved for 8 h, then glucose starved for 1 h. The cells were then incubated in 500 μL glucose production medium, consisting of glucose and phenol red-free Dulbecco's modified Eagle's medium (DMEM) (Thermo Scientific, #A14430-01, USA) with 20 mM sodium lactate, 2 mM sodium pyruvate (Nacalai Tesque, #06977-34, Japan), 2 mM L-glutamine (Nacalai Tesque, #16948-04, Japan), and 15 mM HEPES (Nacalai Tesque, #17557-94, Japan) for 24 h. Treatments were added to their final concentrations in the glucose production medium and incubated for 24 h.

A volume of 50 μL of the glucose production medium was assayed with the Amplex Red Glucose/Glucose Oxidase Assay Kit (Thermo Scientific, #A22189, USA). Glucose concentration in the glucose production media was tabulated in μM. Cells remaining in each plate well were lyzed with NP-40 (NP-40 Cell Lysis Buffer, 2007) to obtain respective protein concentration using the Bradford assay (Sigma-Aldrich, #B6916, USA) (Kruger, 2002). The glucose concentration obtained from each well was normalized with respective protein concentration and presented as μM glucose per μg protein.

Reverse-Transcription Quantitative Polymerase Chain Reaction

The treatment steps for reverse-transcription quantitative polymerase chain reaction (RT-qPCR) were identical to those of *in vitro* glucose production assay, except that assay was done in 1 mL of glucose production media in a 6 well plate (Yoon et al., 2001). At the end of the treatment, RNA was extracted with the RNeasy Mini Kit (Qiagen, #74104, USA). cDNA was synthesized with the Bioline Tetro cDNA Synthesis Kit (Bioline, #65043, UK) according to manufacturer's instructions. Quantitative PCR was performed with KAPA SYBR Fast qPCR Master Mix (KAPA Biosystems, KAPA-KK4600, USA) and Illumina Eco Real Time PCR System (Illumina, EC101-1001, USA) according to the manufacturer's protocol. Target gene expression was normalized against the acidic ribosomal phosphoprotein P0, also known as 36B4 (Akamine et al., 2007). Results were analyzed using the comparative threshold cycle method (Schmittgen and Livak, 2008).

Primer sequences used for RT-qPCR were as follows (Integrated DNA Technologies, Singapore): *PPARG* forward: CGTGGCCGCAGATTTGAA; *PPARG* reverse: CTTCCATTACGGAGAGATCCAC; *PCK1* forward: AAGAGACACAGTGCCCATCC; *PCK1* reverse: ACGTAGGGTGAATCCGTCAG; *G6PC* forward: GAGACTGGCTCAACCTCGTC; *G6PC* reverse: CCTGGTCCAGTCTCACAGGT; *RPLP0* forward: CCGTGATGCCCAGGGAAGACAG; *RPLP0* reverse: TTAGTCGAAGAGACCGAATCCC.

Statistical Analysis

All data were presented as mean ± standard error of mean (SEM). Statistical tests were performed using one-way

analysis of variance with the Tukey's post-hoc test using GraphPad Prism version 7.03 (GraphPad Software, USA). For multiple comparisons, a significance level of less than 0.05 ($p < 0.05$) is considered significant. For gene expression, a fold change of more than 2 accompanied by a significance level of less than 0.05 is considered significant.

Results

Cell Viability Assay

HepG2 and H4IIE cells were treated with increasing concentrations of c9,t11-CLA and t10,c12-CLA in serum-free medium to assess their cytotoxic effects on cells as well as to determine a suitable concentration for subsequent experiments. Generally, cell viability decreased with increasing concentrations. In HepG2, IC_{50} was 37 µM for c9,t11-CLA and 50 µM for t10,c12-CLA (Fig. 1a). For H4IIE, IC_{50} was 76.6 µM for c9,t11-CLA and 71 µM for t10,c12-CLA (Fig. 1b). From this assay, 20 µM was chosen for both CLA isomers in subsequent assays, as this concentration showed efficacy without compromising cell viability.

Effect of Isomers of CLA on HGP

To determine whether isomers of CLA directly act on hepatocytes to modulate gluconeogenesis, both human and rat hepatoma cells were separately exposed to 20 µM c9,t11-CLA and t10,c12-CLA. As insulin has been well demonstrated to suppress the gluconeogenesis (Hatting et al., 2018), insulin (100 nM) was used as a positive control in all experiments. Also, 20 µM linoleic acid (LNA)C18:2 n-6) was tested in parallel with CLA isomers to elucidate any structure-specific or isomer-specific effects.

As shown in Fig. 2a, the HepG2 cells exposed to 100 nM insulin for 24 h had reduced glucose production as expected. Administration of 20 µM of c9,t11-CLA decreased glucose production by 62.5% compared to untreated cells ($p < 0.001$, Fig. 2a). Conversely, the exposure of HepG2 cells with 20 µM of t10,c12-CLA rendered no change in glucose production ($p > 0.05$). Of note, administering both CLA isomers (10 µM of c9t11-CLA and 10 µM of t10c12-CLA) reduced the glucose production by 42.6% ($p < 0.05$, Fig. 2a). Administering 20 µM of LNA rendered no change of glucose production in both HepG2 and H4IIE (Fig. 2a, b).

To further validate the results obtained from HepG2, human hepatocarcinoma cells, the effects of CLA isomers on glucose production were tested in H411E, rat hepatoma cells.

In H4IIE cells (Fig. 2b), it was found that administration of 100 nM insulin, 20 µM of c9,t11-CLA, and 1:1 mixture of CLA isomers has significantly reduced the glucose production by 69.9%, 80.1%, and 65.7%, respectively, compared to control ($p < 0.01$). Similar to the observations in HepG2 cells, administration of 20 µM of t10,c12-CLA led to no change in glucose production in H4IIE cells. Together, these results were comparable to the results obtained from HepG2 cells.

Effect of CLA Isomers on the Expression of *PCK1* and *G6PC* in HepG2

To elucidate whether the effects of CLA isomers on HGP are linked with the downregulation of hepatic gluconeogenic enzymes, the HepG2 cells exposed to CLA

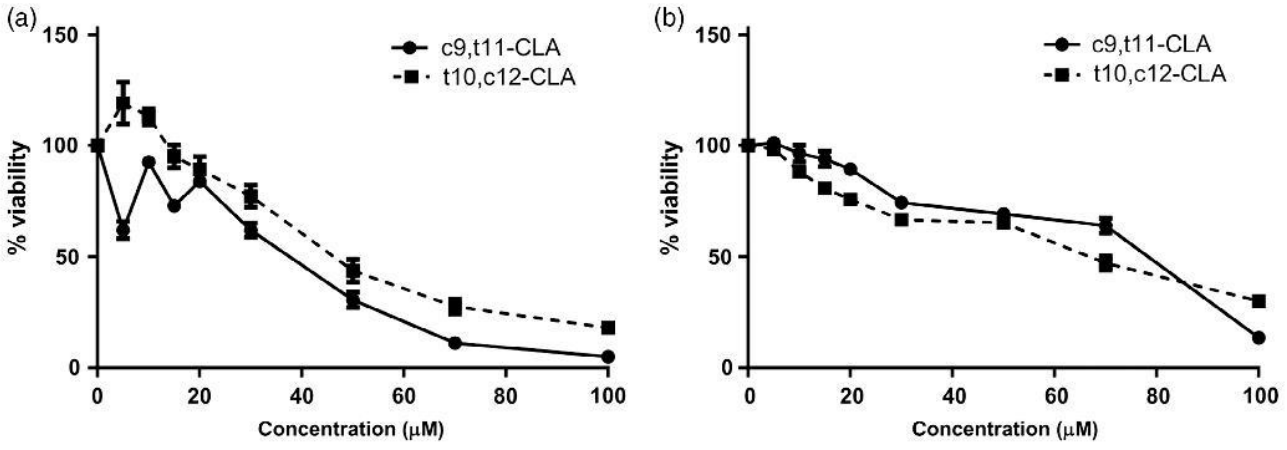


Fig. 1 Cell viability of HepG2 and H4IIE when treated with c9,t11-CLA and t10,c12-CLA. (A) HepG2 (B) H4IIE. Cells grown in 96 well plates were treated with increasing concentration of c9,t11-CLA and t10,c12-CLA in serum-freemedium for 24 h. The percentage of cell viability was determined using the MTT assay. Data were presented as mean ± SEM (standard error of mean)

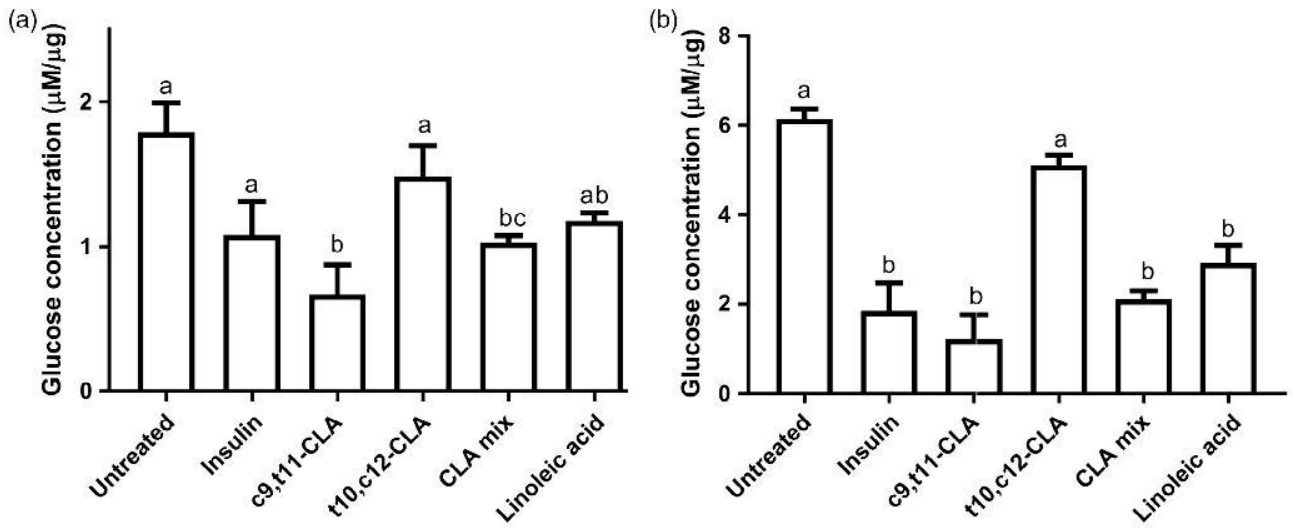


Fig. 2 Glucose production by HepG2 and H4IIE cells exposed with conjugated linoleic acid (CLA) isomers. (A) HepG2 or (B) H4IIE cells grown in 24 well plates were serum and glucose starved. They were then incubated for 24 h with the treatments including: 10 μL of PBS (untreated control), 100 nM of insulin, 20 μM of c9, t11-CLA, t10c12-CLA. or CLA mix: c9,t11 10 μM + t10,c12 10 μM, respectively, and 20 μM linoleic acid. A volume of 50 μL of media from each well was assayed to quantify the glucose content with the Amplex Red Glucose/Glucose Oxidase Assay Kit. The glucose concentration obtained from each well was normalized with respective protein concentration and presented as μM glucose per μg protein. Data were mean ± SEM (standard error of mean), $n = 6$ independent experiments. Groups with different letters on top of bar indicate statistical significance

isomers were analyzed for the mRNA expression of PEPCK, specifically cytosolic phosphoenolpyruvate carboxykinase (*PCK1*) and glucose-6-phosphatase catalytic subunit (*G6PC*) in HepG2 cells and compared with untreated control.

The HepG2 cells exposed to 100 nM insulin led to 82.47% reduction of *PCK1* expression ($p < 0.05$, Fig. 3a) but not *G6PC* (Fig. 3b) compared to control. Likewise, the reduction of gluconeogenesis in c9,t11-CLA administration was accompanied by 87.7% reduction in *PCK1* expression

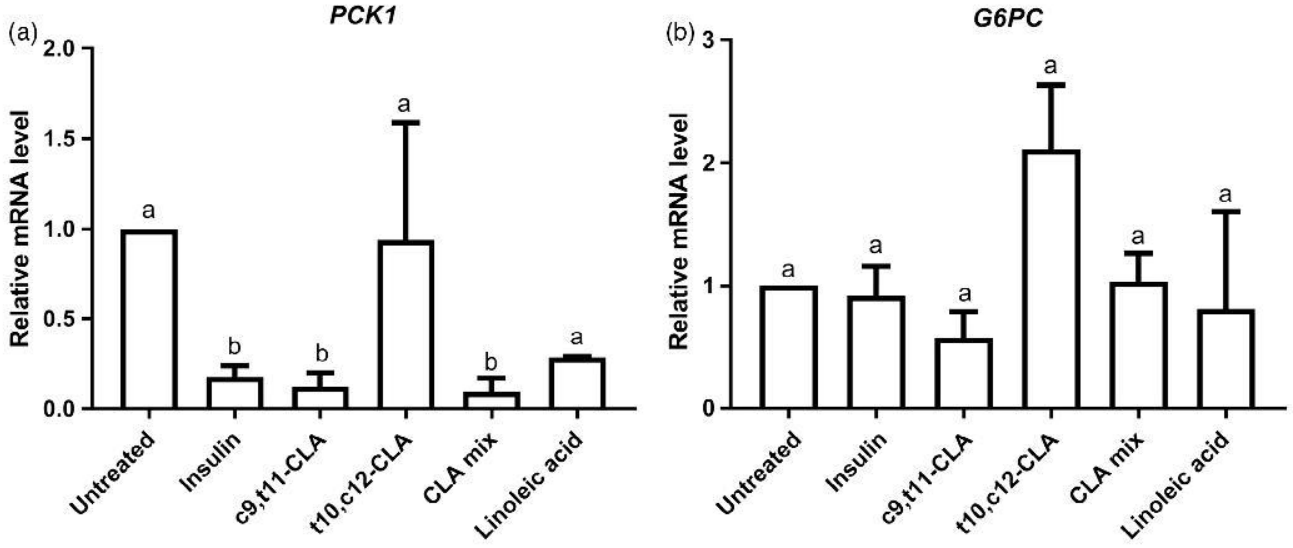


Fig. 3 HepG2 mRNA expression of gluconeogenic genes when treated with conjugated linoleic acid (CLA). Serum-deprived and glucose-deprived HepG2 cells were cultured in 24 well plates and incubated for 24 h with the treatments including, 10 μL of PBS (untreated control), 100 nM of insulin, 20 μM of c9, t11-CLA, t10c12-CLA, or CLA mix: 10 μM of c9,t11+ 10 μM of t10,c12, respectively, and 20 μM linoleic acid. The RNA was isolated from respective treatment wells, cDNA was synthesized and the quantitative polymerase chain reaction (qPCR) was performed. Target gene expression (A) *PCK1* and (B) *G6PC* was normalized with *RPLP0* as the reference gene. Results were analyzed using the comparative threshold cycle method. All data were mean ± SEM (standard error of mean), $n = 6$ independent experiments. A fold change of more than 2 accompanied by different letters on top of bar indicates statistical significance.

($p < 0.05$, Fig. 3a) and but no significant reduction in *G6PC* (Fig. 3b). Conversely, the null effect of t10,c12-CLA is accompanied by no change in *PCK1* expression (Fig. 3a) and a nonsignificant 2.1 fold increase in *G6PC* expression (Fig. 3b). Of note, the combined administration of CLA isomers led to 90.6% reduction in *PCK1* ($p < 0.05$, Fig. 3a) but no change in *G6PC* (Fig. 3b). The effect of 20 μM of LNA on both *PCK1* and *G6PC* was found to be insignificant.

Effect of PPAR Agonist or Antagonist on HGP in CLA Isomer-Treated HepG2

CLA isomers have been shown to be agonists of PPARγ in adipocytes (Belury et al., 2002; Benjamin et al., 2005). To understand whether the PPARγ activation or inhibition has any influence on the effects of CLA isomers on hepatic gluconeogenesis, the effect of conventional PPAR agonist or antagonist in the presence or absence of CLA isomers was examined. In this regard, we first ensured PPARγ (*PPARG*) is expressed in HepG2 cells by RT-PCR (Fig. S1, Supporting Information).

The exposure of HepG2 cells with 10 μM rosiglitazone, a conventional PPARγ agonist led to 72.9% reduction of glucose production ($p < 0.05$, Fig. 4a). However, rosiglitazone combined with CLA isomers either individually or mix had mixed responses. HGP in the combined c9,t11-CLA and rosiglitazone had 75% reduced compared to control ($p < 0.05$, Fig. 4a). Conversely, the presence of t10,12-CLA or CLA mix had abrogated the suppressive effects of rosiglitazone on hepatic gluconeogenesis (Fig. 4a). The administration of GW 9662 at 10 μM [30], a PPARγ antagonist, had 70.2% reduction in hepatic gluconeogenesis, compared to control ($p < 0.005$, Fig. 4b). GW 9662 was found to further decrease HGP when combined with either individual CLA isomers c9,t11 (80.9% reduction), t10,c12 (85.2% reduction) or CLA mix (87.4% reduction) ($p < 0.0001$, Fig. 4b).

Effect of PPAR Agonist or Antagonist on *PCK1* and *G6PC* Expression in CLA Isomer-Treated HepG2 Cells

The expression of *PCK1* was reduced by 95.0% upon exposure to rosiglitazone alone ($p < 0.0001$, Fig. 5a). The combination of c9,t11-CLA, t10,c12-CLA, or CLA mix with rosiglitazone had 89.8% ($p < 0.0001$), 92.0% ($p < 0.0001$), and 94.% ($p < 0.0001$) lowered expression of *PCK1*, respectively (Fig. 5a). In contrast, the expression of *G6PC* had changed neither with rosiglitazone alone nor in combination with individual CLA isomers or CLA mix (Fig. 5b). As shown in Fig. 5c, the administration of 10 μM GW 9662 led to near undetectable expression of *PCK1* either in the presence or absence of CLA, compared to untreated control ($p < 0.0001$). The *G6PC* mRNA level was found to be 86% decreased with cotreatment of GW 9662 and t10,c12-CLA ($p < 0.05$, Fig. 5d); 80.1% decreased with cotreatment of GW 9662 and CLA mix ($p < 0.05$, Fig. 5d).

Discussion

Our findings establish that c9,t11-CLA is able to act directly on liver cells to reduce gluconeogenesis by

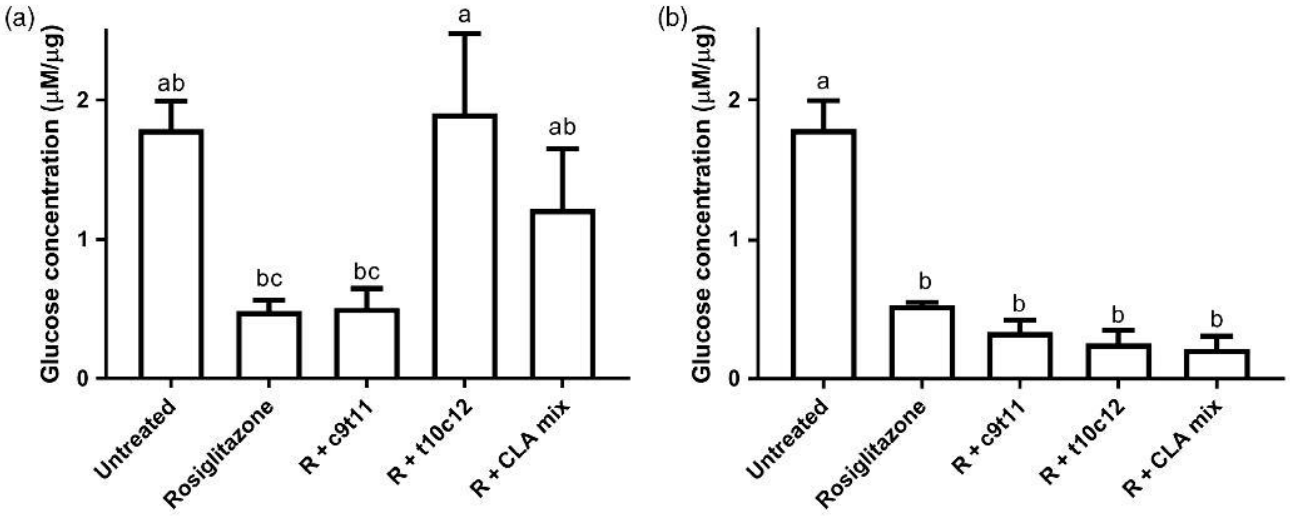


Fig. 4 PPAR agonist or antagonist on hepatic glucose production (HGP) in conjugated linoleic acid (CLA) isomer-treated HepG2 cells. Cells grown in 24-well plates were serum and glucose starved. They were incubated with 10 μM rosiglitazone (A) or 10 μM GW 9662 (B) or cotreated with CLA isomers for 24 h. Fifty microliters of media were assayed for glucose content with Amplex red glucose/glucose oxidase kit. Data were mean ± SEM (standard error of mean), $n = 6$ independent experiments. Different letters on top of bar indicate statistical significance

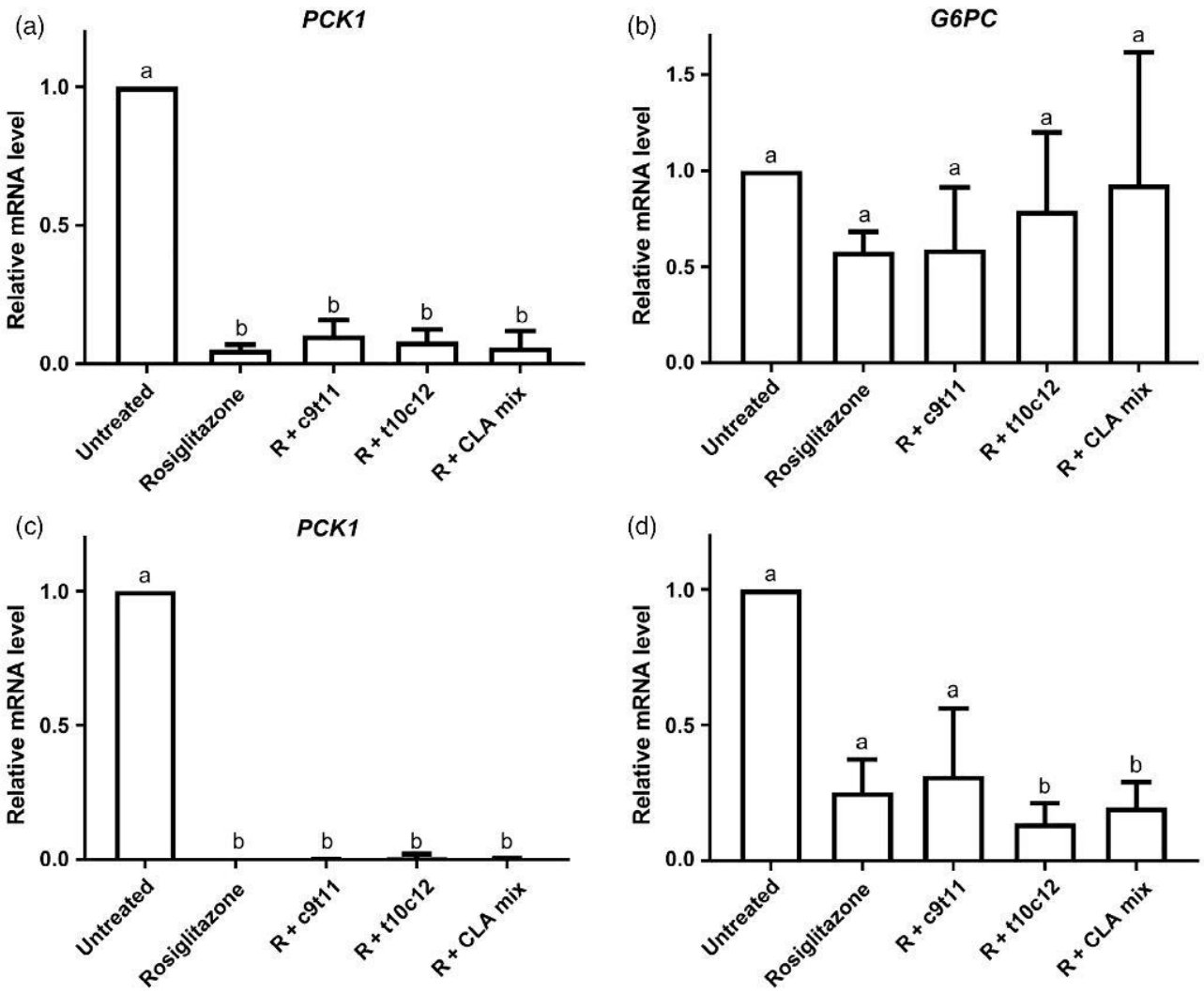


Fig. 5 Rosiglitazone or GW 9662 on *PCK1* and *G6PC* expression in conjugated linoleic acid (CLA) isomers-treated HepG2 cells. Cells grown in 6-well plates were serum and glucose starved. They were incubated with 10 μM rosiglitazone (A, B) or 10 μM GW 9662 (C, D) or cotreated with CLA isomers for 24 h. For gene expression, RNA was extracted, cDNA was synthesized and quantitative polymerase chain reaction (qPCR) was performed. The mRNA expression levels of *PCK1* (A, C) and *G6PC* (B, D) were normalized with *RPLP0* as the reference gene. Data were mean ± SEM (standard error of mean), $n = 6$ independent experiments. A fold change of more than 2 accompanied by different letters on top of bar indicates significance

suppressing *the PCK1* and this effect was comparable to rosiglitazone, a PPAR agonist. However, the exposure of t10,c12 CLA on liver cells have modulated neither the HGP nor the levels of gluconeogenic enzymes. Of note, t10,c12 CLA abrogated the effects of rosiglitazone on HGP. Taken together, our findings suggest the isomer-specific effects of CLA and the possibilities of dairy food constituents interacting with PPAR activation or inhibition to bring about health benefits, which fall into the category of functional foods. Functional food is defined as "any food or food ingredient that provides health benefit beyond its traditional nutritional value" by Institute of Medicine Food and Nutrition Board (Institute of Medicine, 1994). Unfortunately, recent clinical studies on the effect of CLA in glucose homeostasis has been inconsistent and beneficial effects may not be apparent in low dose and short term (<16 weeks), but well tolerated across subjects in terms of safety (Kim et al., 2016).

In T2DM, the increase in hepatic gluconeogenesis is due to elevated basal gluconeogenesis (Erion et al., 2009). Hepatic gluconeogenesis contributes to 75% of hepatic glucose output in T2DM, with the rest contributed by glycogenolysis and glycogen cycling (Hundal et al., 2000). It was established that hepatic gluconeogenesis is less sensitive to inhibition by insulin compared to glycogenolysis (Girard, 2006a). Basal gluconeogenesis is unaffected by insulin because it is transcriptionally controlled by p300, a CREB-like protein not regulated by phosphorylation

(He et al., 2012, 2013). The primacy of gluconeogenesis in T2DM is demonstrated by the overexpression of PEPCK in animal models, which developed T2DM-like state with selective hepatic insulin resistance (Sun et al., 2002; Valera et al., 1994). Alternatively, persistent activation gluconeogenic transcription factors lead to hepatic insulin resistance (Hogan et al., 2015). Although hepatic gluconeogenesis may not be the primary contributor to hyperglycemia, it is thought to contribute to a feedback loop that worsens insulin resistance over time. The improvement of the metabolic profile in diabetic rats can be achieved by knocking down *PCK1* (Gómez-Valadés et al., 2006). Therefore, inhibition of hepatic gluconeogenesis is a viable strategy to alleviate hyperglycemia and other symptoms of T2DM. Because insulin is unable to reduce basal gluconeogenesis, compounds able to exert reduction in basal gluconeogenesis will be of interest, taken that CLA is able to reduce the activity of gluconeogenic enzymes at the transcriptional level. Although the precise mechanism is unknown, it is suggested that CLA reduces gluconeogenesis by disrupting membrane integrity of hepatocytes, judging from the observation of increased lactate dehydrogenase release *in vitro* at high CLA concentrations (Cantwell et al., 1999). It is worth noting that the lowest concentration of CLA used in a previous study (Cantwell et al., 1999) is equivalent to 17.8 μM, but the authors had only observed a significant effect at the equivalent of 71 μM; while we managed to show the efficacy of CLA at 20 μM. Besides that, the modulation of p300 by CLA and its dependence of PPAR shall be the subject of future investigations.

Rosiglitazone is an antidiabetic drug belonging to a class of insulin sensitizers known as thiazolidinediones. Administration of rosiglitazone has been shown to inhibit hepatic gluconeogenesis (Gastaldelli et al., 2006). Our experimental results demonstrated that the reduction in the rate of hepatic gluconeogenesis when the cells were treated with rosiglitazone and CLA corresponded to the expression level of *PCK1* and *G6PC* mRNA, except for the combination of rosiglitazone and c9,t11-CLA. Our observation for rosiglitazone is at odds with a previous observation that reported no change in *PCK1* mRNA levels in rats (Davies et al., 2001). PEPCK activity is controlled by abundance of PEPCK protein in the liver, as the enzyme is neither regulated by allosteric binding nor phosphorylation/dephosphorylation (Scott et al., 1998). Our main caveat was that we were only measuring gene expression at the mRNA but not at the protein level.

It has been reviewed that PPARγ activity has an inverted U-shaped relationship with gluconeogenesis (Picard and Auwerx, 2002). PPAR response element (PPARE) is present in the enhancer region of cytosolic PEPCK (PEPCK-C) gene, which is bound by PPARγ, and it has been shown in mice that PPARE is indispensable for PEPCK-C expression in adipose tissue (Olswang et al., 2002; Tontonoz et al., 2015). In nonadipose cells, forced expression of PPARγ is able to activate the PEPCK-C enhancer of the said cells (Tontonoz et al., 2015). PPARγ antagonist GW 9662 has been shown to inhibit PEPCK expression *in vivo* (Kim et al., 2017). GW 9662 binds to PPARγ at an IC_{50} of 3.3 nM (Leesnitzer et al., 2002), therefore, we reasoned that the reduction of HGP in the presence of GW 9662 is attributed to inhibition of PPARγ binding to PPARE instead of CLA activation.

In spite of our result that centered on the dependence of PPARγ, the long held paradigm of activating PPAR as the key to treating metabolic diseases has been challenged by recent discoveries. Rosiglitazone has traditionally been regarded as a potent and specific agonist for PPARγ (Edvardsson et al., 1999), whereas CLA has been regarded as a weaker agonist with an IC_{50} difference between 940–2176- fold (Belury et al., 2002). Emerging evidence is pointing to thiazolidinediones exerting an insulin-sensitizing effect independent of the PPARγ pathway (Davies et al., 2001; Derlacz et al., 2008), which is further proven by reports of glitazone mimetics improving insulin sensitivity despite a lack of PPAR agonist activity (Bolten et al., 2007). It is essential to take note that this PPAR independence may involve no change in basal PPAR receptor activity. Instead, the authors proposed that modulation of mitochondrial biogenesis as well as direct modulation of mitochondrial metabolism contribute to the pharmacology of thiazolidinediones. There is emerging evidence that points to mitochondrial targets for insulin-sensitizing drugs. Thiazolidinediones have been shown to target the pyruvate carrier complexes of the mitochondria (Colca et al., 2013; Divakaruni et al., 2013; Wright et al., 2014). Metformin has been identified as an inhibitor of mitochondrial glycerophosphate dehydrogenase to suppress gluconeogenesis (Madiraju et al., 2014). It is suggested that these insulin-sensitizing drugs, rather than acting through a linear pathway of activating downstream targets, they lead to a change in the energy state by binding to mitochondrial proteins (Colca et al., 2014). The change in the mitochondrial energy state led to a cellular response of increasing sensitivity to insulin. Based on our observations, it will be useful to determine PPAR independence action of CLA.

The c9,t11 isomer is the most abundant CLA isomer in nature. Hence, the single administration of c9,t11 is highly applicable to the consumption of CLA from dietary sources. The t10,c12 isomer is present in low natural abundance, but high amounts in artificial preparations of CLA mixtures sold commercially. The consumption of t10,c12-CLA in high amounts is relevant in CLA supplements, as these supplements are made from artificial CLA preparations.

A myriad of studies has shown that actions of CLA are isomer dependent. While the c9,t11 isomer is associated

with increase of insulin sensitivity (Bissonauth et al., 2006; Choi et al., 2004, 2007; de Almeida et al., 2014; Kelley et al., 2004; Moloney et al., 2007), the sole consumption of the t10,c12 isomer is associated with adverse effects such as insulin resistance (Risérus et al., 2002), lipoatrophy, hepatic steatosis and hyperinsulinemia (Clément et al., 2002; Kennedy et al., 2010; Poirier et al., 2005), and adipose tissue inflammation (Poirier et al., 2006). *In vivo*, consumption of a mixture of c9,t11-CLA and t10,c12-CLA increased serum high-density lipoprotein (HDL) cholesterol, but led to insulin resistance in Wistar rats, leading to authors' suggestion that CLA supplement should be approached with caution for weight management (de Almeida et al., 2015). Likewise, we have shown that combination of CLA mixture and rosiglitazone decreased insulin resistance but increased atherogenicity by virtue of the serum non-HDL to HDL ratio in Sprague–Dawley rats (Chai et al., 2018). *In vitro*, 1:1 CLA has been shown to inhibit glucose uptake in cultured primary rat adipocytes (Pérez-Matute et al., 2007). To account for our observations, t10,c12-CLA must either inhibit the ability of c9,t11-CLA and thiazolidinediones to bind to their mitochondrial targets, or antagonize the activity of PPARγ. While there is no publication describing the effect of t10,c12-CLA in modulating mitochondrial metabolism, evidence is emerging for t10,c12-CLA antagonism of activated PPARγ activity (Granlund et al., 2003; Yeganeh et al., 2016). Because c9,t11-CLA and t10,c12-CLA are equally efficient in activating PPARγ (Granlund et al., 2003), the outcome cannot be attributed to binding of CLA isomers to PPARγ *per se*, but alternative pathways activated by CLA (Clément et al., 2002). The pathways leading to direct suppression of hepatic gluconeogenesis are a subject of future investigation.

In summary, we have demonstrated that c9,t11-CLA is able to exert an insulin-like effect directly on the liver to bring about reduction in hepatic gluconeogenesis, that is mediated by reduction in *PCK1* and *G6PC* expression. In contrast, t10,c12-CLA increases hepatic gluconeogenesis by increasing *G6PC* expression at the transcriptional level.

Acknowledgements We would like to acknowledge the generous infrastructure provided by the University of Nottingham Malaysia Campus (UNMC). This research was supported by UNMC and the Fundamental Research Grant Scheme from the Ministry of Higher Education, Malaysia (grant number: FRGS/1/2014/SKK01/UNIM/03/2/64924).

Conflict of Interest The authors declare that they have no conflict of interest.

References

Akamine, R., Yamamoto, T., Watanabe, M., Yamazaki, N., Kataoka, M., Ishikawa, M., … Shinohara, Y. (2007) Usefulness of the 5′ region of the cDNA encoding acidic ribosomal phosphoprotein P0 conserved among rats, mice, and humans as a standard probe for gene expression analysis in different tissues and animal species. *Journal of Biochemical and Biophysical Methods*, **70**:481–486.

Alibin, C. P., Kopilas, M. A., & Anderson, H. D. I. (2008) Suppression of cardiac myocyte hypertrophy by conjugated linoleic acid: Role of peroxisome proliferator-activated receptors alpha and gamma. *The Journal of Biological Chemistry*, **283**:10707–10715.

Belury, M., Moya-Camarena, S., & Lu, M. (2002) Conjugated linoleic acid is an activator and ligand for peroxisome proliferator-activated receptor-gamma (PPARγ). *Nutrition Research*, **22**:817–824.

Benjamin, S., Hanhoff, T., Börchers, T., & Spener, F. (2005) An improved molecular test system for the screening of human PPAR transactivation by conjugated linoleic acid isomers and their precursor fatty acids. *European Journal of Lipid Science and Technology*, **107**:706–715.

Benjamin, S., & Spener, F. (2009) Conjugated linoleic acids as functional food: An insight into their health benefits. *Nutrition & Metabolism*, **6**:36.

Bhattacharya, A., Banu, J., Rahman, M., Causey, J., & Fernandes, G. (2006) Biological effects of conjugated linoleic acids in health and disease. *Journal of Nutritional Biochemistry*, **17**:789–810.

Bissonauth, V., Chouinard, Y., Marin, J., Leblanc, N., Richard, D., & Jacques, H. (2006) The effects of t10,c12 CLA isomer compared with c9,t11 CLA isomer on lipid metabolism and body composition in hamsters. *Journal of Nutritional Biochemistry*, **17**:597–603.

Boden, G., Chen, X., & Stein, T. P. (2001) Gluconeogenesis in moderately and severely hyperglycemic patients with type 2 diabetes mellitus. *American Journal of Physiology, Endocrinology and Metabolism*, **280**:E23–E30.

Bolten, C. W., Blanner, P. M., McDonald, W. G., Staten, N. R., Mazzarella, R. a., Arhancet, G. B., … Colca, J. R. (2007) Insulin sensitizing pharmacology of thiazolidinediones correlates with mitochondrial gene expression rather than activation of PPAR gamma. *Gene Regulation and Systems Biology*, **1**:73–82.

Cantwell, H., Devery, R., O'Shea, M., & Stanton, C. (1999) The effect of conjugated linoleic acid on the antioxidant enzyme defense system in rat hepatocytes. *Lipids*, **34**:833–839.

Chai, B. K., Lau, Y. S., Loong, B. J., Mustafa, M. R., Ting, K. N., Murugan, D. D., & Mohankumar, S. K. (2018) Co-administration of conjugated linoleic acid and rosiglitazone increases atherogenic co-efficicient and alters isoprenaline-induced vasodilatation in rats fed high fat diet. *Physiological Research*, **67**:729–740.

Choi, J. S., Jung, M. H., Park, H. S., & Song, J. (2004) Effect of conjugated linoleic acid isomers on insulin resistance and mRNA levels of genes regulating energy metabolism in high-fat-fed rats. *Nutrition*, **20**:1008–1017.

Choi, J. S., Koh, I.-U., Jung, M. H., & Song, J. (2007) Effects of three different conjugated linoleic acid preparations on insulin signalling, fat oxidation and mitochondrial function in rats fed a high-fat diet. *The British Journal of Nutrition*, **98**:264–275.

Churruca, I., Fernández-Quintela, A., & Portillo, M. P. (2008) Conjugated linoleic acid isomers: Differences in metabolism and biological effects. *BioFactors (Oxford, England)*, **35**:105–111.

Clément, L., Poirier, H., Niot, I., Bocher, V., Guerre-Millo, M., Krief, S., … Besnard, P. (2002) Dietary trans-10,cis-12 conjugated linoleic acid induces hyperinsulinemia and fatty liver in the mouse. *Journal of Lipid Research*, **43**:1400–1409.

Colca, J. R., McDonald, W. G., Cavey, G. S., Cole, S. L., Holewa, D. D., Brightwell-Conrad, A. S., … Kletzien, R. F. (2013) Identification of a mitochondrial target of thiazolidinedione insulin sensitizers (mTOT)-relationship to newly identified mitochondrial pyruvate carrier proteins. *PLoS One*, **8**:1–10.

Colca, J. R., Mcdonald, W. G., & Kletzien, R. F. (2014) Mitochondrial target of thiazolidinediones. *Diabetes, Obesity and Metabolism*, **16**:1048–1054.

Conde-Aguilera, J. A., Lachica, M., Nieto, R., & Fernández-Fígares, I. (2012) Metabolic regulation of fatty acid esterification and effects of conjugated linoleic acid on glucose homeostasis in pig hepatocytes. *Animal*, **6**:254–261.

Davies, G. F., Khandelwal, R. L., Wu, L., Juurlink, B. H. J., & Roesler, W. J. (2001) Inhibition of phosphoenolpyruvate carboxykinase (PEPCK) gene expression by troglitazone: A peroxisome proliferator-activated receptor-γ (PPARγ)-independent, antioxidant-related mechanism. *Biochemical Pharmacology*, **62**: 1071–1079.

de Almeida, M. M., De Souza, Y. O., Dutra Luquetti, S. C. P., Sabarense, C. M., Corrêa, A., do, J. O., … González Garcia, R. M. (2015) *Cis*-9, *trans*-11 and *trans*-10, *cis*-12 CLA mixture does not change body composition, induces insulin resistance and increases serum HDL cholesterol level in rats. *Journal of Oleo Science*, **64**: 539–551.

de Almeida, M. M., Luquetti, S. C. P. D., Sabarense, C. M., Corrêa, J. O. d. A., dos Reis, L. G., da Conceição, E. P. S., … Garcia, R. M. G. (2014) Butter naturally enriched in cis-9, trans-11 CLA prevents hyperinsulinemia and increases both serum HDL cholesterol and triacylglycerol levels in rats. *Lipids in Health and Disease*, **13**:200.

DeClercq, V., Taylor, C. G., & Zahradka, P. (2012) Isomer-specific effects of conjugated linoleic acid on blood pressure, adipocyte size and function. *The British Journal of Nutrition*, **107**:1413–1421.

Dentin, R., Liu, Y., Koo, S.-H., Hedrick, S., Vargas, T., Heredia, J., … Montminy, M. (2007) Insulin modulates gluconeogenesis by inhibition of the coactivator TORC2. *Nature*, **449**:366–369.

Derlacz, R. A., Hyc, K., Usarek, M., Jagielski, A. K., Drozak, J., & Jarzyna, R. (2008) PPAR-gamma-independent inhibitory effect of rosiglitazone on glucose synthesis in primary cultured rabbit kidney-cortex tubules. *Biochemistry and Cell Biology = Biochimie et biologie cellulaire*, **86**:396–404.

Dilzer, A., & Park, Y. (2012) Implication of conjugated linoleic acid (CLA) in human health. *Critical Reviews in Food Science and Nutrition*, **52**:488–513.

Divakaruni, A. S., Wiley, S. E., Rogers, G. W., Andreyev, A. Y., Petrosyan, S., Loviscach, M., … Murphy, A. N. (2013) Thiazolidinediones are acute, specific inhibitors of the mitochondrial pyruvate carrier. *Proceedings of the National Academy of Sciences*, **110**:5422–5427.

Edvardsson, U., Bergström, M., Alexandersson, M., Bamberg, K., Ljung, B., & Dahllöf, B. (1999) Rosiglitazone (BRL49653), a PPARgamma-selective agonist, causes peroxisome proliferator-like liver effects in obese mice. *Journal of Lipid Research*, **40**: 1177–1184.

Ehrich, M., & Sharova, L. (2001) In vitro methods for detecting cytotoxicity. *Current Protocols in Toxicology*, **3**:2.6.1–2.6.27.

Erion, D. M., Yonemitsu, S., Nie, Y., Nagai, Y., Gillum, M. P., Hsiao, J. J., … Shulman, G. I. (2009) SirT1 knockdown in liver decreases basal hepatic glucose production and increases hepatic insulin responsiveness in diabetic rats. *Proceedings of the National Academy of Sciences of the United States of America*, **106**: 11288–11293.

Fuke, G., & Nornberg, J. L. (2017) Systematic evaluation on the effectiveness of conjugated linoleic acid in human health. *Critical Reviews in Food Science and Nutrition*, **57**:1–7.

Gastaldelli, A., Miyazaki, Y., Pettiti, M., Santini, E., Ciociaro, D., DeFronzo, R. A., & Ferrannini, E. (2006) The effect of rosiglitazone on the liver: Decreased gluconeogenesis in patients with type 2 diabetes. *Journal of Clinical Endocrinology and Metabolism*, **91**:806–812.

Giralt, A., Denechaud, P. D., Lopez-Mejia, I. C., Delacuisine, B., Blanchet, E., Bonner, C., … Fajas, L. (2018) E2F1 promotes hepatic gluconeogenesis and contributes to hyperglycemia during diabetes. *Molecular Metabolism*, **11**:104–112.

Girard, J. (2006a) The inhibitory effects of insulin on hepatic glucose production are both direct and indirect. *Diabetes*, **55**:S65–S69.

Girard, J. (2006b) Insulin's effect on the liver: "Direct or indirect?" continues to be the question. *Journal of Clinical Investigation*, **116**: 302–304.

Givens, D. I. (2018) Review: Dairy foods, red meat and processed meat in the diet: Implications for health at key life stages. *Animal*, **2035**:1–13.

Gómez-Valadés, A. G., Vidal-Alabró, A., Molas, M., Boada, J., Bermúdez, J., Bartrons, R., & Perales, J. C. (2006) Overcoming diabetes-induced hyperglycemia through inhibition of hepatic phosphoenolpyruvate carboxykinase (GTP) with RNAi. *Molecular Therapy*, **13**:401–410.

Granlund, L., Juvet, L. K., Pedersen, J. I., & Nebb, H. I. (2003) Trans10, cis12-conjugated linoleic acid prevents triacylglycerol accumulation in adipocytes by acting as a PPARgamma modulator. *Journal of Lipid Research*, **44**:1441–1452.

Griinari, J. M., Corl, B. A., Lacy, S. H., Chouinard, P. Y., Nurmela, K., & Bauman, D. E. (2000) Conjugated linoleic acid is synthesized endogenously in lactating dairy cows by Δ9-desaturase1,2. *The Journal of Nutrition*, **130**:2285–2291.

Gupta, N. (2006) Direct and indirect effects of insulin on hepatic glucose production in diabetic depancreatized dogs during euglycemia. *Journal of Endocrinology*, **190**:695–702.

Hatting, M., Tavares, C. D. J., Sharabi, K., Rines, A. K., & Puigserver, P. (2018) Insulin regulation of gluconeogenesis. *Annals of the New York Academy of Sciences*, **1411**:21–35.

He, L., Cao, J., Meng, S., Ma, A., Radovick, S., & Wondisford, F. E. (2013) Activation of basal gluconeogenesis by coactivator p300 maintains hepatic glycogen storage. Molecular endocrinology (Baltimore, Md.), **27**:1322–1332.

He, L., Naik, K., Meng, S., Cao, J., Sidhaye, A. R., Ma, A., … Wondisford, F. E. (2012) Transcriptional co-activator p300 maintains basal hepatic gluconeogenesis. *Journal of Biological Chemistry*, **287**:32069–32077.

Hogan, M. F., Ravnskjaer, K., Matsumura, S., Huising, M. O., Hull, R. L., Kahn, S. E., & Montminy, M. (2015) Hepatic insulin resistance following chronic activation of the CREB Coactivator CRTC2. *Journal of Biological Chemistry*, **290**:25997–26006.

Houseknecht, K. L., Heuvel, J. P. V., Moya-Camarena, S. Y., Portocarrero, C. P., Peck, L. W., Nickel, K. P., & Belury, M. A. (1998) Dietary conjugated linoleic acid normalizes impaired glucose tolerance in the Zucker diabetic Fattyfa/faRat. *Biochemical and Biophysical Research Communications*, **244**:678–682.

Hundal, R. S., Krssak, M., Dufour, S., Laurent, D., Lebon, V., Chandramouli, V., … Shulman, G. I. (2000) Mechanism by which metformin reduces glucose production in type 2 diabetes. *Diabetes*, **49**:2063–2069.

Institute of Medicine.(1994) Enhancing the food supply. In P. R. Thomas & R. Earl (Eds.), *Opportunities in the nutrition and food sciences* (p. 109). Washington, DC: National Academies Press.

Kay, J. K., Mackle, T. R., Auldist, M. J., Thomson, N. A., & Bauman, D. E. (2004) Endogenous synthesis of cis-9, trans-11 conjugated linoleic acid in dairy cows fed fresh pasture. *Journal of Dairy Science*, **87**:369–378.

Kelley, D. S., Bartolini, G. L., Warren, J. M., Simon, V. A., Mackey, B. E., & Erickson, K. L. (2004) Contrasting effects of t10,c12- and c9,t11-conjugated linoleic acid isomers on the fatty acid profiles of mouse liver lipids. *Lipids*, **39**:135–141.

Kelly, M. L., Berry, J. R., Dwyer, D. A., Griinari, J. M., Chouinard, P. Y., Van Amburgh, M. E., & Bauman, D. E. (1998) Dietary fatty acid sources affect conjugated linoleic acid concentrations in Milk from lactating dairy cows. *The Journal of Nutrition*, **128**:881–885.

Kennedy, A., Martinez, K., Chung, S., LaPoint, K., Hopkins, R., Schmidt, S. F., … McIntosh, M. (2010) Inflammation and insulin resistance induced by trans-10, cis-12 conjugated linoleic acid depend on intracellular calcium levels in primary cultures of human adipocytes. *Journal of Lipid Research*, **51**:1906–1917.

Kim, J. H., Kim, Y. Y. J., Kim, Y. Y. J., & Park, Y. (2016) Conjugated linoleic acid: Potential health benefits as a functional food ingredient. *Annual Review of Food Science and Technology*, **7**: 221–244.

Kim, K., Boo, K., Yu, Y. S., Oh, S. K., Kim, H., Jeon, Y., … Baek, S. H. (2017) RORα controls hepatic lipid homeostasis via negative regulation of PPARγ transcriptional network. *Nature Communications*, **8**:162.

Kramer, J. K., Cruz-Hernandez, C., Deng, Z., Zhou, J., Jahreis, G., & Dugan, M. E. (2004) Analysis of conjugated linoleic acid and trans 18:1 isomers in synthetic and animal products. *The American Journal of Clinical Nutrition*, **79**:1137S–1145S.

Kruger, N. J. (2002) The Bradford method for protein quantitation. In J. M. Walker (Ed.), *Protein protocols handbook* (pp. 15–22). Totowa, NJ: The. Humana Press.

Leesnitzer, L. M., Parks, D. J., Bledsoe, R. K., Cobb, J. E., Collins, J. L., Consler, T. G., … Blanchard, S. G. (2002) Functional consequences of cysteine modification in the ligand binding sites of peroxisome proliferator activated receptors by GW9662. *Biochemistry*, **41**:6640–6650.

Madiraju, A. K., Erion, D. M., Rahimi, Y., Zhang, X., Braddock, D. T., Albright, R. A., … Shulman, G. I. (2014) Metformin suppresses gluconeogenesis by inhibiting mitochondrial glycerophosphate dehydrogenase. *Nature*, **510**:542–546.

Matsumoto, M., & Sakai, M. (2012) Glucose production assay in primary mouse hepatocytes. *Bio-Protocol*, **2**:5–8.

Mohankumar, S. K., Taylor, C. G., Siemens, L., & Zahradka, P. (2012) Acute exposure of L6 myotubes to cis-9, trans-11 and trans-10, cis-12 conjugated linoleic acid isomers stimulates glucose uptake by modulating Ca2+/calmodulin-dependent protein kinase II. *The International Journal of Biochemistry & Cell Biology*, **44**: 1321–1330.

Mohankumar, S. K., Taylor, C. G., Siemens, L., & Zahradka, P. (2013) Activation of phosphatidylinositol-3 kinase, AMP-activated kinase and Akt substrate-160 kDa by trans-10, cis-12 conjugated linoleic acid mediates skeletal muscle glucose uptake. *The Journal of Nutritional Biochemistry*, **24**:445–456.

Moloney, F., Toomey, S., Noone, E., Nugent, A., Allan, B., Loscher, C. E., & Roche, H. M. (2007) Antidiabetic effects of cis-9, trans-11-conjugated linoleic acid may be mediated via anti-inflammatory effects in white adipose tissue. *Diabetes*, **56**: 574–582.

Noone, E. J., Roche, H. M., Nugent, A. P., & Gibney, M. J. (2002) The effect of dietary supplementation using isomeric blends of conjugated linoleic acid on lipid metabolism in healthy human subjects. *The British Journal of Nutrition*, **88**:243–251.

Noto, A., Zahradka, P., Yurkova, N., Xie, X., Nitschmann, E., Ogborn, M., & Taylor, C. G. (2006) Conjugated linoleic acid reduces hepatic steatosis, improves liver function, and favorably modifies lipid metabolism in obese insulin-resistant rats. *Lipids*, **41**: 179–188.

NP-40 Cell Lysis Buffer. (2007) *Cold Spring Harbor Protocols*, 2007: pdb.rec11188.

Olswang, Y., Cohen, H., Papo, O., Cassuto, H., Croniger, C. M., Hakimi, P., … Reshef, L. (2002) A mutation in the peroxisome proliferator-activated receptor -binding site in the gene for the cytosolic form of phosphoenolpyruvate carboxykinase reduces adipose tissue size and fat content in mice. *Proceedings of the National Academy of Sciences*, **99**:625–630.

Pérez-Matute, P., Marti, A., Martínez, J. A., Fernández-Otero, M. P., Stanhope, K. L., Havel, P. J., & Moreno-Aliaga, M. J. (2007) Conjugated linoleic acid inhibits glucose metabolism, leptin and adiponectin secretion in primary cultured rat adipocytes. *Molecular and Cellular Endocrinology*, **268**:50–58.

Picard, F., & Auwerx, J. (2002) PPARγ and glucose homeostasis. *Annual Review of Nutrition*, **22**:167–197.

Poirier, H., Niot, I., Clément, L., Guerre-Millo, M., & Besnard, P. (2005) Development of conjugated linoleic acid (CLA)-mediated lipoatrophic syndrome in the mouse. *Biochimie*, **87**:73–79.

Poirier, H., Shapiro, J. S., Kim, R. J., & Lazar, M. a. (2006) Nutritional supplementation with trans-10, cis-12-conjugated linoleic acid induces inflammation of white adipose tissue. *Diabetes*, **55**: 1634–1641.

Rice, B. H. (2014) Dairy and cardiovascular disease: A review of recent observational research. *Current Nutrition Reports*, **3**: 130–138.

Risérus, U., Arner, P., Brismar, K., & Vessby, B. (2002) Treatment with dietary trans10cis12 conjugated linoleic acid causes isomer-specific insulin resistance in obese men with the metabolic syndrome. *Diabetes Care*, **25**:1516–1521.

Schmittgen, T. D., & Livak, K. J. (2008) Analyzing real-time PCR data by the comparative CT method. *Nature Protocols*, **3**: 1101–1108.

Scott, D. K., Doherty, R. M. O., Stafford, M., Newgard, C. B., Granner, D. K., & Stafford, J. M. (1998) The repression of hormone-activated PEPCK gene expression by glucose is insulin-independent but requires glucose metabolism the repression of hormone-activated PEPCK gene expression by glucose is insulin-independent but requires glucose metabolism. *The Journal of Biological Chemistry*, **273**:24145–24151.

Shin, S., Lee, H.-W., Kim, C. E., Lim, J., Lee, J., & Kang, D. (2017) Association between Milk consumption and metabolic syndrome among Korean adults: Results from the health examinees study. *Nutrients*, **9**:1102.

Sun, Y., Liu, S., Ferguson, S., Wang, L., Klepcyk, P., Yun, J. S., & Friedman, J. E. (2002) Phosphoenolpyruvate carboxykinase overexpression selectively attenuates insulin signaling and hepatic insulin sensitivity in transgenic mice. *Journal of Biological Chemistry*, **277**:23301–23307.

Tontonoz, P., Hu, E., Devine, J., Beale, E. G., & Spiegelman, B. M. (2015) PPAR gamma 2 regulates adipose expression of the phosphoenolpyruvate carboxykinase gene. *Molecular and Cellular Biology*, **15**:351–357.

Valera, A., Pujol, A., Pelegrin, M., & Bosch, F. (1994) Transgenic mice overexpressing phosphoenolpyruvate carboxykinase develop non-insulin-dependent diabetes mellitus. *Proceedings of the National Academy of Sciences of the United States of America*, **91**: 9151–9154.

Wright, M. B., Bortolini, M., Tadayyon, M., & Bopst, M. (2014) Minireview: Challenges and opportunities in development of PPAR agonists. *Molecular Endocrinology (Baltimore, Md.)*, **28**: 1756–1768.

Yeganeh, A., Taylor, C. G., Poole, J., Tworek, L., & Zahradka, P. (2016) Trans10, cis12 conjugated linoleic acid inhibits 3T3-L1 adipocyte adipogenesis by elevating β-catenin levels. *Biochimica et Biophysica Acta (BBA)—Molecular and Cell Biology of Lipids*, **1861**:363–370.

Yoon, J. C., Puigserver, P., Chen, G., Donovan, J., Wu, Z., Rhee, J., Spiegelman, B. M. (2001) Control of hepatic gluconeogenesis through the transcriptional coactivator PGC-1. *Nature*, **413**: 131–138.